Turton, Stephen Michael (1991) ***Solar radiation regimes in rainforest understoreys, gaps and clearings, with special reference to Northeast Queensland.*** **PhD thesis, James Cook University.**

SOLAR RADIATION REGIMES IN RAINFOREST UNDERSTOREYS, GAPS AND CLEARINGS, WITH SPECIAL REFERENCE TO NORTHEAST QUEENSLAND

VOLUME 2

Thesis submitted by

Stephen Michael TURTON MSc (*Cant*)

in January 1991

for the degree of Doctor of Philosophy in

the Department of Geography at

James Cook University of North Queensland

CHAPTER 7

TEMPORAL AND SPATIAL DISTRIBUTION OF SOLAR RADIATION ABOVE AND BENEATH SOME NORTHEAST QUEENSLAND RAINFORESTS

The main aim of this chapter is to evaluate the results of the various field experiments described in Chapter 6. In an attempt to achieve the last five specific aims of this thesis, already described at the end of Chapter 2, this chapter will be presented in three main sections: (1) daily irradiation and photosynthetic photon flux density (PPFD) at Topaz, El-Arish and Atherton, North Queensland; (2) diurnal variations in irradiance and PPFD above and beneath tropical rainforest canopies; and (3) seasonal variations in daily PPFD above and beneath tropical rainforest canopies.

7.1 DAILY IRRADIATION AND PHOTOSYNTHETIC PHOTON FLUX DENSITY (PPFD) AT TOPAZ, EL-ARISH AND ATHERTON, NORTH QUEENSLAND

As discussed in Section 6.4.1, daily measurements of total irradiation and total PPFD were made over a period of one year at three sites in the wet tropics region - Topaz, El-Arish and Atherton (Table 5.2), with the aim being to collect some baseline data on solar radiation variability within the region to be compared with the only existing record at Pin Gin Hill, near Innisfail (Fig. 5.3).

Tables 7.1, 7.2 and 7.3 show monthly means for total daily irradiation (Q), the ratio of total to extraterrestrial (Q/Q_o) irradiation, and total daily PPFD at Topaz, El-Arish and Atherton, respectively. It should be noted that the observational periods are not the same, but they do overlap. As expected, given its lower annual rainfall (Fig. 5.3), Atherton experienced the greatest amount of irradiation over the year (6639 MJ m^{-2} per year), followed by Topaz (6055 MJ m^{-2} per year) and El-Arish (5668 MJ m^{-2} per year). These data compare well with the annual mean of about 5800 MJ m^{-2} per year at Pin Gin Hill, based on the nine year record (Hopkins and Graham, 1989). The annual mean Q/Q_oratio of 0.51 for Atherton (Table 7.3) is very similar to that of 0.519 for the 25 humid tropical stations evaluated in Table 3.3. On the other hand, the mean Q/Q_o ratios of 0.45 and 0.46 for El-Arish and Topaz, respectively, are closer to those found for the 25 stations during the wet months where Q/Q_o was equal to 0.47 (Table 3.3). The proximity of Topaz and El-Arish to the coastal ranges (Fig. 5.2) and associated high annual rainfall (Fig. 5.3) are the most likely explanations for

TOPAZ

Month	Irradiation (MJ m^{-2} per day) mean±1 S.D.	Q/Q_0 (ratio) mean±1 S.D.	PPFD (mol m^{-2} per day) mean±1 S.D.
January	22.2±2.28	0.54±0.056	43.0±4.43
February	16.8±4.86	0.42±0.123	32.0±9.46
March	18.0±2.76	0.48±0.075	34.9±5.37
April	13.1±4.50	0.39±0.131	25.3±8.77
May	12.3±4.52	0.42±0.157	23.7±8.81
June	9.4±3.84	0.35±0.142	18.1±7.48
July	12.9±4.42	0.46±0.153	24.9±8.62
August	16.0±3.65	0.50±0.104	30.9±7.11
September	15.2±4.99	0.42±0.144	29.3±9.73
October	20.0±3.23	0.51±0.084	38.8±6.28
November	21.5±3.25	0.52±0.077	41.7±6.33
December	21.7±3.77	0.52±0.091	42.0±7.34
Annual mean	16.59	0.46	32.22
Annual total	6055	-	11760
No. of days	365	365	365

Table 7.1. Mean monthly total irradiation (MJ m^{-2} per day), the mean monthly ratio of total irradiation (Q) to extraterrestrial irradiation (Q_0), and mean monthly photosynthetic photon flux density (PPFD) (mol m^{-2} per day) at Topaz, north Queensland (17° 27' S., 145° 44' E., 680 m asl). The data were collected on a daily basis over the period October 1986 to September 1987. Site characteristics are given in Table 5.2.

EL-ARISH

Month	Irradiation (MJ m^{-2} per day) mean±1 S.D.	Q/Q_0 (ratio) mean±1 S.D.	PPFD (mol m^{-2} per day) mean±1 S.D.
January	18.8±2.14	0.45±0.052	37.6±4.28
February	16.8±2.98	0.42±0.075	33.5±5.95
March	16.3±2.22	0.43±0.059	32.5±4.44
April	13.8±3.23	0.42±0.096	27.6±6.46
May	14.0±3.06	0.48±0.109	27.9±6.11
June	12.1±4.04	0.45±0.149	24.2±8.07
July	14.7±3.59	0.53±0.127	29.3±7.18
August	15.4±2.11	0.49±0.062	30.7±4.21
September	15.3±2.76	0.43±0.079	30.6±5.52
October	17.7±2.57	0.45±0.065	35.4±5.13
November	16.5±2.61	0.40±0.063	33.0±5.21
December	no data	no data	no data
Annual mean	15.53	0.45	31.05
Annual total	5668	-	11333
No. of days	321	321	321

Table 7.2. Mean monthly total irradiation (MJ m^{-2} per day), the mean monthly ratio of total irradiation (Q) to extraterrestrial irradiation (Q_0), and mean monthly photosynthetic photon flux density (PPFD) (mol m^{-2} per day) at El-Arish, north Queensland (17° 52' S., 146° 03' E., 28 m asl). The data were collected on a daily basis over the period January to November 1987. Site characteristics are given in Table 5.2. The missing data for December have been compensated for in the calculation of the annual mean and total.

ATHERTON

Month	Irradiation (MJ m^{-2} per day) mean±1 S.D.	Q/Q_o (ratio) mean±1 S.D.	PPFD (mol m^{-2} per day) mean±1 S.D.
January	21.4±0.96	0.52±0.024	42.1±1.89
February	19.3±2.25	0.48±0.057	37.9±4.44
March	19.1±2.06	0.51±0.061	37.6±4.07
April	16.6±1.91	0.50±0.048	32.7±3.78
May	16.0±2.29	0.54±0.083	31.4±4.52
June	12.7±3.19	0.47±0.116	25.0±6.30
July	16.2±2.69	0.57±0.092	31.9±5.31
August	17.4±2.02	0.55±0.054	34.1±3.98
September	18.1±2.53	0.50±0.074	35.7±4.99
October	21.2±2.35	0.54±0.061	41.7±4.64
November	19.6±2.76	0.48±0.067	38.5±5.45
December	20.7±2.52	0.50±0.061	40.7±4.97
Annual mean	18.19	0.51	35.62
Annual total	6639	-	13001
No. of days	365	365	365

Table 7.3. Mean monthly total irradiation (MJ m^{-2} per day), the mean monthly ratio of total irradiation (Q) to extraterrestrial irradiation (Q_o), and mean monthly photosynthetic photon flux density (PPFD) (mol m^{-2} per day) at Atherton, north Queensland (17° 16' S., 145° 30' E., 760 m asl). The data were collected on a daily basis over the period February 1987 to January 1988. Site characteristics are given in Table 5.2.

these lower Q/Q_0 ratios compared with Atherton which is located on the drier western tableland.

Total daily irradiation and PPFD are highest during the pre-monsoon months of September-December at Topaz and Atherton and lowest at all three sites in winter (June-July). Pin Gin Hill exhibits similar trends to Topaz and Atherton (Hopkins and Graham, 1989). However, El-Arish does not exhibit such a marked variation between September-December (pre-monsoon) and January-March (monsoon) as the other three sites. The reason for this result is not clear, but it may be due to El-Arish's lowland maritime location combined with its proximity to the coastal range which together facilitate high levels of cloudiness throughout the year.

Figure 7.1 illustrates mean daily irradiation and PPFD and their standard deviations for the three sites. Topaz has the greatest variability followed by Atherton and El-Arish, which have similar variability. All sites differed significantly among each other for daily irradiation over the year (Student's t-test: values ranged from 2.94-10.19, $P<0.01$). However, for daily PPFD Topaz and El-Arish did not differ significantly ($t=1.68$, $P>0.05$), while Topaz and Atherton and El-Arish and Atherton were significantly different from each other (respective values for t were: 5.07 and 8.69, $P<0.01$).

These trends are further illustrated in Fig. 7.2 which shows the distribution of percentile values for irradiation and PPFD at each site over the year. These box plots also show that Topaz has the greatest spread of daily totals followed by Atherton and El-Arish. Median daily irradiation is 17.42, 16.42 and 18.5 MJ m^{-2} per day at Topaz, El-Arish and Atherton, respectively. Corresponding median daily PPFD at these sites is 33.8, 32.7 and 36.33 mol m^{-2} per year.

Figures 7.3 and 7.4 show frequency distributions for irradiation and PPFD, respectively at the three sites over the year. At Topaz about 30% of the days over the year had irradiation totals between 15 and 20 MJ m^{-2} per day; this compares with 63.9% at El-Arish and 51.0% at Atherton. Similar trends are evident at Topaz for PPFD, with 32.3% of the days having totals between 30 and 40 mol m^{-2} per day, compared with 63.2% at El-Arish and 52.9% at Atherton.

7.2 DIURNAL VARIATIONS IN IRRADIANCE AND PPFD ABOVE AND BENEATH TROPICAL RAINFOREST CANOPIES

This section presents results of short-term measurements of irradiance and PPFD above and beneath tropical rainforest canopies. Field sampling and data analysis techniques have already been described in Section 6.4.2.

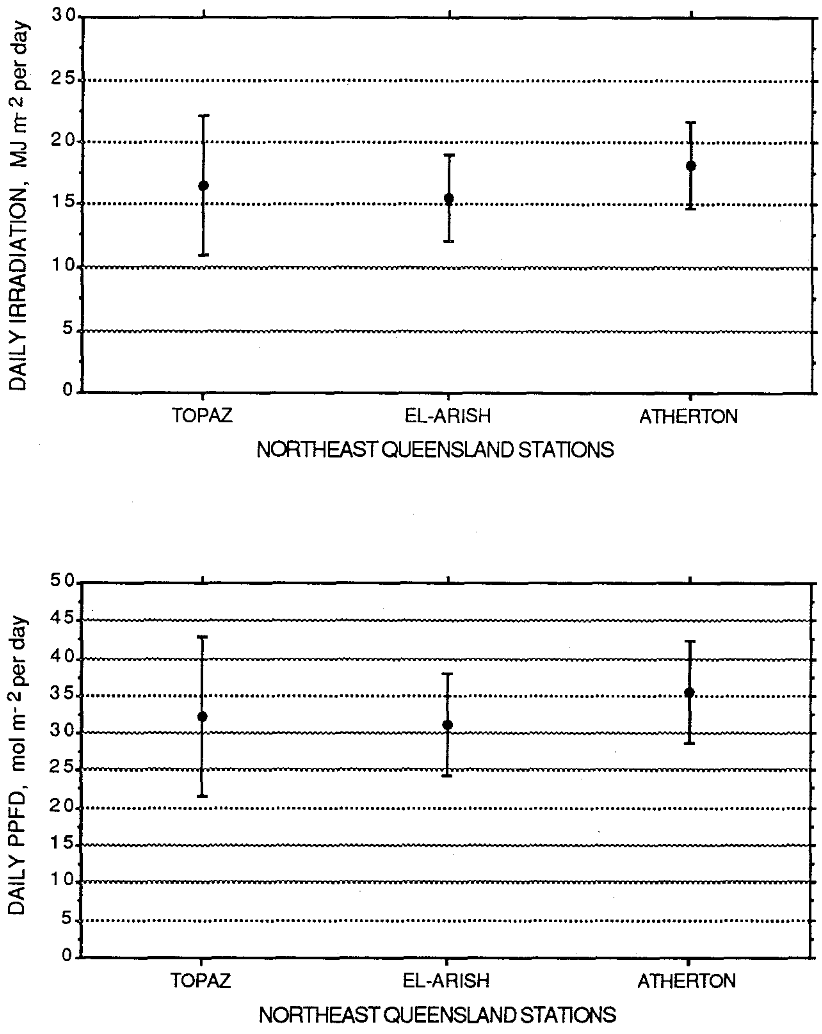

Figure 7.1. Annual mean irradiation (MJ m^{-2} per day) and photosynthetic photon flux density (PPFD) (mol m^{-2} per day) at Topaz, El-Arish and Atherton, northeast Queensland. The error bars represent the standard deviations.

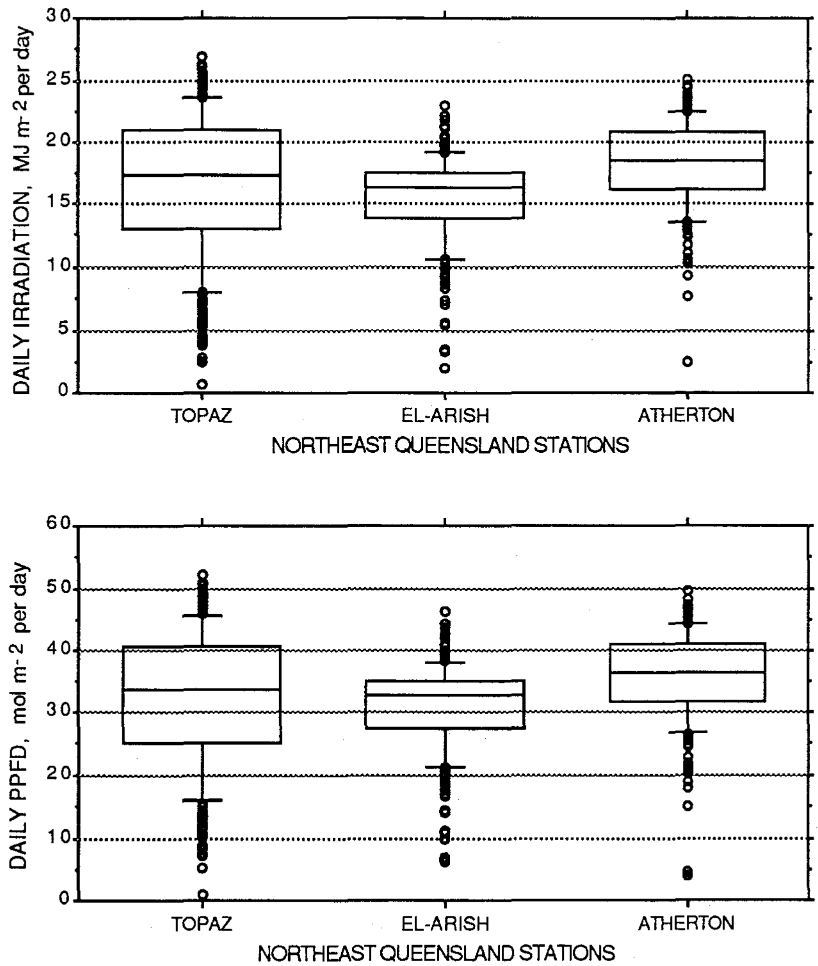

Figure 7.2. Distribution of percentiles for daily irradiation (MJ m^{-2} per day) and photosynthetic photon flux density (PPFD) (mol m^{-2} per day) over the year at Topaz, El-Arish and Atherton, northeast Queensland. The five horizontal lines on the box plot show the 10, 25, 50, 75 and 90th percentiles, with values above and below the 10th and 90th percentile represented as data points.

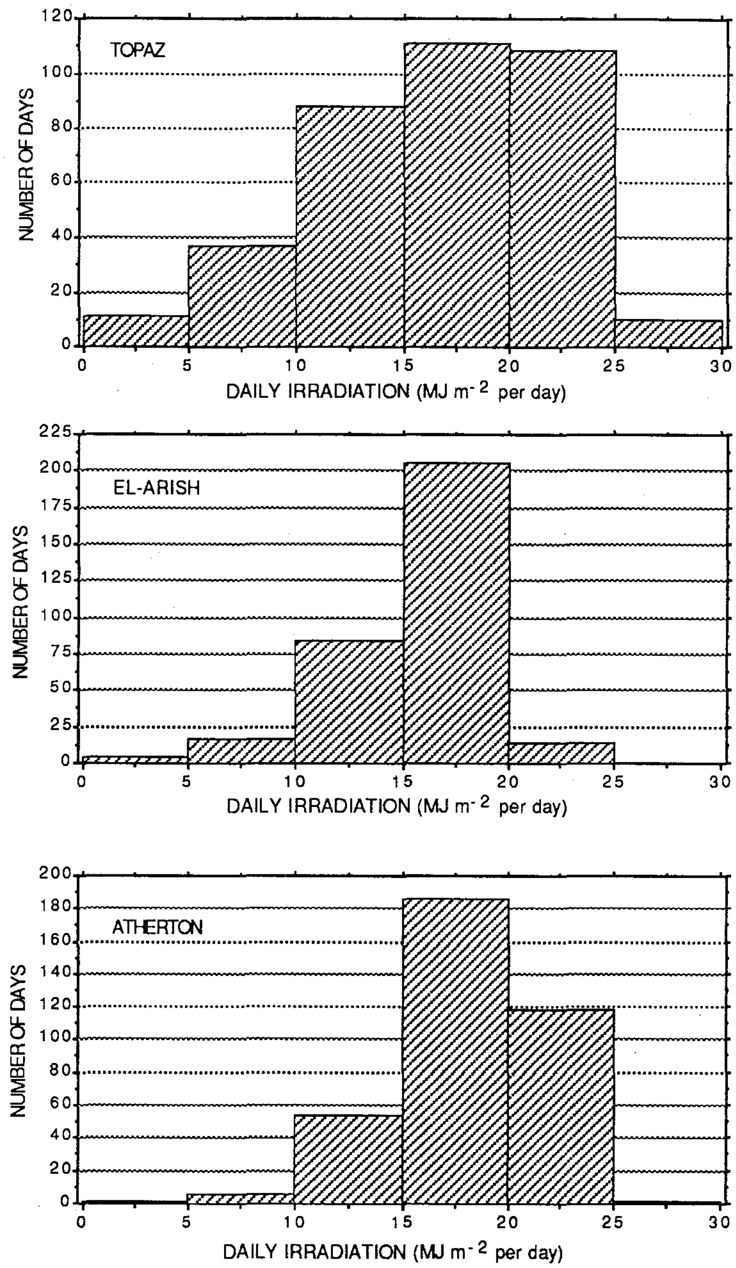

Figure 7.3. Frequency distributions of daily irradiation (MJ m^{-2} per day) over the year at Topaz, El-Arish and Atherton, northeast Queensland.

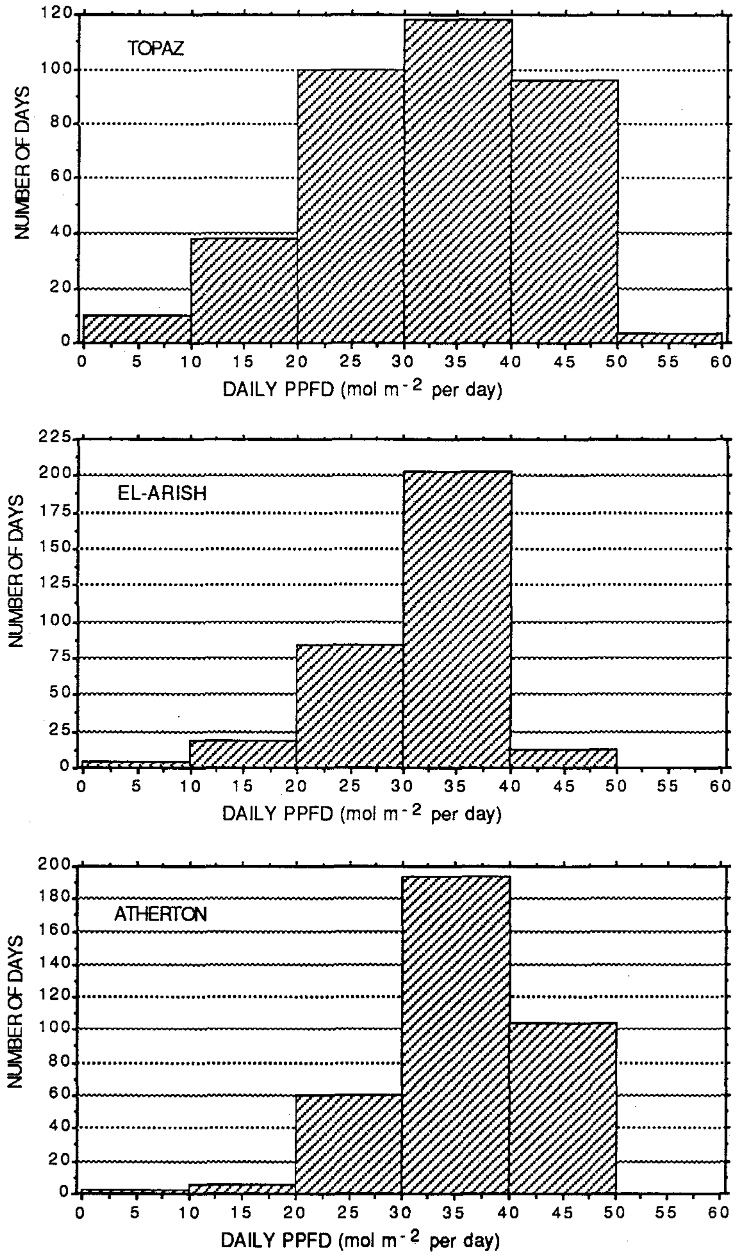

Figure 7.4. Frequency distributions of daily photosynthetic photon flux density (PPFD) (mol m^{-2} per day) over the year at Topaz, El-Arish and Atherton, northeast Queensland.

It is now widely accepted that sunflecks play a key role in the ecophysiology and dynamics of understorey vegetation (Chazdon, 1988). At the temporal scale, sunflecks lasting from a few seconds to several minutes, may affect photosynthesis rates, stomatal responses, leaf temperature, seed germination, and morphogenesis (Fig. 2.6). Furthermore, changes in light availability at the spatial scale (Fig. 2.7) will also influence these ecophysiological processes. Thus, temporal and spatial distributions of light are both required to fully characterise the complex understorey light environment in rainforests. However, the majority of rainforest canopy trees depend on treefall gaps to reach maturity (Hartshorn 1980, Brokaw 1985). It is essential, therefore, that temporal and spatial distributions of light in treefall gaps be analysed as well as those in the shaded understorey.

To account for variations in irradiance and PPFD over time and space, the field data will be analysed in two ways: (1) variations *among* characteristic micro-environments, such as canopy, gap and understorey; and (2) variations *within* these micro-environments themselves.

7.2.1 Variations Among Characteristic Micro-Environments

As discussed in Section 6.4.2.2, field measurements were made with radiometric and photometric sensors at different times of the year to account for changes in sun-earth geometry. Sampling techniques applied to these sensors were standardised for all measurements (ie 10-sec scans averaged every 10-min), with two detailed experiments examining 10-sec instantaneous readings of PPFD within various micro-environments. For purposes of discussion these will be evaluated separately.

7.2.1.1 10-sec Instantaneous Readings of PPFD

(a) Variations Over a Full Day (0700-1700-h)

The frequency distribution of PPFD within the Curtain Fig forest (Fig. 5.4) over a sunny summer's day (January 14, 1987) is shown in Fig. 7.5. The instantaneous 10-sec readings have been analysed for canopy, gap and understorey micro-environments using the linear and logarithmic classifications shown in Table 6.17. The linear classification is useful for evaluating order-of-magnitude differences among these micro-environments. However, because of the non-linear photosynthetic response to light, the logarithmic

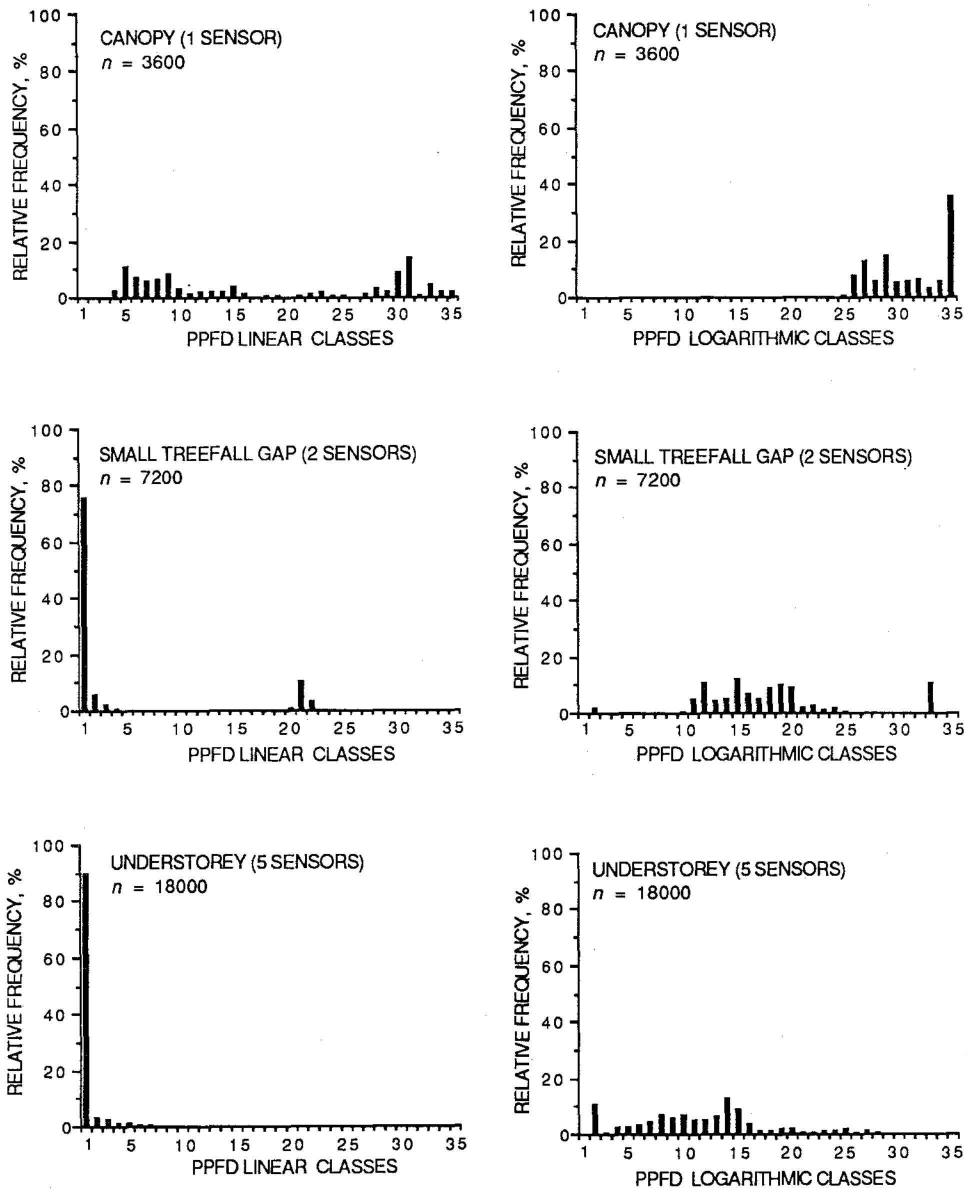

Figure 7.5. Frequency distributions of 10-sec instantaneous readings for photosynthetic photon flux density (PPFD) above the canopy, within a small treefall gap and the understorey of the Curtain Fig forest over a full sunny day (0700-1700-h), January 14, 1987. The data have been sorted using the 35 linear and logarithmic classes shown in Table 6.17.

classification is also very useful because it emphasises the lower (sensitive) end of the PPFD scale (Table 6.17).

The linear classification of PPFD for each micro-environment over a full day (Fig. 7.5) indicates significant differences among the three micro-environments (Kolmogorov-Smirnov, *D*-test: values ranged from 0.16-0.96, $P < 0.01$). The distribution of PPFD above the forest, which may be considered as similar to that experienced by canopy emergents, is relatively uniform over the day. On the other hand, the small treefall gap and understorey have frequency distributions which are noticeably skewed in a positive direction, with about 75% of PPFDs in the gap and 90% of PPFDs in the understorey occurring in class 1 (ie intensities less than 72 μ mol m^{-2} s^{-1}). However, the small treefall gap experiences a secondary peak with intensities between 1440 and 1656 μ mol m^{-2} s^{-1}, associated with the midday sun penetrating through the small canopy gap and reaching the forest floor. Although this secondary peak represents only 10% of PPFD recordings reaching the gap centre over the day, in absolute terms it accounts for over 80% of the daily total PPFD within the gap.

When the same data are sorted into logarithmic classes (Table 6.17), differences among the three micro-environments (Fig. 7.5) are even more significant (*D*-test: values ranged from 0.44-0.96, $P<0.01$). The logarithmic classification has the effect of skewing the frequency distribution of PPFD above the forest in a negative direction with all PPFDs occurring above class 25 (ie between 199.5-2511.9 μ mol m^{-2} s^{-1}). However, the logarithmic classification also has the effect of normalising the positively-skewed gap and understorey frequency distributions. If photosynthetic rates of plants growing in gap and understorey environments are of interest, then the logarithmic classification provides a more detailed evaluation of frequency distributions of PPFD in such habitats, compared with the linear classification (Fig. 7.5). In the small treefall gap, most PPFDs were between classes 10 and 25 (ie 6.3-251.1 μ mol m^{-2} s^{-1}) with the midday secondary peak referred to earlier occurring in class 33 (ie 1259.0-1584.9 μ mol m^{-2} s^{-1}). Moreover, the logarithmic classification is particularly useful for evaluating the frequency distribution of PPFD in the understorey (Fig. 7.5). For example, it is possible to differentiate between shade light (diffuse PPFD) and sunflecks (direct PPFD); if class 18 is used as the minimum level for direct PPFD (ie intensities greater than 50 μ mol m^{-2} s^{-1}), then in absolute terms sunflecks represent 70% of the daily total PPFD in the understorey.

(b) <u>Variations Over the Middle of a Day (1030-1330-h)</u>

The frequency distribution of PPFD within the Curtain Fig forest (Fig. 5.4) over the middle of a sunny summer's day (January 18, 1987) is shown in Fig. 7.6. In the same way

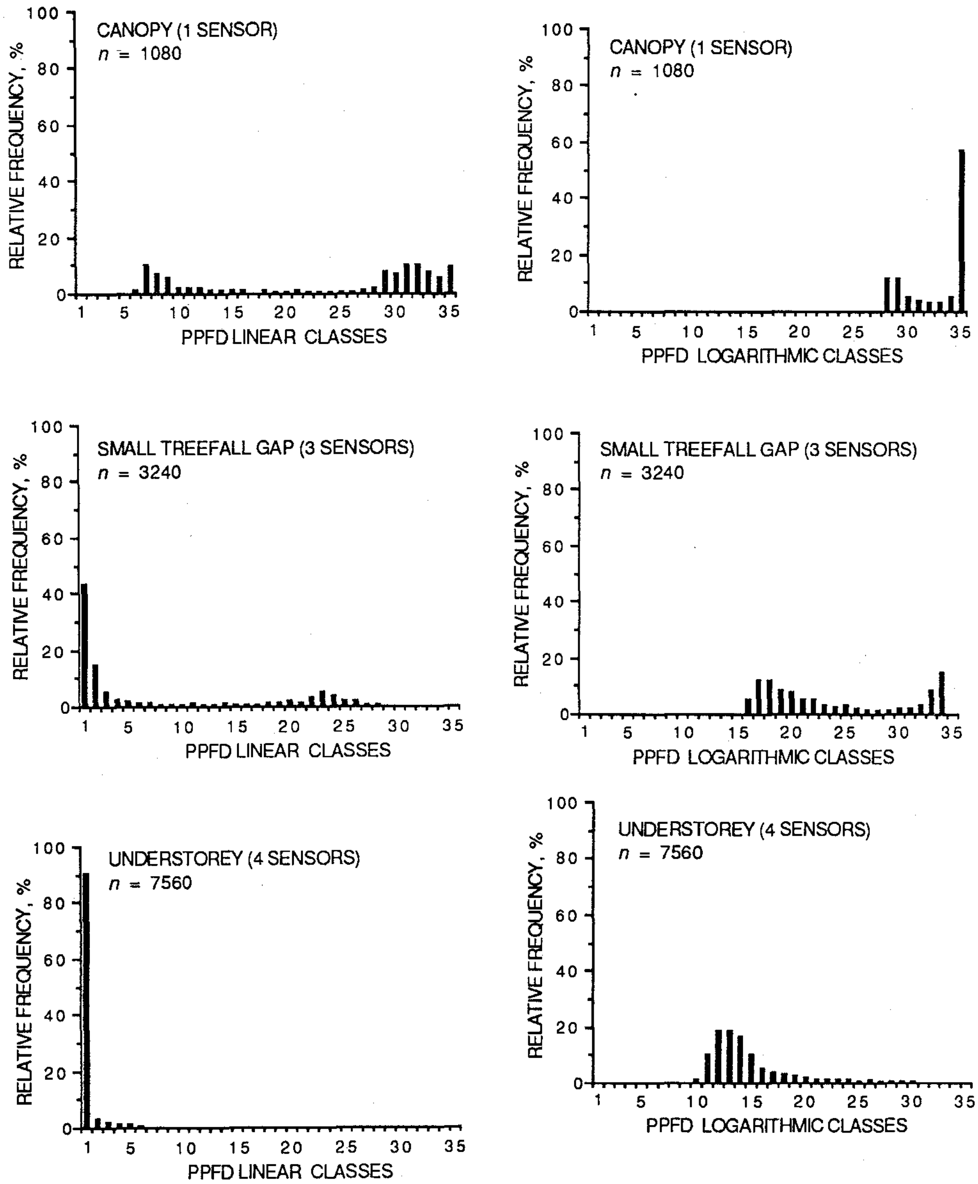

Figure 7.6. Frequency distributions of 10-sec instantaneous readings for photosynthetic photon flux density (PPFD) above the canopy, within a small treefall gap and the understorey of the Curtain Fig forest over the middle of a sunny day (1030-1330-h), January 18, 1987. The data have been sorted using the 35 linear and logarithmic classes shown in Table 6.17.

as the results explained above, instantaneous 10-sec readings have been analysed for canopy, gap and understorey micro-environments using the linear and logarithmic classifications shown in Table 6.17.

The linear classification of PPFD for each micro-environment between 1030-1330-h (Fig. 7.6) indicates significant differences among the three micro-environments (*D*-test: values ranged from 0.47-0.98, $P<0.01$). The distribution of PPFD above the forest is uniform over the middle of the day, with most PPFDs above class 29 (ie intensities greater than 2015.9 μ mol m^{-2} s^{-1}), corresponding with the high midday solar angles. The distribution of PPFDs in the small treefall gap (Fig. 7.6, linear classes) are positively skewed, but not to the same extent as those over a full day (Fig. 7.5, linear classes). Hence, the full-day and midday frequency distributions are significantly different for the gap ($D=0.33$, $P<0.01$). However, the understorey full-day distribution (Fig. 7.5, linear classes) is not significantly different ($D=0.016$, $P>0.05$) to that over the middle of the day (Fig. 7.6, linear classes).

When the same data ares sorted into logarithmic classes (Table 6.17), differences among micro-environments (Fig. 7.6) are very significant (*D*-test: values ranged from 0.68-0.98, $P<0.01$). The logarithmic classification also highlights important differences between full-day frequency distributions (Fig. 7.5) and midday frequency distributions (Fig. 7.6). For example, there are no PPFDs below class 16 (ie intensities less than 25.1 μ mol m^{-2} s^{-1}) in the small gap over the middle of the day (Fig. 7.6, logarithmic classes), yet over the full day about 40% of PPFDs occur below this class (Fig. 7.5, logarithmic classes). Hence, the full-day and midday frequency distributions are significantly different for the gap ($D=0.433$, $P<0.01$).

Furthermore, while the linear classifications of PPFD in the understorey over the full day (Fig. 7.5) and over the middle of the day (Fig. 7.6) are not significantly different, the frequency distributions for logarithmic classes are significantly different from each other ($D=0.43$, $P<0.01$). This demonstrates the utility of the logarithmic classification of light within forest understoreys. For example, over the middle of the day in the understorey (Fig. 7.6, logarithmic classes), there are no PPFDs below class 10 (ie intensities less than 6.3 μ mol m^{-2} s^{-1}), yet over the full day about 37% of PPFDs occur below this class (Fig. 7.5, logarithmic classes).

(c) Variations at Different Times of the Day

The frequency distributions of PPFD within the Curtain Fig forest (Fig. 5.4) at three times of the day for linear and logarithmic classes are shown in Figs. 7.7, 7.8 and 7.9 for canopy, small gap and understorey micro-environments, respectively. The temporal distribution of PPFD for the three given times of the day at each micro-environment is

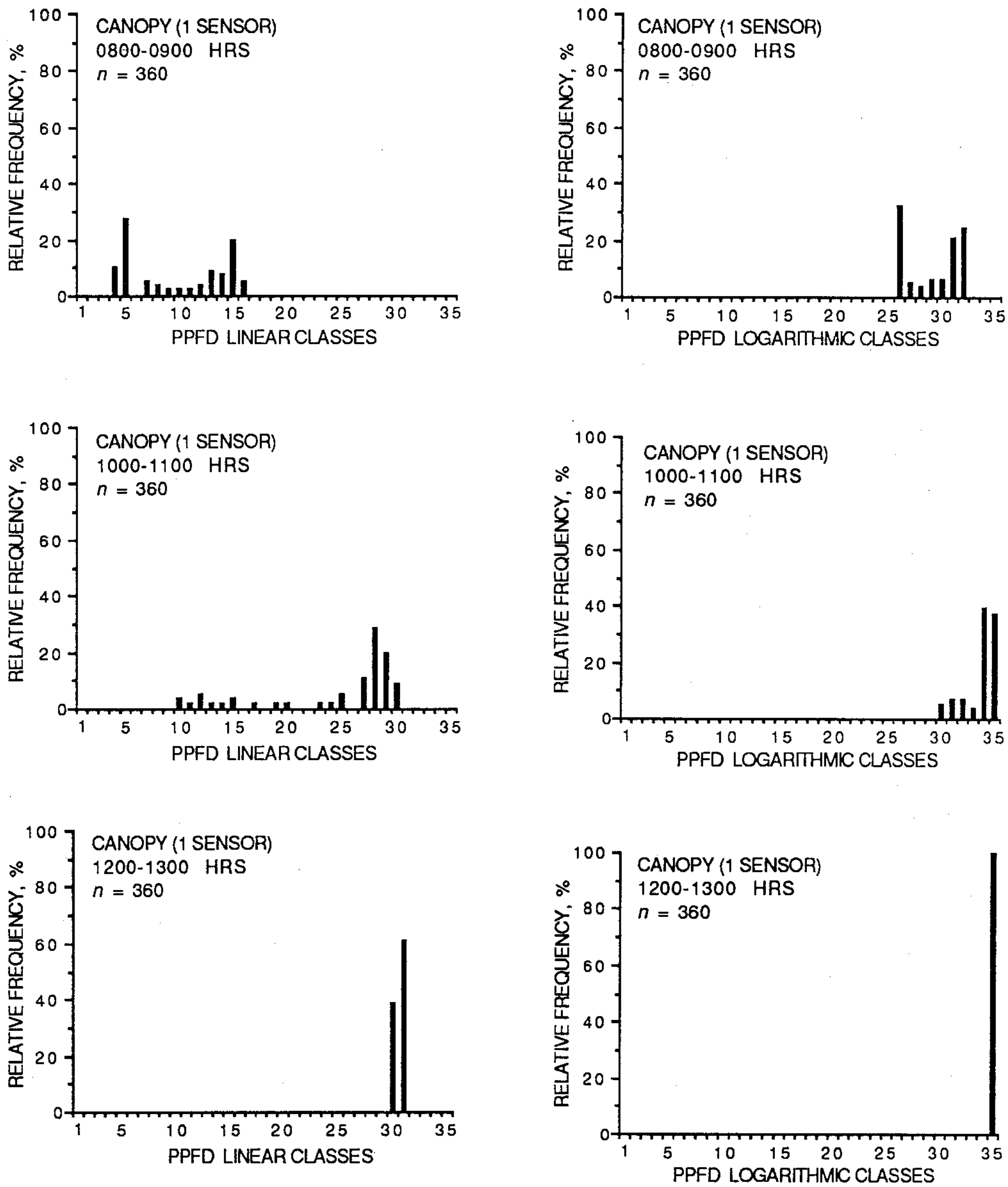

Figure 7.7. Frequency distributions of 10-sec instantaneous readings for photosynthetic photon flux density (PPFD) above the Curtain Fig forest at three times of the day under sunny conditions, January 14, 1987. The data have been sorted using the 35 linear and logarithmic classes shown in Table 6.17.

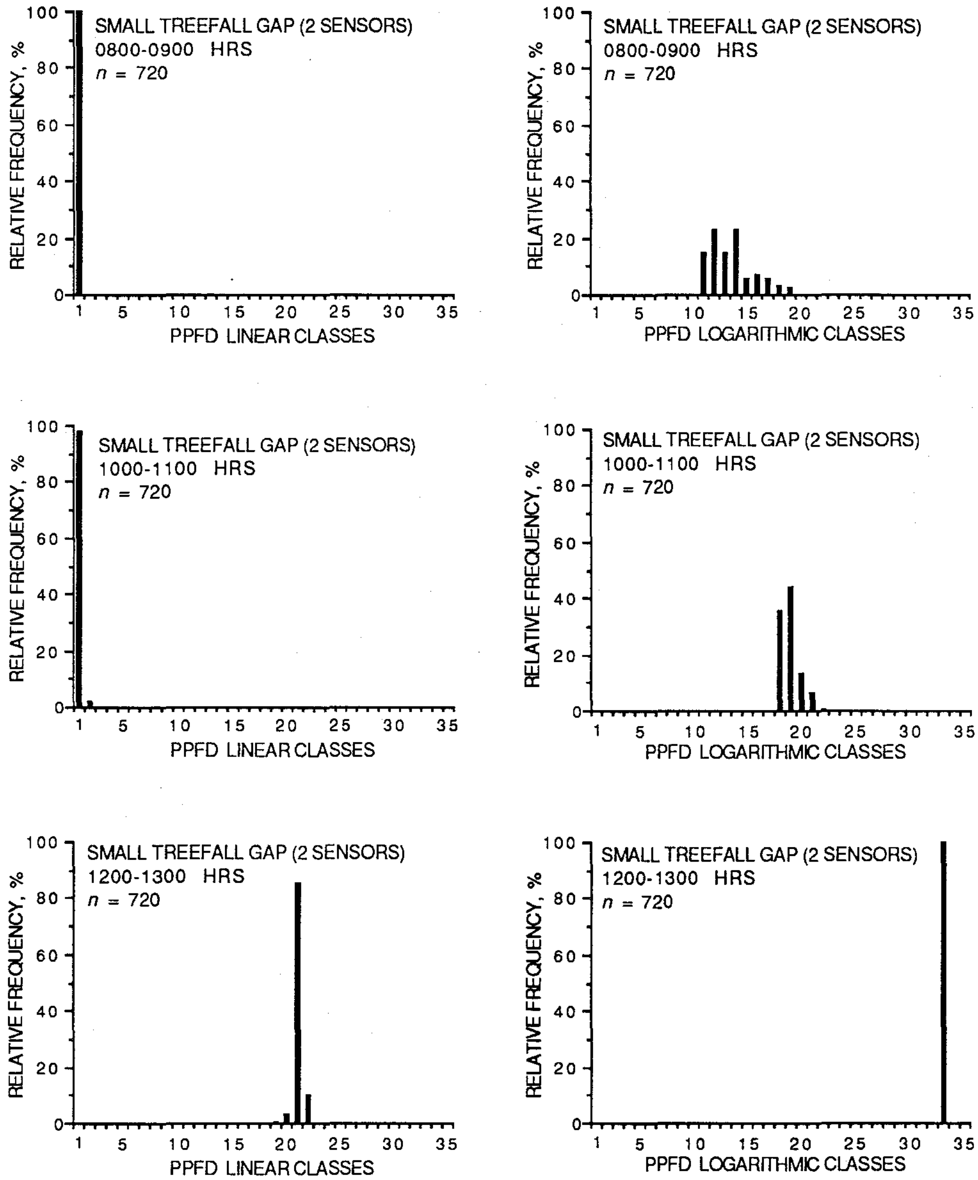

Figure 7.8. Frequency distributions of 10-sec instantaneous readings for photosynthetic photon flux density (PPFD) at the centre of a small treefall gap in the Curtain Fig forest at three times of the day under sunny conditions, January 14, 1987. The data have been sorted using the 35 linear and logarithmic classes shown in Table 6.17.

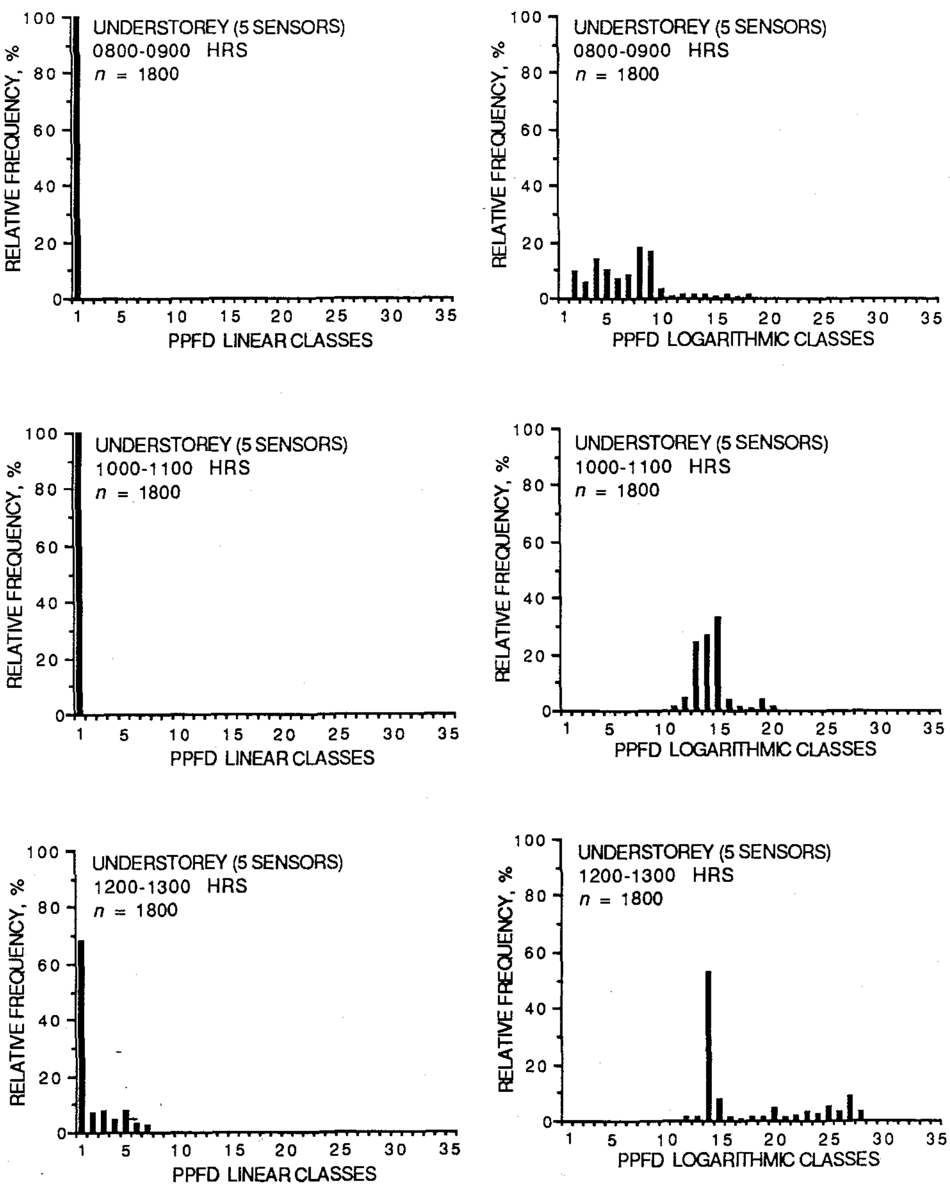

Figure 7.9. Frequency distributions of 10-sec instantaneous readings for photosynthetic photon flux density (PPFD) within the understorey of the Curtain Fig forest at three times of the day under sunny conditions, January 14, 1987. The data have been sorted using the 35 linear and logarithmic classes shown in Table 6.17.

essentially a function of solar altitude and forest architecture. The linear frequency distributions above the canopy at the three times (Fig. 7.7) are significantly different from each other (D values ranged from 0.49-1.00, $P<0.01$). For the gap (Fig. 7.8, linear classes) and understorey (Fig. 7.8, linear classes) only the 1200-h distribution is significantly different from the other times (D values ranged from 0.32-1.00, $P<0.01$). The most dramatic change occurs between 1100-1200-h in the gap (Fig. 7.8), whereby the modal linear class shifts from 1 (ie less than 72 μ mol m^{-2} s^{-1}) to 21 (between 1440.0-1511 μ mol m^{-2} s^{-1}), representing a 20-fold increase. However, the change in the understorey (Fig. 7.9) is less dramatic with the modal linear class being 1 for the three given times of day.

The results of the logarithmic classification of PPFD at each micro-environment (Figs. 7.7, 7.8 and 7.9) show significant differences among the three times (D values ranged from 0.29-1.00, $P<0.01$). The modal logarithmic class above the forest (Fig. 7.7) changes from 26 (ie 251.2-316.1 μ mol m^{-2} s^{-1}) at 0800-0900-h to class 35 (ie 1995.4-2511.9 μ mol m^{-2} s^{-1}) at 1200-1300-h. In the gap (Fig. 7.8), the modal logarithmic class changes from 12 (ie 10.0-12.5 μ mol m^{-2} s^{-1}) at 0800-0900-h to class 33 (ie 1259.0-1584.0 μ mol m^{-2} s^{-1}) at 1200-1300-h. In the understorey (Fig. 7.9), the modal logarithmic class changes from 8 (ie 4.0-4.9 μ mol m^{-2} s^{-1}) at 0800-0800-h to class 14 (ie 20.0-25.0 μ mol m^{-2} s^{-1}) at 1200-1300-h.

Comparisons of the linear frequency distributions at three times of the day among micro-environments illustrates important temporal differences. As expected, the canopy micro-environment is significantly different (D values ranged from 0.98-1.00, $P<0.01$) to each of the other micro-environments at the three given times (Figs. 7.7, 7.8 and 7.9, linear classes).

Similarly, at 1200-1300-h the small gap and understorey micro-environments (Figs. 7.8 and 7.9, linear classes) are significantly different (D=1.00, $P<0.01$) ; this is because over 80% of PPFDs in the gap occur in class 21 (ie between 1440.0-1511 μ mol m^{-2} s^{-1}) and about 65% of PPFDs in the understorey occur in class 1 (ie between 0.0-71.9 μ mol m^{-2} s^{-1}). However, at 0800-0900-h and 1000-1100-h the gap and understorey micro-environments are not significantly different from each other (D values ranged from 0.00-0.02, $P>0.05$); this is because mostly diffuse PPFDs (ie intensities less than 72.9 μ mol m^{-2} s^{-1}) are reaching the forest floor at these times (Figs. 7.8 and 7.9, linear classes). On the other hand, when the same data is sorted into logarithmic classes (Figs. 7.7, 7.8 and 7.9), differences among micro-environments are all significant at the three given times (D values ranged from 0.91-1.00, $P<0.01$). This result also emphasises the sensitivity of the logarithmic classification scheme compared with the linear scheme.

7.2.1.2 10-min Average Readings of Irradiance and PPFD

(a) Curtain Fig Forest (January and July)

Table 7.4 summarises results of various descriptive statistics applied to 10-min average readings of irradiance and PPFD at canopy, gap and understorey micro-environments within the Curtain Fig forest (Fig. 5.4) at two contrasting times of the year. Because solar altitude (α) at solar noon was about 87° over the 6-day measurement period in January and only 54° during the 4-day measurement period in July, one would expect significant differences in mean irradiance and PPFD between these times.

The results in Table 7.4 support this claim; daily average irradiance and PPFD above the canopy in January were found to be significantly different from mean fluxes above the canopy in July (Student's t-test: respective values were 6.45, $P<0.01$; and 3.74, $P<0.01$). This result emphasises the fact that the wet tropics study area is located in the 'peripheral tropics' and hence the forest experiences a significant seasonal variation in solar input between January (summer) and July (winter).

Similarly, daily average irradiance and PPFD within small treefall gaps in January were found to be significantly different from mean fluxes within small gaps in July (for irradiance, t=9.79, $P<0.01$; and for PPFD, t=12.63, $P<0.01$). Moreover, mean irradiance levels in the small gap are 4.5-times higher in January than in July, and mean PPFD levels are about 5-times higher in January than in July.

On the other hand, the results for the understorey (Table 7.4) show that only daily average PPFD is significantly different between January and July (t=3.97, $P<0.01$), while daily average irradiance does not differ significantly between these times (t=0.202, $P>0.05$). Hence, mean irradiance levels in the understorey are almost identical at both times, and mean PPFD levels are only about 1.5-times higher in January than in July. This difference is probably due to the fact that irradiance was measured with linear pyranometers, which have an in-built averaging feature, and PPFD was measured with instruments which were capable of measuring individual sunflecks with little or no averaging over space (refer to Section 6.1).

Both irradiance and PPFD differed significantly among micro-environments in January and July (multiple *a priori* t-test values ranged from 7.60-51.59, $P<0.01$ for irradiance and from 11.62-79.5, $P<0.01$ for PPFD). Both the small gap and understorey experienced a wide-range of radiant flux and photosynthetic photon flux densities over the 6-day measurement period in January (Table 7.4). The highest PPFD in the gap (2045.4 μ mol m^{-2} s^{-1}) represents about 80% of the maximum PPFD above the forest canopy. However, the maximum PPFD in the understorey (442.6 μ mol m^{-2} s^{-1}), associated with a sunfleck, represents only 17.2% of the maximum PPFD above the

Month Micro-environment (No. of days)	Irradiance (W m^{-2}) Average flux (mean±1 SD) (range) Coefficient of variation	Daily total (MJ m^{-2} per day)	PPFD (μ mol m^{-2} s^{-1}) Average flux (mean±1 SD) (range) Coefficient of variation	Daily total (mol m^{-2} per day)	Mean Ratio (irradiance:PPFD)
January CANOPY (6-days)	617.0±323.4 (3.3-1308.6) 52.6% *n*=389	28.65	1221.0±626.3 (25.2-2567.2) 51.3% *n*=389	56.70	1:1.98
January SMALL GAP (6-days)	114.7±216.4 (0.0-1060.1) 188.6% *n*=925	5.33 (18.6)*	173.5±366.9 (0.0-2045.4) 211.5% *n*=2092	8.06 (14.2)*	1:1.51
January UNDERSTOREY (6-days)	17.5±16.9 (0.0-104.7) 96.9% *n*=510	0.812 (2.8%)*	17.7±30.5 (0.0-442.6) 172.1% *n*=1020	0.823 (1.5%)*	1:1.01
July CANOPY (4-days)	439.4±188.3 (24.4-894.7) 42.9% *n*=157	17.39	981.5±377.3 (209.6-1779.2) 38.4% *n*=105	38.87	1:2.24
July SMALL GAP (4-days)	25.7±16.1 (2.0-118.4) 62.7% *n*=569	1.02 (5.9%)*	35.2±42.6 (0.0-727.8) 121.1% *n*=1132	1.39 (3.6%)*	1:1.36
July UNDERSTOREY (4-days)	17.7±8.5 (0.0-51.0) 48.2% *n*=263	0.70 (4.0%)*	12.0±10.8 (0.0-129.0) 90.1% *n*=467	0.474 (1.2%)*	1:0.68

* Refers to the percentage of the daily total within the micro-environment relative to that above the forest canopy.

Table 7.4. Values of daily average irradiance (W m^{-2}), total daily irradiation (MJ m^{-2} per day), daily average photosynthetic photon flux density (PPFD) (μ mol m^{-2} s^{-1}), total daily PPFD (mol m^{-2} per day) and the mean ratio of irradiance to PPFD within three micro-environments in the Curtain Fig forest, northeast Queensland (January and July, 1987).

canopy. In July, these relative values decrease somewhat; the highest PPFDs for the gap (727.8 μ mol m^{-2} s^{-1}) and understorey (129.0 μ mol m^{-2} s^{-1}), relative to maximum PPFD above the forest, are only 40.9% and 7.3%, respectively.

Enormous differences in the light regimes of the three micro-environments are also illustrated by comparing the the daily totals for irradiation and PPFD (Table 7.4). Daily total irradiation above the forest in January was, on average, 5.4-times greater than irradiation in the small gap and 35-times greater than in the understorey. In January, total daily PPFD above the forest was 7-times greater than in the small gap and almost 70-times greater than in the understorey. In comparison, total daily irradiation above the forest in July was 17-times greater than irradiation in the small gap and 25-times greater than in the understorey, and total daily PPFD above the forest was 28-times greater than in the small gap and 82-times greater than in the understorey.

Percentages of daily irradiation and PPFD, relative to levels above the canopy, ranged from 1.2% for PPFD within the understorey in July to 18.6% for irradiation within the small gap in January (Table 7.4). The transmission of daily PPFD within gaps and understoreys at both times of the year is lower than that for irradiance because photosynthetically active wavelengths (400-700 nm) are selectively absorbed by leaves in the canopy (Fig. 2.10). This effect is demonstrated by comparing the ratio of mean daily irradiance to PPFD among micro-environments (Table 7.4). While there are some differences between the two times of year for the three micro-environments, it can be seen that the ratio of irradiance to PPFD decreases with increasing overstorey density.

Important differences among the three micro-environments are further illustrated in Figs 7.10 and 7.11 which show, respectively, the distribution of percentile values for irradiance and PPFD in January and July. As shown in Fig. 7.10, median radiant flux densities above the forest, within the small gap, and within the shaded understorey in January were 591.4, 40.1, and 14.4 W m^{-2}, respectively. The corresponding median radiant flux densities within these micro-environments in July were 424.6, 23.7, and 18.0 W m^{-2}, respectively. By comparison, median PPFDs above the forest, within the gap, and understorey in January (Fig. 7.11) were 1186.0, 39.0 and 11.8 μ mol m^{-2} s^{-1}, with corresponding median PPFDs for July being 964.4, 27.2, and 10.5 μ mol m^{-2} s^{-1}, respectively.

The box plots (Figs. 7.10 and 7.11) are useful for visually differentiating between direct and diffuse radiant flux densities and PPFDs within gap and understorey micro-environments, but some care should be taken with irradiance measurements because they were obtained with a linear pyranometer which has an in-built averaging feature. However, as a first-order approximation, direct fluxes (sunflecks) in the

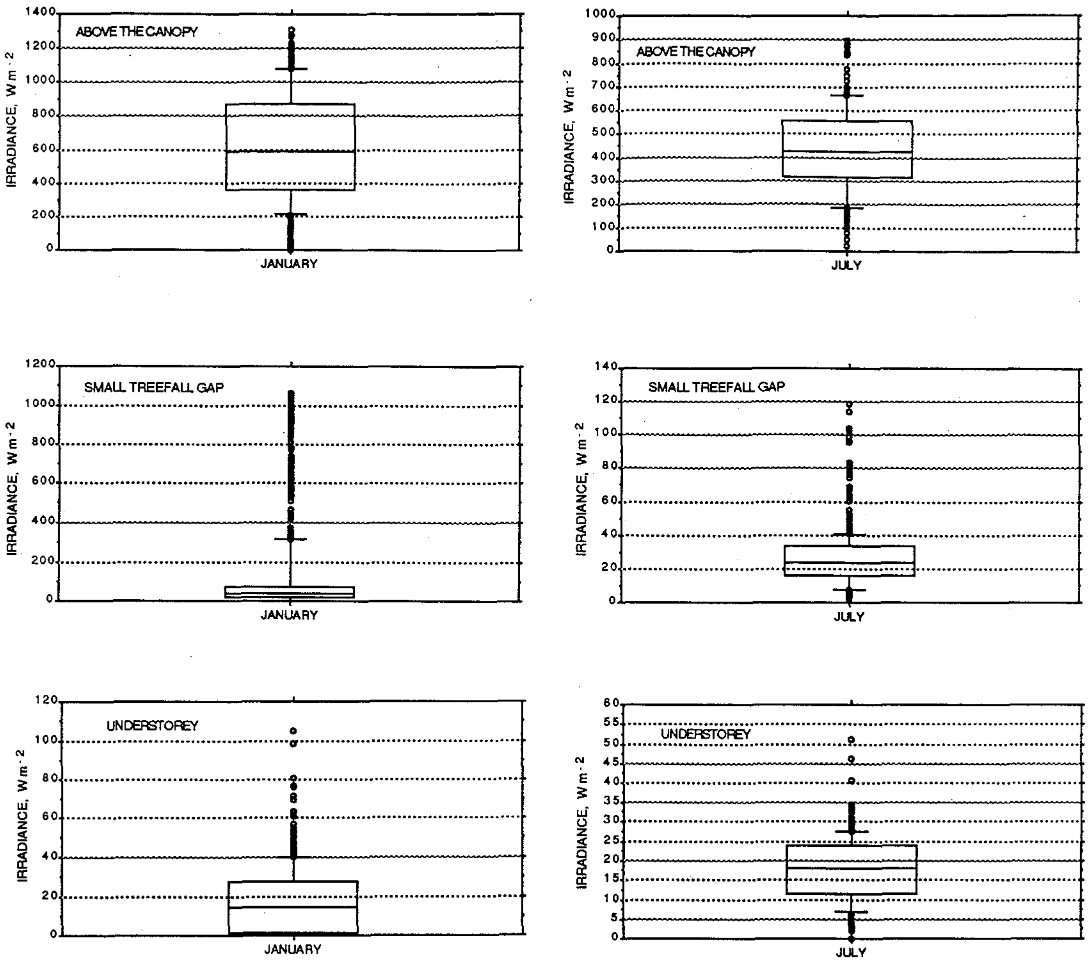

Figure 7.10. Distributions of percentiles (10-min average readings) for irradiance (W m^{-2}) above the canopy, within a small treefall gap and the understorey of the Curtain Fig forest at two contrasting times of the year (January and July). The five horizontal lines on the box plot show the 10, 25, 50, 75 and 90th percentiles, with values above and below the 10th and 90th percentile represented as data points. Note differences in vertical scales.

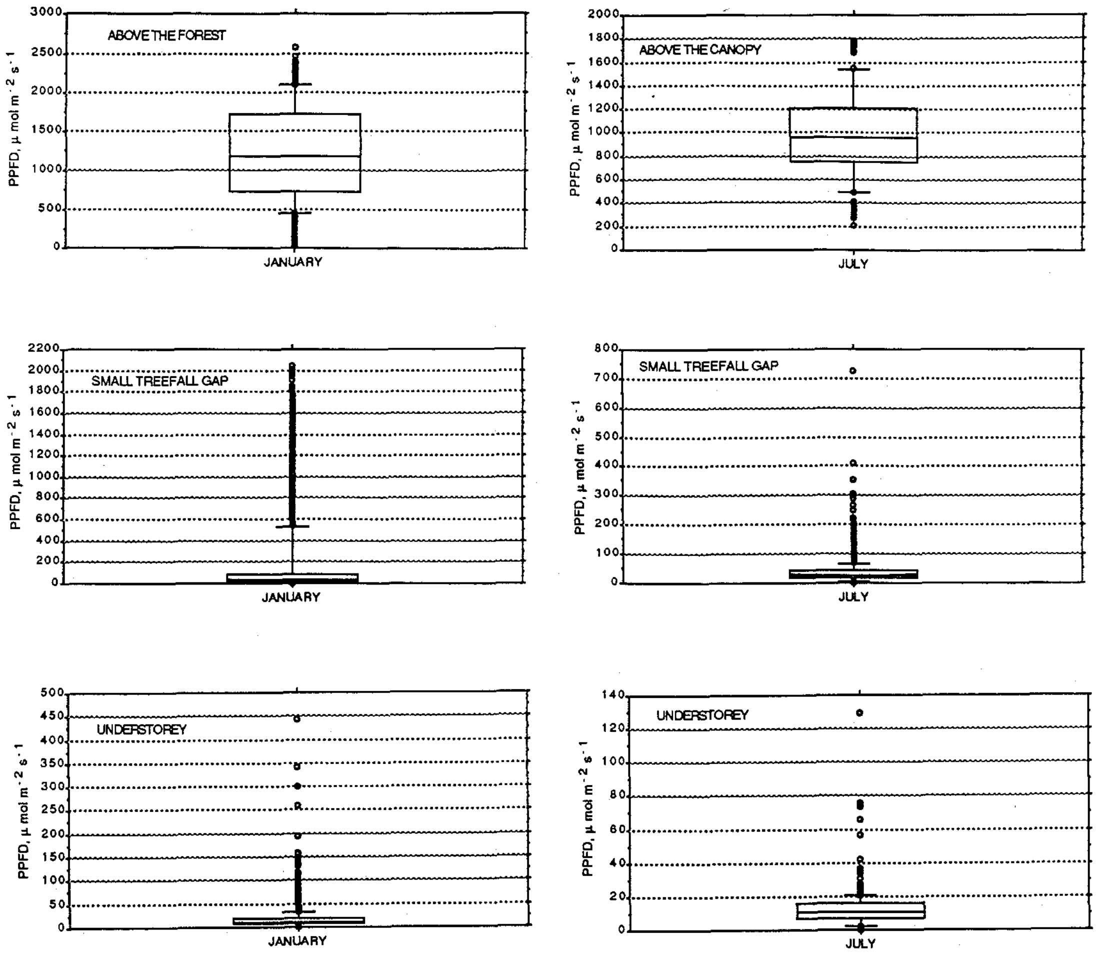

Figure 7.11. Distributions of percentiles (10-min average readings) for photosynthetic photon flux density (PPFD) (μ mol m^{-2} s^{-1}) above the canopy, within a small treefall gap and the understorey of the Curtain Fig forest at two contrasting times of the year (January and July). The five horizontal lines on the box plot show the 10, 25, 50, 75 and 90th percentiles, with values above and below the 10th and 90th percentile represented as data points. Note differences in vertical scales.

understorey correspond closely with data points above the 90th percentile horizontal line on the box plot diagrams. Hence, the box represents diffuse fluxes which dominate the understorey micro-environment throughout the year. However, because the gap experiences a prolonged period of direct radiation around the middle of the day in January (Figs. 7.10 and 7.11), the 90th percentile does not correspond with the boundary between direct and diffuse fluxes; the 75th percentile horizontal line is a better indicator of this boundary. On the other hand, the 90th percentile is a better boundary between direct and diffuse fluxes within small gaps in July (Figs. 7.10 and 7.11); this is because at this latitude (17° S.), the gap centre does not experience a prolonged period of direct radiation around the middle of the day in July. Hence, sunflecks are the only source of direct radiation in the small treefall gap during the low-solar period from May-July. Seasonal variations of daily PPFD within treefall gaps of varying sizes and configurations will be discussed in greater detail in Section 7.3.

The frequency distributions of 10-min average readings within canopy, gap and understorey micro-environments for January and July are shown in Fig. 7.12 for irradiance and Fig. 7.13 for PPFD. As stated in Section 6.4.2.2, frequency distributions of 10-min average readings for irradiance and PPFD were sorted into class intervals suited to the range of fluxes measured within particular micro-environments.

The frequency distributions of irradiance (Fig. 7.12) and PPFD (Fig. 7.13) above the forest in January and July have a low degree of positive skewness (ie values less than 0.3), and they are all platykurtic (ie values less than 3.0). The modal classes for irradiance above the forest in January and July (Fig. 7.12) represent 12.9% and 20.4% of the radiant flux densities over the respective measurement periods. Similarly, the modal classes for PPFD above the forest in January and July (Fig. 7.13) represent 14.4% and 21.9% of the PPFDs over the respective measurement periods. Consequently, emerging trees in the rainforest canopy experience a wide-range of radiant flux densities and PPFDs, and the diurnal distribution of these fluxes is unimodal.

In comparison, the frequency distributions of irradiance (Fig. 7.12) and PPFD (Fig. 7.13) within the small treefall gap and understorey in January and July have a moderate to high degree of positive skewness (ie values greater than 0.3), and they are all leptokurtic (ie values greater than 3.0). This means there is a tendency for radiant flux densities and PPFDs to concentrate towards the lower end of their respective intensity scales; this indicates that mostly diffuse (shade) light is reaching plants growing in these micro-environments.

However, there are noteworthy differences in the degree of kurtosis among micro-environments and types of radiation. For example, the degree of kurtosis is very high for PPFD within the small gap and understorey in July (Fig. 7.13), whereby 78.5% of PPFDs in the gap are between 0 and 50 μ mol m^{-2} s^{-1}, and 95.3% of PPFDs in the

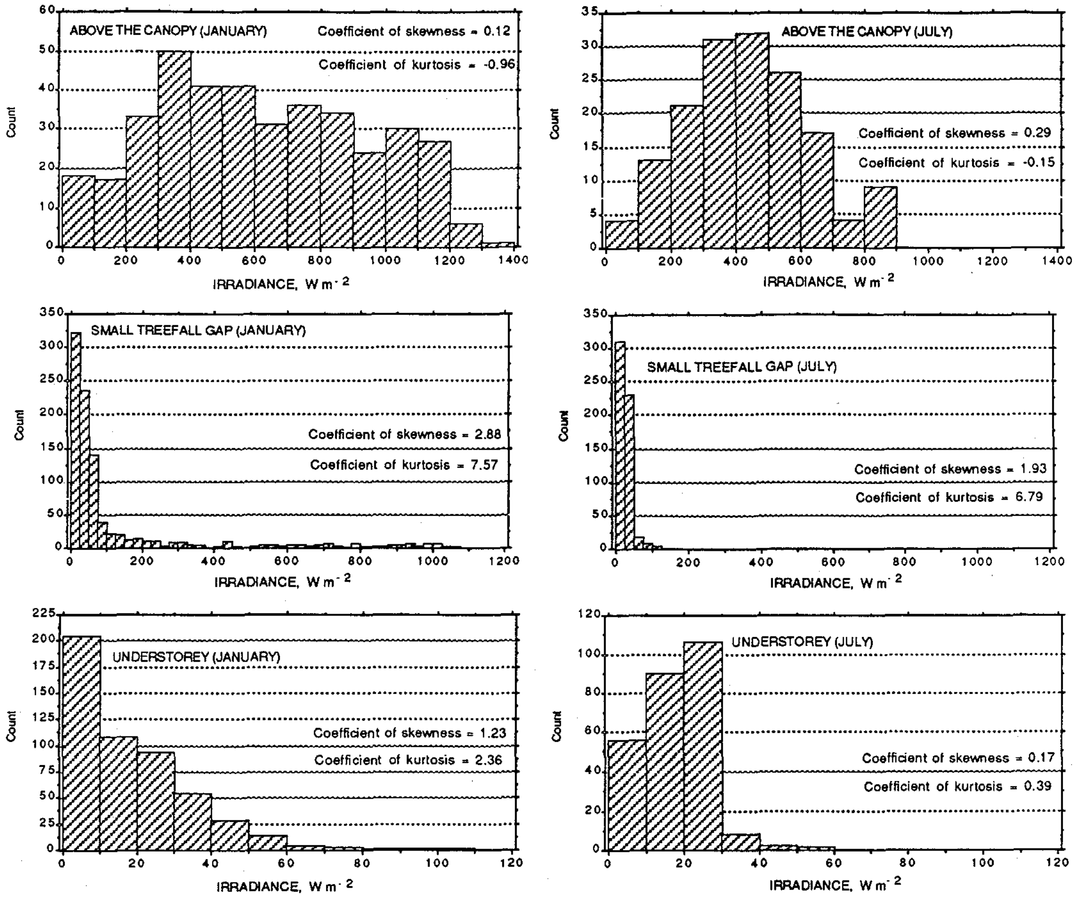

Figure 7.12. Frequency distributions of 10-min average readings for irradiance (W m^{-2}) above the canopy, within a small treefall gap and the understorey of the Curtain Fig forest at two contrasting times of the year (January and July). Note differences in horizontal scales (class intervals).

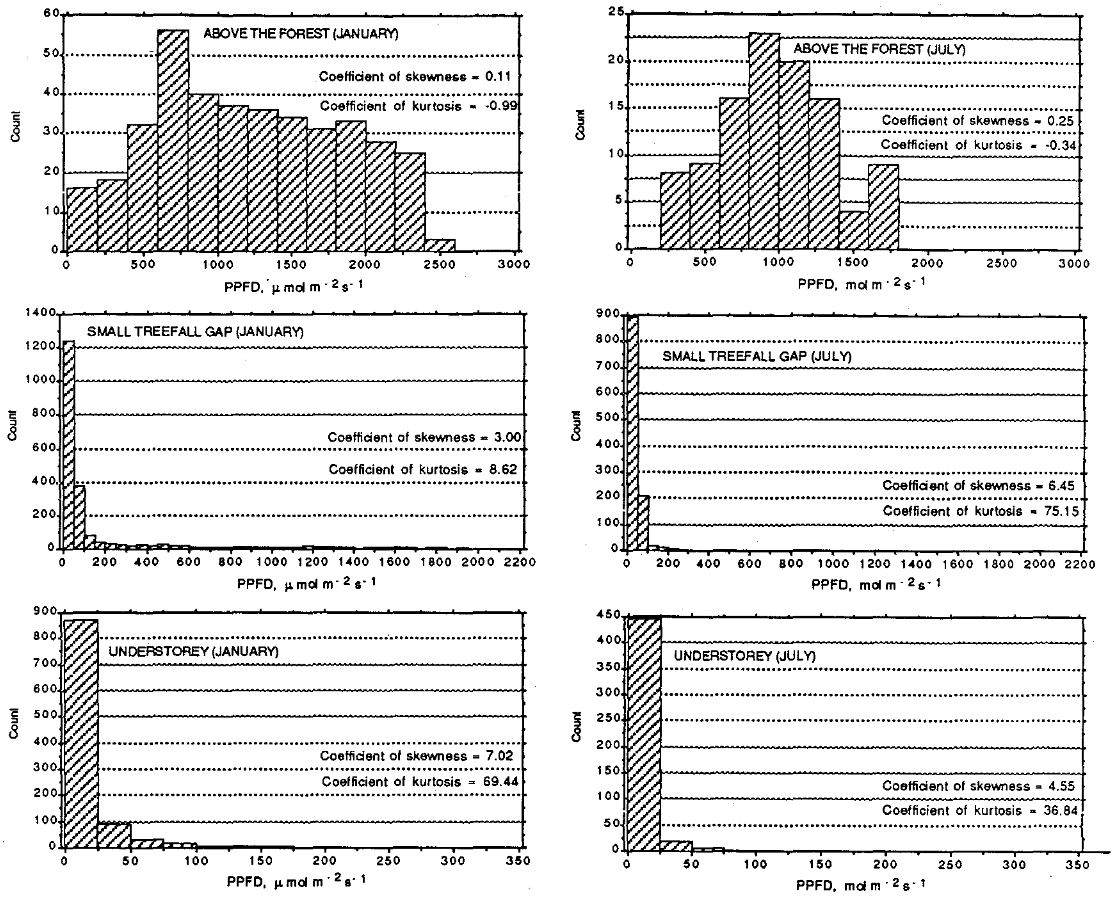

Figure 7.13. Frequency distributions of 10-min average readings for photosynthetic photon flux density (PPFD) (μ mol m^{-2} s^{-1}) above the canopy, within a small treefall gap and the understorey of the Curtain Fig forest at two contrasting times of the year (January and July). Note differences in horizontal scales (class intervals).

understorey are between 0 and 25 μ mol m^{-2} s^{-1}. In comparison, the degree of kurtosis for these micro-environments is not as high in January because there is a greater proportion of high PPFDs (sunflecks) reaching the gap centre and understorey at this time; specifically, 59.4% of PPFDs in the gap are between 0 and 50 μ mol m^{-2} s^{-1}, and 85.2% of PPFDs in the understorey are between 0 and 25 μ mol m^{-2} s^{-1}.

The degree of kurtosis for irradiance in the understorey in July is very low (Fig. 7.12) compared with PPFD at the same time (Fig. 7.13). This apparent discrepancy may be explained by the nature of the instruments used to measure radiant flux densities (irradiance) and PPFDs. As discussed in Section 6.1.1, irradiance was measured within the forest with linear pyranometers which are designed to average radiant fluxes over an area of about 160 cm^2, whereas PPFD was measured with purpose-built sensors (Section 6.1.2.2), designed to measure the intensity of sunflecks (or shade) over an area of about 3.8 cm^2. In other words, the gap and understorey data, shown as frequency histograms in Fig. 7.12, represent 'spatial averages' rather than individual 'spot' measurements.

The results presented in Fig. 7.12 show that 40% of 10-min average irradiance readings within the small gap and 5% within the understorey in January were attributed to irradiance levels greater than 50 W m^{-2}, compared with 6% and 2% in July, respectively. Unfortunately, because the irradiance data is a spatial average, it is not possible to determine accurately the proportion of irradiance contributed by sunflecks within these micro-environments. However, conservative estimates of the proportion of daily total irradiation contributed by sunflecks (taken here as radiant flux densities greater than 50 W m^{-2}) for the two micro-environments are as follows: (1) small treefall gap, January 83%, July 12%; and (2) understorey, January 13%, July 3%.

Similarly, the results presented in Fig. 7.13 show that 41% of 10-min average PPFD readings within the small gap and 6% within the understorey in January were attributed to sunflecks (ie PPFDs greater than 50 μ mol m^{-2} s^{-1}); this compares with 21% and 2% in July, respectively. On the basis of these measurements, the proportions of daily total PPFD contributed by sunflecks within these micro-environments are as follows: (1) small treefall gap, January 85%, July 39%; and (2) understorey, January 21%, July 5%. The understorey value for January (21%) is considerably lower than the estimate of 70% described earlier for the understorey of the same forest at the same time of year (Fig. 7.5). The reason for this difference is that the value given here (Fig. 7.13) is based on 10-min average readings, while the other value (Fig. 7.5) is based on 10-sec instantaneous readings.

(b) Mt Bellenden Ker Forest (June)

Table 7.5 summarises results of various descriptive statistics applied to 10-min average readings of irradiance and PPFD at clearing, lower-canopy, gap and understorey micro-environments within montane tropical rainforest on the summit ridge of Mt Bellenden Ker (Fig. 5.6) over two days (June 23-24, 1987). To test the hypothesis that 'reduction in PPFD by cloudiness decreases productive capacities of montane rainforests compared with lowland rainforests in northeast Queensland', it was necessary to obtain readings at or near the winter solstice (June 21/22), when daily clear-sky potential irradiation is at its lowest for the year. Solar altitude at solar noon (α) was about 50° over the two days, which is similar to that above the Curtain Fig forest in July, when it was 54°. This permits comparisons between the two forest types.

Daily average irradiance within the Mt Bellenden Ker forest ranged from 32.2 W m^{-2} in the understorey to over 400 W m^{-2} in the clearing (Table 7.5); the clearing has similar light conditions experienced by emerging trees in the upper canopy. Similarly, daily average PPFD ranged from 20.5 to over 800 μ mol m^{-2} s^{-1} at corresponding sites, respectively. Both irradiance and PPFD differed significantly among micro-environments in the Mt Bellenden Ker forest (one-way ANOVA: for irradiance F=216.4, P<0.01; and for PPFD F=250.8, P<0.01). Multiple comparisons among sites have shown that all the micro-environments are significantly different from each other (t values ranged from 4.58 to 23.25, P<0.01), except for irradiance in the lower canopy and small gap (t=0.13, P>0.05).

Mean radiant flux densities and PPFDs in the clearing (Table 7.5) compare closely with those above the Curtain Fig forest in July (Table 7.4). However, mean fluxes within the Mt Bellenden Ker forest understorey and gap sites are higher than those in similar micro-environments in the Curtain Fig forest. This can be explained by the fact that the Mt Bellenden Ker forest (Fig. 5.6) is less than half as tall as the Curtain Fig forest (Fig. 5.4) which has a similar structure. Hence, there are fewer leaf layers in the Mt Bellenden Ker forest to intercept the light as it passes through to the forest floor. However, maximum PPFDs within the gap and understorey micro-environments for the Mt Bellenden Ker forest (Table 7.5) are somewhat lower then those found within the Curtain Fig forest at the same time of year (Table 7.4, July). The maximum PPFDs in the small gap (167.0 μ mol m^{-2} s^{-1}) and understorey (60.3 μ mol m^{-2} s^{-1}), represent only 8.8% and 3.2%, respectively, of the maximum PPFD within the clearing (Table 7.5). On the other hand, the highest PPFD in the lower-canopy (436.0 μ mol m^{-2} s^{-1}) represents about 23% of the maximum PPFD in the clearing, which is closer to the maximum PPFDs reported within the small gap in the Curtain Fig forest in July (Table 7.4). It would appear that persistent cloudiness over the measurement

Micro-environment (No. of days)	Irradiance (W m^{-2}) Average flux (mean±1 SD) (range) Coefficient of variation	Daily total (MJ m^{-2} per day)	PPFD (μ mol m^{-2} s^{-1}) Average flux (mean±1 SD) (range) Coefficient of variation	Daily total (mol m^{-2} per day)	Mean Ratio (irradiance:PPFD)
CLEARING (2-days)	407.5±236.4 (17.8-941.4) 58.0% n=94	16.14	805.6±463.5 (60.0-1900.0) 57.5% n=94	31.9	1:1.97
LOWER-CANOPY (2-days)	46.8±35.3 (1.0-281.2) 75.4% n=94	1.85 (11.5%)*	83.5±65.7 (7.3-436.0) 78.7% n=94	3.31 (10.4%)*	1:1.79
SMALL GAP (2-days)	47.4±29.3 (0.0-161.6) 61.7% n=94	1.88 (11.6%)*	48.4±34.2 (7.9-167.0) 70.7% n=94	1.92 (6.0%)*	1:1.02
UNDERSTOREY (2-days)	32.2±18.4 (0.0-83.6) 57.1% n=188	1.27 (7.9%)*	20.5±13.3 (1.0-60.3) 64.8% n=188	0.81 (2.5%)*	1:0.64

* Refers to the percentage of the daily total within the micro-environment relative to that in the clearing.

Table 7.5. Values of daily average irradiance (W m^{-2}), total daily irradiation (MJ m^{-2} per day), daily average photosynthetic photon flux density (PPFD) (μ mol m^{-2} s^{-1}), total daily PPFD (mol m^{-2} per day) and the mean ratio of irradiance to PPFD within four micro-environments in the Mt Bellenden Ker forest, northeast Queensland (June, 1987).

period has reduced the incidence of sunflecks within the Mt Bellenden Ker forest, but low overstorey density has maintained relatively high background (diffuse) radiation levels in the understorey.

Percentages of daily irradiation and PPFD, relative to those in the clearing ranged from 2.5% for PPFD in the understorey to 11.6% for irradiance in the small gap (Table 7.5). In absolute terms, total daily irradiation in the clearing was about 9-times greater than irradiation in the small gap and lower-canopy, and 13-times greater than in the understorey. In comparison, total daily PPFD in the clearing was 9.6-times greater than in the lower-canopy, 16.6-times greater than in the small gap, and 39-times greater than in the understorey. Thus, in a similar manner to the Curtain Fig forest (Table 7.4), the ratio of irradiance to PPFD decreases with increasing overstorey density.

The absolute differences in the light regimes of these four micro-environments are further illustrated in Figs. 7.14 and 7.15 which show, respectively, the distribution of percentile values for irradiance and PPFD. Median radiant flux densities within the clearing, lower-canopy, small gap and understorey (Fig. 7.14) were 359.8, 42.8, 40.7, and 33.2 W m^{-2}, respectively. By comparison, median PPFDs for corresponding sites (Fig. 7.15) were 688.6, 70.3, 39.2 and 17.4 μ mol m^{-2} s^{-1}, respectively. The 90th percentile line is a useful indicator of the boundary between diffuse and direct fluxes for the understorey and the 75th percentile line represents this boundary for the lower-canopy and small gap.

The frequency distributions of 10-min average readings within clearing, lower-canopy, gap and understorey micro-environments are show in Fig. 7.16 for irradiance and Fig. 7.17 for PPFD. Both irradiance and PPFD within the clearing exhibited a moderate degree of positive skewness (ie values between 0.3 and 0.6), and they were platykurtic. The modal classes for irradiance (Fig. 7.16) and PPFD (Fig. 7.17) within the clearing account for 22.3% and 25.5% of the respective flux densities over the two day measurement period. However, because of the cloudy weather over the measurement interval, the modal classes are somewhat lower than those above the Curtain Fig forest in July (Figs. 7.12 and 7.13).

In comparison to the clearing, the frequency distributions of irradiance (Fig. 7.16) and PPFD (Fig. 7.17) within the lower-canopy and small gap have a high degree of positive skewness, and they are leptokurtic. Thus, most radiant flux densities and PPFDs within these habitats are concentrated towards the lower end of their respective intensity scales. For example, the modal classes for irradiance in the lower canopy (25-75 W m^{-2}) and small gap (25-50 W m^{-2}), account for 66% and 46% of the respective radiant flux densities over the measurement period (Fig. 7.16). Similarly,

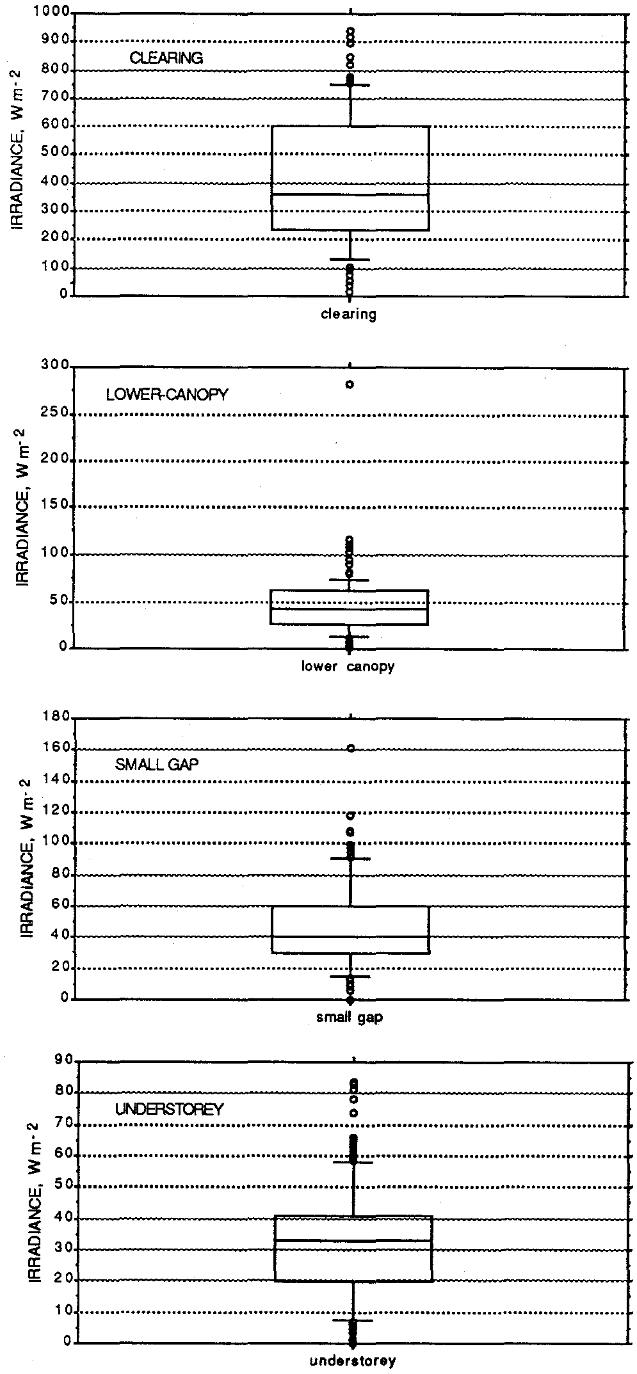

Figure 7.14. Distributions of percentiles (10-min average readings) for irradiance (W m^{-2}) within a forest clearing, the lower-canopy, a small treefall gap and the understorey of the Mt Bellenden Ker forest in June. The five horizontal lines on the box plot show the 10, 25, 50, 75 and 90th percentiles, with values above and below the 10th and 90th percentile represented as data points. Note differences in vertical scales.

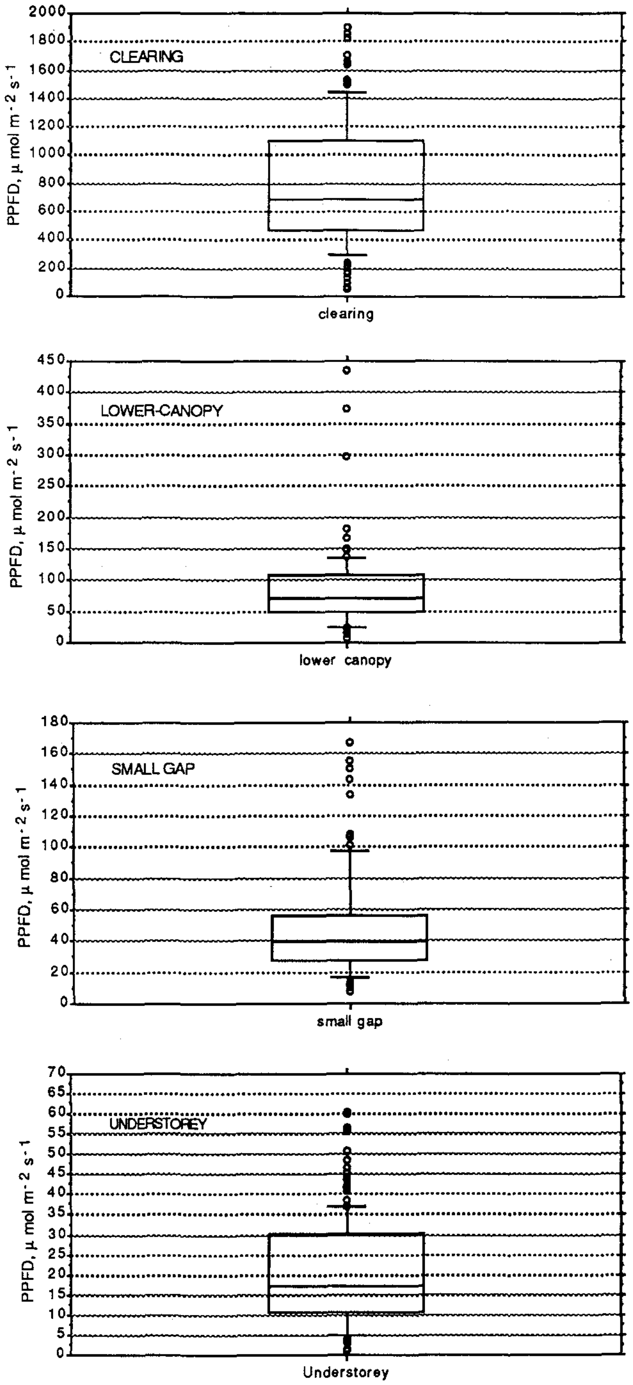

Figure 7.15. Distributions of percentiles (10-min average readings) for photosynthetic photon flux density (PPFD) (μ mol m^{-2} s^{-1}) within a forest clearing, the lower-canopy, a small treefall gap and the understorey of the Mt Bellenden Ker forest in June. The five horizontal lines on the box plot show the 10, 25, 50, 75 and 90th percentiles, with values above and below the 10th and 90th percentile represented as data points. Note differences in vertical scales.

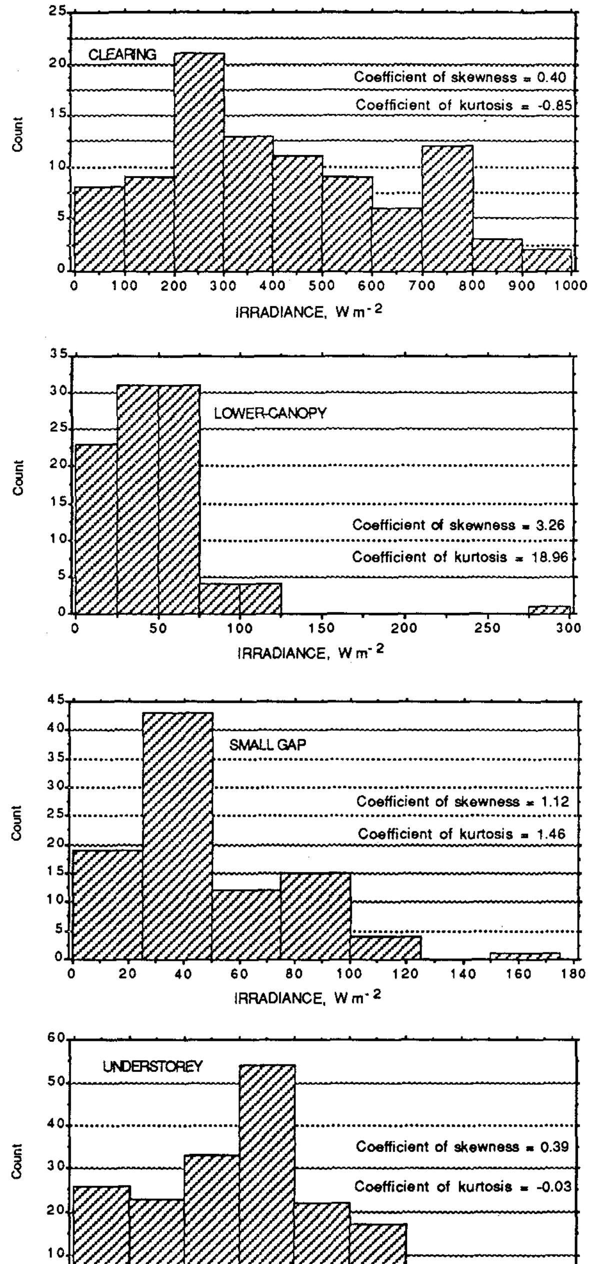

Figure 7.16. Frequency distributions of 10-min average readings for irradiance (W m^{-2}) within a forest clearing, the lower-canopy, a small treefall gap and the understorey of the Mt Bellenden Ker forest in June. Note differences in horizontal scales (class intervals).

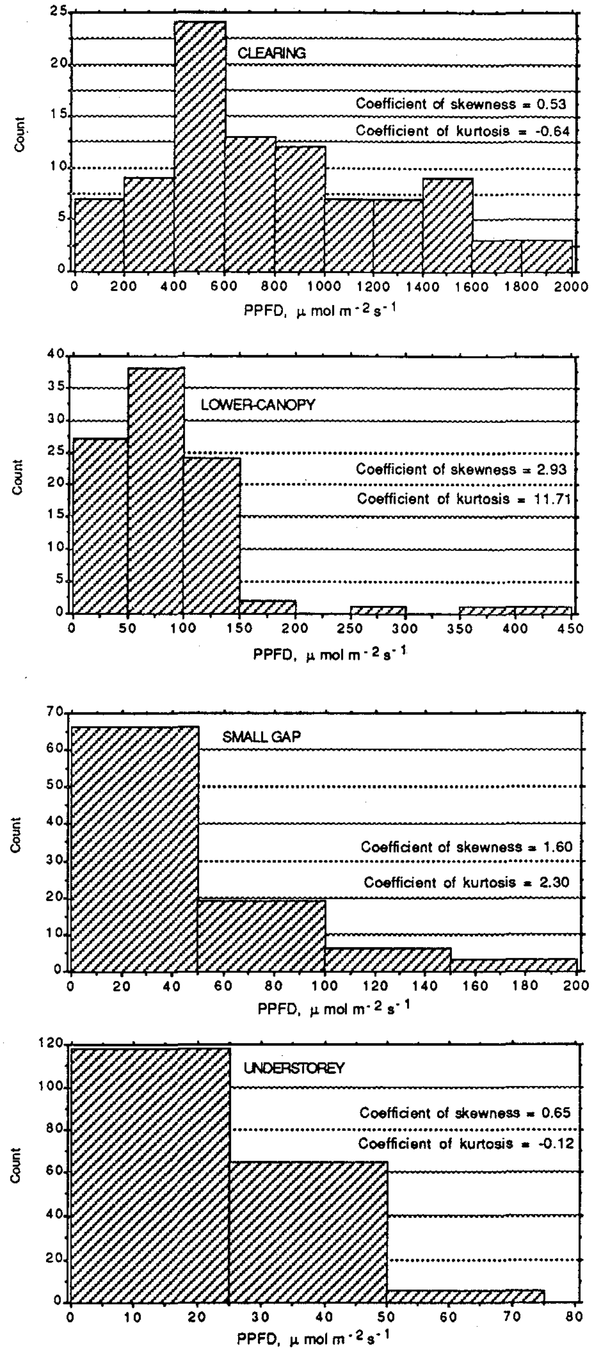

Figure 7.17. Frequency distributions of 10-min average readings for photosynthetic photon flux density (PPFD) (μ mol m^{-2} s^{-1}) within a forest clearing, the lower-canopy, a small treefall gap and the understorey of the Mt Bellenden Ker forest in June. Note differences in horizontal scales (class intervals).

about 40% of PPFDs in the lower-canopy are found in the modal class (50-100 μ mol m^{-2} s^{-1}) and about 70% within the small gap are below 50 μ mol m^{-2} s^{-1} (Fig. 7.17).

On the other hand, the degrees of kurtosis and positive skewness for irradiance in the understorey (Fig. 7.16) are both low, and therefore similar to those for the understorey of the Curtain Fig forest in July (Fig. 7.12). As stated earlier, this pattern is probably due, in part, to the nature of the linear pyranometer used to measure irradiance. However, the degrees of kurtosis and positive skewness for PPFD within the understorey of the Mt Bellenden Ker forest (Fig. 7.17) are both considerably lower than those in the Curtain Fig forest in July (Fig. 7.13). Hence, the distribution of PPFD within the Mt Bellenden Ker forest understorey is platykurtic with about 63% of PPFDs occurring below 25 μ mol m^{-2} s^{-1}; this compares with over 95% below this value within the Curtain Fig forest understorey in July. Moreover, the relatively open nature of the canopy (Fig. 5.6) explains the quite high proportion (35%) of PPFDs between 25 and 50 μ mol m^{-2} s^{-1}; by comparison, only 3.4% of PPFDs occur in this class interval within the Curtain Fig forest in July (Fig. 7.13).

The results presented in Fig. 7.16 show that about 42% of 10-min average readings within the lower-canopy, 34% within the small gap and 16% within the understorey were attributed to irradiance levels greater than 50 W m^{-2}. Hence, conservative estimates of the proportion of daily total irradiation contributed by sunflecks (ie intensities greater than 50 W m^{-2}) for the three micro-environments are as follows: (1) lower-canopy, 62%; (2) small gap, 54%; and (3) understorey, 29%. The values for the gap and understorey are higher than those reported earlier for corresponding micro-environments within the Curtain Fig forest in July.

By comparison, the results presented in Fig. 7.17 show that 71% of 10-min average PPFD readings within the lower-canopy, 30% within the small gap and 3% within the understorey were attributed to sunflecks (ie PPFDs greater than 50 μ mol m^{-2} s^{-1}). On the basis of these measurements, the proportion of daily total PPFD contributed by sunflecks within these micro-environments are as follows: (1) lower-canopy, 87%; (2) small gap, 51%; and (3) understorey, 6%. The value for the small gap is less than that reported earlier for the small gap in the Curtain Fig forest in July, while the value for the understorey is similar to that found for the Curtain Fig understorey.

7.2.2 Variations Within Characteristic Micro-Environments

7.2.2.1 10-sec Instantaneous Readings of PPFD Within the Understorey

The frequency distributions of PPFD at five understorey sites within the Curtain Fig forest (Fig. 5.4) over a sunny summer's day (January 14, 1987) are shown in Fig. 7.18. In the same way as the results described in Section 7.2.1.1, instantaneous 10-sec readings have been analysed for the five understorey sites using the linear and logarithmic classifications shown in Table 6.17.

The linear classification (Fig. 7.18) indicates that the distribution of 10-sec readings of PPFD is not uniform within the understorey. Statistical analysis reveals that the following understorey sites are significantly different from each other: sites 1 and 2, sites 1 and 3, sites 2 and 3, sites 3 and 4, and sites 3 and 5 (Kolmogorov-Smirnov, D-test: values ranged from 0.10-0.21, P<0.01). Despite these differences among understorey sites, the modal class is 1 at each site (ie PPFDs are mostly less than 72 μ mol m^{-2} s^{-1}). Hence, the sites differ mainly in the proportion of sunflecks received. For example, at site 1, about 2% of PPFDs over the day exceeded 71.9 μ mol m^{-2} s^{-1}, compared with 23% at site 3.

Differences in the distribution of PPFD within the understorey of this forest are emphasised more clearly when the same data are sorted into logarithmic classes (Fig. 7.18). All sites are significantly different from each other (D-test: values ranged from 0.14-0.25, P<0.01), except sites 2 and 4 (D=0.06, P>0.05). Moreover, the proportion of daily total PPFD contributed by sunflecks (direct PPFD) varies considerably within the understorey. For example, if class 18 is again used as the minimum level for direct PPFD (ie intensities greater than 50 μ mol m^{-2} s^{-1}), then in absolute terms sunflecks represent 15 and 90% of the daily total PPFD at sites 1 and 3, respectively.

7.2.2.2 10-min Average Readings of Irradiance Within the Understorey

(a) Curtain Fig Forest (November and July)

Table 7.6 summarises results of various descriptive statistics applied to 10-min average readings of irradiance at four understorey sites within the Curtain Fig forest in November 1985 and July 1986. Because solar altitude (α) at solar noon was about 90° over the November measurement period and only 51° over the July measurement period, one would expect mean radiant flux densities to be lower in the understorey in July compared with November. However, these results have been affected by Tropical

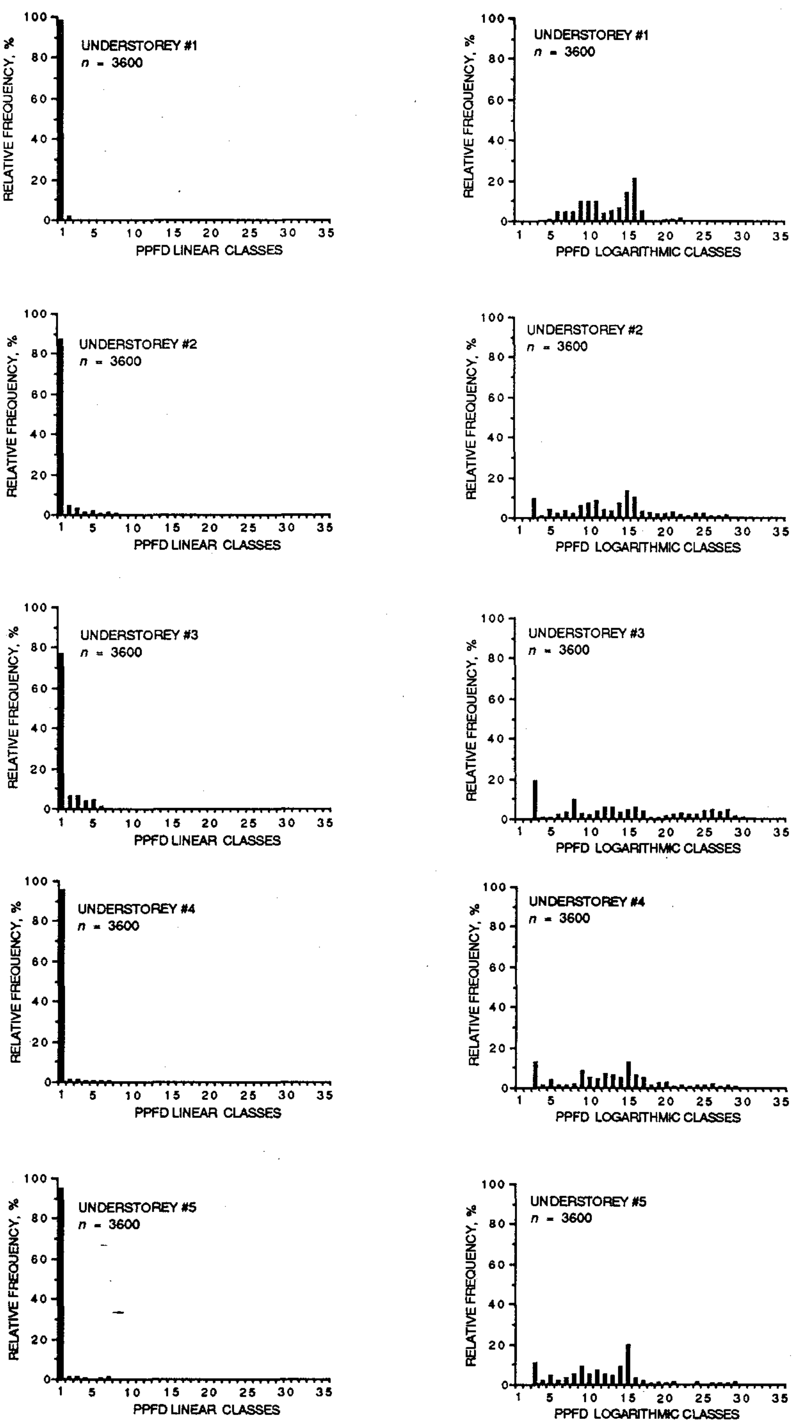

Figure 7.18. Frequency distributions of 10-sec instantaneous readings for photosynthetic photon flux density (PPFD) at five understorey sites within the Curtain Fig forest over a full sunny day (0700-1700-h), January 14, 1987. The data have been sorted using the 35 linear and logarithmic classes shown in Table 6.17.

Understorey Sites	NOVEMBER Irradiance (W m^{-2}) Average flux (mean±1 SD) (range) Coefficient of variation	Daily total (MJ m^{-2} per day)	JULY Irradiance (W m^{-2}) Average flux (mean±1 SD) (range) Coefficient of variation	Daily total (MJ m^{-2} per day)
#1	16.6±17.0 (0.0-131.6) 102.5% *n*=104	0.76 (2.6)*	25.3±4.2 (0.0-34.3) 16.5% *n*=46	1.00 (5.3)*
#2	23.8±17.6 (0.0-118.7) 74.0% *n*=104	1.09 (3.8)*	27.2±8.3 (0.0-51.4) 30.5% *n*=46	1.08 (5.7)*
#3	25.6±16.0 (0.0-86.2) 62.6% *n*=104	1.17 (4.1)*	31.2±12.8 (0.0-80.6) 41.2% *n*=46	1.23 (6.5)*
#4	21.3±12.1 (0.0-51.3) 56.6% *n*=104	0.97 (3.4)*	24.8±5.8 (0.0-38.4) 23.4% *n*=46	0.98 (5.2)*

* Refers to the percentage of the daily total within the understorey relative to that above the forest canopy.

Table 7.6. Values of daily average irradiance (W m^{-2}) and total daily irradiation (MJ m^{-2} per day) within four understorey sites in the Curtain Fig forest, northeast Queensland (November, 1985 and July, 1986).

Cyclone 'Winifred' which caused slight-to-moderate canopy damage at this site in February 1986. Hence, mean radiant flux densities are higher in July, about 5-months after the cyclone, than in the previous November. Statistical analyses have shown that all sites, except site 2, have experienced a significant increase in mean irradiance levels from November to July (site 1: t=3.43, P<0.01; site 2: t=1.25, P>0.05; site 3: t=2.08, P<0.05; and site 4: t=1.84, P<0.05). Therefore, the higher mean radiant flux densities in the understorey in July compared with November are strong evidence of a reduction in canopy density following the cyclone because mean irradiance levels above the canopy are significantly higher in November than in July (t=3.11, P<0.01).

The results shown in Table 7.6 indicate that irradiance is not uniform within the understorey of the Curtain Fig forest, despite the in-built spatial averaging feature in the radiation instruments. Statistical analyses have shown that irradiance differs significantly among understorey sites at both times of the year (one-way ANOVA: for November F=6.37, P<0.01; and for July F=5.48, P<0.01). However, multiple comparisons among sites shown that only some are significantly different from each other (for November: sites 1 and 2 t=3.30, P<0.01; sites 1 and 3 t=4.11, P<0.01; and for July: sites 1 and 3 t=3.35, P<0.01; sites 3 and 4 t=3.65, P<0.01). A wide range of radiant flux densities was experienced within the understorey over the 2-day measurement period in November (Table 7.6). The range of maximum radiant flux densities at the four sites (51.3-131.6 W m^{-2}) represents 5 to 12% of the maximum irradiance above the forest canopy. By comparison, in July the range of maximum radiant flux densities (34.3-80.6 W m^{-2}) represents 4 to 9% of the maximum irradiance above the forest canopy.

Percentages of daily irradiation at the four understorey sites, relative to that above the forest, were higher in July than November (Table 7.6). In absolute terms, total daily irradiation above the forest in November was about 38-times greater than that at site 1 and about 25-times greater than that at site 2. In comparison, total daily irradiation above the forest in July was about 19-times greater than that at site 4 and about 15-times greater than that at site 3.

The absolute differences in irradiance levels within the understorey are explained further in Fig. 7.19 which shows the distribution of percentile values for the four sites in November and July. Median radiant flux densities at sites 1 to 4 in November were 13.5, 22.7, 26.3 and 20.6 W m^{-2}, respectively. The corresponding median values in July were 25.7, 26.6, 29.3 and 24.4 W m^{-2}, respectively. Thus, median values for the four understorey sites are higher in July than in November and this, together with the fact that median values above the forest were 640.2 W m^{-2} in November and 507.2 W m^{-2} in July, are further evidence in support of reduced canopy density following the February cyclone.

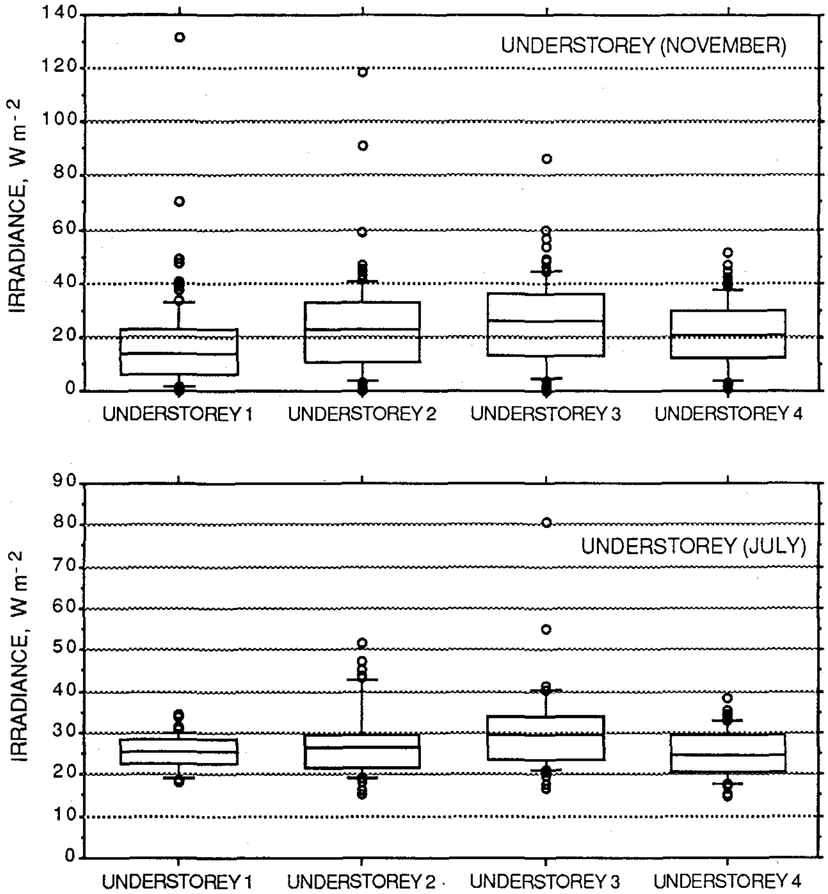

Figure 7.19. Distributions of percentiles (10-min average readings) for irradiance (W m^{-2}) within four understorey sites in the Curtain Fig forest at two contrasting times of the year (January and July). The five horizontal lines on the box plot show the 10, 25, 50, 75 and 90th percentiles, with values above and below the 10th and 90th percentile represented as data points. Note differences in vertical scales.

In a similar way to the box plots shown in Figs. 7.10 and 7.14 for irradiance in the understorey, the 90th percentile horizontal lines (Fig. 7.19) correspond closely with the boundary between diffuse and direct irradiance. However, there is some variability in the 90th percentile (P_{90}) among sites. For example, in November the P_{90} values for sites 1 and 3 are 32.7 and 44.1 W m^{-2}, respectively; in July the P_{90} values for sites 1 and 2 are 30.0 and 42.8 W m^{-2}, respectively.

The frequency distributions of 10-min average irradiance readings at the four understorey sites for November and July are shown in Fig. 7.20. The data have been sorted into class intervals of 10 W m^{-2}. The histograms demonstrate marked differences in solar radiation availability within the understorey (Fig. 7.20). In November, sites 1 to 3 exhibited a strong degree of positive skewness, while sites 1 and 2 were leptokurtic. On the other hand, site 4 exhibited a low degree of positive skewness, and sites 3 and 4 were platykurtic. Similar variability occurred among these four sites in July (Fig. 7.20): sites 2 to 4 exhibited a moderate to strong degree of positive skewness, while only site 2 was leptokurtic; site 1 was normally distributed, and sites 1, 2 and 4 were platykurtic. The greatest variability in modal classes among the four sites occurs in November, with all sites having different values (Fig. 7.20). By comparison, the modal class in July is constant among the sites.

In November, about 1% of 10-min average readings at site 4 were attributed to irradiance levels greater than 50 W m^{-2} (Fig. 7.20); corresponding values for the other sites were: site 1, 2%; site 2, 2.9%; and site 3, 4.8%. By comparison, the values for July were: site 1, 0%; site 2, 2.2%; site 3, 6.5%; and site 4, 0%. Hence, conservative estimates of the proportion of daily total irradiation contributed by sunflecks (ie intensities greater than 50 W m^{-2}) within the understorey ranges from 2.2 to 10.2% for November and from 0 to 14% for July.

(b) Pine Creek Forest (July)

Table 7.7 summarises results of various descriptive statistics applied to 10-min average readings of irradiance at four understorey sites within the Pine Creek forest (Fig. 5.5) over two days (July 18-19, 1986). Solar altitude (α) at solar noon was about 52° during this time. It is therefore possible to compare these results with those described in the preceding section for the Curtain Fig forest in July. Furthermore, mean irradiance above the Curtain Fig forest in July (Table 7.6) is not significantly different (t=0.80, P>0.05) from that above the Pine Creek forest (Table 7.7).

Unlike the Curtain Fig forest, the Pine Creek forest site only received slight canopy disturbance as a result of Tropical Cyclone 'Winifred'. However, because the Pine Creek forest (Fig. 5.5) is not as tall as the Curtain Fig forest (Fig. 5.4), there are

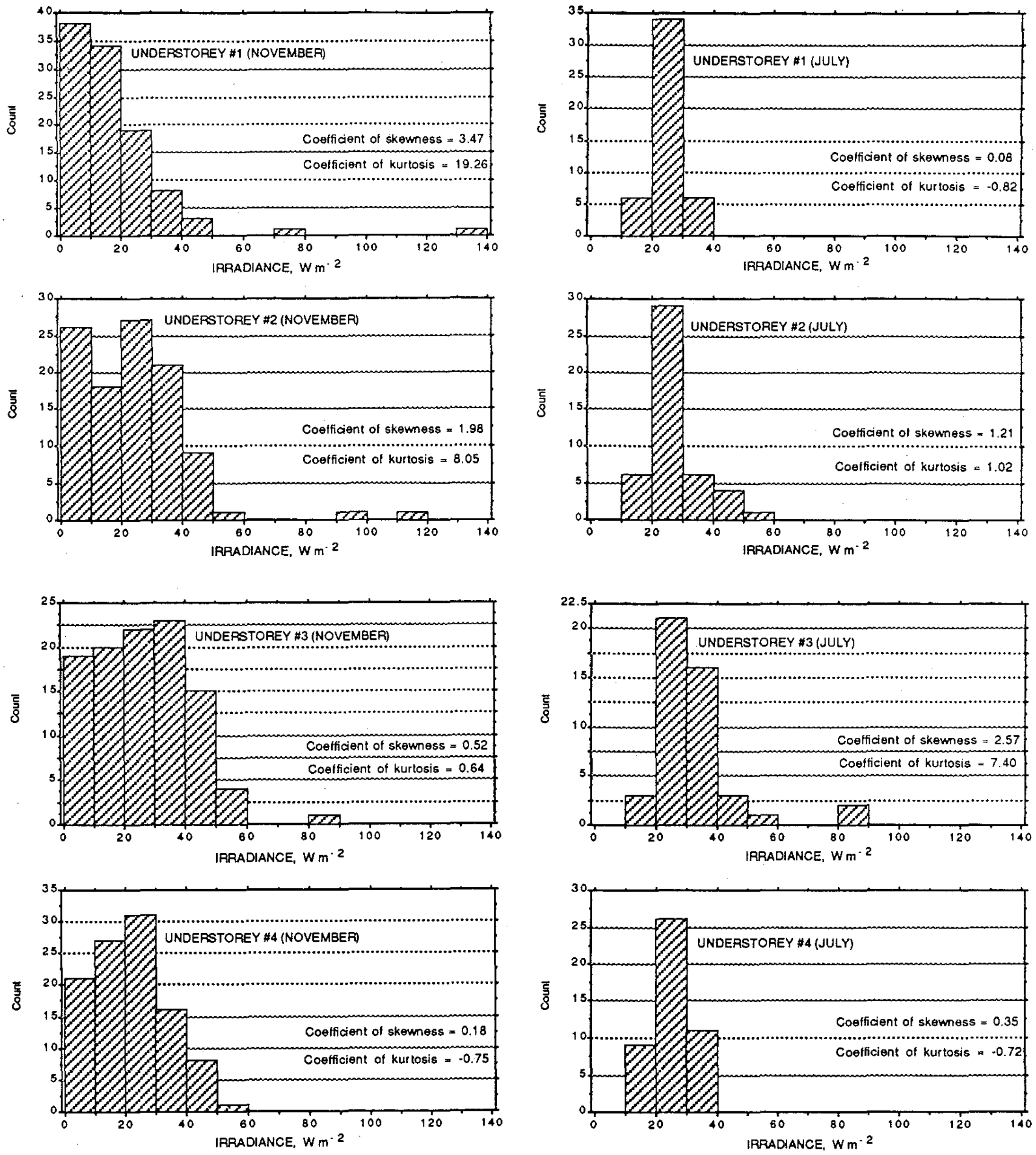

Figure 7.20. Frequency distributions of 10-min average readings for irradiance (W m^{-2}) within four understorey sites in the Curtain Fig forest at two contrasting times of the year (January and July).

Understorey Sites	Irradiance (Wm^{-2}) Average flux (mean± 1 SD) (range) Coefficient of variation	Daily total ($MJ\ m^{-2}$ per day)
#1	27.2±24.1 (0.0-131.6) 88.5% *n*=94	1.08 (6.2)*
#2	35.7±35.7 (0.0-232.7) 100.2% *n*=94	1.43 (8.1)*
#3	35.6±27.6 (0.0-190.8) 77.6% *n*=94	1.42 (8.1)*
#4	45.7±45.8 (0.0-238.4) 100.1% *n*=94	1.83 (10.4)*

* Refers to the percentage of the daily total within the understorey relative to that above the forest.

Table 7.7. Values of daily average irradiance (W m^{-2}) and total daily irradiation (MJ m^{-2} per day) at four understorey sites within the Pine Creek forest, northeast Queensland (July, 1986).

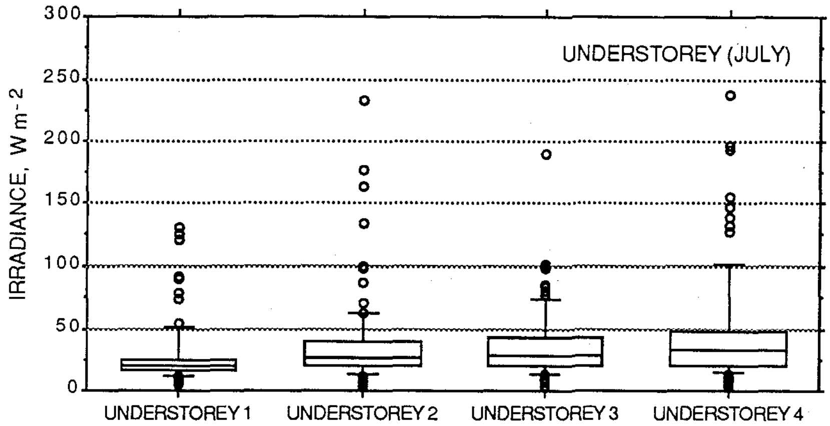

Figure 7.21. Distributions of percentiles (10-min average readings) for irradiance (W m^{-2}) within four understorey sites in the Pine Creek forest in July. The five horizontal lines on the box plot show the 10, 25, 50, 75 and 90th percentiles, with values above and below the 10th and 90th percentile represented as data points.

fewer leaf layers to intercept the penetrating light, and one would therefore expect light levels to be higher in the former. The results in Table 7.7 support this argument; mean radiant flux densities within the Pine Creek forest understorey are significantly higher (t=3.43, P<0.01) than those within the Curtain Fig forest understorey in July (Table 7.6). Moreover, the maximum radiant flux densities within the Pine Creek understorey (Table 7.7) are, on average, about 4-times greater than those measured in the Curtain Fig understorey in July, and about 2-times greater than in November (Table 7.6).

The results indicate that irradiance is not uniform within the Pine Creek forest understorey (Table 7.7), with a similar degree of variability to that found within the Curtain Fig understorey (Table 7.6). Statistical analyses have shown that irradiance differs significantly among the four understorey sites in the Pine Creek forest (one-way ANOVA: F=4.58, P<0.01). However, multiple comparisons have shown that only sites 1 and 4 are significantly different from each other (t=3.70, P<0.01). Nonetheless, a wide-range of radiant flux densities were experienced within the understorey over the 2-day measurement period (Table 7.7). The range of maximum radiant flux densities at the four sites (131.6-238.4 W m^{-2}) represent 13 to 23% of the maximum irradiance above the forest canopy, and are therefore considerably higher than those given earlier for the Curtain Fig forest.

Percentages of daily irradiation at the four understorey sites in the Pine Creek forest, relative to that above the canopy, ranged from 6.2 to 10.4% (Table 7.7). In absolute terms, total daily irradiation above the forest was about 16-times greater than that at site 1 and about 10-times greater than that at site 4. Both values are somewhat lower than those described earlier for the Curtain Fig forest which adds further to the argument that light levels are generally higher in the Pine Creek understorey.

The absolute differences in irradiance levels within the Pine Creek understorey are examined in more detail in Fig. 7.21 which shows the distribution of percentiles for the four sites. Median radiant flux densities at sites 1 to 4 were 20.2, 26.6, 28.2 and 32.9 W m^{-2}, respectively. These values are not greatly different to the median values for the Curtain Fig understorey in July (Fig. 7.19). However, the 90th percentiles are much higher within the Pine Creek understorey, ranging from 50.9 W m^{-2} at site 1 to 101.7 W m^{-2} at site 4 (Fig. 7.21). Thus, there are considerably more high intensity long-duration sunflecks within the Pine Creek understorey, with most exceeding the highest values measured within the Curtain Fig understorey in November and July (Fig. 7.19).

The frequency distributions of 10-min average irradiance readings at the four understorey sites are shown in Fig 7.22. The histograms indicate some variability in the distribution of irradiance (10 W m^{-2} classes) within the understorey. However,

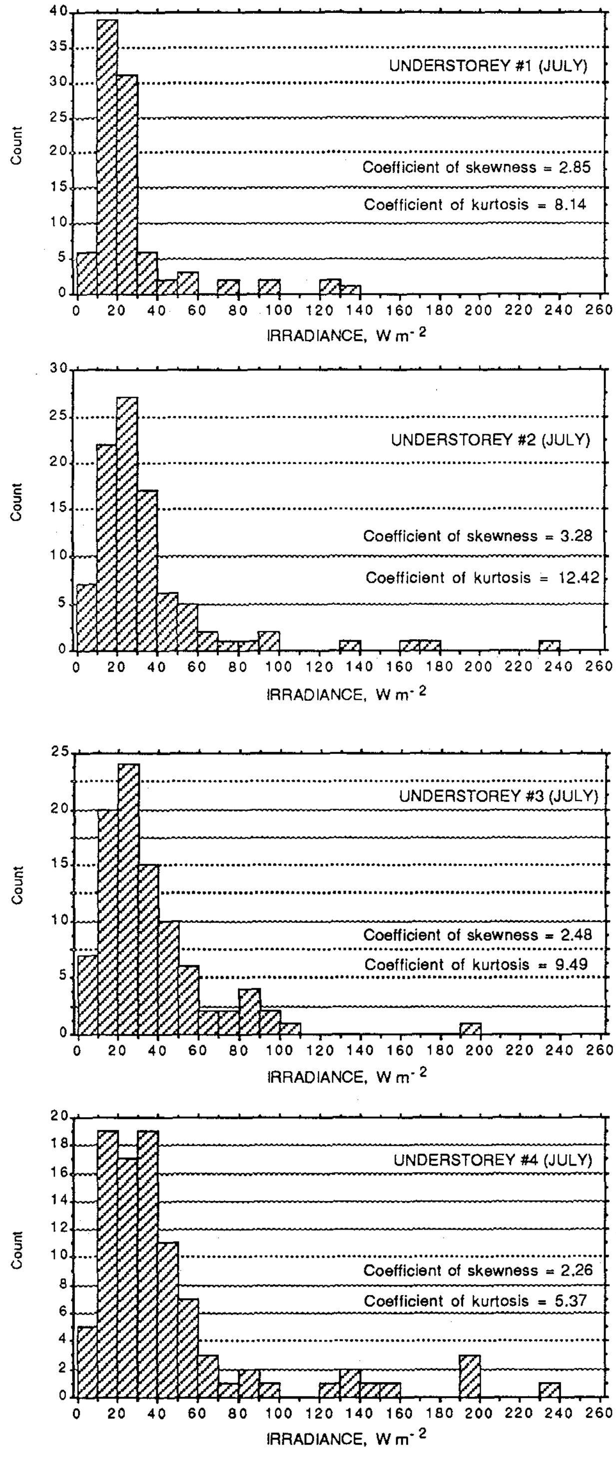

Figure 7.22. Frequency distributions of 10-min average readings for irradiance (W m^{-2}) within four understorey sites in the Pine Creek forest in July.

differences among sites are not as marked as those shown in Fig. 7.20 for the Curtain Fig forest. In the Pine Creek forest (Fig. 7.22), all the understorey sites exhibited a high degree of positive skewness, and they were all leptokurtic. About 11% of 10-min average readings at site 1 were attributed to irradiance levels greater than 50 W m^{-2} (Fig. 7.22); corresponding values for the other sites were: site 2, 16%; site 3, 19.2%; and site 4, 24.5%. Hence, conservative estimates of the proportion of daily total irradiation contributed by sunflecks (ie intensities greater than 50 W m^{-2}) within the understorey ranges from 30.8 to 53.1%. This range is much higher than that reported earlier for the four understorey sites in the Curtain Fig forest in July.

7.2.2.3 10-min Average Readings of PPFD Within the Understorey

Table 7.8 summarises results of various descriptive statistics applied to 10-min average readings of PPFD at four understorey sites within the Curtain Fig forest (Fig. 5.4) in January and three understorey sites within the same forest in July. Because the combined understorey data for January and July have already been compared (Table 7.4), only the spatial variability of PPFD within the understorey will be discussed here.

The results shown in Table 7.8 indicate that PPFD is not uniform within the understorey of the Curtain Fig forest. However, statistical analyses have shown that PPFD differs among sites for January only (one-way ANOVA: F=3.83, P<0.01; compared with July: F=0.904, P>0.05). Furthermore, multiple comparisons among sites for January have shown that only some of the sites are significantly different from each other (sites 2 and 3: t=2.56, P<0.05; and sites 3 and 4: t=3.18, P<0.01). A wide-range of PPFDs were experienced within the understorey over the January measurement period (Table 7.8). The range of maximum PPFDs at the four sites (51.5-442.6 μ mol m^{-2} s^{-1}) represent 2.1 to 18.5% of the maximum PPFD above the forest canopy. By comparison, in July the range of maximum PPFDs at the three sites (26.7-129.0 μ mol m^{-2} s^{-1}) represent 1.5 to 7.4% of the maximum PPFD above the forest canopy.

Percentages of daily total PPFD within the understorey, relative to that above the forest, were similar in January and July (Table 7.8). In absolute terms, total daily PPFD above the forest in January was about 95-times greater than that at site 4 and about 45-times greater than that at site 3. In comparison, total daily PPFD above the forest in July was about 70-times greater than that at site 2 and 55-times greater than that at site 1.

The absolute differences in PPFD levels within the understorey are explained further in Fig. 7.23 which shows the distribution of percentiles for the four sites in

Understorey Sites	JANUARY PPFD (μ mol m^{-2} s^{-1}) Average flux (mean±1 SD) (range) Coefficient of variation	JANUARY Daily total (mol m^{-2} per day)	JULY PPFD (μ mol m^{-2} s^{-1}) Average flux (mean±1 SD) (range) Coefficient of variation	JULY Daily total (mol m^{-2} per day)
#1	16.1±28.3 (0.0-258.7) 175.7% n=121	0.75 (1.4)*	14.4±17.5 (0.4-129.0) 121.8% n=55	0.57 (1.8)*
#2	14.6±19.6 (0.0-157.5) 133.7% n=121	0.68 (1.3)*	11.3±7.0 (0.5-26.7) 61.7% n=55	0.45 (1.4)*
#3	25.3±53.9 (0.0-442.6) 213.3% n=121	1.17 (2.2)*	12.0±11.1 (0.0-66.0) 92.4% n=55	0.58 (1.5)*
#4	12.1±8.7 (0.0-51.5) 71.7% n=268	0.56 (1.1)*		

* Refers to the percentage of the daily total within the understorey relative to that above the forest canopy.

Table 7.8. Values of daily average photosynthetic photon flux density (PPFD) (μ mol m^{-2} s^{-1}) and total daily PPFD (mol m^{-2} per day) within four understorey sites in the Curtain Fig forest, northeast Queensland (January and July, 1987).

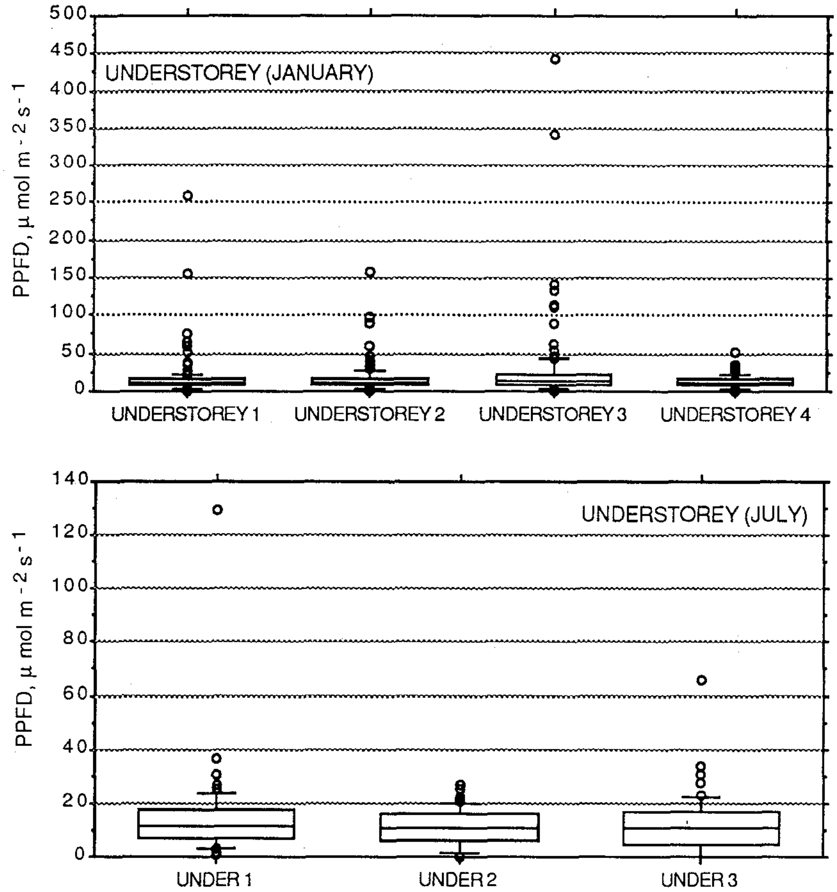

Figure 7.23. Distributions of percentiles (10-min average readings) for photosynthetic photon flux density (PPFD) (μ mol m^{-2} s^{-1}) within four understorey sites in the Curtain Fig forest at two contrasting times of the year (January and July). The five horizontal lines on the box plot show the 10, 25, 50, 75 and 90th percentiles, with values above and below the 10th and 90th percentile represented as data points. Note differences in vertical scales.

January and the three sites in July. Median PPFDs at sites 1 to 4 in January were 11.2, 10.6, 13.5 and 11.0 μ mol m^{-2} s^{-1}, respectively. The median values for sites 1 to 3 in July were 11.7, 10.0 and 10.6 μ mol m^{-2} s^{-1}, respectively. Thus, median values are similar for both times of the year (Fig. 7.23). Moreover, the 90th percentiles are only slightly higher in January (range: 21.7-44.1 μ mol m^{-2} s^{-1}) than in July (range: 19.7-23.5 μ mol m^{-2} s^{-1}). However, there are more high intensity long-duration sunflecks in the understorey in January compared with July (Fig. 7.23).

The frequency distributions of 10-min average PPFD readings at the four understorey sites for January and the three understorey sites for July are shown in Fig. 7.24. The histograms indicate some variability in the distribution of PPFD (25 μ mol m^{-2} s^{-1} classes) within the understorey at these times. In January, all the understorey sites exhibited a high degree of positive skewness, and they were all leptokurtic. The understorey sites in July exhibited similar trends, with the exception of site 2 which was normally distributed and platykurtic (Fig. 7.24). At both times of the year the modal classes were constant (ie 0-25 μ mol m^{-2} s^{-1}) which indicates that most PPFDs received in the understorey consisted of diffuse radiation.

In January, about 1% of 10-min average readings at site 4 were due to sunflecks (ie PPFDs greater than 50 μ mol m^{-2} s^{-1}); corresponding values for the other sites were: site 1, 5%; site 2, 3.3%; and site 3, 8.3% (Fig. 7.24). By comparison, the values for July were: sites 1 and 3, 1.8%; and site 2, 0%. On the basis of these measurements, the proportion of daily total PPFD contributed by sunflecks within the understorey ranges from 2.3 to 35% in January and from 0 to 9.4% in July.

7.2.2.4 10-min Average Readings of Irradiance Within an Elliptical Treefall Gap

Table 7.9 summarises results of various descriptive statistics applied to 10-min average readings of irradiance at three sites within a small elliptical (north-south) treefall gap in the Curtain Fig forest (Fig. 5.4) in January and July. A hemispherical canopy photograph of this gap is shown in Plate 7.5 (Section 7.3.2). Because solar altitude (α) at solar noon was about 87° over the 4-day measurement period in January and only 51° over the 3-day measurement period in July, one would expect mean radiant flux densities to be considerably lower within this small gap in July compared with January.

The results in Table 7.9 support this notion; mean radiant flux densities at each gap site in January are significantly higher than corresponding sites in July (t values ranged from 4.14-9.17, P<0.01). Specifically, mean irradiance levels at the southern end of the gap are 3.4-times higher in January than in July, while those at the centre

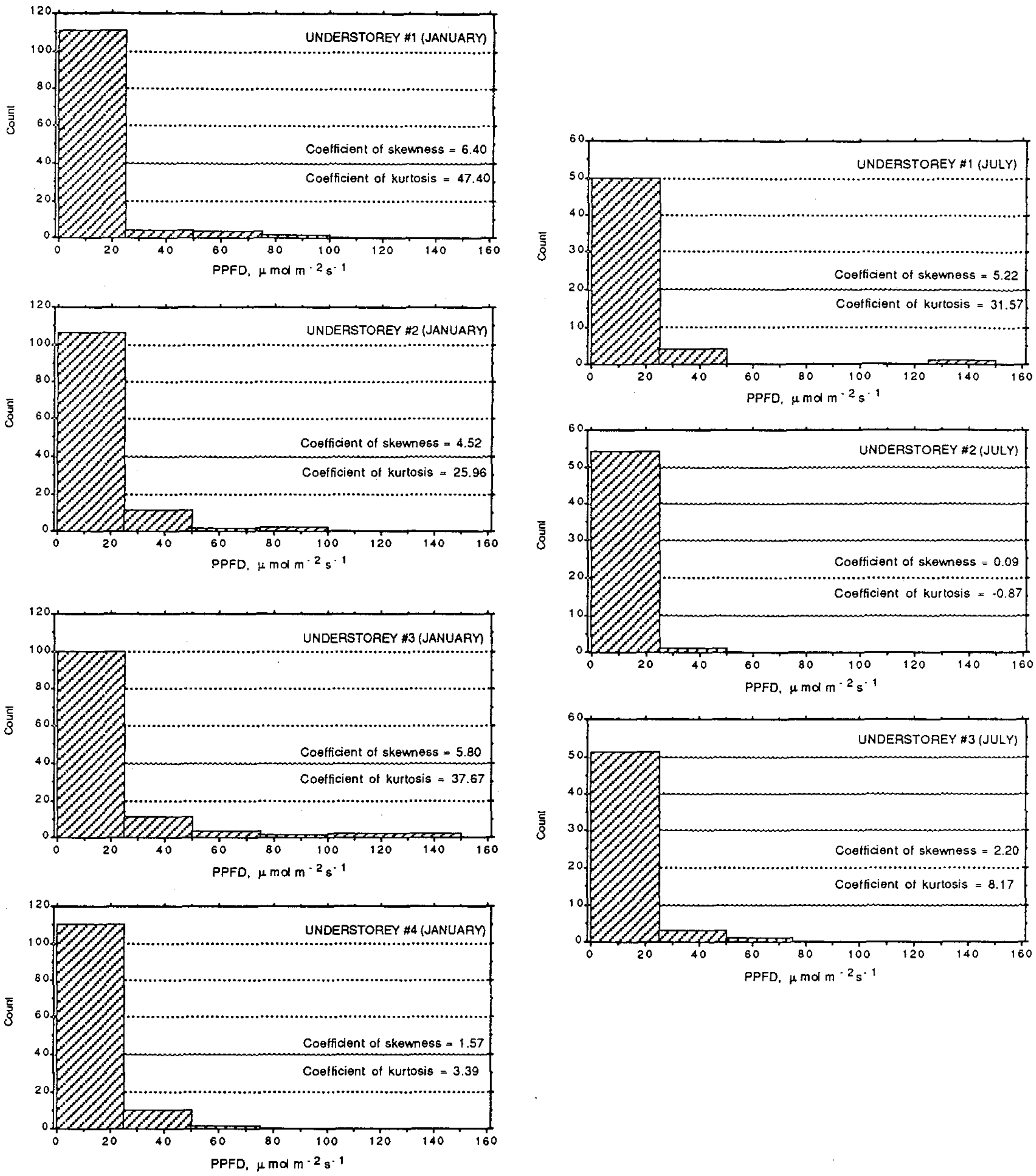

Figure 7.24. Frequency distributions of 10-min average readings for photosynthetic photon flux density (PPFD) (μ mol m^{-2} s^{-1}) within four understorey sites in January and three understorey sites in July in the Curtain Fig forest.

Treefall gap Sites	JANUARY Irradiance (W m^{-2}) Average flux (mean±1 SD) (range) Coefficient of variation	Daily total (MJ m^{-2} per day)	JULY Irradiance (W m^{-2}) Average flux (mean±1 SD) (range) Coefficient of variation	Daily total (MJ m^{-2} per day)
Gap (south)	85.8±180.1 (0.0-1060.1) 209.9% *n*=268	3.99 (13.5)*	25.3±16.9 (3.4-114.0) 66.9% *n*=153	1.00 (5.4)*
Gap centre	122.0±227.5 (0.0-992.7) 186.5% *n*=268	5.66 (19.2)*	25.8±15.9 (3.6-102.6) 61.7% *n*=153	1.02 (5.5)*
Gap (north)	127.6±249.8 (0.0-1047.5) 195.7% *n*=268	5.93 (20.1)*	28.0±18.5 (5.0-118.4) 65.9% *n*=153	1.11 (6.0)*

* Refers to the percentage of the daily total within the understorey relative to that above the forest canopy.

Table 7.9. Values of daily average irradiance (W m^{-2}) and total daily irradiation (MJ m^{-2} per day) at three sites within an elliptical treefall gap in the Curtain Fig forest, northeast Queensland (January and July, 1987).

and northern end of the gap are, respectively, 4.7- and 4.6-times higher in January than in July.

The results shown in Table 7.9 also indicate that irradiance is not uniform within the gap in January with the northern end having the highest mean over the 4-day measurement period. This pattern is due to the position of the midday sun in the southern sky at this time of the year which favours the penetration of direct irradiance into the northern, rather than southern, end of the treefall gap. However, statistical analyses have shown that irradiance does not differ significantly among the three gap sites in January (one-way ANOVA: F=2.82, P>0.05). Likewise, irradiance does not differ significantly among these sites in July (F=0.42, P>0.05). Consequently, a small range of maximum radiant flux densities were experienced within the gap in January (992.7-1060.1 W m^{-2}) and July (102.8-118.4 W m^{-2}), representing 76 to 81% and 11 to 13% of the maximum irradiance above the forest canopy at the respective times of year.

Percentages of daily irradiation at the three gap sites, relative to that above the forest, were considerably higher in January than in July (Table 7.9). In absolute terms, total daily irradiation above the forest in January was about 5- to 7-times greater than levels in the gap. In comparison, total daily irradiation above the forest in July was about 16- to 18-times greater than levels within the treefall gap.

The absolute differences in irradiation levels within the treefall gap are examined in more detail in Fig. 7.25 which shows the distribution of percentiles for the three sites in January and July. Median radiant flux densities at the southern end of the gap, gap centre and northern end of the gap in January were 36.0, 43.1 and 35.9 W m^{-2}, respectively. The corresponding median values in July were 23.1, 23.7 and 25.0 W m^{-2}, respectively. Thus, despite the obvious differences in mean values between January and July (Table 7.9), differences in median values are not as large (Fig. 7.25). However, the 90th percentiles are considerably higher in January (range: 179.6-498.5 W m^{-2}) than in July (range: 40.1-47.9 W m^{-2}); the higher values in January being associated with unintercepted direct irradiance reaching the forest floor beneath the gap over the middle of the day (refer to Plate 7.5).

In addition, the box plots for January (Fig. 7.25) highlight differences in irradiance among the three sites within the gap, particularly the positions of the 90th percentile lines which increase from the southern to the northern end of the gap for reasons explained earlier. The data points above these lines are associated with the intense midday sun penetrating directly through to the floor. On the other hand, the 90th percentile horizontal lines for July are more or less the same across the gap (Fig. 7.25), with data points above the lines being only associated with sunflecks because the midday sun is unable to penetrate directly through this gap at this time of year.

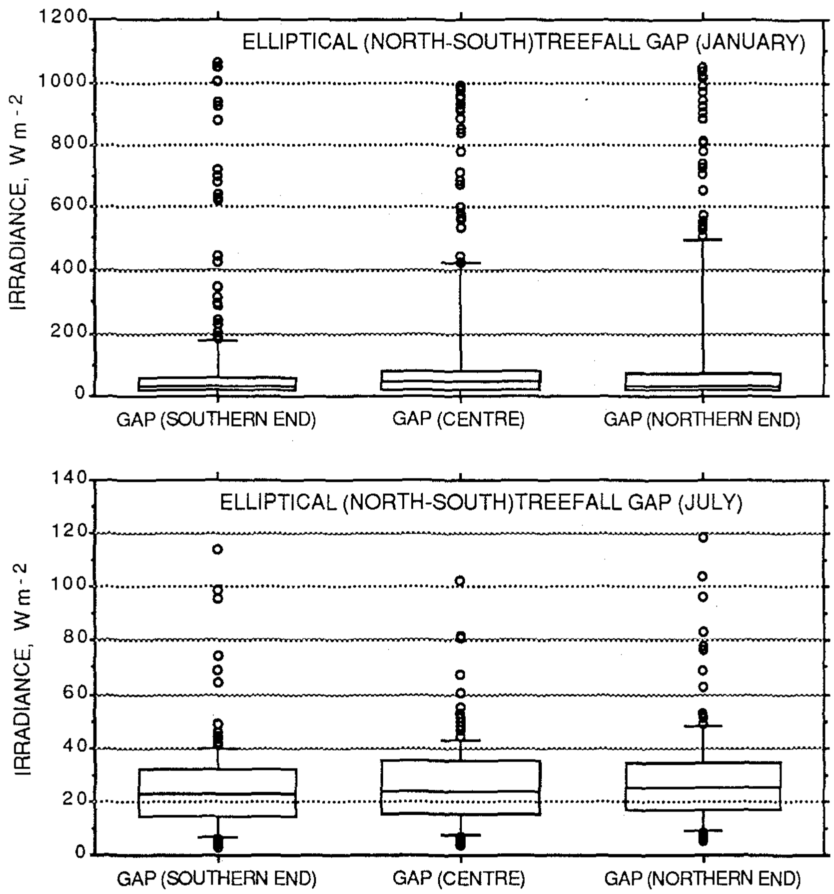

Figure 7.25. Distributions of percentiles (10-min average readings) for irradiance (W m^{-2}) at three sites within an elliptical treefall gap in the Curtain Fig forest at two contrasting times of the year (January and July). The five horizontal lines on the box plot show the 10, 25, 50, 75 and 90th percentiles, with values above and below the 10th and 90th percentile represented as data points. Note differences in vertical scales.

The frequency distributions of 10-min average irradiance readings at the three sites within the treefall gap for January and July are shown in Fig. 7.26. The data have been sorted into class intervals of 25 W m^{-2}. The histograms indicate little variability in the distribution of irradiance within the gap. In both January and July, the three sites within the gap exhibited a high degree of positive skewness, and they were all leptokurtic. At both times of the year the modal classes were constant among sites (ie 0-25 W m^{-2}) which indicates that most radiant flux densities received in the gap consisted of diffuse radiation, although allowance must be made for the in-built spatial averaging feature in the radiation instruments.

However, there are strong differences in the distribution of radiant flux densities within the gap between January and July (Fig. 7.26). In January, about 35% of 10-min average readings at the southern end of the gap were due to sunflecks (ie radiant flux densities greater than 50 W m^{-2}); corresponding values for the centre of the gap and northern end of the gap were 40 and 37%, respectively. By comparison, the values for July were: southern end of gap, 4%; centre of gap, 6.5%; and northern end of gap, 8.5%. On the basis of these measurements, conservative estimates of the proportion of daily total irradiation contributed by sunflecks (ie intensities greater than 50 W m^{-2}) within the small treefall gap ranges from 77 to 84% in January and from 9.7 to 18.7% in July. Hence, there is a marked seasonal change in the availability of direct irradiance within the gap.

7.2.2.5 <u>10-min Average Readings of PPFD Within an Elliptical Treefall Gap</u>

Table 7.10 summarises results of various descriptive statistics applied to 10-min average readings of PPFD at six sites within the same elliptical treefall gap described above over the same measurement intervals. The results in Table 7.10 are therefore similar to those given in Table 7.9 for irradiance at three sites within this gap. Mean PPFDs at each gap site in January are also significantly higher than at corresponding sites in July (*t* values ranged from 3.3-5.0, $P<0.01$). Specifically, mean PPFD levels at the two gap sites at the southern end of the gap are 3.7-times higher than those in July (Table 7.10), while those at the centre and northern end of the gap are both 5.4-times higher than those in July.

The results in Table 7.10 also show that PPFD is not uniform within the gap in January, but unlike irradiance (Table 7.9), the centre and northern end of the gap experience similar PPFD levels. Overall, there appears to be more variability in PPFD within the gap (Table 7.10) compared with irradiance (Table 7.9), and this is expected given the small size of the sensors used to measure PPFD compared with those

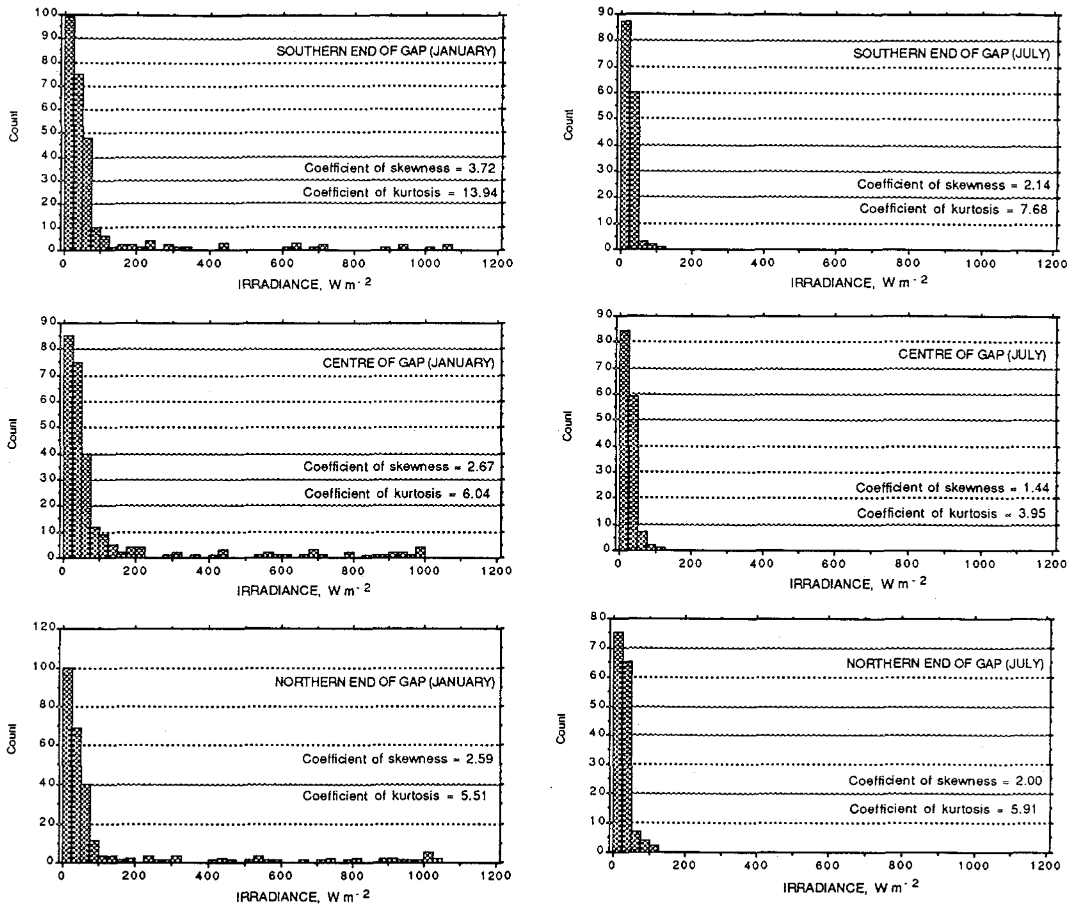

Figure 7.26. Frequency distributions of 10-min average readings for irradiance (W m^{-2}) at three sites within an elliptical treefall gap in the Curtain Fig forest at two contrasting times of the year (January and July).

Treefall Gap Sites	JANUARY PPFD (μ mol m^{-2} s^{-1}) Average flux (mean±1 SD) (range) Coefficient of variation	JANUARY Daily total (mol m^{-2} per day)	JULY PPFD (μ mol m^{-2} s^{-1}) Average flux (mean±1 SD) (range) Coefficient of variation	JULY Daily total (mol m^{-2} per day)
Gap (South #1)	120.9±312.0 (0.0-1709.7) 258.0% *n*=268	5.62 (9.6)*	33.0±41.0 (2.6-307.8) 123.9% *n*=152	1.31 (3.4)*
Gap (South #2)	138.22±319.8 (0.0-1710.2) 231.4% *n*=268	6.42 (11.0)*	36.8±32.0 (0.5-223.1) 87.0% *n*=152	1.46 (3.8)*
Gap (Centre #1)	215.6±434.7 (0.0-1832.4) 201.6% *n*=268	10.0 (17.2)*	39.8±46.1 (1.3-410.4) 115.8% *n*=152	1.57 (4.1)*
Gap (Centre #2)	183.0±393.9 (0.0-1720.3) 215.3% *n*=268	8.5 (14.6)*	34.4±28.5 (1.3-194.8) 82.9% *n*=152	1.36 (3.6)*
Gap (North #1)	227.2±497.1 (0.0-2045.4) 218.8% *n*=268	10.6 (18.1)*	34.9±39.4 (1.5-301.1) 113.0% *n*=152	1.38 (3.6)*
Gap (North #2)	152.7±340.7 (0.0-1697.0) 223.0% *n*=268	7.09 (12.2)*	36.2±48.8 (0.9-354.1) 134.8% *n*=152	1.43 (3.7)*

* Refers to the percentage of the daily total within the understorey relative to that above the forest canopy.

Table 7.10. Values of daily average photosynthetic photon flux density (PPFD) (μ mol m^{-2} s^{-1}) and total daily PPFD (mol m^{-2} per day) at three (paired) sites within an elliptical treefall gap in the Curtain Fig forest, northeast Queensland (January and July, 1987).

used to measure irradiance. However, statistical analyses have shown that PPFD differs significantly among the six gap sites in January only (one-way ANOVA: F=3.73, P<0.01; compared with July: F=0.52, P>0.05). Furthermore, multiple comparisons among sites for January showed that only some of the sites are significantly different from each other (gap south 1 and gap centre 1: t=3.15, P<0.01; gap south 1 and gap north 1: t=3.50, P<0.01; and gap south 2 and gap north 1: t=2.67, P<0.05). Nonetheless, a wide range of maximum PPFDs was experienced within the gap in January (1697.0-2045.4 μ mol m^{-2} s^{-1}) and July (194.8-410.4 μ mol m^{-2} s^{-1}), representing 66 to 80% and 11 to 20% of the maximum PPFD above the forest canopy at the respective times of the year. These ranges are much greater than those shown in Table 7.9 for maximum irradiance within the same gap over the same measurement intervals, but this discrepancy is accounted for by the spatially averaged irradiance measurements.

Percentages of daily PPFD at the six gap sites, relative to that above the forest, were considerably higher in January than in July (Table 7.10). In absolute terms, total daily PPFD above the forest in January was about 6- to 10-times greater than levels within the gap. In comparison, total daily PPFD above the forest in July was about 24- to 29-times greater than levels in the treefall gap. These figures confirm the fact that less PPFD reaches the forest floor compared with irradiance, particularly during July when solar altitudes are generally lower (Table 7.9).

The absolute differences in PPFD levels within the treefall gap are explained further in Fig. 7.27 which shows the distribution of percentiles for the six sites in January and July. The trends are similar to those shown in Fig. 7.25 for irradiance; median PPFDs within the gap in January (range: 25.8-43.9 μ mol m^{-2} s^{-1}) are similar to those in July (range: 23.4-31.2 μ mol m^{-2} s^{-1}), while the 90th percentiles are also considerably higher in January (range: 281.7-970.3 μ mol m^{-2} s^{-1}) than in July (range: 56.2-75.7 μ mol m^{-2} s^{-1}) for reasons stated earlier.

Furthermore, the box plots for January (Fig. 7.27) emphasise differences in PPFD among the six sites within the gap. In particular, the positions of the 90th percentile lines indicate a general increase across the gap from south to north, but the trend is not as clear as that shown in Fig. 7.25 for irradiance. Otherwise, the PPFD patterns within the gap for January (Fig. 7.27) are much the same as those exhibited for irradiance at the same time (Fig. 7.25), with data points above the 90th percentile lines corresponding with the direct penetration of the midday sun. Similarly, the 90th percentile lines are almost constant across the gap in July (Fig. 7.27), with data points above these lines being associated with major sunfleck events.

The frequency distributions of 10-min average PPFD readings at the six sites within the treefall gap for January and July are shown in Fig. 7.28. The data have been

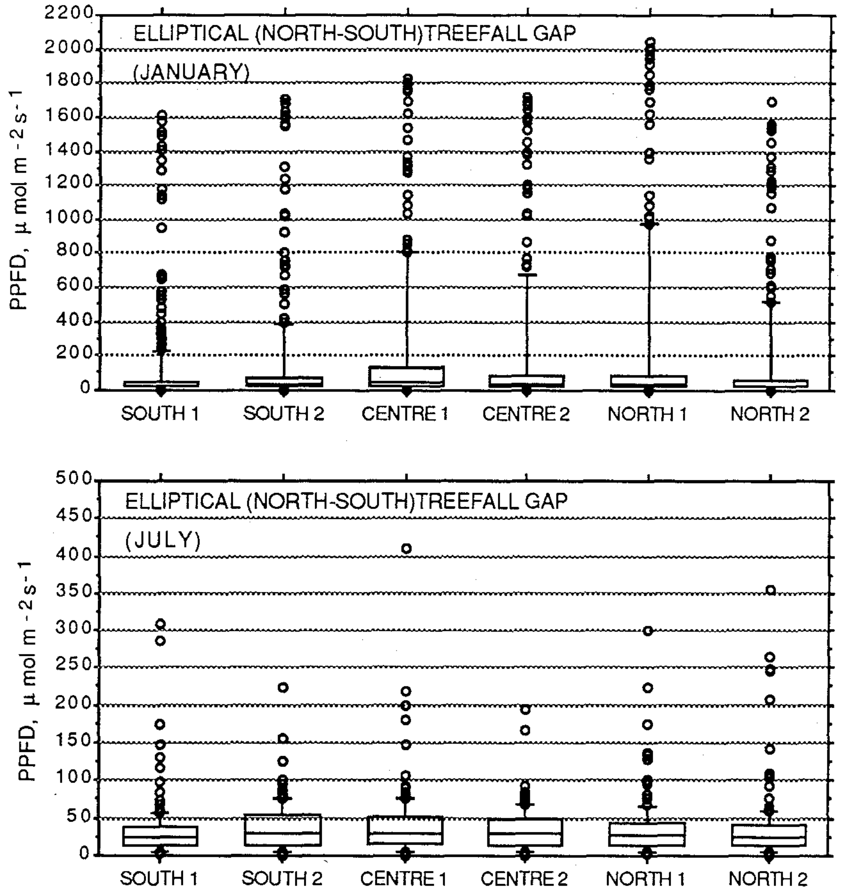

Figure 7.27. Distributions of percentiles (10-min average readings) for photosynthetic photon flux density (PPFD) (μ mol m^{-2} s^{-1}) at three (paired) sites within an elliptical treefall gap in the Curtain Fig forest at two contrasting times of the year (January and July). The five horizontal lines on the box plot show the 10, 25, 50, 75 and 90th percentiles, with values above and below the 10th and 90th percentile represented as data points. Note differences in vertical scales.

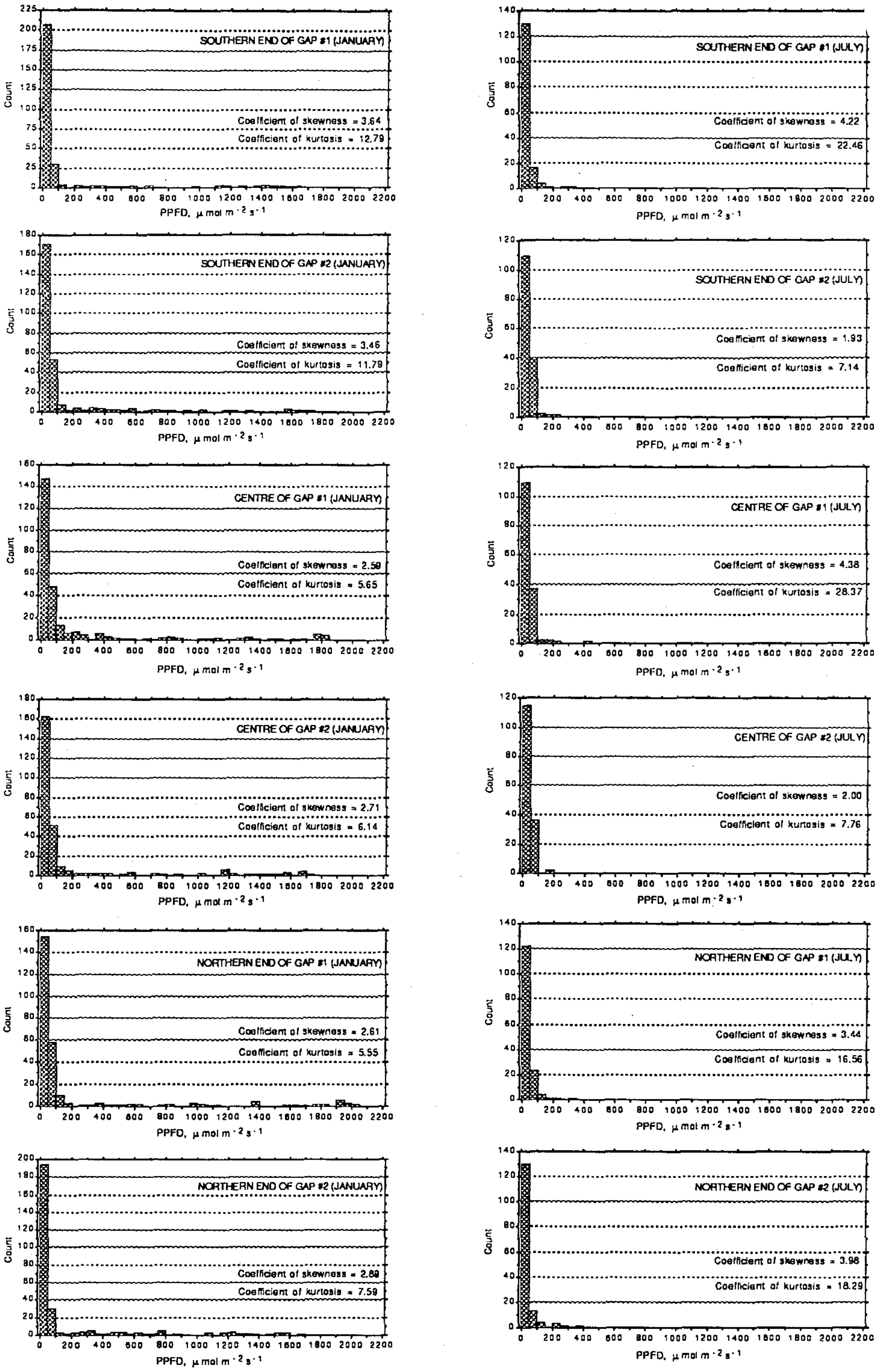

Figure 7.28. Frequency distributions of 10-min average readings for photosynthetic photon flux density (PPFD) (μ mol m^{-2} s^{-1}) at three (paired) sites within an elliptical treefall gap in the Curtain Fig forest at two contrasting times of the year (January and July).

sorted into class intervals of 50 μ mol m^{-2} s^{-1}. The histograms show little variability in the distribution of PPFD within the gap and the trends are very similar to those described earlier for irradiance (Fig. 7.26). In both January and July, the six sites within the gap also exhibited a high degree of positive skewness, and they were all leptokurtic. Moreover, at both times of the year the modal classes were also constant among sites (ie 0-50 μ mol m^{-2} s^{-1}) which provides further evidence that most PPFDs received in the gap consisted of diffuse radiation.

There are also marked differences in the distribution of PPFDs within the gap between January and July (Fig. 7.28). In January, about 23% of 10-min average readings at the most shaded site (gap south 1) were due to sunflecks (ie PPFDs greater than 50 μ mol m^{-2} s^{-1}) and about 43% at the least shaded site (gap north 1). By comparison, in July the values at the most shaded site (gap south 1) and least shaded site (gap centre 1) were 15 and 28%, respectively. On the basis of these measurements, the proportion of daily total PPFD contributed by sunflecks in the most and least shaded sites within the gap ranges from 73 to 89% in January and from 32 to 48% in July.

7.2.2.6 10-min Average Readings of PPFD Within a Circular Treefall Gap

Table 7.11 summarises results of various descriptive statistics applied to 10-min average readings of PPFD at four sites within a small circular treefall gap in the Curtain Fig forest (Fig. 5.4) in January and July. A hemispherical canopy photograph of this gap is shown in Plate 7.4 (Section 7.3.2). Because these measurements were made under similar sky conditions and solar angles to those described in the preceding section for a small elliptical gap in the same forest, it is possible to compare PPFD levels between these two gap types. Such a comparison may prove useful because the two gap types represent the most common sizes and configurations to be found in rainforests; the small circular gap (Plate 7.4) typifies that associated with the gradual *in situ* breakdown of a large canopy tree, while the small elliptical gap (Plate 7.5) typifies that associated with the forced toppling of a single intact canopy tree.

Despite the obvious differences in the configuration of the two canopy gaps, statistical analyses have shown that mean PPFD within the circular gap in January and July (Table 7.11) are not significantly different to those within the elliptical gap (Table 7.10) at the same times of year (for January: t=0.51, P>0.05; and for July: t=1.82, P>0.05). Hence, the distribution of PPFD within this small circular gap (Plate 7.4) is similar to that found in the small elliptical gap (Plate 7.5). However, this similarity would not necessarily occur if the same elliptical gap was aligned east-west, rather than north-south. This fact is explored in Section 7.3.2, when the results of modelling

Treefall Gap Sites	JANUARY PPFD (μ mol m^{-2} s^{-1}) Average flux (mean±1 SD) (range) Coefficient of variation	Daily total (mol m^{-2} per day)	JULY PPFD (μ mol m^{-2} s^{-1}) Average flux (mean±1 SD) (range) Coefficient of variation	Daily total (mol m^{-2} per day)
#1	163.0±303.1 (0.0-1360.2) 185.9% *n*=121	7.57 (14.3)*	40.1±22.0 (0.0-79.5) 54.8% *n*=55	1.59 (5.1)*
#2	179.6±285.5 (0.0-1331.8) 159.0% *n*=121	8.34 (15.7)*	39.1±31.1 (0.0-187.2) 79.5% *n*=55	1.55 (5.0)*
#3	155.6±251.5 (0.0-1305.5) 213.3% *n*=121	7.23 (13.6)*	19.5±14.5 (0.0-82.9) 74.5% *n*=55	0.77 (2.5)*
#4	225.4±306.5 (0.0-1468.1) 213.3% *n*=121	10.47 (19.7)*	19.3±11.8 (0.0-38.9) 61.5% *n*=55	0.76 (2.4)*

* Refers to the percentage of the daily total within the understorey relative to that above the forest canopy.

Table 7.11. Values of daily average photosynthetic photon flux density (PPFD) (μ mol m^{-2} s^{-1}) and total daily PPFD (mol m^{-2} per day) at four sites within a circular treefall gap in the Curtain Fig forest, northeast Queensland (January and July, 1987).

the penetration of PPFD into gaps of varying sizes and configurations are presented. Thus, in a similar manner to the elliptical gap (Table 7.10), mean PPFDs at the four sites within the circular gap in January are significantly higher than at corresponding sites in July (t values ranged from 3.0-4.98, $P<0.01$). Specifically, mean PPFDs within the gap are 8- to 12-times higher than those in July (Table 7.11).

There also appears to be some variability in the distribution of PPFD within the gap (Table 7.11). However, statistical analyses have shown that PPFD differs significantly among the four sites in July only (one-way ANOVA: $F=16.67$, $P<0.01$; compared with January: $F=1.44$, $P>0.05$). Multiple comparisons of means have shown that only sites 1 and 2 and sites 3 and 4 were not significantly different from each other (respective values were: $t=0.24$, $P>0.05$; and $t=0.26$, $P>0.05$). This result opposes that found for the elliptical gap (Table 7.10), whereby differences among sites were significant for January and not July. The reason for this discrepancy is likely to be related to the position of the sensors within the respective gaps, and hence emphasises the sampling problems associated with light measurement within complex vegetation.

Percentages of daily PPFD at the four gap sites, relative to that above the forest, were also considerably higher in January than in July (Table 7.11). In absolute terms, total daily PPFD above the forest in January was about 5- to 7-times greater than levels within the circular gap. In comparison, total daily PPFD in July was about 18- to 41-times greater than levels in the gap. These figures compare well with those given earlier for PPFD within the small elliptical gap (Table 7.10), and therefore demonstrate marked seasonal differences in light availability within small treefall gaps at this latitude.

These seasonal trends are examined further in Fig. 7.29 which shows the distribution of percentiles for PPFD at the four sites within the small circular gap in January and July. Median PPFDs within this gap in January (range: 54.6-79.4 μ mol m^{-2} s^{-1}) are only slightly higher than those within the same gap in July (range: 20.6-40.9 μ mol m^{-2} s^{-1}). However, in a similar way to the small elliptical gap (Fig. 7.27), the 90th percentiles in the circular gap (Fig. 7.29) are considerably higher in January (range: 435.7-599.5 μ mol m^{-2} s^{-1}) than in July (range: 33.4-68.7 μ mol m^{-2} s^{-1}). Hence, the data points above the 90th percentile lines in January (Fig. 7.29) are associated with the direct penetration of the midday sun into the gap, and those in July are only associated with major sunfleck events.

The frequency distribution of 10-min average PPFD readings at the four sites within the small circular gap for January and July are shown in Fig. 7.30. In January, the trends are very similar to those illustrated in Fig. 7.28 for the small elliptical gap at the same time of year; whereby all sites showed high degrees of positive skewness and kurtosis (Fig. 7.30). However, two of the four sites in July exhibited moderate to

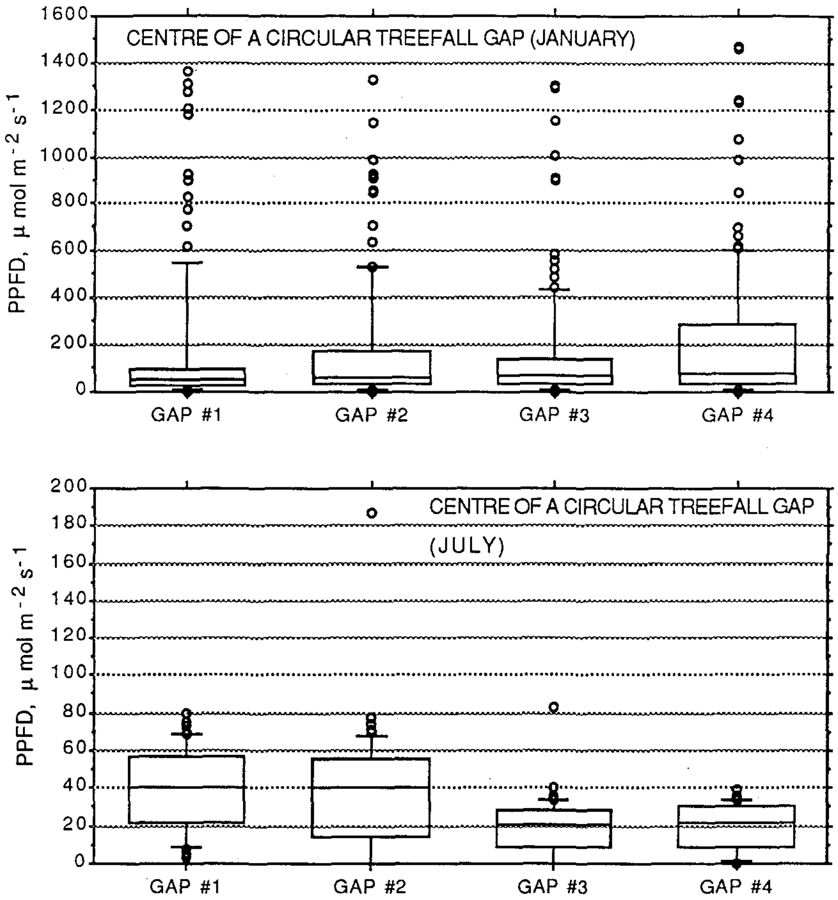

Figure 7.29. Distributions of percentiles (10-min average readings) for photosynthetic photon flux density (PPFD) (μ mol m^{-2} s^{-1}) at four sites within a circular treefall gap in the Curtain Fig forest at two contrasting times of the year (January and July). The five horizontal lines on the box plot show the 10, 25, 50, 75 and 90th percentiles, with values above and below the 10th and 90th percentile represented as data points. Note differences in vertical scales.

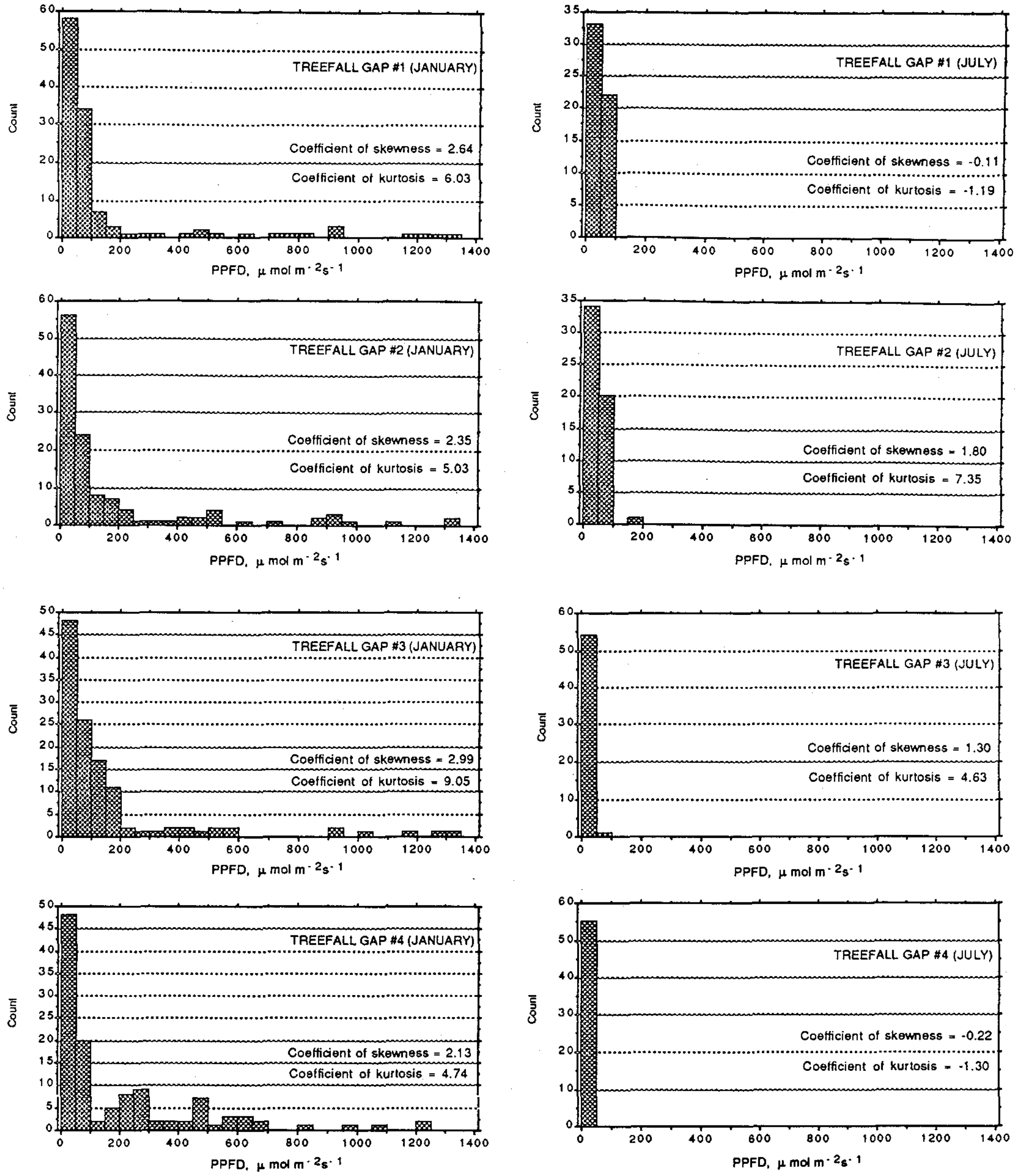

Figure 7.30. Frequency distributions of 10-min average readings for photosynthetic photon flux density (PPFD) (μ mol m^{-2} s^{-1}) at four sites within a circular treefall gap in the Curtain Fig forest at two contrasting times of the year (January and July).

high degrees of negative skewness, and generally low kurtosis. The position of the sensors in the gap, together with the generally cloudy weather conditions over the measurement interval are likely reasons for this apparent anomaly. Nonetheless, at both times of the year the modal classes are constant (0-50 μ mol m^{-2} s^{-1}), showing in the same way as the elliptical gap (Fig. 7.28), that most PPFDs within the circular gap consist of diffuse radiation.

There are also marked differences in the distribution of PPFDs within the circular gap between January and July (Fig. 7.30). In January, about 50% of 10-min average readings at the most shaded site (#3) were due to sunflecks (ie PPFDs greater than 50 μ mol m^{-2} s^{-1}) and about 60% at the least shaded site (#4). By comparison, in July the values at the most shaded site (#4) and least shaded site (#1) were 0 and 40%, respectively. On the basis of these measurements, the proportion of daily total PPFD contributed by sunflecks in the most and least shaded sites within the small circular gap ranges from 87 to 91% in January and from 0 to 57% in July.

7.3 SEASONAL VARIATIONS IN DAILY PPFD ABOVE AND BENEATH TROPICAL RAINFOREST CANOPIES

This section presents results of hemispherical (fisheye) canopy photography measurements of daily PPFD for the 22nd day of each month within rainforest understoreys and gaps, and across the rainforest-open forest boundary (ecotone). Field sampling and data analysis techniques have already been described in Section 6.4.3.

The results evaluated here are considered as the first attempt to model light availability above and beneath rainforest canopies under a range of sky conditions. This was made possible by combining Anderson's (1971) manual technique for determining diffuse and direct site factors beneath plant canopies from fisheye photographs (Section 6.3.2) with the sky-irradiance computer model described in Section 3.1.

7.3.1 Understorey Light Regimes

7.3.1.1 Curtain Fig Forest Before and After Tropical Cyclone Winifred

Table 7.12 summarises results of various descriptive statistics applied to diffuse and direct site factors for the 22nd day of each month, obtained from 20 photosites within the understorey of the Curtain Fig forest (Fig. 5.4) before and immediately after

FULL YEAR	DIFFUSE SITE FACTORS (%) Pre-Cyclone mean±1 SD median (range) cv	Post-Cyclone mean±1 SD median (range) cv	Post-hoc comparison of means (Scheffe *F*-test)
	7.38±3.35 7.03 (2.35-15.71) 45.4%	16.01±5.6 14.45 (6.60-20.12) 35.0%	*F*=37.43 (*P*<0.01)

SOLAR DECLINATION (Approximate date)	DIRECT SITE FACTORS (%) Pre-Cyclone mean±1 SD median (range) cv	Post-Cyclone mean±1 SD median (range) cv	Post-hoc comparison of means (Scheffe *F*-test)
-23.5° (Dec 22)	2.95±2.87 2.08 (0.44-11.02) 97.4%	7.37±4.81 6.05 (1.93-20.92) 65.3%	*F*=12.45 (*P*<0.01)
-20.0° (Jan 22/ Nov 22)	2.84±2.39 2.07 (0.31-9.15) 84.2%	7.65±6.02 6.23 (1.28-20.12) 78.6%	*F*=11.05 (*P*<0.01)
-11.0° (Feb 22/ Oct 22)	2.73±2.12 2.49 (0.38-7.11) 77.9%	8.50±6.44 5.96 (1.84-23.30) 75.7%	*F*=14.55 (*P*<0.01)
0.0° (Mar 21/ Sep 23)	2.67±2.80 1.78 (0.09-11.27) 104.9%	8.28±6.76 6.45 (1.67-31.55) 81.6%	*F*=11.79 (*P*<0.01)
+11.0° (Apr 22/ Aug 22)	1.26±0.87 1.27 (0.08-3.92) 68.8%	4.78±2.67 4.21 (1.24-10.87) 56.2%	*F*=31.08 (*P*<0.01)
+20.0° (May 22/ Jul 22)	1.31±1.19 0.99 (0.12-5.01) 91.2%	4.39±2.81 3.73 (1.10-12.21) 64.0%	*F*=20.43 (*P*<0.01)
+23.5 (Jun 22)	1.27±1.33 0.90 (0.02-5.68) 104.1%	3.80±2.26 3.35 (0.59-9.78) 59.5%	*F*=18.57 (*P*<0.01)

Table 7.12. Values of average diffuse and direct site factors (%) obtained from 20 hemispherical (fisheye) canopy photographs taken at 5-m intervals along a 100-m transect through the understorey of the Curtain Fig forest, northeast Queensland in July 1985 (pre-cyclone) and February 1986 (post-cyclone). The direct site factors are given for solar declinations approximately equal to the 22nd day of each month, while a full-year diffuse site factor is given (cv = coefficient of variation, %).

Tropical Cyclone 'Winifred'. This unique record of potential light availability within the understorey of a tropical rainforest before and after a cyclone is a valuable contribution towards understanding rainforest dynamics in regions affected by such weather systems. It should be noted that this forest site experiences some seasonal variation in canopy cover, with the greatest leaf loss from August-October.

Both diffuse and direct site factors increased significantly in the understorey of the Curtain Fig forest as a consequence of the slight-to-moderate canopy disturbance inflicted by the cyclone (Table 7.12; *post-hoc* Scheffe F-test, $P<0.01$). The marked change in overstorey density, before and after the cyclone, is demonstrated in Plates 7.1 and 7.2, respectively. The fisheye canopy photographs represent photosites where the diffuse site factors are similar to the median values obtained from the before and after measurements taken along the 100-m transect (Table 7.12). The cyclone appears to have resulted in a more uniform light environment in the rainforest understorey because the coefficients of variation for the diffuse and direct site factors are somewhat lower after the cyclone than before (Table 7.11). Therefore, not only has the cyclone increased the amount of light within the understorey, it has also reduced the complexity of the rainforest light regime.

As discussed in Section 2.5.3.3, the red to far-red (R:FR) ratio is an important consideration in any study concerned with light regimes in rainforests because of its profound influence on growth and development in understorey plants. Lee (1987) examined the relationship between log percentage of full sun PPFD and R:FR at two Central American rainforest sites, and found a high degree of correlation between the two variables at both sites ($r>0.95$). If the data for the two sites is combined and Lee's original equation re-arranged, then the following regression function may be used for the estimation of the R:FR:

$$\text{Log (R:FR)} = (\text{TOTAL SITE FACTOR} + 2.943)\ /2.26, \qquad (7.3.1)$$

where the total site factor (obtained from fisheye photographs) represents the percentage of full sun PPFD under cloudless skies.

The distribution of percentile values for total site factors and R:FR ratios (estimated using Eqn 7.3.1) before and after the cyclone are shown in Fig. 7.31. The box plots indicate that median total site factors and R:FR ratios have increased substantially following the cyclone. For example, median total site factors before the cyclone ranged from 2.5% on June 22 to 3.4% on October 22/February 22; immediately after the cyclone, median total site factors ranged from 6.0% on June 22 to 8.6% on November 22/January 22. Likewise, median R:FR ratios before the cyclone ranged from 0.38 on June 22 to 0.45 on October 22/February 22, while median values after the cyclone

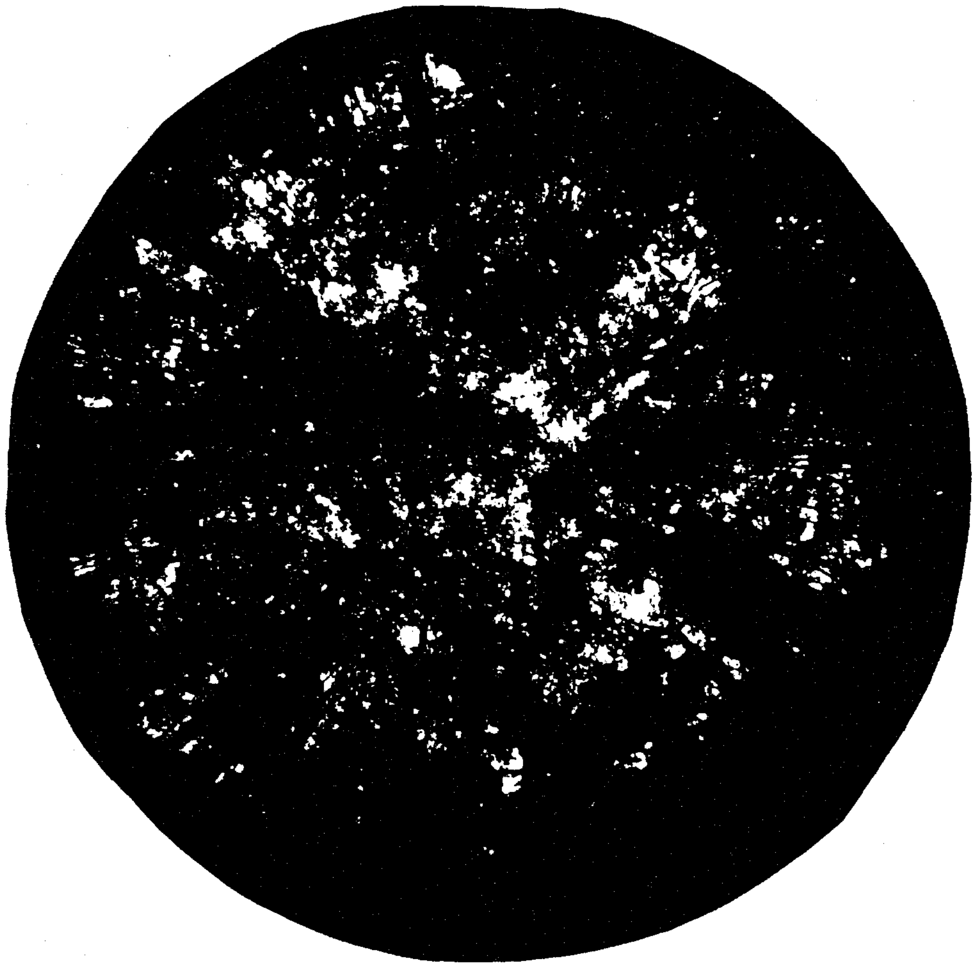

Plate 7.1. A hemispherical (fisheye) canopy photograph taken at photosite 19 within the Curtain Fig forest, northeast Queensland before Tropical Cyclone Winifred (July 1985). The diffuse site factor of 6.97% is similar to the median value for the 20 photosites along the 100-m transect (Table 7.12).

Plate 7.2. A hemispherical (fisheye) canopy photograph taken at photosite 13 within the Curtain Fig forest, northeast Queensland immediately after Tropical Cyclone Winifred (February 1986). The diffuse site factor of 14.36% is similar to the median value for the 20 photosites along the 100-m transect (Table 7.12).

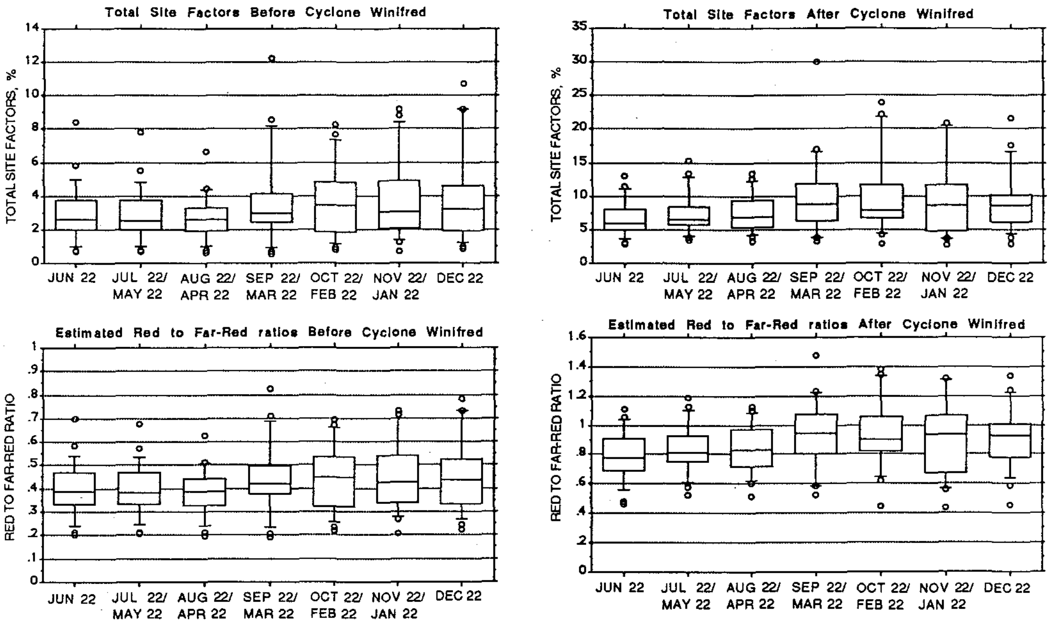

Figure 7.31. Distributions of percentiles for total site factors (%) and estimated red to far-red (R:FR) ratios obtained from 20 hemispherical (fisheye) canopy photographs taken at 5-m intervals along a 100-m transect in the understorey of the Curtain Fig forest, northeast Queensland in July 1985 (pre-cyclone) and February 1986 (post-cyclone). Total site factors (%) and R:FR ratios are given for solar declinations approximately equal to the 22nd day of each month. The R:FR ratios were estimated using Eqn 7.3.1. The five horizontal lines on the box plot show the 10, 25, 50, 75 and 90th percentiles, with values above and below the 10th and 90th percentile represented as data points. Note differences in vertical scales.

ranged from 0.78 on June 22 to 0.94 on November 22/January 22. Hence, cyclone-induced canopy disturbance has altered both the quantity and quality of light available to plants in the understorey of this forest.

The photoelectric measurements have shown that the percentage of daily total PPFD within the understorey of the Curtain Fig forest under sunny conditions ranged from 1.1 to 2.2% in January and from 1.4 to 1.8% in July (Tables 7.4 and 7.8). On the other hand, the total site factors before the cyclone, determined from fisheye photographs, ranged from 0.7 to 9.2% in January and from 0.7 to 7.8% in July. There are two main explanations for this apparent discrepancy: (1) the photoelectric measurements in the field were subject to intervening cloud periods and leaf flutter , which would reduce the incidence of sunflecks in the understorey; and (2) the photographic measurements ignore penumbral effects and hence they tend to over-estimate the quantities of direct PPFD reaching the understorey.

Nonetheless, the fisheye technique is very useful for determining order-of-magnitude seasonal differences among micro-environments, such as gap and understorey, as well as proving its worth as a means of assessing the degree of change in the light environment of a rainforest understorey due to canopy disturbance caused by a tropical cyclone, and hence has applications for assessment of the effects of various human practices such as logging.

Table 7.13 summarises results of various descriptive statistics applied to daily total PPFD under four sky conditions for the 22nd day of each month, obtained from the 20 understorey photosites before and after the cyclone. As expected, given the substantial increase in diffuse and direct site factors immediately after the cyclone (Table 7.12), daily total PPFD is higher in the understorey after the cyclone at all times of the year and under all sky conditions. For example, under cloudless skies mean daily PPFD after the cyclone on June 22 is 2.4-times higher than that before the cyclone, while mean daily PPFD after the cyclone on October 22/February 22 is 2.7-times higher than that before. Likewise, under the three cloud types (Table 7.13), mean daily PPFD after the cyclone is over 2-times higher than that before the cyclone throughout the year.

In agreement with the photoelectric measurements of PPFD discussed in the previous section, the fisheye photography results also demonstrate seasonal changes in light availability in the understorey of this forest both before and after the cyclone (Table 7.13). Statistical analyses of the before-cyclone data have shown that daily total PPFD differs significantly among the seven times of year under all sky conditions (one-way ANOVA: for cloudless F=3.93, P<0.01; for cirrostratus F=3.39, P<0.01; for altostratus F=3.45, P<0.01; and for stratus F=3.56, P<0.01). However, multiple comparisons among the seven times of year indicate that only some months are

Solar Declination (approx. date)	BEFORE CYCLONE TOTAL PPFD PPFD (CLOUDLESS) (mol m^{-2} per day) mean±1 SD (range) median	PPFD (CIRROSTRATUS) (mol m^{-2} per day) mean±1 SD (range) median	PPFD (ALTOSTRATUS) (mol m^{-2} per day) mean±1 SD (range) median	PPFD (STRATUS) (mol m^{-2} per day) mean±1 SD (range) median
-23.5° (Dec 22)	2.75±2.04 (0.59-7.67) 2.30	2.96±1.79 (0.77-6.71) 2.61	2.66±1.21 (0.85-5.67) 2.54	1.59±0.72 (0.51-3.38) 1.51
-20.0° (Nov 22/ Jan 22)	2.68±1.76 (0.51-6.58) 2.19	2.89±1.63 (0.71-6.45) 2.48	2.65±1.20 (0.84-5.66) 2.53	1.58±0.71 (0.50-3.36) 1.50
-11.0° (Oct 22/ Feb 22)	2.53±1.58 (0.54-5.72) 2.37	2.77±1.49 (0.73-5.80) 2.51	2.56±1.16 (0.82-5.45) 2.44	1.52±0.69 (0.48-3.24) 1.45
-0.0° (Sep 22/ Mar 22)	2.39±1.81 (0.36-7.78) 1.90	2.59±1.60 (0.60-7.23) 2.27	2.35±1.07 (0.75-5.01) 2.24	1.40±0.63 (0.44-2.97) 1.33
+11.0° (Aug 22/ Apr 22)	1.49±0.77 (0.34-3.70) 1.43	1.93±0.93 (0.55-4.46) 1.78	2.03±0.92 (0.65-4.32) 1.93	1.20±0.55 (0.38-2.56) 1.15
+20.0° (Jul 22/ May 22)	1.38±0.80 (0.34-3.73) 1.21	1.76±0.88 (0.51-4.18) 1.63	1.76±0.80 (0.56-3.74) 1.67	1.03±0.47 (0.33-2.20) 0.98
+23.5° (Jun 22)	1.31±0.79 (0.3-3.76) 1.16	1.67±0.83 (0.48-3.96) 1.52	1.65±0.75 (0.52-3.50) 1.57	0.97±0.44 (0.31-2.07) 0.93

Solar Declination (approx. date)	AFTER CYCLONE TOTAL PPFD PPFD (CLOUDLESS) (mol m^{-2} per day) mean±1 SD (range) median	PPFD (CIRROSTRATUS) (mol m^{-2} per day) mean±1 SD (range) median	PPFD (ALTOSTRATUS) (mol m^{-2} per day) mean±1 SD (range) median	PPFD (STRATUS) (mol m^{-2} per day) mean±1 SD (range) median
-23.5° (Dec 22)	6.53±3.43 (2.05-15.56) 6.11	6.74±2.98 (2.35-13.90) 6.08	5.78±2.02 (2.38-9.65) 5.22	3.44±1.20 (1.42-5.75) 3.11
-20.0° (Nov 22/ Jan 22)	6.66±4.10 (1.95-14.88) 6.17	6.87±3.46 (2.26-13.70) 6.25	5.77±2.02 (2.38-9.62) 5.20	3.43±1.20 (1.41-5.72) 3.09
-11.0° (Oct 22/ Feb 22)	6.92±4.21 (1.93-16.56) 5.46	6.92±3.68 (2.23-15.10) 5.80	5.56±1.94 (2.29-9.27) 5.01	3.30±1.15 (1.36-5.50) 2.73
-0.0° (Sep 22/ Mar 22)	6.32±3.98 (2.13-19.19) 5.56	6.36±3.23 (2.32-15.96) 5.79	5.11±1.79 (2.11-8.52) 4.61	3.03±1.06 (1.25-5.05) 2.73
+11.0° (Aug 22/ Apr 22)	4.09±1.66 (1.80-7.44) 3.79	4.71±1.75 (2.14-8.35) 4.15	4.40±1.54 (1.82-7.35) 3.97	2.61±0.91 (1.08-4.36) 2.36
+20.0° (Jul 22/ May 22)	3.54±1.54 (1.61-7.36) 3.15	4.11±1.57 (1.86-7.52) 3.49	3.81±1.33 (1.57-6.36) 3.44	2.24±0.78 (0.92-3.74) 2.02
+23.5° (Jun 22)	3.19±1.29 (1.40-6.16) 2.87	3.78±1.38 (1.62-6.55) 3.31	3.57±1.25 (1.47-5.96) 1.57	2.11±0.74 (0.87-3.53) 1.91

Table 7.13. Values of average daily total photosynthetic photon flux density (PPFD) (mol m^{-2} per day) within the understorey of the Curtain Fig forest under four sky conditions before and immediately after Tropical Cyclone 'Winifred' (n=20 photographs). Daily total PPFDs are given for solar declinations approximately equal to the 22nd day of each month.

PRE-CYCLONE MULTIPLE COMPARISONS							
Solar Declination	-23.5° (Dec 22)	-20.0° (Nov 22/ Jan 22)	-11.0° (Oct 22/ Feb 22)	0.0° (Sep 22/ Mar 22)	+11.0° (Aug 22/ Apr 22)	+22.0° (Jul 22/ May 22)	+23.5.0° (Jun 22)
-23.5°(Dec 22)		cl. n.s cs. n.s as. n.s st. n.s	cl. n.s cs. n.s as. n.s st. n.s	cl. n.s cs. n.s as. n.s st. n.s	cl.# cs. n.s as. n.s st. n.s	cl.# cs.# as.# st.#	cl.## cs.# as.## st.##
-20.0° (Nov 22/ Jan 22)	cl. n.s cs. n.s as. n.s st. n.s		cl. n.s cs. n.s as. n.s st. n.s	cl. n.s cs. n.s as. n.s st. n.s	cl.# cs. n.s as. n.s st. n.s	cl.# cs.# as.# st.#	cl.# cs.# as.## st.##
-11.0° (Oct 22/ Feb 22)	cl. n.s cs. n.s as. n.s st. n.s	cl. n.s cs. n.s as. n.s st. n.s		cl. n.s cs. n.s as. n.s st. n.s	cl. n.s cs. n.s as. n.s st. n.s	cl. n.s cs. n.s as. n.s st. n,s	cl.# cs. n.s as.# st.#
0.0° (Sep 22/ Mar 22)	cl. n.s cs. n.s as. n.s st. n.s	cl. n.s cs. n.s as. n.s st. n.s	cl. n.s cs. n.s as. n.s st. n.s		cl. n.s cs. n.s as. n.s st. n.s	cl. n.s cs. n.s as. n.s st. n.s	cl. n.s cs. n.s as. n.s st. n.s
+11.0° (Aug 22/ Apr 22)	cl.# cs. n.s as. n.s st. n.s	cl.# cs. n.s as. n.s st. n.s	cl. n.s cs. n.s as. n.s st. n.s	cl. n.s cs. n.s as. n.s st. n.s		cl. n.s cs. n.s as. n.s st. n.s	cl. n.s cs. n.s as. n.s st. n.s
+20.0° (Jul 22/ May 22)	cl.# cs.# as.# st.#	cl.# cs.# as.# st.#	cl. n.s cs. n.s as. n.s st. n.s	cl. n.s cs. n.s as. n.s st. n.s	cl. n.s cs. n.s as. n.s st. n.s		cl. n.s cs. n.s as. n.s st. n.s
+23.5°(Jun 22)	cl.## cs.# as.## st.##	cl.# cs.# as.## st.##	cl.# cs. n.s as.# st.#	cl. n.s cs. n.s as. n.s st. n.s	cl. n.s cs. n.s as. n.s st. n.s	cl. n.s cs. n.s as. n.s st. n.s	

A priori multiple comparison of means (t-test): ##, highly significant difference ($P<0.01$); #, significant difference ($P<0.05$); n.s, no significant difference ($P>0.05$).
cl. = cloudless sky; cs. = cirrostratus cloud; as. = altostratus cloud; st. = stratus cloud.

POST-CYCLONE MULTIPLE COMPARISONS							
Solar Declination	-23.5° (Dec 22)	-20.0° (Nov 22/ Jan 22)	-11.0° (Oct 22/ Feb 22)	0.0° (Sep 22/ Mar 22)	+11.0° (Aug 22/ Apr 22)	+22.0° (Jul 22/ May 22)	+23.5.0° (Jun 22)
-23.5°(Dec 22)		cl. n.s cs. n.s as. n.s st. n.s	cl. n.s cs. n.s as. n.s st. n.s	cl. n.s cs. n.s as. n.s st. n.s	cl. n.s cs. n.s as. n.s st. n.s	cl.# cs.# as.## st.##	cl.## cs.## as.## st.##
-20.0° (Nov 22/ Jan 22)	cl. n.s cs. n.s as. n.s st. n.s		cl. n.s cs. n.s as. n.s st. n.s	cl. n.s cs. n.s as. n.s· st. n.s	cl.# cs. n.s as. n.s st. n.s	cl.## cs.## as.## st.##	cl.## cs.## as.## st.##
-11.0° (Oct 22/ Feb 22)	cl. n.s cs. n.s as. n.s st. n.s	cl. n.s cs. n.s as. n.s st. n.s		cl. n.s cs. n.s as. n.s st. n.s	cl.# cs. n.s as. n.s st. n.s	cl.## cs.## as.## st.##	cl.## cs.## as.## st.##
0.0° (Sep 22/ Mar 22)	cl. n.s cs. n.s as. n.s st. n.s	cl. n.s cs. n.s as. n.s st. n.s	cl. n.s cs. n.s as. n.s st. n.s		cl. n.s cs. n.s as. n.s st. n.s	cl.# cs.# as. n.s st. n.s	cl.## cs.# as.# st.#
+11.0° (Aug 22/ Apr 22)	cl. n.s cs. n.s as. n.s st. n.s	cl.# cs. n.s as. n.s st. n.s	cl.# cs. n.s as. n.s st. n.s	cl. n.s cs. n.s as. n.s st. n.s		cl. n.s cs. n.s as. n.s st. n.s	cl. n.s cs. n.s as. n.s st. n.s
+20.0° (Jul 22/ May 22)	cl.# cs.# as.## st.##	cl.## cs.## as.## st.##	cl.## cs.## as.## st.##	cl.# cs.# as. n.s st. n.s	cl. n.s cs. n.s as. n.s st. n.s		cl. n.s cs. n.s as. n.s st. n.s
+23.5°(Jun 22)	cl.## cs.## as.## st.##	cl.## cs.## as.## st.##	cl.## cs.## as.## st.##	cl.## cs.# as.# st.#	cl. n.s cs. n.s as. n.s st. n.s	cl. n.s cs. n.s as. n.s st. n.s	

A priori multiple comparison of means (t-test): ##, highly significant difference ($P<0.01$); #, significant difference ($P<0.05$); n.s, no significant difference ($P>0.05$).
cl. = cloudless sky; cs. = cirrostratus cloud; as. = altostratus cloud; st. = stratus cloud.

Table 7.14. *A priori* multiple comparisons (t-tests) of mean daily total photosynthetic photon flux density (PPFD) among seven times of the year (solar declinations) for cloudless skies, and cirrostratus, altostratus and stratus cloud types, within the understorey of the Curtain Fig forest before and immediately after the cyclone.

significantly different from each other (Table 7.14, before-cyclone). Generally, daily PPFD levels in the understorey of the Curtain Fig forest are significantly lower during the winter months (May-July) than those during the summer months (October-February).

Statistical analyses of the after-cyclone data have also shown that daily total PPFD differs significantly among the seven times of year under all sky conditions (one-way ANOVA: for cloudless F=5.42, P<0.01; for cirrostratus F=5.51, P<0.01; for altostratus F=5.80, P<0.01; and for stratus F=5.98, P<0.01). Furthermore, multiple comparisons among the times of year indicate highly significant differences among a larger number of months than those found for the before-cyclone data (Table 7.14). A cursory examination of the canopy before the cyclone (Plate 7.1) compared with that immediately after (Plate 7.2) reveals that there are a greater number of canopy openings near the zenith after the cyclone than before. This result supports the idea that cyclone-induced canopy disturbance results in more significant seasonal variations in light availability within the understorey of this forest because during the summer months (September-March) more direct PPFD (sunflecks) are able to penetrate through the disturbed canopy (Plate 7.2) compared with the undisturbed canopy (Plate 7.1).

7.3.1.2 Pine Creek Forest

Table 7.15 summarises results of various descriptive statistics applied to daily total PPFD under four sky conditions for the 22nd day of each month, obtained from 20 photosites within the understorey of the Pine Creek forest (Fig. 5.5) in July 1985. Diffuse and direct site factors are also included in the table for the understorey of this forest. Because these photographs were obtained at more or less the same times as those taken in the Curtain Fig forest before the cyclone (Tables 7.12 and 7.13), it is possible to compare light conditions between the two forest types.

Statistical analyses have shown that there are no significant differences in both diffuse and direct site factors between the Pine Creek understorey and the Curtain Fig understorey before the cyclone (t values ranged from 0.13-1.95, P>0.05). It would appear, therefore, that light conditions are similar within both understoreys despite the fact that the Curtain Fig forest (Fig. 5.4) is almost twice as tall as the Pine Creek forest (Fig. 5.5). However, the almost continuous layer of fan palms (*Licuala ramsayii*) in the Pine Creek forest sub-canopy (Fig. 5.5) exerts a strong blocking effect on light penetration into the understorey. This is demonstrated in Plate 7.3 which shows a fisheye canopy photograph taken within the understorey of this forest at a photosite where the diffuse site factor is similar to the median value obtained from the 20

Solar Declination (approx. date)	PPFD (CLOUDLESS) (mol m^{-2} per day) mean±1 SD (range) median	PPFD (CIRROSTRATUS) (mol m^{-2} per day) mean±1 SD (range) median	PPFD (ALTOSTRATUS) (mol m^{-2} per day) mean±1 SD (range) median	PPFD (STRATUS) (mol m^{-2} per day) mean±1 SD (range) median	DIRECT SITE FACTORS (%) mean±1 SD (range) median	FULL-YEAR DIFFUSE SITE FACTOR (%) mean±1 SD (range) median
	TOTAL PPFD					
-23.5° (Dec 22)	3.17±2.10 (0.49-7.59) 2.75	3.42±1.82 (0.73-6.61) 3.10	3.14±1.31 (0.94-5.31) 2.96	1.87±0.78 (0.56-3.16) 1.76	3.34±2.95 (0.17-10.33) 2.76	8.71±3.66 (2.60-14.70) 8.20
-20.0° (Nov 22/ Jan 22)	3.22±2.20 (0.48-7.03) 2.43	3.51±1.94 (0.73-6.39) 2.91	3.13±1.31 (0.94-5.29) 2.95	1.86±0.78 (0.56-3.15) 1.78	3.45±3.18 (0.20-9.87) 2.17	
-11.0° (Oct 22/ Feb 22)	2.77±1.64 (0.44-5.90) 2.55	3.11±1.58 (0.70-6.12) 2.91	3.02±1.26 (0.90-5.10) 2.85	1.79±0.75 (0.54-3.03) 1.69	2.82±2.11 (0.13-6.98) 2.53	
-0.0° (Sep 22/ Mar 22)	2.79±1.46 (0.37-5.48) 2.82	3.06±1.38 (0.65-5.21) 3.00	2.78±1.16 (0.83-4.69) 2.62	1.65±0.69 (0.49-2.78) 1.55	3.21±2.23 (0.03-7.44) 3.14	
+11.0° (Aug 22/ Apr 22)	2.07±1.11 (0.43-4.20) 1.73	2.46±1.16 (0.69-4.57) 2.26	2.39±1.00 (0.72-4.04) 2.26	1.42±0.59 (0.42-2.40) 1.34	2.24±1.58 (0.13-5.44) 1.66	
+20.0° (Jul 22/ May 22)	1.82±0.96 (0.37-3.69) 1.60	2.22±1.05 (0.60-3.99) 2.01	2.07±0.87 (0.62-3.50) 1.95	1.22±0.51 (0.36-2.06) 1.15	2.08±1.50 (0.03-5.27) 1.64	
+23.5° (Jun 22)	1.71±0.88 (0.49-3.49) 1.44	2.04±0.94 (0.60-3.78) 1.85	1.94±0.81 (0.58-3.28) 1.83	1.15±0.48 (0.34-1.94) 1.08	1.98±1.48 (0.41-5.19) 1.56	

Table 7.15. Values of average daily total photosynthetic photon flux density (PPFD) (mol m^{-2} per day) within the understorey of the Pine Creek forest under four sky conditions obtained from 20 hemispherical (fisheye) canopy photographs taken at 5-m intervals along a 100-m transect through the understorey in July 1985. Daily total PPFDs and direct site factors (%) are given for solar declinations approximately equal to the 22nd day of each month, while a full-year diffuse site factor (%) is given.

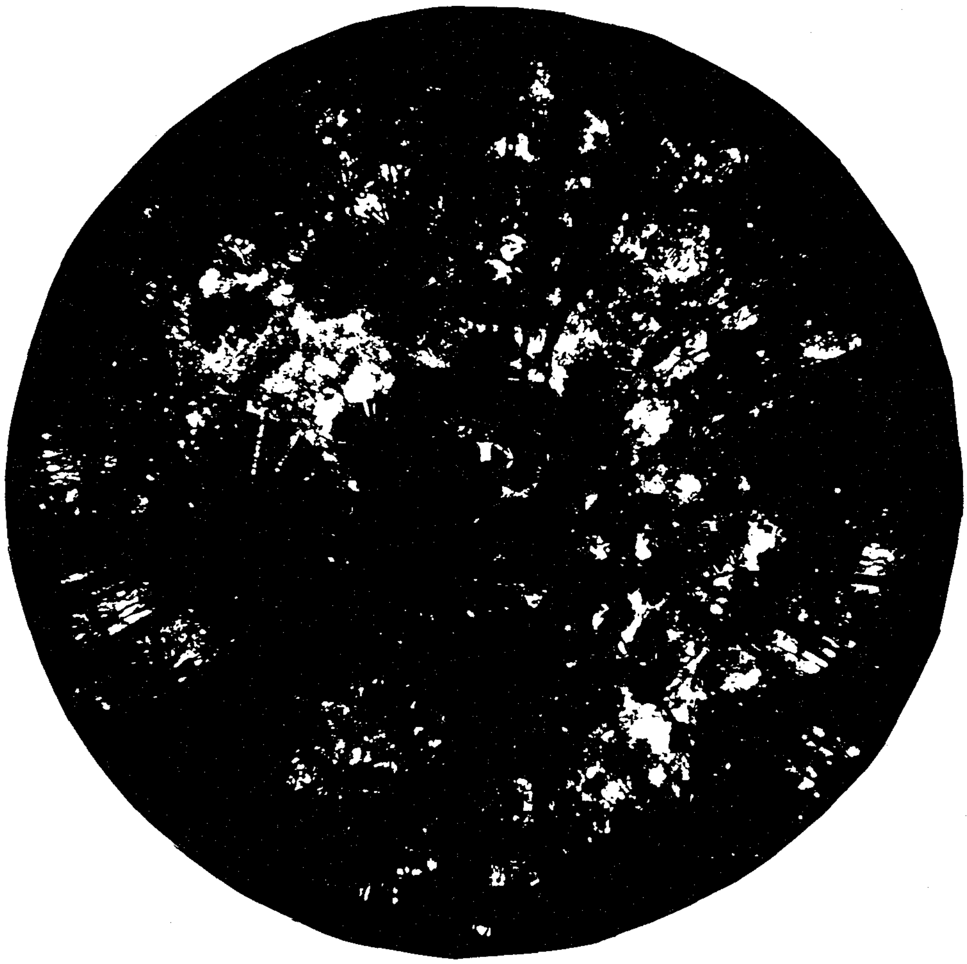

Plate 7.3. A hemispherical (fisheye) canopy photograph taken at photosite 11 within the Pine Creek forest, northeast Queensland in July 1985. The diffuse site factor of 8.00% is similar to the median value for the 20 photosites along the 100-m transect (Table 7.15).

photosites along the 100-m transect (Table 7.15). Because the fan palms have almost horizontal leaf angles, they tend to obscure the sky (and hence prevent the penetration of direct light) at solar angles greater than about 60° above the horizon (Plate 7.3). On the other hand, the deeper canopy layer in the Curtain Fig forest (Fig. 7.4) facilitates a more gradual interception of light by leaves in the canopy and this results in a diffuse site factor for this forest (Plate 7.1) that is similar to that for the Pine Creek forest (Plate 7.3). In other words, the Pine Creek forest intercepts most of the penetrating light within the comparatively narrow fan palm layer, while the Curtain Fig forest intercepts a similar amount of light but over a considerably deeper layer of leaves.

Differences and similarities between the two forest types are illustrated further by comparing the distribution of percentiles for total site factors and red to far-red (R:FR) ratios for the Pine Creek understorey (Fig. 7.32) with those obtained for the Curtain Fig understorey before the cyclone (Fig. 7.31). Median total site factors in the Pine Creek understorey are similar to those reported earlier for the Curtain Fig understorey, ranging from 3.2% on June 22 to 4.4% on September 22/March 22. Likewise, median R:FR ratios are also similar to the Curtain Fig understorey, ranging from 0.44 to 0.55 at corresponding times of the year, respectively. The fact that total site factors reach their highest median value at the equinoxes (September 22/March 22) is most likely related to the blocking effect caused by the fan palms described earlier, which reduces understorey direct site factors (and hence total site factors) during the high solar (summer) months (Table 7.15). By comparison, direct site factors are highest in the understorey of the Curtain Fig forest during the summer months (Table 7.2) because this forest does not have a continuous sub-canopy layer of fan palms (Fig. 5.4).

Seasonal variations in daily total PPFD under the four sky conditions described earlier within the Pine Creek understorey are evident in Table 7.5. In a similar way to the Curtain Fig understorey, statistical analyses have shown that daily total PPFD in the Pine Creek understorey differs significantly among the seven times of year under all sky conditions (one-way ANOVA: for cloudless F=2.62, P<0.05; for cirrostratus F=2.64, P<0.05; for altostratus F=3.26, P<0.01; and for stratus F=3.36, P<0.01). However, in comparison to the Curtain Fig forest, the Pine Creek forest experiences a less marked seasonal variation in light availability in its understorey, particularly under sunny (ie cloudless or cirrostratus cloud) conditions. For example, multiple comparisons among the seven times of the year indicate that only a small number of months are significantly different to each other (Table 7.16). The low seasonal variability in daily total PPFD within the understorey of this forest under sunny conditions is most likely due to the effect of the fan palm layer described above.

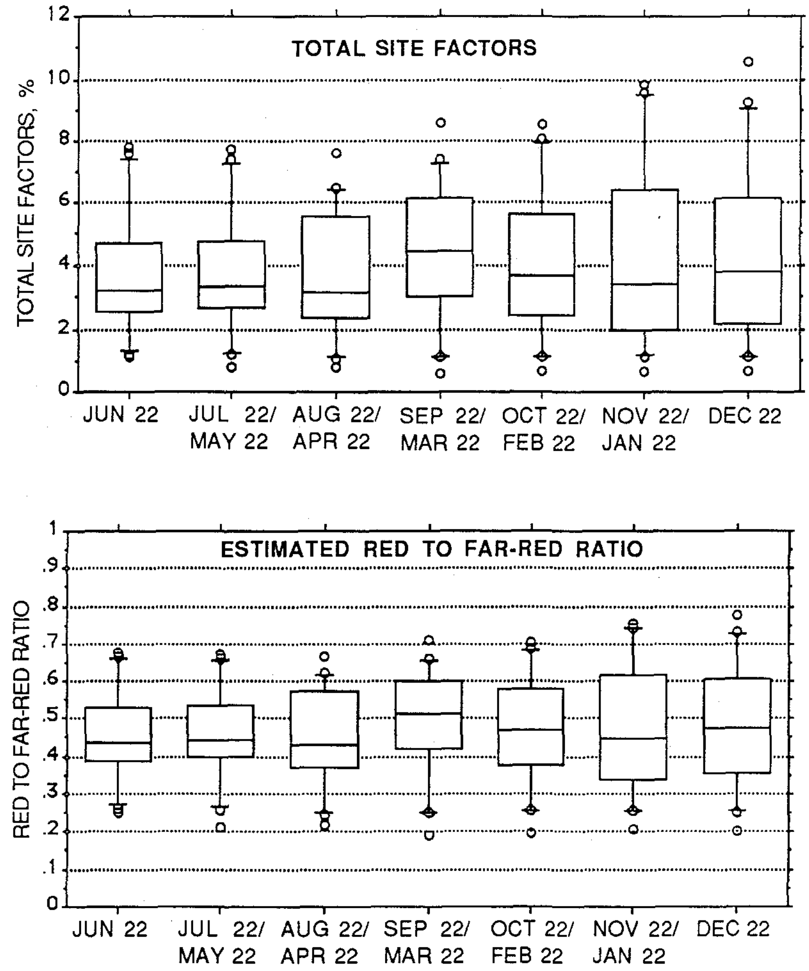

Figure 7.32. Distributions of percentiles for total site factors (%) and estimated red to far-red (R:FR) ratios obtained from 20 hemispherical (fisheye) canopy photographs taken at 5-m intervals along a 100-m transect in the understorey of the Pine Creek forest, northeast Queensland in July 1985. Total site factors (%) and R:FR ratios are given for solar declinations approximately equal to the 22nd day of each month. The R:FR ratios were estimated using Eqn 7.3.1. The five horizontal lines on the box plot show the 10, 25, 50, 75 and 90th percentiles, with values above and below the 10th and 90th percentile represented as data points.

Solar Declination	-23.5° (Dec 22)	-20.0° (Nov 22/ Jan 22)	-11.0° (Oct 22/ Feb 22)	0.0° (Sep 22/ Mar 22)	+11.0° (Aug 22/ Apr 22)	+22.0° (Jul 22/ May 22)	+23.5.0° (Jun 22)
	MULTIPLE COMPARISONS						
-23.5°(Dec 22)		cl. n.s cs. n.s as. n.s st. n.s	cl. n.s cs. n.s as. n.s st. n.s	cl. n.s cs. n.s as. n.s st. n.s	cl. n.s cs. n.s as. n.s st. n.s	cl. n.s cs. n.s as.* st.*	cl.* cs.* as.* st.*
-20.0° (Nov 22/ Jan 22)	cl. n.s cs. n.s as. n.s st. n.s		cl. n.s cs. n.s as. n.s st. n.s	cl. n.s cs. n.s as. n.s st. n.s	cl. n.s cs. n.s as. n.s st. n.s	cl. n.s cs. n.s as.* st.*	cl.* cs.* as.* st.*
-11.0° (Oct 22/ Feb 22)	cl. n.s cs. n.s as. n.s st. n.s	cl. n.s cs. n.s as. n.s st. n.s		cl. n.s cs. n.s as. n.s st. n.s	cl. n.s cs. n.s as. n.s st. n.s	cl. n.s cs. n.s as. n.s st. n.s	cl. n.s cs. n.s as.* st.*
0.0° (Sep 22/ Mar 22)	cl. n.s cs. n.s as. n.s st. n.s	cl. n.s cs. n.s as. n.s st. n.s	cl. n.s cs. n.s as. n.s st. n.s		cl. n.s cs. n.s as. n.s st. n.s	cl. n.s cs. n.s as. n.s st. n.s	cl. n.s cs. n.s as. n.s st. n.s
+11.0° (Aug 22/ Apr 22)	cl. n.s cs. n.s as. n.s st. n.s	cl. n.s cs. n.s as. n.s st. n.s	cl. n.s cs. n.s as. n.s st. n.s	cl. n.s cs. n.s as. n.s st. n.s		cl. n.s cs. n.s as. n.s st. n.s	cl. n.s cs. n.s as. n.s st. n.s
+20.0° (Jul 22/ May 22)	cl. n.s cs. n.s as.* st.*	cl. n.s cs. n.s as.* st.*	cl. n.s cs. n.s as. n.s st. n.s	cl. n.s cs. n.s as. n.s st. n.s	cl. n.s cs. n.s as. n.s st. n.s		cl. n.s cs. n.s as. n.s st. n.s
+23.5°(Jun 22)	cl.* cs.* as.* st.*	cl.* cs.* as.* st.*	cl. n.s cs. n.s as.* st.*	cl. n.s cs. n.s as. n.s st. n.s	cl. n.s cs. n.s as. n.s st. n.s	cl. n.s cs. n.s as. n.s st. n.s	

A priori multiple comparison of means (*t*-test): **, highly significant difference ($P<0.01$);
*, significant difference ($P<0.05$); n.s, no significant difference ($P>0.05$).
cl. = cloudless sky; cs. = cirrostratus cloud; as. = altostratus cloud; st. = stratus cloud.

Table 7.16. *A priori* multiple comparisons (*t*-tests) of mean daily total photosynthetic photon flux density (PPFD) among seven times of the year (solar declinations) for cloudless skies, and cirrostratus, altostratus and stratus cloud types, within the understorey of Pine Creek forest.

7.3.2 Treefall Gap Light Regimes

Given the importance of treefall gaps as sites for rainforest regeneration, a range of rainforest gaps of varying sizes and configurations were photographed using the fisheye lens-camera system described in Section 6.3.2. This section presents the results of modelling seasonal changes in light availability at the centre of four types of treefall gap found within several northeast Queensland rainforests: (1) a small circular gap (Plate 7.4); (2) a small elliptical gap (Plate 7.5); and (3) a large circular gap (Plate 7.6); and (4) a large elliptical gap (Plate 7.7). However, because the orientation of non-circular gaps is likely to influence light availability at the forest floor, the so-called elliptical gaps (Plates 7.5 and 7.7) were analysed with their long axes orientated north-south and east-west. Hence, the number of gap types presented here may effectively be increased from four to six.

Table 7.17 shows diffuse and direct site factors for the six contrasting treefall gaps described above. As expected, the large circular gap (Plate 7.6) has the highest direct and diffuse site factors, followed by the large elliptical gap (Plate 7.7). The modelling procedure demonstrates how the orientation of an elliptical gap profoundly affects its direct site factors over the year (Table 7.17). For example, when the small elliptical gap (Plate 7.5) is orientated north-south, its direct site factors range from 1.9 to 18.5%; when the exact same gap is orientated east-west, direct site factors range from 0.7 to 28.4%. A similar trend is apparent for the large elliptical gap (Table 7.17); when the gap (Plate 7.7) is orientated north-south, direct site factors range from 3.8 to 33.6%. By comparison, when this gap is orientated east-west, direct site factors range from 3.4 to 47.7%. Hence, the yearly range of direct site factors is more extreme within treefall gaps that are orientated east-west.

The effects of gap size and orientation on the red to far-red (R:FR) ratio is shown in Table 7.18 for the six gap types. In the large circular gap, the estimated R:FR ratio under cloudless skies is greater than 1.00 throughout the year and is therefore similar to that found in the open or above the forest (Smith and Morgan, 1981). However, R:FR ratios are generally less than 1.00 during the winter months (April-August) in the other gaps, except for the small elliptical north-south orientated gap where values are less than 1.00 throughout the year. Because these R:FR ratios were estimated using the same method as those in the understorey (ie Eqn 7.3.1), it is possible to compare the annual means for these micro-environments. Generally, R:FR ratios within the large circular gap (Table 7.18) are about 3-times higher than those within the Curtain Fig understorey before the cyclone and 1.4-times higher than those within the same understorey after the cyclone. On the other hand, R:FR ratios within the small elliptical north-south orientated gap are 2-times higher than those within the

Plate 7.4. A hemispherical (fisheye) canopy photograph taken at the centre of a small circular gap created by the forced toppling of a single tree during Tropical Cyclone 'Winifred'. The gap is located in the Curtain Fig forest, northeast Queensland. The diffuse site factor for the site was 19.4% when photographed immediately after the cyclone in February 1986.

Plate 7.5. A hemispherical (fisheye) canopy photograph taken at the centre of a small elliptical (north-south) gap created by the forced toppling of a single tree at an unknown time. The gap is located in the Curtain Fig forest, northeast Queensland. The diffuse site factor for the site was 17.8% when photographed in November 1985.

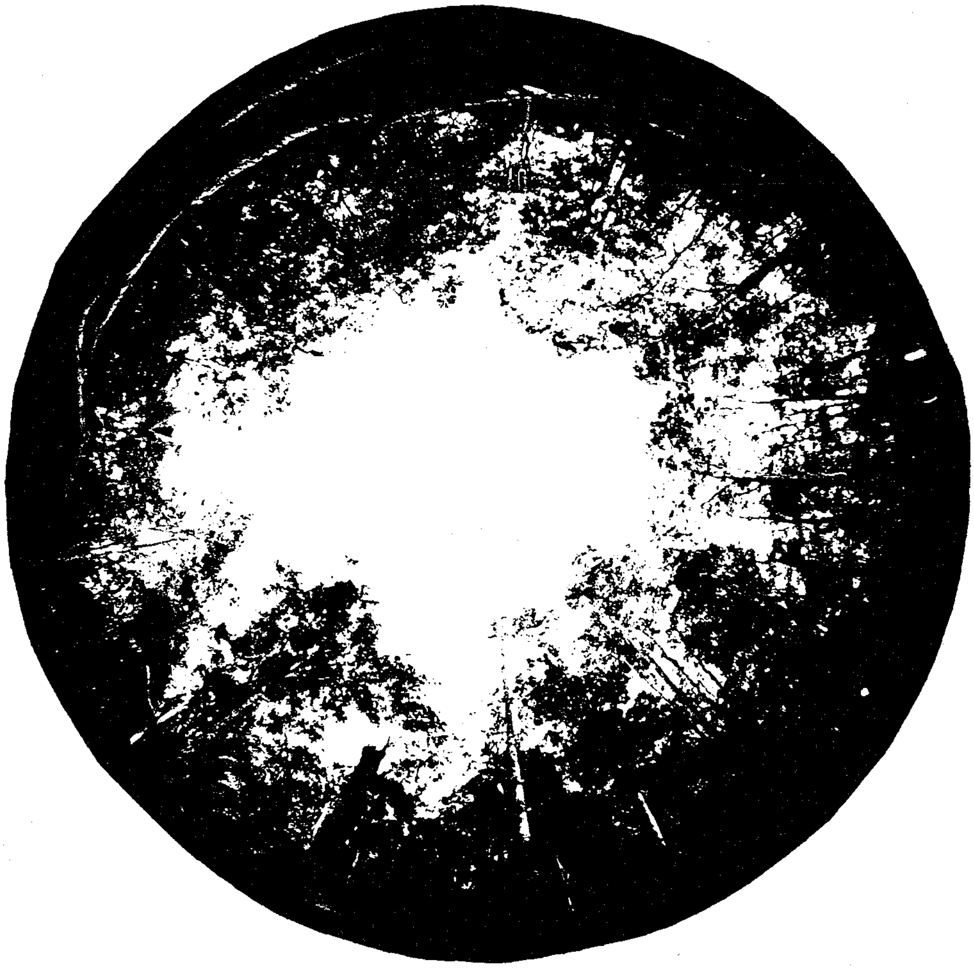

Plate 7.6. A hemispherical (fisheye) canopy photograph taken at the centre of a large circular gap created by the death and forced toppling of a large fig tree (*Ficus* spp.) at an unknown time. The gap is located in the Wongabel forest, northeast Queensland. The diffuse site factor for the site was 54.1% when photographed in October 1990.

Plate 7.7. A hemispherical (fisheye) canopy photograph taken at the centre of a large elliptical (east-west) gap created by the forced toppling of a single tree during Tropical Cyclone 'Winifred'. The gap is located in the Pine Creek forest, northeast Queensland. The diffuse site factor for the site was 34.5% when photographed immediately after the cyclone in February 1986.

SOLAR DECLINATION (APPROX. DATE)	DIRECT SITE FACTORS (%) SMALL CIRC. GAP	LARGE CIRC. GAP	SMALL ELLIP. GAP (N/S)#	SMALL ELLIP. GAP (E/W)	LARGE ELLIP. GAP (N/S)	LARGE ELLIP. GAP (E/W)#
-23.5° (22 Dec)	24.7	57.8	17.5	9.9	33.6	28.8
-20.0° (22 Jan/Nov)	21.9	62.8	18.4	28.4	33.5	39.9
-11.0° (22 Feb/Oct)	22.6	53.4	18.5	28.0	27.8	47.7
0.0° (22 Mar/Sep)	6.1	27.8	7.3	9.5	24.6	32.1
+11.0° (22 Apr/Aug)	2.1	25.8	3.1	3.8	12.1	13.3
+20.0° (22 May/Jul)	1.3	9.5	2.3	1.0	4.6	5.0
+23.5° (22 Jun)	0.7	10.9	1.9	0.7	3.8	3.4
ANNUAL MEAN	11.3	37.4	9.9	11.6	20.0	24.3
FULL-YEAR DIFFUSE SITE FACTOR (%)	19.4	54.1	17.8	17.8	34.5	34.5

Refers to the orientation of the long axis of the actual elliptical gap:
N/S = north-south; E/W = east-west

Table 7.17. Values of diffuse and direct site factors (%) obtained from hemispherical (fisheye) canopy photographs taken at the centre of six contrasting treefall gaps within several rainforest types in northeast Queensland (refer to text for location details). The direct site factors are given for solar declinations approximately equal to the 22nd day of each month, while a full-year diffuse site factor is given. Both the large and small elliptical gaps have been analysed for north-south and east-west orientations for modelling purposes.

SOLAR DECLINATION (APPROX. DATE)	ESTIMATED RED TO FAR-RED RATIOS					
	SMALL CIRC. GAP	LARGE CIRC. GAP	SMALL ELLIP. GAP (N/S)#	SMALL ELLIP. GAP (E/W)	LARGE ELLIP. GAP (N/S)	LARGE ELLIP. GAP (E/W)#
-23.5° (22 Dec)	1.07	1.42	0.96	0.80	1.21	1.16
-20.0° (22 Jan/Nov)	1.03	1.45	0.97	1.11	1.21	1.26
-11.0° (22 Feb/Oct)	1.04	1.40	0.97	1.11	1.15	1.33
0.0° (22 Mar/Sep)	0.72	1.20	0.74	0.80	1.12	1.20
+11.0° (22 Apr/Aug)	0.60	1.19	0.62	0.65	0.95	0.97
+20.0° (22 May/Jul)	0.60	1.03	0.61	0.57	0.85	0.84
+23.5° (22 Jun)	0.59	1.05	0.61	0.57	0.82	0.82
ANNUAL MEAN	0.81	1.25	0.78	0.80	1.04	1.08

Refers to the orientation of the long axis of the actual elliptical gap:
N/S = north-south; E/W = east-west

Table 7.18. Estimated red to far-red (R:FR) ratios for six contrasting treefall gaps within several rainforest types in northeast Queensland (refer to text for location details). The R:FR ratios were estimated using Eqn 7.3.1. and are given for solar declinations approximately equal to the 22nd day of each month.

Curtain Fig forest understorey before the cyclone and almost equal to those within the same understorey after the cyclone. Similar differences to those given for the Curtain Fig understorey before the cyclone would be expected for the Pine Creek understorey.

Figure 7.33 shows daily total PPFD under cloudless skies, and cirrostratus, altostratus and stratus cloud types above the forest and at the centre of the six treefall gaps described above. Seasonal changes in light availability above the forest and within the six gap types are shown for solar declinations approximately equal to the 22nd day of each month. In agreement with the gap simulations presented in Section 4.3 (Fig. 4.8), at a similar latitude to northeast Queensland, there is a noticeable decrease in daily total PPFD above the forest with increasing cloud depth at all times of the year (Fig. 7.33). However, in a similar manner to the gap simulations shown in Fig. 4.8, on June 22 daily total PPFD is higher within all six gap types under cirrostratus and altostratus cloud than under cloudless skies because of higher levsls of diffuse radiation, and on December 22 daily total PPFD is higher within these gaps under cloudless skies than under the three cloud types (Fig. 7.33).

The seven graphs shown in Fig. 7.33 also emphasise absolute differences in light availability among the six gap types over the year. For example, on December 22 daily total PPFD in the large circular gap under cloudless skies is 1.8-times higher than that in the large elliptical east-west gap, 1.6-times higher than that in the large elliptical north-south gap, 2.5-times higher than that in the small circular gap, 5-times higher than that in the small elliptical east-west gap, and 3.3-times higher than that in the small elliptical north-south gap. In comparison, on June 22 daily total PPFD in the large circular gap under cloudless skies is about 2.5-times higher than that in either the large elliptical east-west or large elliptical north-south gaps, 3.7-times higher than that in the small circular gap, 4.2-times higher than that in the small elliptical east-west gap, and 3.4-times than that in the small elliptical north-south gap.

The photoelectric measurements have shown that the percentage of daily total PPFD within the small elliptical north-south gap (Plate 7.5) under sunny conditions ranged from 9.6 to 18.1% in January and from 3.4 to 4.1% in July (Table 7.10). Similarly, the total site factors for this gap, estimated from the fisheye photograph, were 17.0% for January 22 and 5.6% for July 22. At the centre of the small circular gap (Plate 7.4), the percentage of daily total PPFD under sunny conditions ranged from 13.6 to 19.7% in January and from 2.4 to 5.1% in July (Table 7.11). Likewise, total site factors for this gap were 19.6% for January 22 and 5.2% for July 22. Hence, there is an acceptable agreement between relative daily PPFD levels obtained from photoelectric measurements within these two gaps under natural conditions, and total site factors obtained from analysis of fisheye photographs of the same gaps.

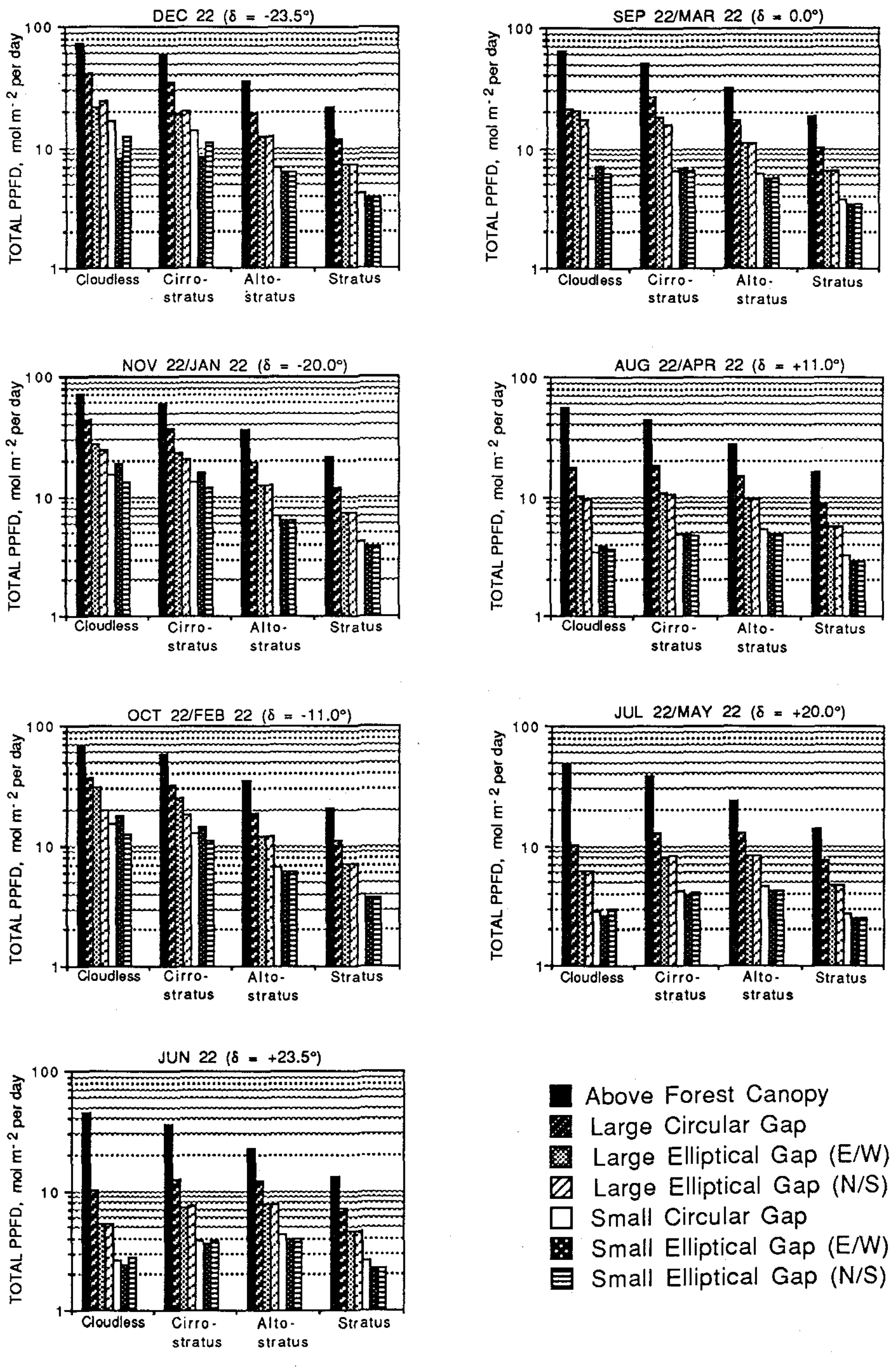

Figure 7.33. Daily total photosynthetic photon flux density (PPFD) (mol m^{-2} per day) under cloudless skies, and cirrostratus, altostratus and stratus cloud types above the forest canopy and at the centre of six contrasting treefall gaps within several rainforest types in northeast Queensland (refer to text for location details). Daily total PPFDs are given for solar declinations approximately equal to the 22nd day of each month.

7.3.3 Rainforest-Open Forest Boundary (Ecotone) Light Regimes

The results presented thus far have focused exclusively on the temporal and spatial distribution of irradiance and PPFD within characteristic micro-environments in rainforests. It is now widely recognised that understanding boundary dynamics between rainforest and open forest is a pre-requisite for the successful management of remaining patches of rainforest in many places in northeast Queensland. Much of the research into aspects of this boundary has focussed on the role of fire in controlling the expansion or contraction of rainforest. Moreover, there is little doubt that light availability to seedlings and saplings in the transition zone (ecotone) between rainforest and open forest is another critical factor controlling boundary dynamics. However, apart from a few spot measurements made by Duff (1987) there are no published studies examining the light regimes across this important transition zone.

As stated in Section 6.4.3, three 50-m transects were established across the rainforest-open forest boundary at Kirrama (Fig. 5.7) and fisheye photographs were taken at 5-m intervals along each transect. However, statistical analyses have shown that there are no significant differences (F-test, $P > 0.05$) in direct and diffuse site factors among the three transects, and it is therefore possible to pool data from the 10 photosites along each transect into a single combined transect.

Table 7.19 summarises results of various descriptive statistics applied to diffuse, direct and site factors for the five vegetation zones across the rainforest-open forest boundary at Kirrama (Fig. 5.7). Fisheye photographs of sites representing the open forest (zone A), ecotone (zone C) and mature rainforest (zone E) are shown in Plates 7.8, 7.9 and 7.10, respectively. The results in Table 7.19 demonstrate a marked decrease in diffuse and direct site factors (and hence total site factors) across the boundary from open forest to rainforest. The coefficients of variation are highest in the dynamic transition zone between tall open forest and young rainforest (zone C), and this result may be attributed to the corresponding complexity of vegetation in this zone (Fig. 5.7).

The effects of canopy cover on the red to far-red (R:FR) ratio is demonstrated by the mean yearly values shown in Table 7.19. Because these R:FR ratios were estimated using the same method as those given earlier for rainforest understoreys (Figs. 7.31 and 7.32) and treefall gaps (Table 7.18), it is possible to make comparative evaluations among micro-environments. It would appear that the mean R:FR ratio in the ecotone (zone C, Table 7.19) falls within the range exhibited by the treefall gaps shown in Table 7.18, with the exception of the large circular gap which has a R:FR ratio similar to those found in the tall open forest (zone B) and open forest (zone A). Likewise, the mean R:FR ratios in the young and mature rainforest (zones D and E) are similar to those found in the Curtain Fig understorey before the cyclone (Fig. 7.31) and the Pine

Vegetation zone	Diffuse site factor (%) mean ± 1 SD (range) coefficient of variation	Direct site factor (%) mean ± 1 SD (range) coefficient of variation	Total site factor (%) mean ± 1 SD (range) coefficient of variation	Mean Red to Far-Red (R:FR) Ratio
(A)	66.4±6.3	38.3±14.2	45.1±11.1	
Open	(59.3-75.9)	(12.6-66.5)	(25.7-68.1)	1.33
forest	9.5%	37.1%	24.6%	
(B)	53.8±18.5	29.5±19.8	35.4±18.4	
Tall open	(18.5-73.7)	(2.3-66.8)	(6.8-68.3)	1.23
forest	34.4%	67.1%	52.0%	
(C)	27.4±19.8	12.5±16.0	16.0±16.5	
Tall open forest	(7.5-67.0)	(0.3-57.7)	(2.4-59.6)	0.92
(rainforest under)	72.3%	128.0%	103.0%	
(D)	10.4±3.3	3.0±2.6	4.7±2.5	
Young	(6.1-15.2)	(0.2-10.1)	(1.8-10.5)	0.53
rainforest	31.7%	86.7%	53.2%	
(E)	9.8±4.2	2.9±2.6	4.5±2.6	
Mature	(5.3-18.0)	(0.1-9.9)	(1.6-10.6)	0.52
rainforest	42.9%	89.7%	57.8%	

Table 7.19. Annual average values of diffuse, direct and total site factors (%) and red to far-red (R:FR) ratios obtained from 30 hemispherical (fisheye) photographs taken at 5-m intervals along three 50-m transects across the open forest-rainforest boundary (ecotone) at Kirrama, northeast Queensland. Site factors are given for the four vegetation zones identified across the boundary. The R:FR ratios were estimated using Eqn 7.3.1.

Plate 7.8. A hemispherical (fisheye) canopy photograph taken at a representative site within the open forest (zone A) at Kirrama, northeast Queensland. The diffuse site factor for the site was 59.3% when photographed in August 1986.

Plate 7.9. A hemispherical (fisheye) canopy photograph taken at a representative site within the open forest-rainforest boundary (zone C) at Kirrama, northeast Queensland. The diffuse site factor for the site was 18.5% when photographed in August 1986.

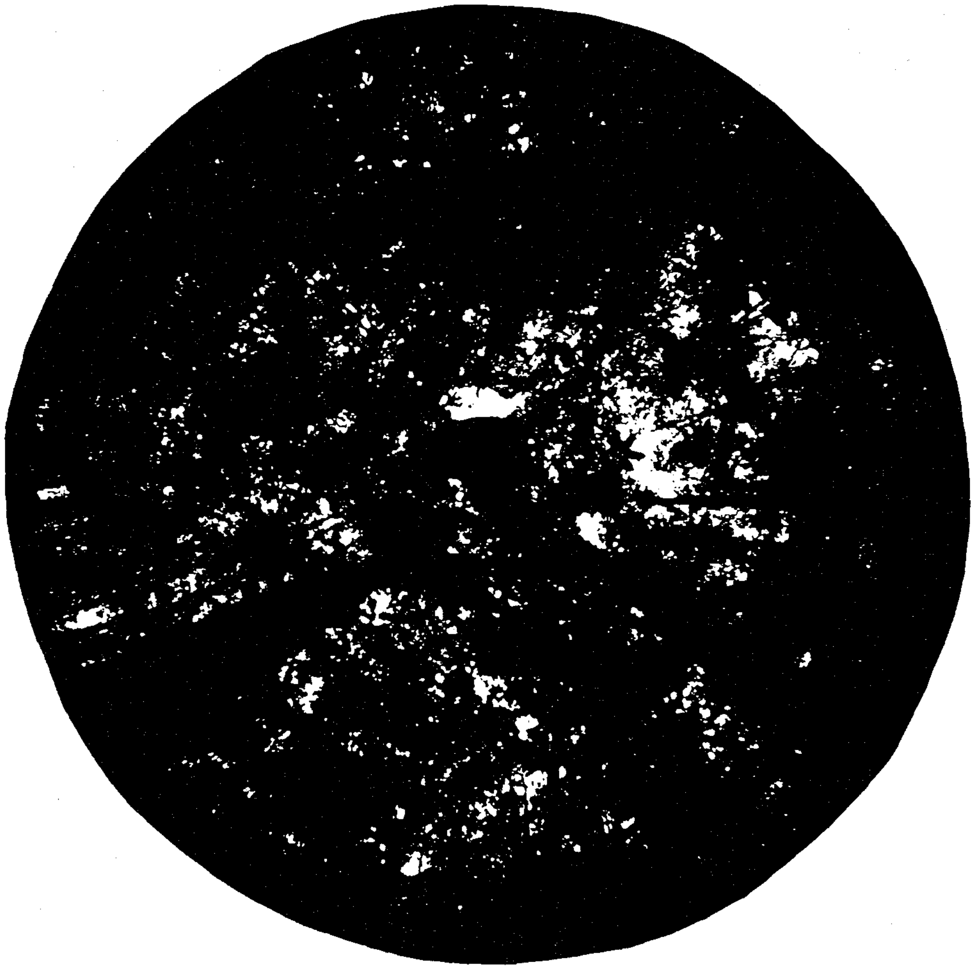

Plate 7.10. A hemispherical (fisheye) canopy photograph taken at a representative site within the mature rainforest (zone E) at Kirrama, northeast Queensland. The diffuse site factor for the site was 9.0% when photographed in August 1986.

Creek understorey (Fig. 7.32). Perhaps the most significant result is that total site factors and R:FR ratios in the ecotone (zone C) are similar to those found in treefall gaps (Table 7.18).

Fig. 7.34 shows potential (cloudless-sky) diffuse, direct and total PPFD (mol m^{-2} per day) across the open forest - rainforest boundary at Kirrama on the 22nd day of each month. To place the daily PPFDs into context, the five vegetation zones shown in Fig. 5.7 are indicated on the line graphs. Seasonal variations in the availability of direct and diffuse light are apparent across this boundary. Specifically, during the summer (high solar) half of the year (September-March) direct PPFD declines semi-exponentially across the boundary, while in the winter (low solar) half of the year (April-August), the decline is more linear. On the other hand, the decline in diffuse PPFD across the boundary appears to be linear throughout the year. Hence, in a similar manner to the light regime found in treefall gaps, there are distinct seasonal changes in the availability of direct PPFD across the open forest-rainforest boundary at northeast Queensland latitudes (13-19° S.). For example, mean daily direct PPFD in the ecotone (zone C) on December 22 is almost 6-times higher than that in the ecotone on June 22 (Fig. 7.34).

Furthermore, seasonal effects are particularly noticeable for the open forest (zones A and B, Fig. 7.34), where relative direct PPFD levels are about 50 to 60% full sun on November 22/January 22 compared to only 20 to 25% full sun on June 22. However, in the rainforest understorey the seasonal differences in the penetration of direct PPFD are less significant.

Although marked seasonal changes are evident across the open forest-rainforest boundary under cloudless skies (Fig. 7.34), these changes are considerably smaller under stratus cloud conditions (Fig. 7.35). For example, mean daily total PPFD in the ecotone (zone C) on December 22 is only 1.5-times higher than that in the ecotone on June 22 (Fig. 7.35). Nonetheless, Figs. 7.34 and 7.35 aim to demonstrate, respectively, the highest and lowest levels of light availability across the boundary, with average conditions likely to fall somewhere between these two extremes.

7.4 SUMMARY

This chapter has provided a detailed evaluation of temporal and spatial distributions of solar radiation above and beneath some northeast Queensland rainforests. Results of field investigations were presented in three main sections.

First, daily irradiation and photosynthetic photon flux density (PPFD) were examined at three sites in the wet tropics region - Atherton, Topaz and El-Arish. It

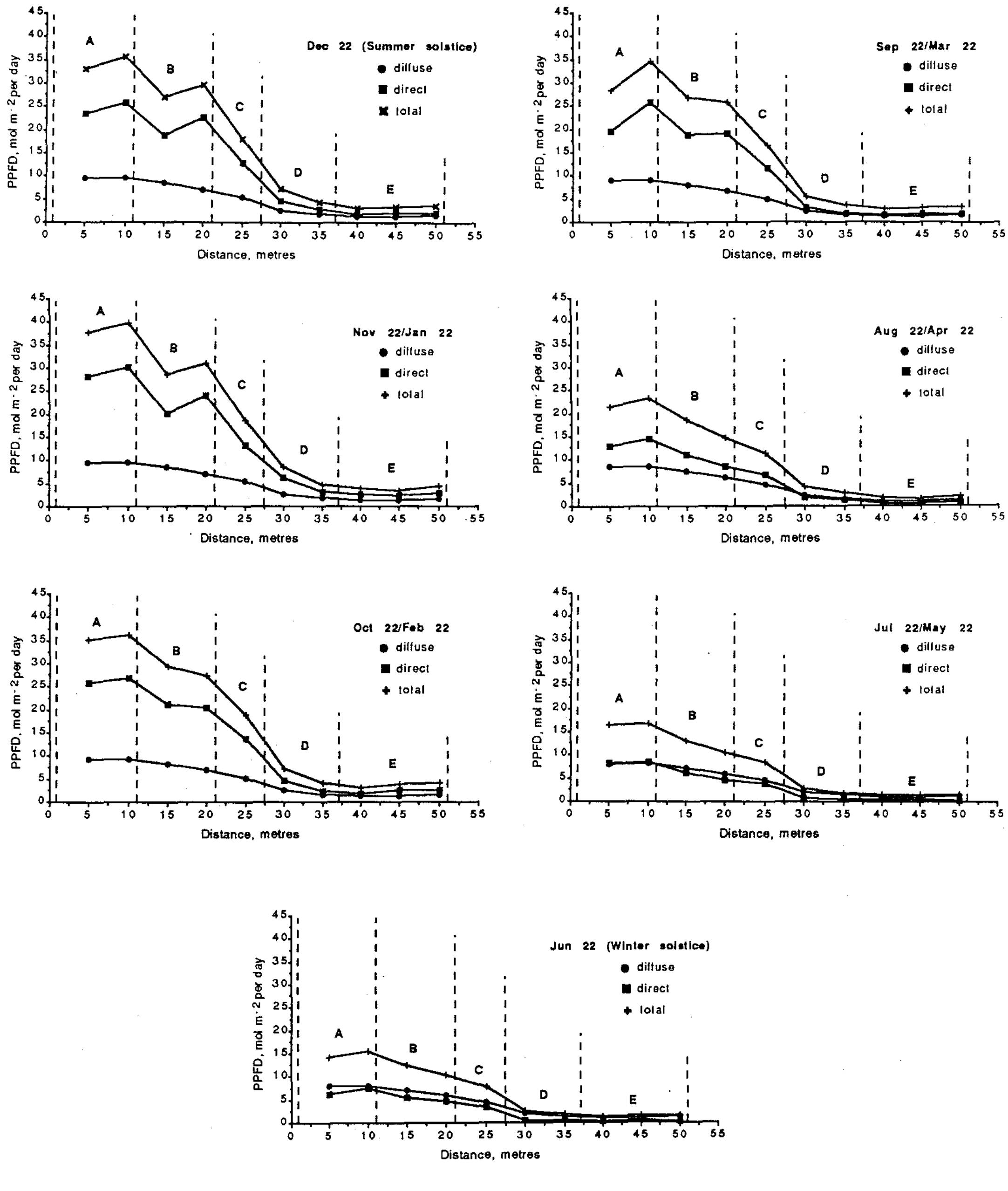

Figure 7.34. Potential (cloudless sky) daily direct, diffuse and total photosynthetic photon flux density (PPFD) (mol m^{-2} per day) at 5-m intervals across the open forest-rainforest boundary at Kirrama, northeast Queensland. Daily integrals are given for solar declinations approximately equal to the 22nd day of each month. The five vegetation zones shown in Fig. 5.7 are superimposed for reference.

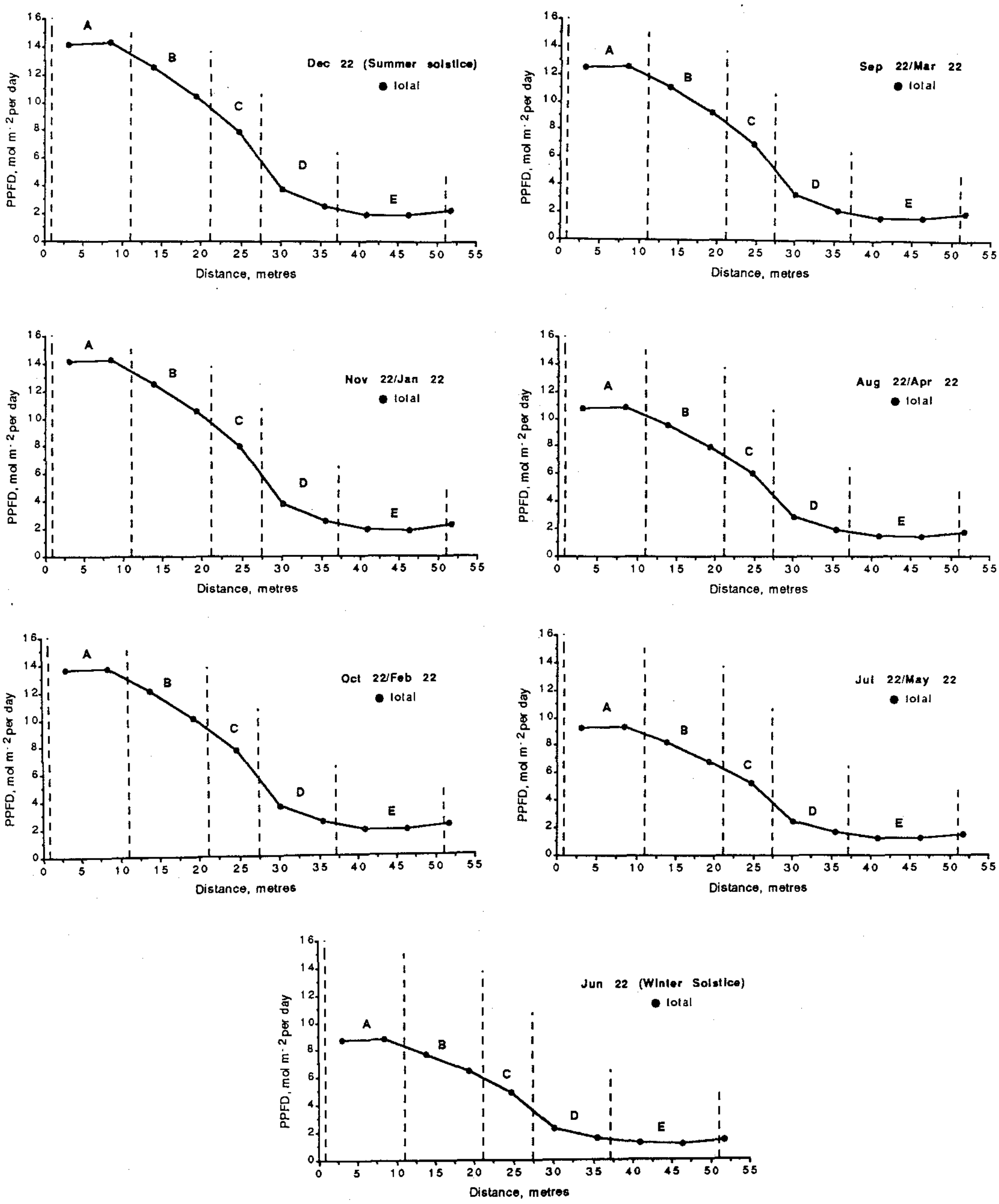

Figure 7.35. Daily total photosynthetic photon flux density (PPFD) (mol m^{-2} per day) under stratus cloud conditions at 5-m intervals across the open forest-rainforest boundary at Kirrama, northeast Queensland. Daily integrals are given for solar declinations approximately equal to the 22nd day of each month. The five vegetation zones shown in Fig. 5.7 are superimposed for reference.

was found that annual average solar radiation was highest at Atherton (6639 MJ m^{-2}), the driest site, followed by Topaz (6055 MJ m^{-2}) and El-Arish (5665 MJ m^{-2}), respectively. Annual average values for these three sites compared closely with a nine year annual average of 5800 MJ m^{-2} at Pin Gin Hill, which is also located in the wet tropics region. Both Atherton and Topaz experienced their highest monthly average solar radiation levels in the pre-monsoon months of September-December, with El-Arish experiencing similar levels throughout the summer months of September-March.

In the second section, diurnal variations in irradiance and PPFD above and beneath several northeast Queensland rainforest canopies were examined. The results presented in this section attempted to account for variations in irradiance and PPFD over time and space by considering variability among characteristic micro-environments, such as canopy, gap and understorey, and then variability within these micro-environments themselves. The micro-environments investigated provide a reasonable representation of the range of light regimes found in rainforests: the understorey illustrates the generally low light conditions prevalent beneath a closed canopy where only extremely shade-tolerant species can survive; the small treefall gaps are fairly typical of the light regimes created by the death or forced toppling of a single tree; and above the forest is representative of the light conditions experienced by emergents in the upper canopy.

On the basis of detailed field measurements within several rainforest types, the following generalisations were made: (1) in summer irradiance levels above rainforests are, on average, 33-times higher than levels in understoreys and 6-times higher than levels in small treefall gaps; (2) in summer PPFD levels above rainforests are, on average, 70-times higher than levels in understoreys and 7-times higher than levels in small treefall gaps; (3) in winter irradiance levels above rainforests are, on average, 16-times higher than levels in understoreys and 15-times higher than levels in small treefall gaps; (4) in winter PPFD levels above rainforests are, on average, 79-times higher than levels in understoreys and 26-times higher than levels in small treefall gaps; (5) in summer median radiant flux densities within understoreys and small treefall gaps ranged from 13.5-26.3 W m^{-2} and 35.9-43.1 W m^{-2}, respectively; (6) in summer median PPFDs within understoreys and small treefall gaps ranged from 10.6-13.5 μ mol m^{-2} s^{-1} and 25.8-43.9 μ mol m^{-2} s^{-1}, respectively; (7) in winter median radiant flux densities within understoreys and small treefall gaps ranged from 18.0-33.2 W m^{-2} and 23.1-40.7 W m^{-2}, respectively; (8) in winter median PPFDs within understoreys and small treefall gaps ranged from 10.0-17.4 μ mol m^{-2} s^{-1} and 23.4-39.2 μ mol m^{-2} s^{-1}, respectively; (9) the highest 10-min average irradiance reading recorded in the understorey was 238.4 W m^{-2}; (10) the highest 10-min average PPFD reading recorded in the understorey was 442.6 μ mol m^{-2} s^{-1}; (11) the highest 10-sec instantaneous PPFD reading (sunfleck) recorded in the understorey was 794.2 μ mol m^{-2} s^{-1}; (12) mean daily total irradiation within small treefall gaps represents about 18% of that available above the rainforest in summer and 6% available above the rainforest in winter; (13) mean daily total PPFD within small treefall gaps represents about 14% of that available above the rainforest in summer and 4% available above the rainforest in winter; (14) mean daily total irradiation within most understoreys represents about 3-5% of that available above the rainforest throughout the year; (15) mean daily total PPFD within most understoreys represents about 1-2% of that available above the rainforest throughout the year; (16) the frequency distributions of irradiance and PPFD within small gaps and understoreys, with few exceptions, have moderate to high degrees of positive skewness and kurtosis; (17) on the basis of 10-min average readings sunflecks represent 0-24.5% of the radiant flux densities and 0-8.3% of the PPFDs reaching the understorey throughout the year, but in absolute terms they account, respectively, for 0-53.1% and 0-35% of the daily total irradiation and PPFD within the understorey; (18) on the basis of 10-sec instantaneous PPFD readings sunflecks represent about 10% of PPFDs reaching the understorey in summer, but in absolute terms account for about 70% of the daily total PPFD within the understorey; (19) on the basis of 10-min average readings sunflecks represent 35-40% of the radiant flux densities and 23-60% of the PPFDs within treefall gaps in summer, but in absolute terms they account, respectively, for 77-84% and 73-91% of the daily total irradiation and PPFD within treefall gaps at this time of year; and (20) on the basis of 10-min average readings sunflecks represent 4-34% of the radiant flux densities and 0-40% of the PPFDs within treefall gaps in winter, but in absolute terms they account, respectively, for 10-54% and 0-57% of the daily total irradiation and PPFD within treefall gaps at this time of year.

In the third and final section, seasonal variations in daily PPFD above and beneath several northeast Queensland rainforest canopies were examined. The results presented in this section are considered as the first attempt to model light availability within rainforest understoreys and gaps, and across the rainforest-open forest boundary under a range of sky conditions.

The availability of light within the understorey of an upland tropical rainforest before and immediately after a tropical cyclone was examined first and the following generalisations were made: (1) direct, diffuse and total site factors and red to far-red (R:FR) ratios increased significantly as a result of the slight-to-moderate canopy disturbance caused by the cyclone; (2) on the basis of estimates for the 22nd day of each month, mean daily total PPFD in the understorey under cloudless skies ranged from 1.3-2.8 mol m^{-2} per day before the cyclone and from 3.2-6.9 mol m^{-2} per day immediately after the cyclone, representing a 2- to 3-fold increase; (3) on the basis of estimates for the 22nd day of each month, mean daily total PPFD in the understorey under stratus cloud ranged from 0.97-1.6 mol m^{-2} per day before the cyclone and from 2.1-3.4 mol m^{-2} per day immediately after the cylone, representing a 2-fold increase; (4) median red to far-red (R:FR) ratios over the year within the understorey ranged from 0.38-0.45 before the cyclone and from 0.78-0.94 immediately after the cyclone, representing a 2-fold increase; and (5) seasonal differences in the availability of light within the understorey were more significant after the cyclone than before, and this result was attributed to the increase in the size and number of canopy openings between 60 and 90° above the horizon that occurred as a result of the cyclone.

Understorey light regimes were also examined within a lowland rainforest using the same fisheye canopy photography technique and the following generalisations were made: (1) the almost continuous sub-canopy layer of fan palms has a strong effect on light penetration into the understorey; (2) on the basis of estimates for the 22nd day of each month, mean daily total PPFD in the understorey ranged from 1.7-3.2 mol m^{-2} per day under cloudless skies and from 1.2-1.9 mol m^{-2} per day under stratus cloud; (3) median red to far-red (R:FR) ratios over the year within the understorey ranged from 0.44-0.55; and (4) seasonal differences in the availability of light within the understorey, particularly under sunny conditions, were less significant in this rainforest compared with the upland rainforest. This result was attributed to the almost continuous horizontal layer of fan palm leaves which prevent the penetration of direct light into the forest when solar angles are greater than about 60°.

Given the importance of treefall gaps as sites for regeneration of most rainforest canopy trees, a range of gaps of varying sizes and configurations were examined using the fisheye photography technique and the following generalisations were made: (1) the yearly range of direct site factors was more extreme in elliptical gaps orientated east-west than those found in the exact same gaps orientated north-south; (2) mean annual diffuse site factors ranged from 17.8% for a small elliptical gap to 54.1% for a large circular gap; (3) mean annual direct site factors ranged from 9.9% for the small elliptical gap orientated north-south to 37.4% for the large circular gap; (4) mean annual R:FR ratios ranged from 0.78 for the small elliptical gap orientated north-south to 1.25 for the large circular gap; (5) the mean annual R:FR ratio for the large circular gap was about 3-times higher than that within the understorey of the same forest type before the cyclone, while the mean annual R:FR ratio within the small elliptical north-south orientated gap was about 2-times higher than that within the understorey of the same forest type before the cyclone; (6) there are strong seasonal differences in light availability within a wide-range of treefall gaps in northeast Queensland: on the basis of estimates for the 22nd day of each month, daily total PPFD at the centre of the large circular gap ranged from 10-40 mol m^{-2} per day under cloudless skies and from

7-13 mol m^{-2} per day under stratus cloud , while daily total PPFD at the centre of the small elliptical gap orientated north-south ranged from 2.8-13 mol m^{-2} per day under cloudless skies and from 2.2-4.0 mol m^{-2} per day under stratus cloud; (7) there are also strong seasonal differences in R:FR ratios within these treefall gaps: on the basis of estimates for the 22nd day of each month, the R:FR ratio at the centre of the large circular gap ranged from 1.03-1.45, while the R:FR ratio at the centre of the small elliptical gap orientated north-south ranged from 0.61-0.97; and (8) it was shown that there are order-of-magnitude differences in light availability across the range of treefall gaps analysed and this undoubtedly controls the microclimate and hence the ecophysiology of plants growing within these treefall gaps.

Seasonal changes in light availability across the open forest-rainforest boundary were also examined using the fisheye photography method and the following generalisations were made: (1) mean annual diffuse site factors decreased from 66.4% in the open forest to 27.4% in the ecotone and then to 9.8% in the mature rainforest; (2) mean annual direct site factors decreased from 38.3% in the open forest to 12.5% in the ecotone and then to 2.9% in the mature rainforest; (3) mean annual R:FR ratios decreased from 1.33 in the open forest to 0.92 in the ecotone and then to 0.52 in the mature rainforest; (4) total site factors and R:FR ratios within the ecotone are very similar to those found within small treefall gaps, and this result has important implications for the ecophysiology of plants growing in the ecotone; (5) under cloudless skies direct PPFD declined semi-exponentially across the boundary during the summer half of the year (September-March) and linearly during the winter half of the year (April-August), while diffuse PPFD declined linearly across the boundary throughout the year; (6) there were strong seasonal differences in light availability within the five vegetation zones across the open forest-rainforest boundary under cloudless skies: on the basis of estimates for the 22nd day of each month, daily total PPFD ranged from 14-38 mol m^{-2} per day in the open forest, from 8-18 mol m^{-2} per day in the ecotone, and from 1.8-4.0 mol m^{-2} per day in the mature rainforest; and (7) there were small seasonal differences in light availability within the five vegetation zones across the boundary under stratus cloud: on the basis of estimates for the 22nd day of each month, daily total PPFD ranged from 9-14 mol m^{-2} per day in the open forest, from 5-8 mol m^{-2} per day in the ecotone, and from 1.5-2.1 mol m^{-2} per day in the mature rainforest.

The results presented in this chapter have numerous outputs towards improving our knowledge and understanding of tropical rainforest regeneration following natural and human disturbance. There are also implications for reforestation of disturbed sites such as road cuttings and open-cast mines, by planting tree species better suited to the prevailing light conditions. And finally, there are implications for the conservation and management of remaining rainforest in northeast Queensland, as a substantial portion occurs as small, isolated patches. These implications will be discussed further in the next chapter.

CHAPTER 8

SOLAR RADIATION IN RELATION TO RAINFOREST STRUCTURE AND FUNCTION: A SYNTHESIS

The primary purpose of this chapter is to synthesise the results presented in Chapters 4 and 7 in the context of rainforest structure and function, by critically evaluating the six research hypotheses described at the end of Chapter 2. To achieve this objective, the chapter will be presented in four main sections: (1) a comparative evaluation of understorey light environments in tropical rainforests; (2) a comparative evaluation of treefall gap light environments in tropical rainforests; (3) light environments within montane tropical rainforest in northeast Queensland; and (4) light environments across the open forest-rainforest boundary in northeast Queensland.

8.1 A COMPARATIVE EVALUATION OF UNDERSTOREY LIGHT ENVIRONMENTS IN TROPICAL RAINFORESTS

A number of generalisations about light environments within rainforest understoreys were made in the earlier review of the literature. It was found that both PPFD and irradiance within rainforest understoreys are highly variable over time and space. It was shown that daily total PPFD in most tropical rainforest understoreys ranges from 0.5 to 3.0% of that above the forest, while daily total irradiation in most understoreys ranges from 1.0 to 5.0% of that above the forest. In addition, it was determined that most sunflecks last less than 2-min and their intensity varies from 50 to 500 μ mol m^{-2} s^{-1}, depending on sky conditions and overstorey canopy structure, and in most understoreys sunflecks contribute 40 to 80% of the daily total PPFD and irradiation under sunny conditions.

Two research hypotheses were developed in regard to understorey light environments in northeast Queensland rainforests:

(1) Relative PPFD and irradiance levels in the understoreys of northeast Queensland rainforests are higher, on average, than tropical rainforests elsewhere because canopy density is lower; and

(2) In comparison to equatorial rainforests, sunflecks represent a less significant portion of the daily total radiation in the understoreys of northeast Queensland rainforests because of the cloudy trade-wind coast climate.

It was originally suggested that prevalent cloud cover associated with the almost constant southeast trade flow and resultant uplift along the eastern highlands would be expected to reduce the incidence of sunflecks in the understorey, but the lower canopy density would facilitate higher levels of background diffuse radiation in the understorey. In other words, a lower incidence of sunflecks in the understorey of northeast Queensland rainforests would be compensated for by higher levels of diffuse radiation.

Table 8.1 compares understorey light environments within lowland, upland and montane rainforests in northeast Queensland with tropical and subtropical rainforests elsewhere. It would appear that the first hypothesis, cited above, should be accepted in part because relative irradiance levels in the understoreys of the various northeast Queensland rainforests are higher, on average, than those published for other rainforest understoreys (Table 8.1). However, the very low percentage transmission for irradiance reported by Bjorkman and Ludlow (1972) in a southeast Queensland rainforest represents the most extreme shade microsite in that forest, and should not be considered as typical of understorey light conditions for the forest as a whole. Nonetheless, across a wide-range of understorey microsites in Costa Rican and Panamanian rainforests, Lee (1987) found mean percentage transmission values for irradiance that are consistently lower than the mean values given for northeast Queensland rainforest understoreys (Table 8.1). In addition, at least two other researchers have reported mean percentage transmission values for irradiance that are lower than those given in Table 8.1 for this study: 1.2% for Amazonian lowland rainforest (Shuttleworth *et al.*, 1984 a); and 3.0% for Nigerian lowland rainforest (Ghuman and Lal, 1987). Moreover, only one study, at the time of writing this thesis, has published a mean percentage transmission value for irradiance in a tropical rainforest that is similar to the range given in Table 8.1 for northeast Queensland rainforests: 5.0% for an upper montane rainforest in Jamaica (Aylett, 1985). In fact, the range of percentage transmission values for irradiance reported for rainforest understoreys in this study are closer to the range of 4 to 17% reported for temperate broadleaf and coniferous forest understoreys (Trapp, 1938; Nageli, 1940; Shirley, 1945; Vezina and Pech, 1964; Gay *et al.*, 1971; Turton, 1985).

Although there is some evidence in support of accepting the first hypothesis in the case of irradiance measurements, it would appear that it should be rejected in the case of PPFD measurements. As shown in Table 8.1, relative PPFD levels in the

Location (Latitude)	Mean percent transmission of irradiance (range)	Mean percent transmission of PPFD (range)	Mean total daily irradiation (range) MJ m^{-2} /day	Mean total daily PPFD (range) mol m^{-2} /day	Maximum intensity of sunflecks μ mol m^{-2} s^{-1}	Percent of daily total irradiation contributed by sunflecks	Percent of daily total PPFD contributed by sunflecks	Mean red to far-red (R:FR) ratio (range)	Reference
Curtain Fig (upland) (17° 17' S.)	4.7 (2.8-6.5)	1.5 (1.2-1.8)	1.00 (0.76-1.23)	0.65 (0.47-0.82)	442.6 (<20)	2-14	5-21	0.29 ## (0.26-0.32)	This study
Curtain Fig (upland) (17° 17' S.)		3.0		0.99 (0.47-1.50)	<250 (10-20)		12-65	0.42 ##	Pearcy (1987)
Curtain Fig (upland) (17° 17' S.) # (pre-cyclone)		3.3 (2.7-3.8)		2.1 (1.3-2.8)			32-61	0.44 ## (0.39-0.47)	This study
Curtain Fig (upland) (17° 17' S.) # (post-cyclone)		8.5 (6.7-10.0)		5.3 (3.2-6.9)			39-68	0.70 ## (0.63-0.76)	This study
Pine Creek (lowland) (16° 59' S.)	8.3 (6.2-10.4)		1.4 (1.08-1.83)			31-53			This study
Pine Creek (lowland) (16° 59' S.) #		4.1 (3.7-4.5)		2.5 (1.7-3.2)			38-61	0.49 ## (0.47-0.52)	This study
Mt Bellenden Ker (montane) (17° 17' S.)	7.9	2.5	1.3	0.81	60.3 (<35)	29	6	0.38 ##	This study
SE Queensland (upland) (28° 15' S.)	2.9 (2.5-3.2)	0.5 (0.4-1.1)	0.35 (0.16-0.53)	0.21 (0.15-0.24)	350 (15)	11	62	0.18 ## (0.17-0.25)	Bjorkman & Ludlow (1972)
Oahu, Hawaii (upland) (21° 30' N.)		2.4 (1.5-3.8)		0.86 (0.55-1.38)	410 (10-30)		40	0.37 ## (0.29-0.47)	Pearcy (1983)

based on estimates derived from fisheye photographs
R:FR estimated using Eqn 7.3.1

Table 8.1. A comparative summary of understorey light environments within tropical and subtropical rainforests. Note definitions of sunfleck activity are specific to each study.

Table 8.1. (Continued).

Location (Latitude)	Mean percent transmission of irradiance (range)	Mean percent transmission of PPFD (range)	Mean total daily irradiation (range) MJ m^{-2} /day	Mean total daily PPFD (range) mol m^{-2} /day	Maximum intensity of sunflecks μ mol m^{-2} s^{-1}	Percent of daily total irradiation contributed by sunflecks	Percent of daily total PPFD contributed by sunflecks	Mean red to far-red (R:FR) ratio (range)	Reference
La Selva, Costa Rica (lowland) (10° 26' N.)		1.5 (1 - 2)		0.32 (0.18-0.55)	ca. 500 (<20)		10-78	0.29 ## (0.24-0.34)	Chazdon & Fetcher (1984)
La Selva, Costa Rica (lowland) (10° 26' N.)	2.8	1.2 (0.1-3.8)			468.8 (36.2)			0.40 (0.13-0.47)	Lee (1987)
B. C. I., Panama (lowland) (9° 9' N.)	3.8	1.5 (0.2-3.6)			307.2 (44.7)			0.35 (0.14-0.46)	Lee (1987)
Thana Dist., India (lowland) (19° 31' N.)		10 (6-15)		3.6 (2.2-5.3)	1430		15-66	0.30	Lee (1989)
Sumatra, Indonesia (lowland) (1° 5' S.)		0.68 (0.25-1.04)		0.21 (0.05-0.37)				0.20 ## (0.15-0.25)	Torquebiau (1988)
Los Tuxlas, Mexico (lowland) (18° 34' S.)							16-44		cited in Chazdon (1984)
Southern Nigeria (lowland) (6° 15' N.)						70			Evans (1956)
Bukit Res., Singapore (lowland) (1° 18' N.)						50			Whitmore & Wong (1959)
Ecuador (lowland) (approx. 3° S.)						60			Grubb & Whitmore (1967)

R:FR estimated using Eqn 7.3.1

understoreys of upland and montane rainforests in northeast Queensland are similar to those published for other rainforest understoreys. For example, the mean percentage transmission for PPFD in the Curtain Fig understorey is within the range reported for Costa Rican and Panamanian rainforests (Table 8.1). An examination of site details reveals that these forests are 20-40 m tall and hence they have relatively closed canopy conditions. However, Pearcy (1987) reported a higher mean percentage transmission for PPFD in the understorey of the Curtain Fig forest than the mean value obtained in this study. The reason for this difference is probably due to the fact that Pearcy's mean value is largely based on measurements made during the dry season (August-October), a period when cloud development is minimal because of weak southeast trades. Furthermore, the canopy is likely to be more open at this time because of the presence of some deciduous and semi-evergreen trees which exhibit heavy leaf fall at times of moisture stress (Tracey, 1982). On the other hand, the mean value given for the present study is based on measurements made in mid-January (wet season), and July (end of the wet) and it is therefore more typical of light conditions within this forest understorey. Likewise, the mean percentage transmission for PPFD in the Mt Bellenden Ker understorey is similar to that reported by Pearcy (1983) for the Hawaiian forest. Both these forests transmit a higher proportion of PPFD because they are only 10-20 m in height and hence have relatively open canopy conditions.

For reasons stated above, the very low percentage transmission for PPFD given by Bjorkman and Ludlow (1972) is only representative of an extreme shade microsite in that forest. The very low percentage transmission for PPFD published by Torquebiau (1988) for the Sumatran rainforest understorey is also indicative of an extreme shade microsite in that forest and should not be considered as typical of understorey light conditions for the entire forest. Both studies emphasise the problem of only measuring light conditions at one site in the understorey of a complex rainforest.

The range of daily total PPFDs in the Curtain Fig understorey over the year (Table 8.1) compare closely with those reported by Pearcy (1987) for the same forest. Likewise, mean daily PPFD in the Mt Bellenden Ker forest understorey is similar to that reported by Pearcy (1983) for the Hawaiian forest understorey. However, some of the results compared in Table 8.1 emphasise the problem of relative versus absolute measurements. For example, the mean percentage transmission of PPFD in the Curtain Fig understorey over the year is the same as the yearly mean given by Chazdon and Fetcher (1984) for the Costa Rican forest understorey; yet in absolute terms, mean daily total PPFD in the Curtain Fig understorey is over twice as much as that given for the Costa Rican forest understorey. Hence, in absolute terms daily total PPFDs within upland and montane rainforest understoreys in the study area are 2- to 5-times greater than values reported for equatorial rainforests (Table 8.1) and are similar to that found in the Hawaiian rainforest at a corresponding latitude.

The literature review emphasised the importance of sunflecks to the energy and carbon balances of understorey plants. It was suggested that evapotranspiration rates experienced by understorey plants would be very low under most conditions because of the low levels of radiant energy experienced in the understorey. However, it is difficult to estimate transpiration rates in these plants because, as well as incident radiant energy, transpiration is also dependent on stomatal conductance, leaf size, leaf orientation, vapour pressure deficit and windspeed. In terms of the carbon balance, it was shown that tree saplings and herbs growing in shaded habitats have low light saturation and compensation points (Table 2.3), and consequently their quantum efficiencies are generally high. Furthermore, recent studies have shown that in most tropical rainforest understoreys, sunflecks contribute 32 to 60% of the daily carbon uptake in seedlings and saplings (Pearcy, 1988, Chazdon, 1988) and that photosynthetic utilisation of sunflecks depends not only on the light intensity but also on their frequency and duration (Chazdon and Pearcy, 1986 a, b). Although sunflecks are important to the daily carbon gain in understorey rainforest plants, background diffuse (shade) light is generally above the light compensation points of understorey plants (1.7-6.3 μ mol m^{-2} s^{-1}, Table 2.3); research from a number of tropical rainforest understoreys has shown that diffuse PPFDs are mostly between 5 and 50 μ mol m^{-2} s^{-1}, depending on overstorey density and sky conditions.

There are some problems with comparing the proportion of daily radiation contributed by sunflecks shown in Table 8.1 because definitions of sunfleck activity are specific to each study. However, all the values shown for PPFD measurements are based on average readings over 5- or 10-min intervals and this permits a reliable comparison among the rainforests. Nonetheless, caution must be applied in the case of irradiance measurements because of the range of instruments and sampling rates used by various researchers. In addition, researchers are not consistent about what radiant and photon flux densities constitute a sunfleck; the definitions used in this thesis for irradiance (50 W m^{-2}) and PPFD (50 μ mol m^{-2} s^{-1}) are similar to those used in recent studies in other forests (eg Pearcy, 1983, 1987; Chazdon and Fetcher, 1984; Chazdon, 1986; Lee, 1987, 1989).

It would appear from the comparisons made in Table 8.1, that the second hypothesis, cited above, should be accepted in part because sunflecks represent a less significant portion of the daily total radiation in the understoreys of upland and montane rainforests in the study area. Apart from the estimates derived from the fisheye photographs that tend to over-estimate direct PPFDs in the understorey, the percentages of daily total PPFD contributed by sunflecks in the Curtain Fig and Mt

Bellenden Ker understoreys range from 6-21%; this compares with a range of 10-78% reported for the other rainforest understoreys shown in Table 8.1. Similarly, the percentages of daily total irradiation contributed by sunflecks in these forest understoreys range from 2-29% compared with 11-70% for rainforest understoreys elsewhere. The discrepancy between the range of values given in this study for the Curtain Fig forest (Table 8.1) and those reported by Pearcy (1987) for the same forest is due to the same factors described earlier.

Further evidence that sunflecks play a less significant role in the carbon and energy balances of understorey plants in upland and montane rainforests is demonstrated by comparing frequency distributions of PPFD among forests. The highest 10-min average reading (sunfleck) recorded in the Curtain Fig understorey was 442.6 μ mol m^{-2} s^{-1}, although most sunflecks were between 50 and 200 μ mol m^{-2} s^{-1} (Fig. 7.11). This observation is supported by independent measurements made by Pearcy (1987) in the understorey of the same forest (Table 8.1), where he reported that most sunflecks were less than 250 μ mol m^{-2} s^{-1}. In the same study, he also found that only 32% of the daily carbon gain in understorey tree seedlings was due to sunflecks. In some tropical rainforest understoreys (Table 2.3), sunflecks are responsible for up to 60% of the daily carbon gain in understorey plants under sunny conditions. Moreover, it would appear that sunflecks play an almost insignificant role in the energy and carbon balances within the Mt Bellenden Ker forest understorey because over the period of measurement, they never exceeded 75 μ mol m^{-2} s^{-1}. The light environments within this montane tropical forest will be discussed further in Section 8.3.

Herein lies the main difference between understorey light conditions in upland and montane rainforests in the study area and those elsewhere: because of the cloudy trade-wind coast climate (Gentilli, 1972), sunflecks are less intense in the Curtain Fig and Mt Bellenden Ker forests than those measured in other tropical rainforests. Leaf flutter due to the steady trade wind would also reduce the intensity and duration of sunflecks in the understoreys of these forests throughout most of the year. However, the frequency distributions of PPFD and irradiance appear to be more or less the same for all rainforests, exhibiting high degrees of positive skewness and kurtosis. In other words, diffuse PPFDs (ie intensities less than 50 μ mol m^{-2} s^{-1}) typically contribute over 90% of those found in the understorey over the course of a day (Bjorkman and Ludlow, 1972; Pearcy, 1983, 1987; Chazdon and Fetcher, 1984; Chazdon, 1986; Lee, 1987; Oberbauer *et al.*, 1988).

Furthermore, it would appear that most diffuse PPFDs within the Curtain Fig understorey (Fig. 7.11) and Mt Bellenden Ker understorey (Fig. 7.15) are above the light compensation points reported thus far for understorey plants (Table 2.3), which implies that sunflecks are less critical for maintaining a positive carbon balance in plants growing in these understoreys. By comparison, in deeply shaded closed-canopy sites in the Costa Rican rainforest described earlier, Chazdon (1986) found that where diffuse midday PPFD was below 5 μ mol m^{-2} s^{-1}, sunflecks provided the light energy needed to maintain the positive carbon balance. In the same study, it was shown for three species of understorey palms, that positive carbon gain occurred at daily total PPFDs greater than 0.20 mol m^{-2} per day. As shown in Table 8.1, mean daily total PPFD for rainforest understoreys examined in this study are well above this amount, ranging from 0.65-5.3 mol m^{-2} per day; this compares with a range of 0.21-3.6 mol m^{-2} per day for rainforest understoreys elsewhere.

In apparent contrast to upland and lowland rainforests in the study area, sunflecks appear to contribute a significant amount to the daily total irradiation in the understorey of the Pine Creek forest (Table 8.1) and, therefore, the second hypothesis should be rejected in the case of this lowland rainforest. Although 10-min average PPFD was not measured in the Pine Creek understorey, it is likely that sunflecks play a more important role in the annual carbon balance of this forest. This generalisation is based on the fact that radiant flux densities are much higher within this forest in July (Table 7.7 and Fig. 7.21) than those within the Curtain Fig forest at the same time of year (Table 7.8 and Fig. 7.23). On the basis of measurements of irradiance and PPFD made within the Curtain Fig forest, it is estimated that sunflecks contributed 40 to 60% of the daily total PPFD within the Pine Creek understorey in July. This range is similar to that reported by Pearcy (1983) for the understorey of the Hawaiian forest which has a similar stature (15-20 m) to the Pine Creek forest (Fig. 5.5). In the same forest, he also found that sunflecks were responsible for up to 60% of the carbon gain in understorey seedlings, almost twice as much as the figure given by Pearcy (1987) for understorey seedlings in the Curtain Fig forest during the dry season.

In regard to light utilisation by understorey plants in the Curtain Fig and Mt Bellenden Ker forests it would appear that post-illumination CO_2 fixation, which allows for the equivalent of a few extra seconds of light-saturated photosynthesis following a sunfleck (Chazdon and Pearcy, 1986 a), may be less important in these understoreys because of the general lack of sunfleck activity, particularly during periods of prolonged cloudy weather. On the other hand, this process is likely to be more important to the total carbon gain of seedlings and saplings in the Pine Creek forest understorey because of the greater sunfleck activity in this forest.

The literature review also made a few generalisations about the non-photosynthetic characteristics of understorey plants. It was shown that beneath dense rainforest canopies there are spectral changes which are of obvious physiological significance, notably the drastic reduction in red and blue wavebands. Research has demonstrated that light quality, as well as the quantity of light received by plants in tropical rainforests, affects numerous life cycle factors, such as germination, establishment, growth, survivorship and reproduction (Figs. 2.6 and 2.7). Variations in light quality, and the red to far-red (R:FR) ratio in particular, appear to control the morphological characteristics of plants growing in the understorey. It was determined that beneath dense canopies, R:FR ratios are generally less than 0.5 and in open daylight they are typically greater than 1.0 (Smith and Morgan, 1981).

Table 8.1 compares mean R:FR ratios for lowland, upland and montane rainforests in the study area with tropical and subtropical rainforests elsewhere. With the exception of the Curtain Fig understorey after the cyclone, mean R:FR ratios for all the understoreys are less than 0.5, with the range of values confirming that the quantity of far-red light in the understorey can be 2- to 8-times that of red light. Such low R:FR ratios, together with generally low PPFDs, must affect growth and development processes in understorey seedlings and saplings within these rainforests.

The pre- and post-cyclone light measurements for the understorey of the Curtain Fig forest (Table 8.1) provide a unique opportunity to discuss the likely effects of this kind of disturbance on the ecophysiology and dynamics of rainforests growing in regions affected by tropical cyclones; the most obvious and dramatic effect being the significant increase in direct, diffuse and total site factors and R:FR ratios as a result of the slight-to-moderate canopy disturbance caused by the cyclone (Table 7.12 and Fig. 7.31). In absolute terms, it was shown that mean (potential) daily PPFD increased by 60% within the understorey immediately after the cyclone (Table 7. 13). Such profound changes in both the quantity and spectral quality of light available to plants in the understorey would have important implications for the physiological and ecological processes shown in Fig. 2.6 and 2.7. The increase in sunfleck activity following the cyclone would immediately affect photosynthesis rates, stomatal responses, leaf temperature, seed germination and morphogenesis (Fig. 2.6). On the other hand, the general increase in light availablity in the understorey would affect plant growth, seedling establishment, morphology, survivorship and reproduction at the scale of weeks to months following the cyclone. However, over longer time scales (perhaps greater than 12-24 months), and assuming no further cyclone damage, one would expect canopy density (and hence understorey light conditions) to return more or less to the pre-cyclone state.

8.2 A COMPARATIVE EVALUATION OF TREEFALL GAP LIGHT ENVIRONMENTS WITHIN TROPICAL RAINFORESTS

Light availability is undoubtedly the major limiting resource in tropical rainforest understoreys. As we have seen, the shaded understorey is noted for its dark, moist appearance interrupted by occasional sunflecks. Very few tree species are able to complete their life cycles in the shaded understorey; they rely instead on openings or gaps in the canopy as a means of receiving sufficient light for growth and reproduction (Denslow, 1987).

As already discussed in the literature review, rainforest trees can be broadly classified into those that only regenerate in gaps (so-called large gap specialists or pioneer species) and those that may be shade tolerant in some stages of their development, but ultimately depend on gaps to reach maturity (so-called small gap specialists or nomad species). Of the 700 plus tree species growing in northeast Queensland rainforests only 20 or so regenerate exclusively in large gaps or open areas (Thompson *et al.*, 1988). The vast majority are able to grow, albeit slowly if not at all, in the understorey, but require a canopy gap to reach maturity. For this reason, it is now widely recognised that gaps caused by the death or forced toppling of a single tree or small group of trees are central to the function and structure of tropical rainforests. Yet, on average, only 1-2% of the canopy area is disturbed each year by treefalls (Denslow, 1987; Whitmore, 1988). Many would argue that this small area is sufficient to maintain structural and floristic diversity in these forests. In other words, we should view a rainforest as a 'dynamic' ecosystem with treefall gaps being constantly created by disturbances and filled-in by regrowth of seedlings and saplings from below and by canopy closure from above.

However, it was concluded that, unlike rainforest understoreys, it is difficult to compare light measurements among treefall gaps because of the combined effect of factors such as latitude, time of year, slope angle and aspect, forest height and gap configuration. Consequently, two research hypotheses were developed in regard to treefall gap light environments in northeast Queensland rainforests:

(1) Because of the relatively high latitude of the study area, seasonal changes in light availability, particularly in small gaps, are more marked than equatorial rainforests where most research has been conducted so far; and

(2) While latitude and effective gap size profoundly influence light availability at the centre of treefall gaps, slope inclination, slope aspect and sky conditions will also affect light availability in gaps and hence influence their vegetation dynamics.

In formulating these hypotheses, it was suggested that it would be naive to consider only gap size and latitude as the main factors affecting gap light regimes and associated vegetation dynamics. The validation of these hypotheses has important implications for improving our knowledge and understanding of: rainforest regeneration in gaps and clearings following natural and human disturbance, rainforest management, plantation forestry practices, and reforestation of degraded areas such as mine sites and road cuttings.

It is evident from the information summarised in Table 8.2, that quantitative data on irradiance and PPFD within treefall gaps in tropical rainforests is rather scant. Chazdon and Fetcher (1984) reported an annual mean percentage transmission of 9% for a 200 m^2 gap in the Costa Rican rainforest referred to in the previous section; this value compares well with the values shown in Table 8.2 for 100-130 m^2 gaps in the Curtain Fig forest. It is also evident that there are considerable differences in relative irradiance and PPFD levels among apparently similar gaps, and this is most likely due to the various factors affecting light availability within gaps described above.

Unfortunately, there are few studies examining seasonal changes in light availability within treefall gaps to compare with this study. However, there is some evidence in support of accepting the first hypothesis cited above. For example, within a 400 m^2 gap in the Costa Rican rainforest described above, Chazdon and Fetcher (1984) found that the percentage transmission of PPFD ranged from 20 to 35% over the year; this compares with a yearly range of 11.9 to 45.4% for 200 m^2 gaps in the Pine Creek forest, and 22.4 to 60.1% for a 500 m^2 gap in the Wongabel forest (Table 8.1). Furthermore, computer simulations in Chapter 4 (Fig. 4.2) have demonstrated that seasonal changes in light availability across a range of gap sizes at 20° S., a similar latitude to northeast Queensland, are greater than at the equator. It is not unreasonable to assume, therefore, that seasonal changes in light availability within small and large rainforest gaps at northeast Queensland latitudes are greater than those found within similar gaps at or near the equator.

Despite the obvious problems in comparing treefall gap light regimes among the various rainforests shown in Table 8.2, it is clear that mean daily total irradiation and PPFD within these gaps are greater than values reported for adjacent understoreys (Table 8.1) and less than values experienced by canopy emergents. Consequently, as a result of the death or forced toppling of a single tree or small group of trees there is a dramatic change in both the quantity and spectral quality of light reaching the forest floor. The constant shade with random patches of direct light (sunflecks), that typifies light conditions in the understorey beneath an intact canopy, is suddenly replaced by a light regime that has more predictable diurnal and seasonal patterns.

Location (Latitude)	Mean percent transmission of irradiance (range)	Mean percent transmission of PPFD (range)	Mean total daily irradiation (range) MJ m^{-2} /day	Mean total daily PPFD (range) mol m^{-2} /day	Mean irradiance (range) W m^{-2}	Mean PPFD (range) μ mol m^{-2} s^{-1}	Mean red to far-red (R:FR) ratio (range)	Reference
Curtain Fig (17° 17' S) 100-130 m^2 gaps (January and July)	12.3 (5.9-18.6)	8.9 (3.6-14.2)	3.18 (1.02-5.33)	4.72 (1.39-8.06)	70.2 (0-1060.1)	104.4 (0-2045.4)	0.72 ## (0.46-0.88)	This study
Curtain Fig (17° 17' S) 300 m^2 gap (October)		36.5		12.6		(0-2000.0)	1.24 ##	Pearcy (1987)
Curtain Fig (17° 17' S) 100-130 m^2 gaps # (Full Year)		11.3 (5.5-26.2)		8.6 (2.4-20.0)			0.80 ## (0.57-1.11)	This study
Wongabel (17° 17' S) 500 m^2 gap # (Full Year)		37.2 (22.4-60.1)		25.4 (10.2-40.3)			1.25 ## (1.05-1.45)	This study
Pine Creek (16° 59' S) 200 m^2 gaps # (Full Year)		23.0 (11.9-45.4)		12.7 (5.3-30.2)			1.06 ## (0.82-1.33)	This study
Mt Bellenden Ker (17° 17' S) 150 m^2 gap (June)	11.6	6.0	1.9	1.9	47.4 (0-161.6)	48.4 (7.9-167.0)	0.60 ##	This study
La Selva, Costa Rica (10° 26' N.) 400 m^2 gap (Wet & Dry seasons)		27.5 (20.0-35.0)		7.2 (3.9-13.6)		166.0 (0-1100.0)	1.13 ## (1.01-1.23)	Chazdon & Fetcher (1984)

based on estimates derived from fisheye photographs
R:FR estimated using Eqn 7.3.1

Table 8.2. A comparative summary of treefall gap light environments within tropical rainforests.

Table 8.2. (Continued).

Location (Latitude)	Mean percent transmission of irradiance (range)	Mean percent transmission of PPFD (range)	Mean total daily irradiation (range) MJ m^{-2} /day	Mean total daily PPFD (range) mol m^{-2} /day	Mean irradiance (range) W m^{-2}	Mean PPFD (range) μ mol m^{-2} s^{-1}	Mean red to far-red (R:FR) ratio (range)	Reference
La Selva, Costa Rica (10° 26' N.) 200 m^2 gap (Dry season)		9.0		2.3 (1.5-3.1)		53.2 (0-220.0)	0.72 ##	Chazdon & Fetcher (1984)
La Selva, Costa Rica (10° 26' N.) unsp. gaps (April)	37.5	28.9 (4.1-90.0)			175.1 (29.5-770.0)	368.0 (44.4-1603.0)	0.90 (0.59-1.25)	Lee (1987)
B. C. I., Panama (9° 9' N.) unsp. gaps (April)	75.5	67.6 (37.4-96.1)			418.0 (158.6-702.0)	994.8 (347.0-1730.0)	1.15 (0.97-1.17)	Lee (1987)
Sumatra, Indonesia (1° 5' S.) 320 m^2 gap (2 days)		19.8		7.2		167.7	1.00 ##	Torquebiau (1988)
Sumatra, Indonesia (1° 5' S.) 320 m^2 gap-edge (2 days)		3.0		1.1		25.3	0.42 ##	Torquebiau (1988)
La Selva, Costa Rica (10° 26' N.) 150 m^2 gap (Wet & Dry seasons)				3.1 (1.0-5.1)				Chazdon (1986)
La Selva, Costa Rica (10° 26' N.) 150 m^2 gap-edge (Wet & Dry seasons)				1.1 (0.8-1.4)				Chazdon (1986)
La Selva, Costa Rica (10° 26' N.) 200 m^2 gap-edge (Wet & Dry seasons)				1.8 (0.2-3.3)				Chazdon (1986)
La Selva, Costa Rica (10° 26' N.) 400 m^2 gap-edge (Wet & Dry seasons)				2.6 (0.6-4.6)				Chazdon (1986)
Penang, W. Malaysia (5° 28' N.) 100 m2 gap (10 mths)		37.0					1.25 ##	Raich (1989)

based on estimates derived from fisheye photographs
R:FR estimated using Eqn 7.3.1

As shown in Table 8.2, a large range of radiant and photon flux densities are experienced within treefall gaps, and like the understorey, the frequency distribution of light exhibits strong degrees of positive skewness and kurtosis (Figs. 7.12 and 7.13). As a rule, diffuse PPFDs (ie intensities less than 50 μ mol m^{-2} s^{-1}) contribute more than 70% of those found in small gaps over the course of a day in tropical rainforests (Fig. 7.13, this study; Chazdon and Fetcher, 1984; Chazdon, 1986). However, unlike the understorey, the direct light component in gaps consists of prolonged periods of unintercepted sunlight during the middle of the day, as well as the usual sunflecks at other times of the day. Superimposed over this diurnal light regime, there are seasonal changes in sun-earth geometry that affect the penetration of direct sunlight into these gaps. The gap light regime is further complicated by the configuration of the gap itself. Results of modelling light availability within treefall gaps (Table 7.17) have shown that seasonal variations in direct light within small and large elliptical gaps that are orientated east-west are greater than those found for the exact same gaps orientated north-south.

In addition to the dramatic increase in light quantity in the understorey following a treefall, there are important changes in the spectral quality of the light. As already discussed in the previous section, the red to far-red (R:FR) ratio is generally less than 0.5 within tropical rainforest understoreys (Table 8.1). Because many plant species have seeds that will not germinate until R:FR ratios are constantly high (Morgan and Smith, 1981), the creation of a gap by a treefall is vital for their survival as the canopy opening results in a significant increase in the proportion of red light reaching the forest floor. It can be seen in Table 8.2, that mean R:FR ratios for various treefall gaps range from 0.42 to 1.25 with an overall mean of 0.94; this compares with an overall mean of 0.37 for the rainforest understoreys shown in Table 8.1.

The literature review also emphasised the extreme microclimate conditions experienced by seedlings and saplings within large treefall gaps. During the middle of the day plants growing in these gaps experience radiant flux densities that are similar in intensity to those experienced by canopy emergents. Consequently, they have to contend with higher leaf temperatures and transpirational demands than plants growing in the understorey and small gaps. Few shade-tolerant tree species are capable of surviving the extreme conditions in large gaps; instead these gaps are colonised by shade-intolerant (pioneer) species that either grow fast or adjust physiologically to the profoundly altered microclimate (Fetcher *et al.*, 1985).

The large gap strategists (pioneers) are generally found in gaps that have average light levels in excess of 10-20% full sun (Schulz, 1960). Conversely, the small gap strategists (shade-tolerant tree species) prefer small gaps that have average light levels less than 10% full sun. Accordingly, large gap strategists have high light compensation points and high rates of maximum (light saturated) photosynthesis, while small gap strategists have comparatively lower light compensation points and rates of maximum photosynthesis (Table 2.3). Consequently, an examination of the various gaps shown in Table 8.2 would suggest that large gap strategists are most likely to be found in gaps over 150 m^2.

Considerable changes in both the quantity and spectral composition of light available to dormant seeds, seedlings and saplings in the understorey following a treefall and subsequent creation of a canopy gap, will undoubtedly affect the physiological and ecological processes shown in Figs. 2.6 and 2.7. The sudden increase in diffuse, and particularly red-enriched direct light, would affect photosynthesis rates, stomatal responses, leaf temperature, seed germination and morphogenesis at time scales lasting from a few seconds to several hours. The general increase in light availability would also affect plant growth, seedling establishment, morphology, survivorship and reproduction at the scale of weeks to months. Finally, depending on the size of the original gap, the increased light availablity would affect phenology, leaf turnover, whole-plant growth, plant architecture and nutrient cycling at the scale of months to years (Fig. 2.6).

As stated in Chapter 4, the results of Simulation 1 (Fig. 4.2, Appendix C: Tables C.1 to C.7) emphasise the profound influence of latitude on solar radiation availability in rainforest gaps and clearings, particularly at higher latitudes Perhaps the most important finding in Simulation 1, is that at 40° S. there is theoretically no time of the day throughout the year, on a horizontal surface, when direct-beam irradiance reaches the centre of rainforest gaps with forest height to gap diameter (*h:d*) ratios greater than 1:1 (Fig. 4.2). In other words, if sunflecks are excluded for modelling purposes, then no direct light will ever reach the centre of small-to-large single treefall gaps within rainforests at this latitude. Given the fact that single treefalls are the most common disturbance event in rainforests (Brokaw, 1985) and the importance of direct light for physiological and ecological processes such as photosynthesis, morphogenesis, seed germination, survivorship and reproduction (Chazdon, 1988), it would appear that geographical location (latitude) is an undisputed limiting factor to rainforest function, particularly gap-phase dynamics. Consequently, the effect of latitude on light availability within small treefall gaps may explain the general decrease in regional rainforest diversity from tropical to temperate eastern Australia (Stocker, 1988).

The results shown in Fig. 4.2 assume that latitude and the effective size of gaps, as determined by the forest height to gap diameter ratio, are the main factors controlling the availability of light in gaps. However, if light availability is the main limiting resource in rainforests, then studies of gap environments and dynamics need to take into account the other factors affecting light availability within gaps. In particular, slope inclination, slope aspect and sky conditions are likely to influence light regimes within treefall gaps. The second hypothesis, cited above, was developed to test this proposal.

The results of Simulations 2 and 3 (Figs. 4.4, 4.5 and 4.8, Appendix C: Tables C.8 to C.28) provide substantial evidence for the acceptance of the second hypothesis. In particular, the results of Simulation 2 support the notion that slope inclination and aspect are more important to rainforest function at higher latitudes than at lower latitudes. It was demonstrated that a steep north-facing (equatorward) slope at 20° S. experiences relatively constant solar radiation conditions throughout the year, compared with a steep south-facing (poleward) slope at the same latitude (Fig. 4.4, Tables C.8 to C.14). This has important implications for energy-balance processes, particularly evaporation and transpiration rates from the soil and vegetation located on these slopes (Oke, 1987). Plants growing on steep north-facing slopes at 20° S. have to contend with constantly high radiation levels, even during the winter months which at this latitude correspond, more often than not, with the dry season. On the other hand, plants growing on south-facing slopes at 20° S. have to contend with the highest radiation levels at the summer solstice because such slopes are inclined towards the sun at this time (Fig. 4.4). However, during the dry winter months south-facing slopes at this latitude are inclined away from the sun and consequently experience lower evapotranspiration rates. It would appear that there is a need for more meso-scale studies examining relationships between species composition and topography in the wet tropics region because the inventory surveys published to-date (eg Webb and Tracey, 1981; and Tracey, 1982) have considered mostly broad scale environmental gradients and interrelationships between species composition and climatic and edaphic factors.

According to Oke (1987: 175), the naturally uneven configuration of the landscape produces a wide spectrum of microclimates, and these have important implications for other aspects of the physical environment, such as hydrologic and geomorphic processes; ultimately, plant and animal habitats are directly and indirectly affected, resulting in distinctly different assemblages of flora and fauna on slopes of different angle and aspect. In northeast Queensland, at a similar latitude to 20° S. (Fig. 4.4), it is not uncommon to find open sclerophyll (fire- and drought-resistant) forest growing on steep north-facing slopes and closed canopy rainforest on remaining slopes, presumably because of some of the factors described above.

At 40° S., there are pronounced differences in solar radiation loadings between north- and south-facing slopes (Fig. 4.5, Tables C.15 to C.21). North-facing slopes experience consistently higher radiation levels than south-facing slopes which are always inclined away from the sun, even at the summer solstice. A study by Aisenshtat (1966), examining the effects of topography on the surface energy balance of bare ground in the Turkestan Mountains (41° N.), showed that a 31° south-facing (equatorward) slope received almost 3-times more net radiation than a 33° north-facing (poleward) slope. It was shown, that the south-facing slope pumped more than 3-times as much sensible heat into its lower atmosphere; Oke (1987) maintains that such strong differential heating is likely to produce local slope winds. Although this study concerned energy-balance conditions above bare ground only, it nevertheless demonstrates the large differences in energy budgets likely to be found among differing slope aspects in the mid-to-high latitudes.

The simulations have also shown, that at 40° S. direct radiation is unable to reach the centre of small-to-large single treefall gaps (ie. *h:d* ratios greater than 1:1) in rainforests growing on horizontal and south-facing slopes (Fig. 4.5). However, at this latitude, small-to-large single treefall gaps located in rainforest growing on north-facing slopes do experience some direct radiation during the summer months (September-March). This undoubtedly promotes forest regeneration within such gaps because of the paramount importance of direct light to physiological and ecological processes, such as photosynthesis, morphogenesis, seed germination, plant growth, survivorship and reproduction (Chazdon, 1988).

The results of Simulation 3 (Fig. 4.5, Appendix C: Tables C.22 to C.28) have demonstrated the important effects of sky conditions on light regimes above and at the centre of rainforest gaps and clearings at 20° S. Some of these simulations have shown that plants growing within small gaps may benefit from increased background diffuse light under cloudy skies, but only in situations where direct light (sunflecks excepted) is unable to reach their leaf surfaces.

The Sky-Canopy-Gap-Irradiance (SCANGIR) Model (Chapter 3) may be used to estimate diurnal and seasonal differences in the availability of diffuse and direct solar radiation within rainforest gaps and clearings for locations experiencing distinct macroclimatic cloud regimes. For example, because of the prevalent cloud cover experienced by montane tropical rainforests, the proportion of direct-beam radiation within large and small treefall gaps in these forests will be significantly lower than that found within similar treefall gaps in lowland tropical rainforests. In the next section, light regimes within montane tropical rainforests will be discussed in more detail.

Accounting for diurnal and seasonal changes in cloudiness and subsequent effects on the availability of light, particularly direct light, within treefall gaps would have important implications for physiological and ecological processes over time (Fig.

2.6) and space (Fig. 2.7). For example, on a seasonal time scale, many tropical areas have distinct wet and dry seasons with corresponding levels of cloudiness. It has already been demonstrated for 20 humid tropical stations that seasonal variations in cloud cover affect total irradiation and sunshine duration at the earth's surface (Table 3.3). Thus, if some index of cloudiness is available from standard meteorological measurements, such as estimates of proportion of cloud cover or number of raindays per month, then it should be possible to fine-tune the estimations of daily PPFD within rainforest understoreys and gaps obtained using the fisheye photography technique.

Likewise, on a diurnal time scale, the SCANGIR Model can be used to simulate a range of sky conditions above a rainforest gap over the course of a day. For example, lowland tropical regions experience a distinct diurnal cloud regime, typically cloudless before solar noon followed by varying depths of cumulus cloud development in the afternoon. This would have implications for plants growing at particular locations within a gap; plants growing on the western-side of the gap would experience more direct light because of the generally cloudless sky conditions before midday, while those growing on the eastern-side of the gap would experience less direct light because of the cloud development in the afternoon. Furthermore, treefall gaps located on steep east-facing slopes would experience greater quantities of direct light than similar treefall gaps located on steep west-facing slopes. The internal heterogeneity of plant species found within treefall gaps in tropical rainforests (Denslow, 1987) may therefore be explained, in part, by the corresponding complexity of the internal gap light regime. Brandani *et al.* (1988), argue that the internal heterogeneity of gaps is probably one of the factors helping to maintain the high tree species richness characteristic of tropical rainforests.

According to Mooney *et al.* (1980: 25), knowledge of the physiological ecology of tropical plants is essential to our understanding of the functioning and effective management of natural tropical ecosystems as well as plantation and agroforestry systems. This is concerned with determining how organisms acquire and allocate resources (light, water and nutrients) in specific environmental complexes. In a partial response to these proposals, this thesis has argued that light availability within understoreys of tropical rainforests is restricted to photosynthetically inactive shade light, interrupted by occasional high intensity, short-duration sunflecks, whose spectral composition is similar to the light above the forest. Research throughout the tropics has shown that very few rainforest tree species can grow and reproduce within the shaded understorey because of the generally low light levels. Over the past decade, researchers have demonstrated experimentally that treefall gaps are central to the functioning of tropical rainforests because of their role as sites for regeneration of most rainforest canopy trees (Denslow, 1987). Perhaps the most important finding to arise out of this research is that the most useful tree species possess a high degree of shade tolerance.

However, at the time of writing this thesis, only one researcher (Hartshorn, 1989) has attempted to design a management system for tropical rainforests that capitalises on forest dynamics and gap dependency. His paper presents preliminary results from a study on the application of gap theory to forest management in the Peruvian Amazon; the aim being to manage heterogeneous tropical forests for sustained yield timber by harvesting narrow strip clear-cuts, which promotes natural regeneration of native tree species. The so-called Palcazu Forest Management Model involves clear-cut strips (30-40 m wide) rotated through a production unit on a 30-40 year cycle. Hartshorn (1989: 568) claims that it is difficult to estimate how many tree species might be lost during subsequent rotations from production forest managed under the strip clear-cut system, but the loss certainly will be much less than losses occurring when large areas are clear-cut or converted to other land use. Moreover, in the conclusion he states that basic research on tropical forest dynamics and gap theory can lead to economically viable and socially attractive management of tropical forests that contributes significantly to the conservation of biological diversity.

Implicit in our understanding of gap dynamics is a detailed understanding of the light environments of gaps, and the SCANGIR Model attempts to account for all the factors affecting light regimes within gaps. As stated in the introduction, ecologists and foresters have tended to only consider latitude and the effective size (forest height to gap diameter) of gaps as the main factors affecting light availability within gaps. The results presented in Chapter 4 of this thesis have demonstrated that, together with latitude and gap size, slope angle, slope aspect and sky conditions also influence the diurnal and seasonal distribution of direct and diffuse radiation within gaps and forest clearings. Hence, the SCANGIR Model could be used in conjunction with the Palcazu Forest Management Model, described above, to produce 'ideal' light conditions for regeneration of shade-tolerant tree species at a particular site. This could be achieved by altering the width and compass direction (orientation) of the clear-cut strips for specific latitudes, forest heights and topographies.

In addition, the SCANGIR Model and gap theory could be applied in the case of rehabilitating rainforest sites in the Wet Tropics World Heritage Area that have been disturbed by activities such mining and road construction, as well as reforestation of degraded areas away from rainforest boundaries on land formerly occupied by rainforest, such as old dairy farms on the Atherton Tableland. The SCANGIR Model would predict diurnal and seasonal distributions of direct and diffuse solar radiation at a particular site in relation to average diurnal and seasonal cloud regimes. On the basis of these estimates and physiologies of native tree species, managers could then apply gap theory to promote the eventual dominance of the site by shade-tolerant (small gap) tree species. In some situations, it may be necessary to manually revegetate sites with suitable tree species, while in other situations it may be necessary to control the growth and subsequent dominance of the site by pioneer (large-gap) tree species that originated from adjacent forest areas. On the other hand, at very exposed sites that have been severely degraded it may be better to revegetate the disturbed area with useful pioneer tree species, planted in monospecific stands, with a view to future timber extraction.

Understanding treefall gap light environments and gap theory may also benefit selective logging practices. This thesis has demonstrated significant differences in light quantity and quality among elliptical gaps with different orientations at 17° S. (Tables 7.17 and 7.18), and because selective felling of individual trees within a rainforest generally results in the formation on an elliptical gap, similar to those shown in Plates 7.5 and 7.7, then it should be possible to manipulate regeneration processes by controlling the direction of treefalls. Forest managers could achieve regeneration of useful shade-tolerant tree species in tropical rainforests by ensuring that trees were felled in a north-south, rather than an east-west, direction because the latter would create light regimes of greater benefit to shade-intolerant (pioneer) tree species that are generally of little commercial value. On the other hand, in subtropical and temperate rainforests, shade-tolerant tree species would benefit from east-west treefall gaps because of the consistently lower solar angles at latitudes corresponding with these forest types (Fig. 4.1). However, forest managers would also need to take into account local forest height and topography at the site of the proposed treefall.

8.3 LIGHT ENVIRONMENTS WITHIN MONTANE TROPICAL RAINFOREST IN NORTHEAST QUEENSLAND

The following research hypothesis was developed in regard to light environments within montane tropical rainforest in northeast Queensland:

Reduction in photosynthetic photon flux density (PPFD) by cloudiness decreases productive capacities of montane rainforests compared with lowland rainforests in northeast Queensland.

This hypothesis was developed as a result of several detailed studies showing that above-ground primary productivity and biomass are generally lower in montane rainforests compared with lowland rainforests (Grubb, 1977; Tanner, 1980; Medina and Klinge, 1983), and the explanation put forward by Richards (1952) and Grubb (1977) that these observations were due to lower temperatures and higher cloud cover (and hence decreased solar radiation) experienced by the montane rainforests. However, Jordan (1983) maintains that there is doubt as to whether the effect is direct or indirect. Leigh (1975) supports an indirect effect by attributing decreased productivity to decreased transpiration rates on mountain tops which results in a slower rate of nutrient uptake through the trees. This so-called 'transpiration theory' argues simply that lower rates of transpiration are caused by higher humidities, which result from lower temperatures. The rejection of the above hypothesis would thereby lend support to Leigh's transpiration theory.

Only limited data are available for detailed comparisons of PPFD measurements in the Mt Bellenden Ker forest with those in other tropical rainforests (Tables 8.1 and 8.2). It would appear that daily total PPFD in the understorey of the Mt Bellenden Ker forest is within the range of values reported for rainforest understoreys in northeast Queensland and elsewhere (Table 8.1). Moreover, there is little evidence that cloud cover has reduced the availability of PPFD above the Mt Bellenden Ker forest because the ratio of irradiance to PPFD in the large clearing (Table 7.5) is similar to those found above the Curtain Fig forest at a lower altitude (Table 7.4).

The results presented for the four micro-environments in the Mt Bellenden Ker forest (Table 7.5) suggest that reduction in PPFD by cloud cover would not limit the rates of photosynthesis. Median PPFD in the large clearing (Fig. 7.14) or upper canopy is nearly always above the range of light saturation levels of 100-800 μ mol m^{-2} s^{-1} measured for rainforest plants (Table 2.3). In the remaining micro-environments (Fig. 7.14), median PPFDs are still higher than known light compensation points for understorey or shade-grown rainforest plants (Table 2.3), even in the shaded understorey. Furthermore, Chazdon (1986) has shown, for three species of understorey palms, that daily total PPFD must be greater than 0.20 mol m^{-2} per day for positive carbon gain over a 24-h period. The daily total for the Mt Bellenden Ker understorey near the winter solstice is about 4-times this amount (Table 7.5).

Table 8.3 provides conservative estimates of daily total irradiation under cloudless skies and nimbostratus cloud for the solstices and equinoxes for Mt Bellenden Ker as calculated by the Sky-Irradiance Model (Section 3.1). In the large clearing, the ratio of surface to extraterrestrial irradiation for the 2-day measurement interval was 0.60 (Table 7.5) which is close to the mean dry season value of 0.57 given in Table 3.3 for the humid tropics, in general. If the canopy transmission coefficients for the Mt Bellenden Ker forest (Table 7.5) are assumed to be constant and daily total irradiation above the forest assumed to be isotropic under the nimbostratus cloud, then on the

Date	Extraterrestrial irradiation (MJ m^{-2} per day)	Cloudless-sky irradiation (MJ m^{-2} per day)	Nimbostratus cloud irradiation (MJ m^{-2} per day)
Dec 22	41.6	29.1	4.5
Mar 21/Sep 23	36.3	25.4	4.1
Jun 22	27.0	18.9	3.1

Table 8.3. Extraterrestrial, cloudless-sky (potential) and heavily overcast (nimbostratus cloud type) irradiation for Mt Bellenden Ker at various times of the year. Estimates calculated using the Sky-Irradiance Model (Chapter 3).

shortest day (June 22) daily total irradiation above the forest will be about 3.1 MJ m^{-2} per day (Table 8.3) and daily irradiation in the understorey will be about 0.24 MJ m^{-2} per day (assumming a canopy irradiance transmission coefficient of 0.079, Table 7.5). Given the mean ratio of irradiance to PPFD of 1: 0.64 (Table 7.5), then the estimated minimal value of daily total PPFD in the understorey under nimbostratus cloud will be 0.17 mol m^{-2} per day, slightly lower than the minimum level for positive carbon gain over 24-h given by Chazdon (1986) for understorey palms. The conservative estimate here is based on the lowest likely daily total PPFD above the forest during heavy nimbostratus cloud conditions, although lower levels are likely beneath cumulonimbus cloud (Reynolds *et al.*, 1975). Using the same procedure, the lowest likely daily total PPFDs in the lower-canopy and small gap under nimbostratus cloud are 0.64 and 0.37 mol m^{-2} per day, respectively.

Two conclusions are pertinent to the perceived effects of cloudiness on canopy productivity in montane tropical rainforests. First, in this study, exposed conditions in the large clearing (or upper canopy) allowed light-saturated levels of photoassimilation, even during heavy cloud. Second, estimated minimum levels of daily irradiation and PPFD in lower-canopy, gap and understorey micro-environments are similar to or exceed values for positive carbon gain in understorey plants reported elsewhere. On the basis of this study, the hypothesis that reduction in PPFD by cloudiness decreases productive capacities of montane (cloud) forests must be seriously questioned, if not rejected, and some other hypotheses put forward to explain the generally lower productivity of these forests, such as the transpiration theory devised by Leigh (1975).

8.4 LIGHT ENVIRONMENTS ACROSS THE OPEN FOREST-RAINFOREST BOUNDARY IN NORTHEAST QUEENSLAND

Changes in the location of boundaries between rainforests and eucalypt forests in the tropics and subtropics of eastern Australia are related to changes in the disturbance regime (Unwin *et al.*, 1985, 1988; Stocker and Unwin, 1986). In the absence of fire, rainforest on many sites will advance into areas dominated by fire-tolerant, open forest or grassland species, mainly of the genus *Eucalyptus*, and in time the pyrophytic vegetation will be replaced. Rainforests may be replaced by pyrophytic vegetation following fire, or other forms of disturbance which results in fire being able to penetrate the rainforest boundary. Boundary dynamics of rainforest in northeast Queensland are of particular importance to the conservation and management of rainforest in this region, as a substantial portion of the remaining rainforest occurs as small, isolated patches (Australian Heritage Commission, 1986).

The dynamic nature of rainforest open forest boundaries in northeast Queensland gives rise to a sharp spatial transition between closed canopy vegetation (rainforest) and sclerophyllous vegetation with a relatively open canopy (Fig. 5.7). This floristic transition is accompanied by marked changes in microclimate: temperature range, humidity and light availability, particularly near the ground (Unwin *et al.*, 1985). Light availability to seedlings and saplings in the transition zone (ecotone) has been identified as one of the critical factors, along with fire, controlling boundary dynamics, and hence short-term stability or instability of rainforest (Unwin *et al.*, 1985; Duff, 1987). The pyrophytic species of open forest and grassland are incapable of early growth under a closed canopy, while young individuals of rainforest species are generally fire sensitive and relatively slow growing in the open forest environment. The boundary may vary, in the space of a few metres, from the extremes of the light intensities experienced in the open to those found in the understorey beneath an intact canopy. This change is most rapid close to the forest floor, and this is likely to exert a strong influence on the distribution, establishment and success of seedlings in the early stages of recruitment. As a result of these observations, the following research hypothesis was developed in regard to light environments across the open forest-rainforest boundary in northeast Queensland:

The light regime experienced by plants growing in the rainforest-open forest boundary (ecotone) is similar to that experienced by plants within treefall gaps.

It has already been demonstrated in the previous section that small treefall gaps are important sites for regeneration of primary (shade-tolerant) tree species, because of the favourable light regime afforded by small canopy openings. Conversely, large gaps are frequently colonised by pioneer (shade-intolerant) tree species that prefer the exposed light regime and associated microclimate afforded by large canopy openings. Hence, validation of the above hypothesis would permit forest managers to apply gap theory to the rainforest-open forest boundary with the view to either stabilising or expanding the rainforest edge.

The range of diffuse site factors in the open forest and tall open forest (Table 7.17: zones A and B) are similar to those reported by Anderson (1981) for open eucalypt forest in southeast Australia of 28 to 56%. Likewise, diffuse site factors for the rainforest understorey (zones D and E) are similar to those reported for lowland and upland rainforest in the study area (Tables 7.12 and 7.15). However, the means given for young and mature rainforest at Kirrama (Table 7.19) are somewhat higher than the value of

1.5% given by Bjorkman and Ludlow (1972) for the deeply shaded subtropical rainforest understorey, described earlier. The reason for this was attributed to the fact that their light measurements were only representative of an extreme shade microsite in that forest.

Unfortunately, direct site factors for open eucalypt forest are not included in the paper by Anderson (1981) to compare with this study. However, the direct site factors given for the Kirrama rainforest understorey (Table 7.19: zones D and E) compare well with those reported for lowland and upland rainforest in the study area (Table 7.12 and 7.15) and also with the range of 0 to 17% reported by Pearcy (1983) for the Hawaiian forest understorey, referred to in Table 8.1.

There is evidence in support of accepting the hypothesis, cited above, because mean diffuse and direct site factors for the ecotone (Table 7.19: zone C) are similar to the range of values reported for small and large treefall gaps within several rainforests in the study area (Table 7.17). Likewise, the mean red to far-red (R:FR) ratio in the ecotone (Table 7.19) is within the range of those found in small and large treefall gaps (Table 7.18). However, because of the high variability in diffuse and direct site factors within the ecotone (Table 7.19: zone C), this zone should be treated by forest managers as a 'transition', with a continuum of light regimes that resemble the following micro-environments: open forest > large gap > small gap > rainforest understorey.

Mean total PPFD (2.72 mol m^{-2} per day) in the mature rainforest (Fig. 7.34, zone E) is within the range of 0.21 to 5.3 mol m^{-2} per day given for the tropical and subtropical rainforest understoreys in the study area and elsewhere (Table 8.1). The results indicate that PPFD levels in the young and mature rainforest understoreys (Fig. 7.34 and 7.35) under cloudless and stratus cloud conditions are more than enough to facilitate daily positive carbon gain in understorey species (Chazdon, 1986). However, daily PPFD in the rainforest understorey is almost certainly insufficient for the shade intolerant (pioneer) tree species that require high light intensities, high R:FR ratios and high soil temperatures for germination and seedling establishment (Bazzaz and Pickett, 1980). These species prefer the more open light environments on the rainforest-tall open forest margin (Unwin *et al.*, 1985) or the light conditions experienced within larger rainforest gaps (Denslow, 1987). Typically, these pioneer species exhibit rapid early growth with characteristic high light-saturated photosynthetic rates but low respiration rates (Table 2.3). Thus, at some point in the transition zone between tall open forest and young rainforest (Fig. 7.34), daily PPFD is probably insufficient for daily positive carbon gain in the pioneer species.

Moreover, the results presented here (Table 7.19 and Fig. 7.34) suggest that, towards the rainforest end of the transition zone, light conditions are probably similar to those experienced within small treefall gaps in mature rainforests. Typically, such light conditions are preferred by shade tolerant (primary) tree species that are unable to grow and reproduce successfully in the adjacent shaded rainforest understorey and to compete with the fast growing pioneer species at the more open end of the transition zone.

It would appear, therefore, that understanding the *light availability continuum* across the open forest-rainforest boundary and the associated plant photosynthetic and photomorphogenetic responses are essential for conservation and management of remaining rainforest patches in northeast Queensland. For example, a detailed study of seed germination across ecotones in the Ivory Coast (Ponce de Leon, 1982) has shown that many rainforest seeds and seedlings do not survive when they are exposed to the high temperature fluctuations, lower humidity and periodic fire that are typical of the nearby open forest (savanna) environment. The exposed savanna environment prevents the establishment of the rainforest tree species in the open forest, but when fire is excluded from the ecotone community, some of the resistant seed species can become established, thereby initiating the colonisation of the open forest by the rainforest (Ponce de Leon, 1982). Over time, as the microclimatic conditions are changed by the presence of the rainforest pioneer (shade-intolerant) species, the remaining rainforest plants can germinate under their shade.

Hence, two management and reforestation strategies are suggested for the rainforest-open forest boundary (ecotone) in northeast Queensland: (1) prevent fire occurring near the rainforest margin (zone C) with the eventual aim of extending rainforest into areas presently occupied by open forest species; and (2) reforestation of severely degraded boundary sites with shade-intolerant (pioneer) tree species to encourage the eventual spread of more shade-tolerant (primary) tree species from the adjacent rainforest. Of the 700 plus tree species growing in northeast Queensland rainforests (Tracey 1982) about 20 or so regenerate exclusively in large gaps or open areas and could therefore be used for this purpose.

CHAPTER 9

CONCLUSION AND RECOMMENDATIONS

9.1. CONCLUSIONS

9.1.1 The Aims

The seven (7) specific aims of this thesis, outlined at the end of chapter 2, have been achieved: (1) a computer model for the estimation of solar radiation regimes within rainforest openings that incorporates gap size, forest height, slope angle and apect, sky conditions, and daily and seasonal variation in the position of the sun was developed and presented in Chapter 3; (2) the results of three computer simulations which demonstrated, respectively, the effects of latitude, slope inclination and sky conditions on solar radiation regimes within rainforest gaps and clearings were evaluated in Chapter 4; (3) the temporal and spatial distributions of photosynthetic photon flux density (PPFD) and irradiance within canopy, gap and understorey micro-environments for lowland, upland and montane rainforests in the study area were evaluated in Chapter 7; (4) the influence of solar declination (time of year) on the standard deviation, skewness and kurtosis about the mean of PPFD and irradiance within canopy, gap and understorey sites was examined for the selected rainforests; (5) conservative estimates of the contribution of sunflecks to the daily total PPFD and irradiation within the selected rainforest understoreys at contrasting times of the year were made; (6) within-gap variability of PPFD and irradiance at contrasting times of the year was examined for the selected rainforests; and (7) seasonal variations in light availability across the open forest-rainforest boundary (ecotone) were also evaluated in Chapter 7.

9.1.2 The Materials and Methods

The materials and methods used to obtain quantitative data on the temporal and spatial distribution of solar radiation above and beneath rainforests were described in Chapters 3 and 6.

The Sky-Canopy-Gap-Irradiance (SCANGIR) Model was developed in Chapter 3. This was in response to indications arising out of the literature review which highlighted that the effective size of treefall gaps (ie forest height to gap diameter) and latitude are not the sole factors controlling the availability of light and associated vegetation dynamics. Three computer simulations were generated using the SCANGIR Model which aimed, respectively, to demonstrate the effects of latitude, slope inclination and sky conditions on light availability across a range of effective gap sizes. The effective gap sizes were adjusted in an attempt to simulate canopy openings created by single- and multiple-treefalls, and human-made forest clearings. It was concluded that the SCANGIR Model is an improvement on existing models of this type because it permits the estimation of *effective gap light regimes* by incorporating, together with forest height, gap size and latitude, factors such as slope angle, slope aspect, sky conditions, and daily and seasonal variation in the position of the sun. It was also proposed that the SCANGIR Model could be applied equally well to non-vegetated surfaces, such as urban canyons.

Chapter 6 dealt with the direct and indirect measurement and analysis of solar radiation in the open and within several northeast Queensland rainforests. Radiometric sensors were used for the measurement of short-wave irradiance (0.3-3.0 μm) and photometric sensors were used for the measurement of photosynthetic photon flux density (PPFD = 0.4-0.7 μm). This chapter also included a critical evaluation of a purpose-built photometric sensor, constructed especially for the project. It was demonstrated that this inexpensive light sensor compares well with a commercial quantum sensor in terms of the following specifications: risetime, spectral characteristics, cosine response and linearity under artificial and natural light conditions. However, the results indicate that the purpose-built sensor is not suitable for field measurements requiring accuracies within ±5%.

Sampling techniques applied to the radiometric and photometric sensors were standardised for all field measurements (ie 10-sec scans averaged every 10-mins), with the exception of some 10-sec instantaneous readings. It was argued that the 10-min average sampling technique would be sufficient to indicate major sunfleck events in rainforest understoreys, while keeping the quantity of data to be analysed to manageable levels. However, the results presented in Chapter 7 for upland and montane rainforests have shown that a shorter averaging period, perhaps 2-mins, would be preferable for forest understoreys with lower levels of sunfleck activity. Furthermore, with the advent of powerful portable microcomputers, it would seem that data management problems are no longer the issue they were previously.

It was argued that temporal and spatial distributions of light are both required to fully characterise the complex light environment in rainforests. To achieve this objective, variations among characteristic micro-environments, such as canopy, gap and understorey, were analysed as well as variations within these micro-environments themselves. It was also argued that these micro-environments represent the range of light regimes experienced by plants in rainforests. The understorey illustrates the generally low light conditions prevalent beneath a closed canopy where only extremely shade-tolerant species can survive and reproduce successfully. The treefall gaps are fairly typical of the light regimes created by the death or forced toppling of a single tree or small group of trees, and such canopy openings are considered as essential for the regeneration of most rainforest trees. Finally, above the forest is representative of the light conditions experienced by emergents in the upper canopy.

Different data analysis techniques were applied to the 10-min average irradiance and PPFD readings and the 10-sec instantaneous PPFD readings obtained from sensors placed within these micro-environments. Together with the usual descriptive statistics, a number of higher-order moments about the mean (ie standard deviation, skewness and kurtosis) were applied to the 10-min average readings. The frequency distributions of 10-min average irradiance and PPFD were also examined using class intervals, adjusted to the range of light intensities experienced within the micro-environments. On the other hand, the 10-sec instantaneous PPFD readings were analysed using linear and logarithmic classification schemes. It was argued that the linear classification is useful for emphasising order-of-magnitude differences among micro-environments, while the logarithmic classification is more useful in conjunction with photosynthesis studies because of the non-linear photosynthetic response to light.

The hemispherical (fisheye) canopy photography method, described in Chapter 6, is considered as the first attempt to model light availability above and beneath rainforest canopies under a range of sky conditions. This was achieved by combining the manual technique for determining direct and diffuse site factors beneath plant canopies from fisheye photographs pioneered by Anderson (1964 a,b) with the Sky-Irradiance Model presented in Chapter 3 of this thesis.

9.1.3 The Results and Synthesis

The results obtained from the computer simulations and field measurements were presented in Chapters 4 and 7, respectively, and comparative evaluations were made in Chapter 8.

Chapter 4 presented the results of three computer simulations. The first simulation attempted to demonstrate the effects of latitude on the availability of solar radiation, and direct-beam radiation in particular, within rainforest gaps and clearings. On the basis of simulations that assumed a cloudless sky, zero slope, no sunflecks and a 10-60 m tall forest, it may be concluded that:

(1) seasonal variations in daily total irradiation above the forest canopy and in small-to-large clearings increase with increasing latitude;

(2) at 40° South, the latitude corresponding with temperate rainforest in Australia and New Zealand, there is theoretically no time of the day throughout the year, when direct irradiance reaches the centre of small-to-large single treefall gaps; and

(3) given the fact that single treefalls are the most common disturbance event in rainforests and the importance of direct light for numerous physiological and ecological processes in forests, then latitude is an undisputed limiting factor to rainforest function, particularly gap-phase dynamics.

The second simulation addressed a deficiency in the literature, by attempting to demonstrate the effects of slope angle and aspect on the availability of solar radiation within rainforest gaps and clearings. The following conclusions may be drawn as a result of the computer simulations for six slope inclinations at 20° and 40° South that assumed cloudless skies, no sunflecks and a 10-60 m tall forest:

(1) slope angle and aspect are more important to rainforest function, particularly gap-phase dynamics, at higher latitudes than at lower latitudes;

(2) small-to-large rainforest clearings located on steep north-facing (equatorward) slopes at 20° South experience relatively constant radiation conditions throughout the year, compared with clearings of the same size located on steep south-facing (poleward) slopes at this latitude;

(3) as a consequence of the effects of slope inclination on radiation loadings within small-to-large rainforest clearings at 20° South, tree seedlings and saplings growing in such clearings located on steep north-facing slopes have to contend with constantly high transpirational demands coupled with high soil evaporation rates, while those located in similar clearings on steep south-facing slopes have only to contend with high transpirational demands and soil evaporation rates at or near the summer solstice; and

(4) at 40° South, small-to-large single treefall gaps located on moderate-to-steep north-facing slopes experience some direct light during the summer months, and this undoubtedly promotes forest regeneration within such gaps.

The third simulation attempted to demonstrate the effects of sky conditions on the availability of solar radiation within rainforest gaps and clearings. This simulation is considered the first of this kind because other models dealing with light regimes in forest openings have only considered potential (cloudless-sky) radiation. As a result of computer simulations for three cloud types at 20° South that assumed zero slope, no sunflecks and a 10-60 m tall forest, it may be said that:

(1) daily total irradiation available at the canopy surface declines steadily with increasing cloud depth (ie. cirrostratus > altostratus > stratus);

(2) during the winter months (April-August), mean irradiance levels within small treefall gaps under cirrostratus and altostratus cloud are almost twice the intensity of levels experienced under cloudless skies because of an increase in the diffuse component of the total radiation under cloudy skies; and

(3) tree seedlings and saplings growing within small treefall gaps may benefit from increased background diffuse light under cirrostratus and altostratus cloud, but only in situations where direct light is unable to reach their leaf surfaces.

Chapter 7 presented the results of field measurements undertaken at three sites in northeast Queensland (Topaz, El-Arish, Atherton) and within lowland, upland and montane rainforest in the study area. It was necessary to obtain base-line data on solar radiation variability within the Wet Tropics study area because long-term records were only available for one site - Pin Gin Hill. The main findings arising from one year's measurement of daily total irradiation at the three sites, may be summarised as follows:

(1) the highest annual total irradiation was recorded at Atherton, the driest site, followed by Topaz and El-Arish, respectively;

(2) daily total irradiation was lowest during the winter months (April-July) because of the lower solar angles and reduced day length, with the effect being enhanced by general cloudiness due to prevalent southeast trades during these months;

(3) daily total irradiation was highest during the pre-monsoon months (September-December) because of the higher solar angles and increased day length, with the generally clear conditions being maintained due to weak southeast trades during these months; and

(4) because of the cloudy trade-wind coast climate, annual total irradiation within the Wet Tropics of northeast Queensland lies at the mid-to-lower end of the range found for other locations in the world's humid tropics.

The detailed field measurements, examining the temporal (diurnal and seasonal) and spatial distributions of solar radiation above and beneath several northeast Queensland rainforest types, are considered to be the most comprehensive in this region to date, and it is hoped that this research will contribute to existing and future studies on the ecophysiology and dynamics of rainforest vegetation in the region and elsewhere.

As a consequence of the results presented in Chapter 7 and the comparative evaluations made in Chapter 8, the following conclusions may be stated about rainforest understorey and gap light environments in the study area:

(1) daily total irradiation and PPFD levels within the understoreys of lowland, upland and montane rainforests in northeast Queensland are 2- to 5-times higher than those reported for several equatorial rainforests and similar to that reported by one researcher for an Hawaiian forest understorey, at a similar latitude to the study area;

(2) because of the cloudy trade-wind coast climate, high intensity, long-duration sunflecks are more the exception than the rule within upland and montane rainforest understoreys in the study area, and are therefore likely to play only a small role in the carbon balance of understorey plants in these forests;

(3) sunfleck activity within the understorey of a lowland rainforest in the study area is similar to that reported for tropical rainforests elsewhere, where studies have confirmed their importance to the carbon balance of understorey plants;

(4) the frequency distributions of irradiance and PPFD within understoreys and treefall gaps in the study area are similar to rainforests elsewhere, exhibiting moderate-to-high degrees of positive skewness and kurtosis, with diffuse fluxes typically contributing over 90% of those found in the understorey over the course of a day;

(5) mean daily (potential) PPFD increased by 60% within the understorey of an upland rainforest in the study area following slight-to-moderate canopy damage caused by a tropical cyclone, and this significant change demonstrates the important effects of this

kind of disturbance on both the quantity and quality of light available to understorey plants;

(6) unlike rainforest understoreys, whose light regimes comprise of constant shade with random sunflecks, the light regimes within treefall gaps have more predictable diurnal and seasonal patterns;

(7) seasonal changes in light availability within small and large treefall gaps in northeast Queensland rainforests are greater than those found within similar treefall gaps in equatorial rainforests;

(8) results of modelling light availability within several treefall gaps in the study area have shown that seasonal variations in direct light in small and large elliptical gaps that are orientated east-west are greater than those found for the exact same gaps orientated north-south; and

(9) there are order-of-magnitude differences in light availability across the range of small-to-large gaps analysed in this study, and this undoubtedly controls the microclimate and subsequently the ecophysiology of tree seedlings and saplings growing within these gaps.

In addition to the studies examining temporal and spatial distributions of solar radiation within rainforest understoreys and treefall gaps, this thesis has presented results from two case-studies examining light environments within montane tropical rainforest and across the open forest-rainforest boundary, respectively.

Light environments within montane tropical rainforests on the summit of Mt Bellenden Ker have several important characteristics, which may be summarised as follows:

(1) reduction in PPFD by cloudiness does not appear to limit the rates of photosynthesis for plants growing within canopy, gap and understorey micro-environments, because median PPFD in the upper canopy is nearly always above the range of light saturation points reported for rainforest plants, and in the lower-canopy, gap and understorey median PPFDs are higher than known light compensation points reported for understorey or shade-grown plants;

(2) estimated minimum levels of daily total PPFD in lower-canopy, gap and understorey micro-environments under nimbostratus cloud are similar to or exceed values for positive carbon gain in understorey plants elsewhere; and
(3) reduction in PPFD by cloudiness does not appear to decrease productive capacities of montane (cloud) forests, and hence the results of this case-study lend support to Leigh's (1975) Transpiration Theory as the main reason for the lower primary productivity of these forests.

Finally, it may be concluded that light environments across the open forest-rainforest boundary (ecotone) at Kirrama exhibited the following features:

(1) under cloudless skies daily direct PPFD declined semi-exponentially across the boundary during the summer months (September-March) and linearly during the winter months (April-August), while daily diffuse PPFD declined linearly across the boundary throughout the year; and

(2) the results presented in this case-study suggest that, towards the rainforest end of the transition zone (ecotone), light conditions are similar to those experienced within small treefall gaps in rainforests, while towards the open forest end of the transition zone, light conditions are similar to those experienced within large treefall gaps in rainforests.

As stated in Chapter 1, the objectives of this thesis have contributed to the call by the National Research Council (1980) for the establishment and continued monitoring of key parameters of the physical and biological environment throughout the tropics. Specifically, the work presented in this thesis has attempted to quantify the temporal and spatial distribution of solar radiation within natural and modified rainforest systems. It has been argued throughout that solar radiation (light) is the major limiting resource in tropical rainforests. Hence, if we are to assess the consequences of rainforest conversion to simpler systems, such as pasture and plantations, then we need to expand our rather limited knowledge of the temporal and spatial distribution of light, as well as other environmental resources such as water and nutrients, within natural and modified systems. Furthermore, it was suggested that detailed studies of these environmental resources serve not only to predict effects of deforestation, but also to minimise the impact by planting vegetation which closely matches natural forest behaviour.

The scientific management implications of the methods and results presented in this thesis were evaluated in Chapter 8. Firstly, this work has contributed to improving our knowledge and understanding of rainforest regeneration following natural disturbances such as treefalls and cyclones. It is hoped that this work will also contribute to studies concerned with the ecophysiology and dynamics of rainforest vegetation. In agreement with research conducted within rainforest understoreys elsewhere, this thesis has shown that only extremely shade-tolerant herbs and shrubs are able to survive and reproduce in the shaded understorey and that treefalls are essential for regeneration of most tree species in rainforests. Given the importance of treefall gaps for rainforest function, it was rather surprising to find that light environments within gaps were so poorly documented in the literature. This thesis has attempted to improve our knowledge of light regimes within treefall gaps, and it may be concluded that if light availability is the main limiting resource in rainforests, then studies of gap environments and dynamics must take into account all the factors likely to influence light availability within gaps, such as forest height, gap diameter, slope angle, slope aspect, sky conditions and daily and seasonal variation in the position of the sun.

Secondly, this work has provided valuable quantitative data on the temporal and spatial distributions of light across the open forest-rainforest boundary (ecotone), and there is little doubt that understanding the light availability continuum and associated plant responses across the boundary are essential for conservation and management of remaining rainforest in northeast Queensland because a substantial portion remains as small, isolated patches.

Thirdly, this work has contributed to forest management strategies following human disturbance, including rehabilitation of degraded sites within rainforest patches or on the rainforest margin, and reforestation of cleared areas away from the rainforest margin, such as abandoned agricultural land. It has been advocated that the SCANGIR Model (Chapter 3) and gap theory can be applied by forest managers to promote the eventual dominance of disturbed sites by shade-tolerant (primary) tree species. To achieve this aim, it may be necessary, in the first instance, to plant shade-intolerant (pioneer) tree species and to subsequently introduce shade-tolerant species beneath the pioneer tree canopy.

Finally, this work has contributed to forestry logging practices. It would seem that understanding treefall gap light environments and gap theory may benefit selective logging practices because this thesis has demonstrated marked differences in light quantity and quality among elliptical gaps with different orientations. It may also be said that the SCANGIR Model has numerous applications in strip clear-cut timber harvesting techniques, whereby it was suggested that 'ideal' light conditions for regeneration of useful shade-tolerant tree species could be achieved by altering the width and orientation of the clear-cut strips in accordance with latitude, forest height and local topography.

9.2 RECOMMENDATIONS FOR FUTURE RESEARCH

(1) The SCANGIR Model (Chapter 3) should be modified to simulate solar radiation regimes in elliptical, rather than only circular gaps, with the diffuse radiation being treated as anisotropic, rather than isotropic.

(2) While the vertical distribution of light within tropical rainforest canopies has been adequately described, virtually nothing is known about the horizontal variability of light within rainforest canopies. It is therefore suggested, that a 'tram-line' system, similar to that used by Baldocchi *et al.* (1984 a, b), be established within the canopy of a tropical rainforest to quantify variations in light across the horizontal plane at several heights within the canopy.

(3) This thesis has only presented preliminary results on seasonal variations in light availability across the open forest-rainforest boundary, as determined from fisheye photographs. Because light availability to seedlings and saplings in the boundary zone (ecotone) has been identified as one of the critical factors controlling boundary dynamics and subsequent rainforest stability, then it is vital that diurnal variations in light across the boundary be quantified as well, preferably in conjunction with ecophysiology studies.

(4) Because of the rapid conversion rates of the world's tropical forests, there is a definite need for comparative studies of light quantity and quality within successional (secondary) forests of different age and species composition; this research should be carried out in collaboration with studies of the ecophysiology and dynamics of regenerating tree seedlings and saplings.

(5) There is a clear need for more research into forest-atmosphere interactions in the Wet Tropics study area. The present study of solar radiation regimes within rainforest understoreys, gaps and clearings should be extended into a general study of radiation exchange (energy balance) within these micro-environments. This would ideally require measurements of incoming and outgoing short- and long-wave radiation above the canopy, within the canopy itself, in treefalls of varying sizes, within the shaded understorey and across the open forest-rainforest boundary (ecotone). If possible,

measurements should be conducted within these micro-environments for rainforest located on slopes with different angles and aspects to account for variations in net radiation and the likely effects on evapotranspiration, environmental heating and photosynthesis. This would seem to be particularly important in the Wet Tropics region because most of the remaining rainforest is located on mountainous terrain. Finally, this knowledge of energy-balance and forest microclimate should be directly applied to the practical problems of rainforest management and silviculture.

REFERENCES

Abacus Concepts (1986). *StatView 512+.* BrainPower Incorporated, Calabasas, California.

Aisenshtat, B.A. (1966). Investigations on the heat budget of Central Asia. In: *Sowremennye Problemy klimatologii.* (Ed. M.I. Budyko), pp. 83-129. Meteorol. Gidrol, Leningrad.

Alexandre, D.Y. (1984). Strata in tropical rain-forest at Tai (Ivory Coast). In: *Tropical Rain-Forest: The Leeds Symposium.* (Eds. A.C. Chadwick and S.L. Sutton), pp. 15-24. Leeds Philosophical Society, Leeds, U.K.

Allee, W.C. (1926). Measurement of environmental factors in the tropical rainforest of Panama. *Ecology* 7, 273-302.

Anderson, M.C. (1964 a). Studies of the woodland light climate I: the photographic computation of light conditions. I *Journal of Ecology* 52, 27-41.

Anderson. M.C. (1964 c). Light relations of terrestrial plant communities and their measurement. Biological Reviews 39, 425-486.

Anderson, M.C. (1966). Stand structure and light penetration II: a theoretical analysis. *Journal of Applied Ecology* 3, 41-54.

Anderson, M.C. (1971). Radiation and crop structure. In: *Plant Photosynthetic Production: A manual of Methods.* (Eds. Z. Sestak, J. Catsky and P.G. Jarvis), pp. 412-466. Dr W. Junk Publishers, The Hague.

Anderson, M.C. (1981). The geometry of leaf distribution on some south-eastern Australian forests. *Agricultural Meteorology* 25, 195-205.

Anderson, M.C. and Miller, E.E. (1974). Forest cover as a solar camera: penumbral effects in plant canopies. *Journal of Applied Ecology* 11, 691-697.

Angstrom, A. (1924). Solar and terrestrial radiation. *Quarterly Journal of the Royal Meteorological Society* 50, 121-126.

Aoki, M., Yabuki, K. and Koyama, H. (1975). Micrometeorology and assessment of primary production of a tropical rain forest in West Malaysia. *Journal of Agricultural Meteorology* 31, 115 - 124.

Ashton, P.S. (1958). Light intensity measurements in rain forest near Santarem, Brazil. *Journal of Ecology* 46, 65-70.

Atkins, E.S. (1957). Light measurement in a study of white pine reproduction. Canada Department of Northern Affairs & Natural Resources, Forestry Branch, *Forest Research Division Technical Note* No. 60.

Atkins, W.R.G., Poole, H.H. and Stanbury, F.A. (1937). The measurement of the intensity and colour of light by means of emission and rectifier photoelectric cells. *Proceedings of the Royal Society* B 121, 427-450.

Aubreville, A. (1938). La foret coloniale: les forets de l'Afrique occidentale francaise. *A. Acad. Sci. Colon.* 9, 1-245.

Augspurger, C.K. (1984). Seedling survival of tropical tree species: interaction of dispersal distance, light-gaps and pathogens. *Ecology* 65, 1705-1712

Augspurger, C.K. and Franson, S. E. (1988). Input of wind-dispersed seeds into light-gaps and forest sites in a neotropical forest. *Journal of Tropical Ecology* 4, 239 - 252

Australian Heritage Commission (1986). *Tropical Rainforests of North Queensland: Their Conservation Significance.* Australian Government Publishing Service, Canberra.

Aylett, G.P. (1985). Irradiance Interception, leaf conductance and photosynthesis in Jamaican upper montane rain forest trees. *Photosynthetica* 19, 323-327.

Baldocchi, D.D., Matt, D.R., Hutchison, B.A and McMillen, R.T. (1984 a). Solar radiation within an oak-hickory forest: an evaluation of the extinction coefficients for several radiation components during fully-leafed and leafless periods. *Agricultural and Forest Meteorology* 32, 307-322.

Baldocchi, D.D, Hutchison, B.A., Matt, D.R. and McMillen, R.T. (1984 b). Seasonal variations in the radiation regime within an oak-hickory forest. *Agricultural and Forest Meteorology* 33, 177-191.

Baldocchi, D.D., Hutchison, B.A., Matt, D.R. and McMillen, R.T. (1986). Seasonal variations in the statistics of photosynthetically active radiation penetration in an oak-hickory forest. *Agricultural and Forest Meteorology* 36, 343-361.

Barry, R.G. and Chorley, R.J. (1987). *Atmosphere, Weather and Climate (5th Ed.).* Methuen, London and New York.

Barton, A. M., Fetcher, N. and Redhead, S. (1989). The relationship between treefall gap size and light flux in a neotropical rain forest in Costa Rica. *Journal of Tropical Ecology* 5, 437-439.

Baumgartner, A. (1956). Untersuchungen uber den Warme und Wasserhaushalt eines jungen Waldes. *Deut. Wetterdienstes Ber.* 5, 4-53.

Bazzaz, F. A. and Pickett, S.T.A. (1980). Physiological ecology of tropical succession: a comparative review. *Annual Reviews of Ecological Systematics* 11, 287 - 310.

Bell, C.D. and Rose, D.A. (1981). Light measurement and the terminology of flow. *Plant, Cell and Environment* 4, 89-96.

Bennett, I. (1969). Correlation of daily insolation with daily total sky cover, opaque sky cover and percentage of possible sunshine. *Solar Energy* 12, 391-393.

Biggs, W.W., Edison, A.R., Eastin, J.D., Brown, K.W., Maranville, J.W. and Clegg, M.D. (1971). Photosynthesis light sensor and meter. *Ecology* 52, 125-131.

Biggs, W.W. (1986). Radiation measurement. In: *Advanced Agricultural Instrumentation.* (Eds. W.G. Gensler), pp. 3-20. Martinus Nijhoff, Dordrecht.

Bjorkman, O. (1981). Responses to different quantum flux densities. In: *Physiological Plant Ecology I: Responses to the Physical Environment.* (Ed. O.L. Lange, P.S. Nobel, C.B. Osmond and H. Ziegler), pp. 57-107. Springer-Verlag, Berlin, Heidelberg and New York.

Bjorkman, O. and Ludlow, M.M. (1972). Characterization of the light climate on the floor of a Queensland rainforest. *Carnegie Institution Washington Yearbook* 71, 85-94.

Bjorkman, O., Ludlow, M.M. and Morrow, P.A. (1972). Photosynthetic performance of two rainforest species in their native habitat analysis of their gas exchange. *Carnegie Institution Washington Yearbook* 71, 94-102.

Black, J.N., Bonython, C.W. and Prescott, J.A. (1954). Solar radiation and the duration of sunshine. *Quarterly Journal of the Royal Meteorological Society* 80, 231-235.

Blackadar, A. (1984). A computer almanac. *Weatherwise,* October 1984.

Bonell, M., Gilmour, D.A. and Cassells, D.S. (1981). Soil hydraulic properties and their effect on surface and subsurface water transfer in a tropical rainforest catchment. *Hydrological Sciences Bulletin* 26, 1-18.

Bonell, M., Cassells, D.S. and Gilmour, D.A. (1983 a). Vertical soil water movement in a tropical rainforest catchment in north-east Queensland. *Earth Surface Processes and Landforms* 8, 253-272.

Bonell, M., Gilmour, D.A. and Cassells, D.S. (1983 b). A preliminary survey of the hydraulic properties of rainforest soils in tropical north-east Queensland and their implications for the runoff process. *Catena Supplement* 4, 57-78.

Bonell, M., Gilmour, D.A. and Cassells, D.S. (1986). The storm runoff response to various rainfall systems on the wet tropical coast of northeast Queensland. East-West Centre, Environment and Policy Institute. Working paper, Honolulu, Hawaii.

Bonell, M., Cassells, D.S. and Gilmour, D.A. (1987). Spatial variations in soil hydraulic properties under tropical rainforest. In: *International Conference on Infiltration, Development and Application.* (Ed. Yu-si Fok), pp. 153-165. University of Hawaii.

Bongers, F. , Popma, J., Meave del Castillo, J., and Carabias, J. (1988). Structure and floristic composition of the lowland rain forest of Los Tuxtlas, Mexico. *Vegetatio* 74, 55 - 80.

Bonhomme, R. and Chartier, P. (1972). The interpretation and automatic measurement of hemispherical photographs to obtain sunlit foliage area and gap frequency. *Israel Journal of Agricultural Research* 22, 53-61.

Bourgeron, P.S. (1981). Diversity pattern in the Tai forest (Ivory Coast). Journal of African Ecology (cited in Bourgeron, 1983).

Bourgeron, P.S. (1983). Spatial aspects of vegetation structure. In: *Ecosystems of the World 14A: Tropical Rain Forest Ecosystems: Structure and Function.* (Ed. F.B. Golley), pp. 29-47. Elsevier Scientific Publishing Co., Amsterdam.

Bourgeron, P.S. and Guillaumet, J.L. (1981). A descriptive model of stratification in the Tai forest (Ivory Coast). cited in Bourgeron (1983).

Brandani, A., Hartshorn, G.S. and Orians, G.H. (1988). Internal heterogeneity of gaps and species richness in Costa Rican tropical wet forest. *Journal of Tropical Ecology* 4, 99-119.

Brokaw, N.V.L. (1982). The definition of a treefall gap and its effect on measures of forest dynamics. *Biotropica* 14, 158-160.

Brokaw, N.V.L. (1985). Treefalls, regrowth, and community structure in tropical forests. In: *The Ecology of Natural Disturbance and Patch Dynamics.* (Ed. S.T.A. Pickett and P.S. White), pp. 53-69. Academic Press, Orlando and London.

Brokaw, N.V.L. (1987). Gap-phase regeneration of three pioneer tree species in a tropical forest. *Journal of Ecology* 75, 9-19.

Brokaw, N.V.L. (1989). Species composition in gaps and structure of a tropical forest. *Ecology* 70, 538-541.

Brunig, E.F. (1970). Stand structure, physiognomy and environmental factors in some lowland forests in Sarawak. *Tropical Ecology* 11, 26-43.

Brunig, E.F. (1983). Vegetation structure and growth. In: *Ecosystems of the World 14A: Tropical Rain Forest Ecosystems: Structure and Function.* (Ed. F.B. Golley), pp. 49-75. Elsevier Scientific Publishing Co., Amsterdam.

Bunning, E. (1947). *In den Waldern Nord-Sumatras.* Dummlers-Verlag, Bonn.

Bureau of Meteorology (1971). *Climatic Survey Northern Region 16 - Queensland.* Bureau of Meterology, Brisbane.

Bureau of Meteorology (1988). *Climatic Averages Australia.* Australian Government Publishing Service, Canberra.

Burgess, M.D. and Cox, L.M. (1975). A bipolar analog integrator for use with net radiometers. *Agricultural Meteorology* 15, 385-391.

Cachan, P. and Duval, J. (1963). Variations microclimatiques verticales et saisonnieres dans la foret sempervirente de Basse Cote D'Ivoire. *Annales De La Faculte Des Sciences Dakar* 8, . .r-r 8, 5-87.

Campbell, G.S. (1974). A micropower electronic integrator for meteorological applications. *Agricultural Meteorology* 13, 399-404.

Campbell, G.S. (1977). *An Introduction to Environmental Biophysics.* Springer-Verlag, Berlin, Heidelberg and New York.

Campbell, G.S. (1981). Fundamentals of radiation and temperature relations. In: *Physiological Plant Ecology I: Responses to the Physical Environment.* (Ed. O.L. Lange, P.S. Nobel, C.B. Osmond and H. Ziegler), pp. 11-40. Springer-Verlag, Berlin, Heidelberg and New York.

Canham, C.D. (1988). Growth and canopy architecture of shade-tolerant trees: response to canopy gaps. *Ecology* 69, 786-795

Carter, G.S. (1934). Reports of the Cambridge Expedition to British Guiana, 1933. *Linnean Society of London Zoological Journal* 38, 579-589.

Cassells, D.S., Gilmour, D.A. and Bonell, M. (1985). Catchment response and watershed management in tropical rainforests in north-eastern Australia. *Forest Ecology and Management* 10, 155-175.

Chan, S.S., McCreight, R.W., Walstad, J.D. and Spies, T.A. (1986). Evaluating forest vegetative cover with computerized analysis of fisheye photographs. *Forest Science* 32, 1085-1091.

Chartier, P. (1966). Etude du microclimat lumineux dans la vegetation. *Annals of Agronomy* 17, 571-602.

Chazdon, R.L. (1986). Light variation and carbon gain in rainforest understorey palms. *Journal of Ecology* 74, 995-1012.

Chazdon, R.L. (1987). Aspectos importantes para el estudio de los regimenes de luz en bosques tropicales. *Rev. Biol. Trop.* 35 (Suppl. 1), 191-196.

Chazdon, R.L. (1988). Sunflecks and their importance to forest understorey plants. *Advances in Ecological Research* 18, 1-63.

Chazdon, R.L. and Fetcher, N. (1984). Photosynthetic light environments in a lowland tropical rainforest in Costa Rica. *Journal of Ecology* 72, 553-564.

Chazdon, R.L. and Fetcher, N. (1986 a). Photosynthetic responses to light variation in rainforest species I: induction under constant and fluctuating light conditions. *Oecologia (Berlin)* 69, 517-523.

Chazdon, R.L. and Fetcher, N. (1986 b). Photosynthetic responses to light variation in rain forest species II: carbon gain and photosynthetic efficiency during lightflecks. *Oecologia (Berlin)* 69, 517-523.

Chazdon R.L. and Field, C.B. (1987 a). Determinants of photosynthetic capacity in six rainforest Piper species. *Oecologia (Berlin)* 73, 222-230.

Chazdon, R.L. and Field, C.B. (1987 b). Photographic estimation of photosynthetically active radiation: evaluation of a computerized technique. *Oecologia (Berlin)* 73, 525-532.

Chazdon, R.L., Williams, K. and Field, C.B. (1988). Interactions between crown structure and light environment in five rainforest *Piper* species. *American Journal of Botany.* (cited in Chazdon, 1988).

Cheke, A.S., Nanakorn, W. and Yankoses, C. (1979). Dormancy and dispersal of seeds of secondary forest species under the canopy of a primary tropical rain forest in northern Thailand. *Biotropica* 11, 88-95.

Chiariello, N.R. , Field, C.B. and Mooney, H.A. (1987). Midday wilting in a tropical pioneer tree. Functional Ecology 1, 3-11.

Chow, W.S., Luping Qian, Goodchild, D.J. and Anderson, J.M. (1988). Photosynthetic acclimation of *Alocasia macrorrhiza* (L.) G. Don to growth irradiance: structure, function and composition of chloroplasts. *Australian Journal of Plant Physiology* 15, 107-122.

C.I.E. (1970). *International Lighting Vocabulary.* Commission International de l'Eclairage, Publication No. 17, Paris.

Cloudsley-Thompson, J.L. and Cloudsley, A. (1984). Microclimatic measurements in neotropical forest, grassland and desert, with faunal observations. *International Journal of Biometeorology* 28, 293-302.

Coombe, D.E. (1957). The spectral composition of shade light in woodlands. *Journal of Ecology* 45, 823-830.

Coombe, D.E. and Evans, G.C. (1960). Hemispherical photography in studies of plants. *Medical and Biological Illustration* 10, 68-75.

Crow, T.R. (1980). A rain forest chronicle: a 30 year record of change in structure and composition at El Verde, Puerto Rico. *Biotropica* 12, 42-55.

Czarnowski, M. and Slomka, J. (1959). Some remarks on the percolation of light through the forest canopy. *Ecology* 40, 312-315.

Data Electronics Australia Ltd (1985). *Users Manual.* Data Electronics Australia Pty Ltd.

Data Electronics Australia Ltd (1985). *Technical Manual.* Data Electronics Australia Pty Ltd.

Denmead, A.K. (1971). *The Atherton Tableland. Geological Excursions Handbook.* (Ed. G. Mayford). A. N. Z. A. S. S , 43rd Congress and Geological Society of Australia Inc., Qld. Division, Brisbane, May 1971, 1-19.

Denslow, J.S. (1980) . Gap partitioning among tropical rainforest trees. *Biotropica* 12 (Suppl), 47-55.

Denslow, J.S. (1987). Tropical rainforest gaps and tree species diversity. *Annual Reviews of Ecological Systematics* 18, 431-451.

De Steven, D. (1988). Light gaps and long-term seedling performance of a neotropical canopy tree (*Dipteryx panamensis,* Leguminosae). *Journal of Tropical Ecology* 4, 407-411.

Dick R.S. (1975). A map of the climates of Australia according to Koppen's principles of definition. *Queensland Geographical Journal* 3, 33-69.

Doley, D., Unwin, G.L. and Yates, D.J. (1988). Spatial and temporal distribution of photosynthesis and transpiration by single leaves in a rainforest tree, *Argyrodendron peralatum. Australian Journal of Plant Physiology* 15, 317-326.

Downs, R.J., Hendricks, S.B., Borthwick, H.A. (1957). Photoreversible control of elongation in Pinto beans and other plants under normal conditions of growth. *Botanical Gazette* 118, 199-208.

Drummond, A.J. and Thekaekara, M.P. (1973). *The Extraterrestrial Solar Spectrum.* Institute of Environmental Science, Illinois, USA.

Ducrey, M. (1975). Utilisation des photographies hemispheriques pour le calcul de la permeabilite des couverts forestiers au rayonnement solaire. *Annals des Science Forestieres* 32, 73-92.

Duff, G.A. (1987). *Physiological Ecology and Vegetation Dynamics of North Queensland Upland Rainforest - Open Forest Ecotones.* Ph.D thesis, James Cook University of North Queensland, Townsville.

Duffie, J.A. and Beckman, W.A. (1980). *Solar Engineering of Thermal Processes.* Wiley, New York.

Egle, K. (1937). Zur kenntnis des lichtfeldes der pflanze und der blattfarbstoffe. *Planta* 26, 546-583.

Evans, G.C. (1939). Ecological studies on the rain forest of Southern Nigeria. *Journal of Ecology* 27, 436-482.

Evans, G.C. (1956) An area survey method of investigating the distribution of light intensity in woodlands, with particular reference to sunflecks. *Journal of Ecology* 44, 391-428.

Evans, G.C. and Coombe, D.E. (1959). Hemispherical and woodland canopy photography and the light climate. *Journal of Ecology* 47, 103-113.

Federer, C.A. and Tanner, C.B. (1966). Spectral distribution of light in the forest. *Ecology* 47, 555-560.

Fetcher, N., Oberbauer, S.F. and Strain, B.R. (1985). Vegetation effects on microclimate in lowland tropical forest in Costa Rica. *International Journal of Biometeorology* 29,145-155.

Forgan, B.W. (1979). The measurement of solar irradiance: instrumentation and measurements in the Adelaide region. PhD thesis, *Flinder's University of South Australia, Research Report* No. 32, School of Earth Sciences, Flinder's University, Bedford Park, SA.

Freyman, S. (1968). Spectral distribution of light in forests of the Douglas Fir zone of southern British Columbia. Canadian *Journal of Plant Science* 48, 326-328.

Fitter, D.J., Knapp, P.H. and Wilson, W.J. (1980). Stand structure and light penetration IV. A sensor for measuring photosynthetically active radiation. *Journal of Applied Ecology* 17, 183-193.

Fitter, A.H. and Hay, R.K.M. (1981). *Environmental Physiology of Plants.*

Fritz, S. and MacDonald, T.H. (1949). Average solar radiation in the United States. *Heat Ventilation* 46, 61-64.

Frohlich, C. and Brusa, R.W. (1981). Solar radiation and its variation in time. *Solar Physics* 74, 209-215.

Garwood, N.C., Janos, D.P. and Borkaw, N. (1979). Earthquake-caused landslides: a major disturbance to tropical forests. *Science* 205, 997-999.

Gates, D.M. (1980). *Biophysical Ecology.* Springer-Verlag, New York.

Gay, L. W., Knoerr, K.R. and Braaten, M.O. (1971). Solar radiation variability on the floor of a pine plantation. *Agricultural Meteorology* 8, 39-50.

Gentilli, J. (1972). *Australian Climate Patterns.* Nelson, Melbourne.

Ghuman, B.S. and Lal, R. (1987). Effects of a partial clearing on microclimate in a humid tropical forest. *Agricultural and Forest Meteorology* 40, 17-29

Gilmour, D.A., Bonell, M. and Sinclair, D.F. (1980). An investigation of storm drainage processes in a tropical rainforest catchment. *Australian Water Resources Council Technical Paper* 56.

Glover, J. and McCulloch, J.S.G. (1958). The empirical relation between solar radiation and hours of bright sunshine. *Quarterly Journal of the Royal Meteorological Society* 84, 172-175.

Grubb, P.J. (1977). Control of forest growth and distribution on wet tropical mountains with special reference to mineral nutrition. *Annual Reviews of Ecological Systematics* 8, 83-107.

Grubb, P.J. and Whitmore, T.C. (1966). A comparison of montane and lowland rainforest in Ecuador II: the climate and its effects on the distribution and physiognomy of the forest. *Journal of Ecology* 54, 303-333.

Grubb, P.J. and Whitmore, T.C. (1967). A comparison of montane and lowland rainforest in Ecuador III: the light reaching the ground vegetation. *Journal of Ecology* 55, 33-57.

Gutschick, V.P., Barron, M.H., Waechter, D.A. and Wolf, M.A. (1985) Portable monitor for solar radiation that accumulates irradiance histograms for 32 leaf-mounted sensors. *Agricultural and Forest Meteorology* 33, 281-290.

Hadfield, W. (1974). Shade in north-east Indian forest tea plantations II: foliar illumination and canopy characteristics. *Journal of Applied Ecology* 11, 151-178.

Halle, F., Oldeman, R.A.A. and Tomlinson, P.B. (1978). *Tropical Trees and Forests: an Architectural Analysis.* Springer-Verlag, Berlin.

Hartshorn, G.S. (1978). Treefalls and tropical forest dymanics. In: *Tropical Trees as Living Systems.* (Eds. R.B. Tomlinson and M. H. Zimmerman), pp. 617-638. Cambridge University Press, Cambridge.

Hartshorn, G.S. (1980). Neotropical forest dynamics. *Biotropica* 12 (Supplement), 23-30.

Hartshorn, G.S. (1989). Application of gap theory to tropical forest management: natural regeneration on strip clear-cuts in the Peruvian Amazon. *Ecology* 70, 567-569.

Hill, R. (1924). A lens for whole sky photographs. *Royal Meteorological Society Quarterly* 50, 227-235.

Hirota, O., Takeda, T. and Saito, Y. (1975). studies on the utilisation of solar radiation by crop stands. *Proceedings of the Crop Science Society of Japan* 44, 357-363.

Hogan, K.P. (1987). Photosynthesis in two neotropical palm species. *Functional Ecology* 2, 371-377.

Holbo, H.R., Childs, S.W. and McNabb, D.H. (1985). Solar radiation at seedling sites below partial canopies. *Forest Ecology and Management* 10, 115-124.

Holmes, M.G. and Smith, H. (1977). The function of phytochrome in the natural environment II: the influence of vegetation canopies on the spectral energy distribution of natural daylight. *Photochemical Photobiology* 25, 539-545.

Holmes, M.G. (1981). Spectral distribution of radiation within plant canopies. In: *Plants and the Daylight Spectrum.* (Ed. H. Smith), pp. 147-158. Academic Press, London.

Hopkins, M. S. and Graham, A. W. (1989). Community phenological patterns of a lowland tropical rainforest in north-eastern Australia. *Australian Journal of Ecology* 14, 399-413.

Hopkins, M.S., Tracey, J.G. and Graham, A.W. (1990). The size and composition of soil seed-banks in remnant patches of three structural rainforest types in north Queensland. *Australian Journal of Ecology* 15,43-50.

Horn, H.S. (1971). *The Adaptive Geometry of Trees.* Princeton University Press, Princeton, New Jersey.

Hussain, M. (1984). Estimation of global and diffuse irradiation from sunshine duration and atmospheric water vapour content. *Solar Energy* 33, 217-220.

Hutchison, B.A. and Matt, D.R. (1976). Beam enrichment of diffuse radiation in a deciduous forest. *Agricultural Meteorology* 17,93-110.

Hutchison, B.A. and Matt, D.R. (1977). The distribution of solar radiation within a deciduous forest. *Ecological Monographs* 47, 185-207.

Iqbal, M. (1983). *An Introduction to Solar Radiation.* Academic Press, Toronto.

Isabell, R.F., Stephenson, P.J., Murtha, G.G., and Gillman, G.P. (1976). Red basaltic soils in north Queensland. *CSIRO Australian Division of Soils Technical Paper No.* 28.

Jahnke, L.S. and Lawrence, D.B. (1965). Influence of photosynthetic crown structure on potential productivity of vegetation, based primarily on mathematical models. *Ecology* 46, 319-326.

Jarvis, P.G., James, G.B. and Landsberg, J.J. (1976). Coniferous forest. In: *Vegetation and the Atmosphere Volume 2: Case Studies.* (Ed. J.L. Montieth), 171-240. Academic Press, London, New York and San Francisco.

Johnson, G.T. and Watson, I.D. (1984). The determination of view-factors in urban canyons. *Journal of Climate and Applied Meteorology* 23, 229-335.

Johnson, G.T. and Watson, I.D. (1985). Calculating view factors using video imagery. School of Mathematics and Physics, *Macquarie University Technical Report No.* 85-015. Macquarie University, NSW.

Johnson, G.T. and Watson, I.D. (1986). Estimating view-factors using video imagery. In: *Proceedings of the International Conference on Development and Application of Computer Techniques to Environmental Studies.* (Ed. P. Zannetti), pp. 627-638. Computational Mechanics Publications, Los Angeles.

Jones, H.G. (1983). *Plants and Microclimate.* Cambridge University Press, Cambridge.

Jordan, C.F. (1969). Derivation of leaf-area index from quality of light on the forest floor. *Ecology* 50, 663-666.

Jordan, C.F. (1983). Productivity of tropical rain forest ecosystems and the implications for their use as future wood and energy sources. In: *Ecosystems of the World 14A: Tropical Rain Forest Ecosystems: Structure and Function.* (Ed. F.B. Golley), pp. 117-136. Elsevier Scientific Publishing Co., Amsterdam.

Jordan, C.F. (1987). (Ed.) *Amazonian Rain Forests: Ecosystem Distrurbance and Recovery: Case-Studies of Ecosystem Dynamics under a Spectrum of Land-Use Intensities.* Springer-Verlag, Berlin-Heidelberg- New York.

Jupp, D.L.B., Anderson, M.C., Adomeit, E.M. and Witts, S.J. (1980). PISCES - a computer program for analysing hemispherical canopy photographs. *CSIRO Technical Memorandum* 80/23, Canberra.

Keto, A.I. (1984). The conservation status of the rainforests of the wet tropics of north-east Queensland. *Occasional Paper No. 1.* Rainforest Conservation Society of Queensland, Brisbane.

Kikkawa, J. (1982). Ecological association of birds and vegetation structure in wet tropical forests of Australia. *Australian Journal of Ecology 7,* 325-345.

Kikkawa, J., Montieth, G.B. and Ingram, G. (1981). Cape York Peninsula, major region of faunal interchange. In: *Ecological Biogeography of Australia.* (Ed. A. Keast), pp. 1695-1742. Dr W. Junk, The Hague.

Kira, T., Shinozaki, K. and Hozumi, K. (1969). Structure of forest canopies as related to their primary productivity. *Plant and Cell Physiology* 10, 129-142.

Klinge, H., Rodrigues, W.A., Brunig, E.F. and Fittkau, E.J. (1974). Biomass and structure in a central Amazonian rainforest. In: *Trends in Tropical Ecology.* (Eds. E. Medina and F. Golley), pp. 115-122. Springer-Verlag, Heidelberg.

Koyama, H. (1981). Photosynthetic rates in lowland rain forest trees of peninsular Malaysia. *Japanese Journal of Ecology* 31, 361-369.

Kubin, S. (1971). Measurement of radiant energy. In: *Plant Photosynthetic Production: Manual of Methods.* (Eds. Z. Sestak, J. Catsky and P.G. Jarvis), pp. 702-765. Dr W. Junk Publishers, The Hague.

Kwesiga, F.R., Grace, J. and Sandford, A.P. (1986). Some photosynthetic characteristics of tropical timber trees as affected by the light regime during growth. *Annals of Botany* 58, 23-32.

Laffan, M.D. (1988). Soils and land use on the Atherton Tableland, north Queensland. *CSIRO Soils and Land Use Series, No.* 61., Canberra.

Lang, A.R.G. (1973). Leaf orientation of a cotton plant. *Agricultural Meteorology* 11, 37-51.

Larcher, W. (1980). *Physiological Plant Ecology (2nd Ed.).* Springer-Verlag, Berlin, Heidelberg, New York.

Lawton, R.O. and Putz, F.E. (1988). Natural disturbance and gap-phase regeneration in a wind-exposed tropical cloud forest. *Ecology* 69, 764-777.

Lee, D.W. (1987). The spectral distribution of radiation in two neotropical rainforests. *Biotropica* 19, 161-166.

Lee, D.W. (1989). Canopy dynamics and light climates in a tropical moist deciduous forest in India. *Journal of Tropical Ecology* 5, 65-79.

Lee, D.W. and Paliwal, K. (1988). The light climate of a South Indian evergreen forest. *GeoBios*. 15, 3-6.

Leigh, E.G. (1975). Structure and climate in tropical rain forest. *Annual Reviews of Ecological Systematics* 2, 67-86.

Lemeur, R. (1973). A method for simulating the direct solar radiation regime in sunflower, Jerusalem artichoke, corn and soybean canopies using actual stand structure data. *Agricultural Meteorology* 12, 229-247.

Liou, K.N. (1976). On the absorption, reflection and transmission of solar radiation in cloudy atmospheres. *Journal of Atmospheric Science* 33, 798-805.

List, R.J. (1971). *Smithsonian Meteorological Tables (6th Ed.).* Smithsonian Institution Press, Washington D.C.

Longman, K.A. (1969). The dormancy and survival of plants in the humid tropics. *Symposium of the Society of Experimental Biology* 23, 471-488.

Longman, K.A. (1978). Control of shoot extension and dormancy - external and internal factors. In: *Tropical Trees as Living Systems.* (Eds. P.B. Tomlinson and M.H. Zimmerman), pp. 465-495. Cambridge University Press, New York.

Longman, K.A. and Jenik, J. (1987). *Tropical Forest and its Environment* (2nd Ed.). Longman, Essex.

Lowman, M.D. (1986). Light interception and its relation to structural differences in three Australian rainforest canopies. *Australian Journal of Ecology* 11, 163-170.

Lugo, A. (1970). Photosynthesis studies on four species of rain forest seedlings. In: *A Tropical Rainforest.* (Eds. H.T. Odum and R.F. Pigeon). Division of Technology Information, United States Atomic Energy Commission.

Mabin, M.C.G. (1989). The eastern highlands of north Queensland. In: *Australian and New Zealand Geomorphology Group 4th Conference, Buchan, Victoria.* (Ed. D.L. Dunkerley), pp. 74-76.

McAlpine, J.R. and Keig, G with Falls, R. (1983). *Climate of Papua New Guinea.* CSIRO in association with ANU Press.

McCree, K.J. (1972). Test of current definitions of photosynthetically active radiation against leaf photosynthesis data. *Agricultural Meteorology* 10, 443-453.

McCree, K.J. (1981). Photosynthetically active radiation. In: *Physiological Plant Ecology I: Responses to the Physical Environment.* (Ed. O.L. Lange, P.S. Nobel, C.B. Osmond and H. Ziegler), pp. 41-55. Springer-Verlag, Berlin, Heidelberg and New York.

McPherson, H.G. (1969). Photocell-filter combinations for measuring photosynthetically active radiation. *Agricultural Meteorology* 6, 347-356.

Madgwick, H.A.I. and Brumfield, G.L. (1969). The use of hemispherical photographs to assess light climate in the forest. *Journal of Ecology* 57, 537-542.

Martinez Ramos, M., Alvarez-Buylla, E., Sarukhan, J and Pinero, D. (1988) Treefall age determination and gap dynamics in a tropical forest. *Journal of Ecology* 76, 700-716.

Martinez-Ramos, M., Alvarez-Buylla, E., and Sarukhan, J. (1989). Tree demography and gap dynamics in a tropical rain forest. *Ecology* 70, 555-558.

Masson, H. (1966). Quantitative evaluation of solar radiation. *Solar Energy* 10, 119-124.

Medina, E. and Klinge, H. (1983). Productivity of tropical forests and tropical woodlands. In: *Physiological Plant Ecology IV: Ecosystem Processes, Mineral Cycling, Productivity and Man's Influence.* (Eds. O.L. Lange, P.S. Nobel, C.B. Osmond and H. Ziegler), pp. 281-303. Springer-Verlag, Berlin, Heidelberg and New York.

Microsoft QuickBASIC (1988). *User's Guide.* Microsoft Corporation, USA.

Miller, D.H. (1959). Transmission of insolation through pine forest canopy as it affects the melting of snow. *Schweiz. Anst. f. Forstl. Versuchsw. Mitt.* 35, 57-79.

Miller, E.E. and Norman, J.M. (1971). A sunfleck theory for plant canopies I: lengths of sunlit segments along a transect. *Agronomy Journal* 63, 735-738.

Mohr, H. and Schaefer, E. (1979). Uniform terminolgy for radiation: a critical comment. *Photochemical Photobiology* 26, 1061-1062.

Molion, L.C.B. (1987). Micrometeorology of an Amazonian rain forest. In: *Geophysiology of Amazonia.* (Ed. R.E. Dickinson), pp. 255-272. John Wiley & Sons, New York.

Monsi, M. and Saeki, T. (1953). Uber den lichtfaktor in den pflanzengesellschaften und seine bedeutung fur die stoffproduktion. *Japanese Journal of Botany* 14, 22-52.

Monteny, B., Humbert, J., L'homme, J.P. and Kalms, J.M. (1981). Le rayonnement net et l'estimation de l'evapotranspiration en Cote d'Ivoire. *Agricultural Meteorology* 23, 45-59.

Montieth, G.B. and Davies, V.T. (1984). *Preliminary Account of a Survey of Arthropods (Insects and Spiders) along an Altitudinal Rainforest Transect in Tropical Queensland.* (unpublished).

Montieth, J.L. (1959). The reflection of short-wave radiation by vegetation. *Quarterly Journal of the Royal Meteorological Society* 85, 386-392.

Moon, P. and Spencer, D.E. (1942). Illumination for a nonuniform sky. *Illumination Engineering* 37, 707-726.

Mooney, H.A. and Ehleringer, J.R. (1978). The carbon gain benefits of solar tracking in a desert annual. *Plant, Cell and Environment* 1, 307-311.

Mooney, H.A., Bjorkman, O., Hall, A.E. , Medina, E. and Tomlinson, P.B. (1980) . The study of the physiological ecology of tropical plants - current status and needs. *Bio Science* 30, 22-26.

Mooney, H.A., Field, C. and Vazquez-Yanes, C. (1984). Photosynthetic characteristics of wet tropical forest plants. In: *Physiological Ecology of Plants of the Wet Tropics.* (Eds. E. Medina, H.A. Mooney and C. Vazquez-Yanes), pp.113-128. Dr W. Junk Publishers, The Hague.

Morgan, D.C. and Smith, H. (1981) Non-photosynthetic responses to light quality. In: *Physiological Plant Ecology I: Responses to the Physical Environment.* (Ed. O.L. Lange, P.S. Nobel, C.B. Osmond and H. Ziegler), pp. 109-134. Springer-Verlag, Berlin, Heidelberg and New York.

Muller, M.J. (1982). *Selected Climate Data for a Global Set of Standard Stations for Vegetation Science.* Dr W. Junk Publishers, The Hague.

Murtha, G.G. (1986). Soils of the Tully - Innisfail area, north Queensland. *CSIRO, Division of Soils Divisional Report No.* 82.

Nageli, W. (1940). Lichtmessungen im Freiland und in geschlossenen Altholzbestanden Schweiz. *Met. Zeitschrift* 53, 409.

National Research Council (1980). *Research Priorities in Tropical Biology.* National Academy of Sciences, Washington D.C.

Njoku, E. (1964). Seasonal periodicity in the growth and development of some forest trees in Nigeria II: observations on seedlings. *Journal of Ecology* 52, 19-26.

Norman, J. M. and Jarvis, P.G. (1974). Photosynthesis in Sitka spruce (*Picea sitchensis* (Bong.) Carr.) III: measurements of canopy structure and interception of radiation. *Journal of Applied Ecology* 11, 375-398.

Norman, J.M. and Tanner, C.B. (1969). Transient light measurements in plant canopies. *Agronomy Journal* 61, 847-849.

Nunez-Farfan, J. and Dirzo, R. (1988). Within-gap spatial heterogeneity and seedling performance in a Mexican tropical forest. *Oikos* 51, 274-284.

Oberbauer, S.F., Clark, D.B., Clark, D.A. and Quesda, M. (1988). Crown light environments of saplings of two species of rainforest emergent trees. *Oecologia* 75, 207-212.

Ogawa, H., Yoda, K., Ogino, K. and Kira, T. (1965). Comparative ecological studies on three main types of forest vegetation in Thailand. 1 Structure and floristic composition. *Nature and Life in SE Asia* 4, 13-48.

Oguntoyinbo, J.S. (1970). Reflection coefficients of natural vegetation crops and urban surfaces in Nigeria. *Quarterly Journal of the Royal Meteorological Society* 96, 430-441.

Oke, T.R. (1987). *Boundary Layer Climates (2nd Ed.).* Methuen, London and New York.

Oldeman, R.A.A. (1978). Architecture and energy exchange of dicotyledonous trees in the forest. In: *Tropical Trees as Living Systems.* (Eds. R.B. Tomlinson and M. H. Zimmerman), pp. 535-560. Cambridge University Press, Cambridge.

Olson, C.E. and Good, R.E. (1961). Seasonal changes in light reflectance from forest vegetation. *Photogrammic Engineering* 27, 492-493.

Ondok, J.P. (1984). Simulation of stand geometry in photosynthetic models based on hemispherical photographs. *Photosynthetica* 18, 231-239.

Orozco-Segovia, A.D.L. (1986). *Fisiologia ecologia del photoblastismo en semillas de cuatro especies del genero.* Piper *L.* Ph.D. Thesis, Universidad Nacional Autonoma de Mexico, Mexico.

Orth, R. (1939). Zur kenntnis des lichtklimas der tropen und subtropen sowie des tropischen urwaldes. *Beitr. Geophys.* 55, 52-102.

Page, C.T. and Clifford, H.T. (1981). Ecological biogeography of Australian conifers and ferns. In: *Ecological Biogeography of Australia.* (Ed. A. Keast), pp. 471-498. Dr W. Junk, The Hague.

Pearcy, R.W. (1983). The light environment and growth of C_3 and C_4 tree species in the understorey of a Hawaiian forest. *Oecologia* 58, 19-25.

Pearcy, R.W. (1987). Photosynthetic gas exchange responses of Australian tropical forest trees in canopy, gap and understory micro-environments. *Functional Ecology* 1, 169-178.

Pearcy, R.W. (1988). Photosynthetic utilisation of lightflecks by understorey plants. *Australian Journal of Plant Physiology* 15, 223-238.

Pearcy, R.W. (1989). Radiation and light measurements. In: *Plant Physiological Ecology: Field methods and Instrumentation.* (Ed. R.W. Pearcy, J.R. Ehleringer, H.A. Mooney and P.W. Rundel), pp. 97-116. Chapman and Hall, London and New York.

Pearcy, R.W. and Calkin, H.W. (1983). Carbon dioxide exchange of C_3 and C_4 tree species in the understorey of a Hawaiian forest. *Oecologia (Berlin)* 58, 26-32.

Pearcy, R.W., Osteryoung, K . and Calkin, H.W. (1985). Photosynthetic responses to dynamic light environments by Hawaiian trees. *Plant Physiology* 79, 896- 902.

Pearcy, R.W., Chazdon, R.L. and Kirschbaum, M.U.F. (1987 a). Photosynthetic utilization of lightflecks by tropical forest plants. In: *Progress in Photosynthesis Research Vol. IV.* (Ed. J. Biggens), pp. 257-260. Martinus Nijhoff, Dordrecht.

Pearcy, R.W., Bjorkman, O., Caldwell, M.M., Keeley, J.E., Monson, R.K. and Strain, B.R. (1987 b). Carbon gain by plants in natural environments. *BioScience* 37, 21-29.

Pinker, R.T., Thompson, O.E. and Eck, T.F. (1980). The albedo of a tropical evergreen forest. *Quarterly Journal of the Royal Meteorological Society* 106, 551-558.

Pinker, R.T. (1982) . The diurnal asymmetry in the albedo of tropical forest vegetation. *Forest Science* 28, 297-304.

Ponce de Leon, L. (1982). L'ecophysiologie de la germination d'especes forestieres et de savanne, en rapport avec la dynamique de la vegetation en Cote d'Ivoire. *Bull. Liason Cher. Lamto, N.S.I.,* pp. 1-44.

Popma, J. and Bongers, F. (1988). The effect of canopy gaps on growth and morphology of seedlings of rain forest species. *Oecologia (Berlin)* 75, 625-632.

Popma, J. Bongers, F, Martinez-Ramos, M. and Veneklaas, E. (1988). Pioneer species distribution in treefall gaps in neotropical rain forest; a gap definition and its consequences. *Journal of Tropical Ecology.* 4, 77-88.

Popma, J., Bongers, F. and Meave del Castillo, J. (1988). Patterns in the vertical structure of the tropical lowland forest of Los Tuxtlas, Mexico. *Vegetatio* 74, 81-91.

Powles, S.B. and Bjorkman, O. (1981). Leaf movement in the shade species *Oxalis oregana* II: role in protection against injury by intense light. *Carnegie Institution Washington Yearbook* 80, 63-66.

Prescott, J.A. (1940). Evaporation from a water surface in relation to solar radiation. *Transactions of the Royal Society of South Australia* 64, 114-118.

Raich, J.W.(1989). Seasonal and spatial variation in the light environment in a tropical dipterocarp forest and gaps. *Biotropica* 21,299-302.

Ramage, C.S. (1968). Role of a tropical 'maritime continent' in the atmospheric circulation. *Monthly Weather Review* 96, 365-370.

Reifsnyder, W.E. and Lull, H.W. (1965). *Radiant Energy in Relation to Forests.* AMS Press, New York.

Reifsnyder, W.E., Furnival , G.M. and Horowitz, J.L. (1971) . Spatial and temporal distribution of solar radiation beneath forest canopies. *Agricultural Meteorology* 9, 21-37.

Reynolds, D.W., Vonder Haar, T.H. and Cox, S.K. (1975). The effect of solar radiation absorption in the tropical troposphere. *Journal of Applied Meteorology* 14, 433-444.

Richards, P.W. (1952). *The Tropical Rainforest: An Ecological Study.* Cambridge University Press, Cambridge.

Richards. P.W. (1983). The three-dimensional structure of tropical rain forest. In: *Tropical Rain-Forest: The Leeds Symposium.* (Eds. A.C. Chadwick and S.L. Sutton), pp. 3-10. Leeds Philosophical Society, Leeds, U.K.

Rietveld, M.R. (1978). A new method for estimating the regression coefficients in the formula relating solar radiation to sunshine. *Agricultural Meteorology* 19, 243-252.

Roberts, J., Cabral, M.R. and De Aguiar, L.F. (1990). Stomatal and boundary-layer conductances in an Amazonian terra firme rain forest. *Journal of Applied Ecology* 27, 336-353.

Robertson, G.W. (1966). The light composition of solar and sky spectra available to plants. *Ecology* 47, 640-643.

Robinson, N. (1966). *Solar Radiation.* Elsevier, Amsterdam.

Rosenberg, N.J., Blad, B.L. and Verma, S.B. (1983). *Microclimate: The Biological Environment (2nd Ed.).* John Wiley and Sons, New York.

Ross, J. (1975). Radiative transfer in plant communities. In: *Vegetation and the Atmosphere Volume 1: Principles.* (Ed. J.L. Montieth), pp.13-55. Academic Press, London, New York and San Francisco.

Ross, J. (1981). *The Radiation Regime and Architecture of Plant Stands.* Dr W. Junk Publishers, The Hague.

Sadler, J.C. and Harris, B.E. (1970). The mean tropospheric circulation and cloudiness over South-East Asia and neighbouring areas. Hawaii Institute of Geophysics, University of Hawaii.

Saffell, R.A., Campbell, G.S. and Campbell, E.C. (1979). An improved micropower counting integrator. *Agricultural Meteorology* 20, 393-396

Salisbury, F.B. (1981). Responses to photoperiod. In: *Physiological Plant Ecology I: Responses to the Physical Environment.* (Ed. O.L. Lange, P.S. Nobel, C.B. Osmond and H. Ziegler), pp. 135-167. Springer-Verlag, Berlin, Heidelberg and New York.

Salminen, R., Hari, P., Kellomaki, S., Korpilahti, E., Kotiranta, M. and Sievanen, R. (1983 a). A measuring system for estimating the frequency distribution of irradiance within plant canopies. *Journal of Applied Ecology* 20, 887-895.

Salminen, R., Nilson, T., Hari, P., Kaipiainen, L. and Ross, J. (1983 b). A comparison of different methods for measuring the canopy light regime. *Journal of Applied Ecology* 20, 897-904.

Schulz, J.P. (1960). *Ecological Studies on Rain Forest in Northern Surinam.* N.V. Noord-Hollandsche Uitgevers Maatschappij, Amsterdam.

Schulze, E.D., Fuchs, M.I. and Fuchs, M. (1977). Spatial distribution of photosynthetic capacity and performance in a mountain spruce forest of northern Germany I: biomass distribution and daily CO_2 uptake in different crown layers. *Oecologia (Berlin)* 29, 43-61.

Schupp, E.W., Howe, H.F., Augspurger, C.K. and Levey, D.J. (1989). Arrival and survival in tropical treefall gaps. *Ecology* 70, 562-564.

Scott, G.A.J. and Street, R.M. (1976). The role of chemical weathering in the formation of Hawaiian Amphitheatre-headed valleys. *Z. Geomorp. NF* 20, 171-189.

Sheehy, J.E. (1985) . Radiation. In: *Instruments for Environmental Physiology.* (Ed. B. Marshall and F.I. Woodward), pp 5-28. Cambridge University Press, Cambridge.

Shell, G.S.G. and Lang, A.R.C. (1976). Movements of sunflower leaves over a 24-hr period. *Agricultural Meteorology* 16, 161-170.

Shirley, H.L. (1935). Light as an ecological factor and its measurement. *Botanical Review* 1, 355-381.

Shirley, H.L. (1945). Light as an ecological factor and its measurement II. *Botanical Review* 11, 497-532.

Shuttleworth, W. J. , Gash, J.H. C., Lloyd, C.R. , Moore, C.J. Roberts, J., Filho, A, D, O. M., Fisch, G., De Paula Silva Filho, V., De Nazare Goes Ribeiro, M., Molion, L.C.B., De Abreu Sa, L. D., Nobre, J.C.A., Cabral, O. M. R., Patel, S. R. and De Moraes, J.C. (1984 a) Eddy correlation measurements of energy partition for Amazonian forest. *Quarterly Journal of the Royal Meteorological Society* 110, 1143-1162.

Shuttleworth, W. J, Gash, J.H. C., Lloyd, C.R. , Moore, C.J. Roberts, J., Filho, A, D, O. M., Fisch, G., De Paula Silva Filho, V., De Nazare Goes Ribeiro, M., Molion, L.C.B., De Abreu Sa, L. D., Nobre, J.C.A., Cabral, O. M. R., Patel, S. R. and De Moraes, J.C. (1984 b). Observations of radiation exchange above and below Amazonian forest. *Quarterly Journal of the Royal Meteorological Society* 110, 1163-1169

Shuttleworth, W.J., Gash, J.H. C., Lloyd, C.R. , Moore, C.J. Roberts, J., Filho, A, D, O. M., Fisch, G., De Paula Silva Filho, V., De Nazare Goes Ribeiro, M., Molion, L.C.B., De Abreu Sa, L. D., Nobre, J.C.A., Cabral, O. M. R., Patel, S. R. and De Moraes, J.C. (1985). Daily variations of temperature and humidity within and above Amazonian forest. *Weather* 40, 102-108.

Simonett, D.A. (1967). Landslide distribution and earthquakes in the Bewani and Torricelli Mountains, New Guinea. In: *Landform studies from Australia and New Guinea.* (Eds. J.N. Jennings and J.A. Mabbutt), pp. 64-68. Cambridge University Press, Cambridge.

Sinclair, T.R. and Knoerr, K.R. (1982). Distribution of photosynthetically active radiation in the canopy of a Loblolly pine plantation. *Journal of Applied Ecology* 19,183-191.

Smith, H. and Morgan, D.C. (1981). The spectral characteristics of the visible radiation incident upon the surface of the earth. In: *Plants and the Daylight Spectrum.* (Ed. H. Smith), pp. 3-20. Academic Press, London.

Smith, J.S. (1936). Light and the forest canopy. *Malaysian Forester* 5, 6-12.

Smith, W.K., Knapp, A.K. and Reiners, Q.A. (1989). Penumbral effects on sunlight penetration in plant communities. *Ecology* 70, 1603-1609.

Spencer, J.W. (1971). Fourier series representation of the position of the sun. *Search* 2, 172.

Spencer, J.W. (1982). A comparison of methods for estimating hourly diffuse solar radiation from global solar radiation. *Solar Energy* 29, 19-32.

Stace, H.C.T., Hubble, G.D., Brewer, R., Northcote, K.H., Sleeman, J.R. Mulcahy, M.J. and Hallsworth, E.G. (1968). *A Handbook of Australian Soils.* Rellim Technical Publications, Glenside, South Australia.

Stanhill, G. (1970). Some results of helicopter measurements of albedo. *Solar Energy* 13, 59-66.

Stephens, G.R. and Waggoner, P.E. (1975). Carbon dioxide exchange of a tropical rain forest. Part I. *BioScience* 20, 1050-1053.

Steyn, D.G. and Hay, J.E. (1986). The determination of sky-view factors in urban environments using video imagery. *Journal of Atmospheric and Oceanic Technology* 3, 759-764.

Stigter, C.J. and Musabilha, V.M.M. (1982). The conservative ratio of photosynthetically active to total radiation in the tropics. *Journal of Applied Ecology* 19, 853-858.

Stocker, G.C. (1988). Tree species diversity in rainforests - establishment and maintenance. *Proceedings of the Ecological Society of Australia* 15, 39-47.

Stocker, G.C. and Mott, J.J. (1981). Fire in the tropical forests and woodlands of northern Australia. In: *Fire and the Australian Biota.* (Eds. A.M. Gill, R.H. Groves and I.R. Noble), pp. 425-439. Australian Academy of Science, Canberra.

Stocker, G.C. and Unwin, G.L. (1986). Fire and the functioning of tropical plant communities. In: *Tropical Plant Communities.* (Eds. H.T. Clifford and R.L. Sprecht), pp. 91-103. University of Queensland, Brisbane.

Stoutjesdijk, P.H. (1972). A note on the spectral transmission of light by tropical rainforest. *Acta. Bot. Neerl.* 22, 346-350.

Stubblebine, W., Langenheim, J.H. and Lincoln, D. (1978). Vegetative response to photoperiod in the leguminous tree *Hymenaea courbaril* L. *Biotropica* 10, 18-29.

Swaine, M.D., Lieberman, D. and Putz, F.E. (1987). The dynamics of tree populations in tropical forest: a review. *Journal of Tropical Ecology* 3, 359-366.

Swaine, M.D. and Hall, J.B. (1988). The mosaic theory of forest regeneration and the determination of forest composition in Ghana. *Journal of Tropical Ecology* 4, 253-269.

Szeicz, G. (1985). Instruments and their exposure. In: *Vegetation and the Atmosphere Volume 1: Principles.* (Ed. J.L. Montieth), pp. 229-273. Academic Press, London, New York and San Francisco.

Szeicz, G., Monteith, J.L. and Dos Santos, J.M. (1964). Tube solarimeters to measure radiation among plants. *Journal of Applied Ecology* 1, 169-174.

Tanner, E.V.J. (1980).. Studies on the biomass and productivity in a series of montane rain forests in Jamaica. *Journal of Ecology* 68, 573-588.

Thompson, W.A., Stocker, G.C. and Kriedemann, P.E. (1988). Growth and photosynthetic response to light and nutrients of *Flindersia brayleyana* F. Muell., a rainforest tree with broad tolerance to sun and shade. *Australian Journal of Plant Physiology* 15, 299-315.

Tomlinson, P.B. (1987). Architecture of tropical plants. *Annual Reviews of Ecological Systematics.* 18, 1-21.

Torquebiau, E.F. (1988). Photosynthetically active radiation environment, patch dynamics and architecture in a tropical rainforest in Sumatra. *Australian Journal of Plant Physiology* 15, 327-342.

Tracey, J.G. (1982). *The Vegetation of the Humid Tropical Region of North Queensland.* CSIRO, Melbourne.

Tracey, J.G. and Webb. L.J. (1975). *Vegetation of the Humid Tropical Region of North Queensland.* (15 maps at 1:100,000 scale + key). CSIRO, Long Pocket Laboratories, Indooroopilly, Queensland.

Trapp, E. (1938). Untersuchung uber die Verteilung der Helligkeits in einem Buchenbestand. *Bioklimatologie Ser. B* 5, 153-158.

Tucker, D.J. and Mansfield, T.A. (1972). Effects of light quality on apical dominance in *Xanthium strumarium* and the associated changes in endogenous levels of abscisic acid and cytokinins. *Planta* 102, 140-151.

Turton, S.M. (1985). The relative distribution of photosynthetically active radiation within four tree canopies, Craigieburn Range, New Zealand. *Australian Forest Research* 15, 383-394.

Uhl, C., Clark, K., Dezzeo, N, and Maquirino, P. (1988). Vegetation dynamics in Amazonian treefall gaps. *Ecology* 69, 751-763.

Unwin, G.L., Stocker, G.C. and Sanderson, K.D. (1985). Fire and the forest ecotone in the Herberton highland, north Queensland. *Proceedings of the Ecological Society of Australia* 13, 215-224.

Unwin, G.L., Applegate, G.B., Stocker, G.C. and Nicholson, D.I. (1988). Initial effects of tropical cyclone 'Winifred' on forests of north Queensland. *Proceedings of the Ecological Society of Australia* 15, 283-296.

Ustin, S.L., Woodward, R.A., Barbour, M.G. (1984). Relationships between sunfleck dynamics and red fir seedling distribution. *Ecology* 65,1420-1428.

Vazquez-Yanes, C. and Smith, H. (1982). Phytochrome control of seed germination in the tropical rain forest pioneer trees *Cecropia obtusifolia* and *Piper auritum* and its ecological significance. *New Phytologist* 92, 477-485.

Vazquez-Yanes, C. and Segovia, A. (1984). Ecophysiology of seed germination in the tropical humid forests of the world: a review. In: *Physiological Ecology of Plants of the Wet Tropics.* (Eds. E. Medina, H.A. Mooney and C. Vazquez-Yanes), pp.51-84. Dr W. Junk Publishers, The Hague.

Vezina, P.E. (1961). Variations in total solar radiation in three Norway spruce plantations. *Forest Science* 3, 257-264.

Vezina, P.E. and Pech, G.Y. (1964). Solar radiation beneath conifer canopies in relation to crown closure. *Forest Science* 10, 443-451.

Vezina, P.E. and Boulter, D.W.K. (1966). The spectral composition of near ultra-violet and visible radiation beneath forest canopies. *Canadian Journal of Botany* 4, 1267-1284.

Vince-Prue, D. (1975). *Photoperiodism in Plants.* McGraw-Hill Book Company, London.

Vince-Prue, D. (1981). Daylight and photoperiod. In: *Plants and the Daylight Spectrum.* (Ed. H. Smith), pp. 223-242. Academic Press, London.

Walker, J.W. (1976). Comparative pollen morphology and phylogeny of the ranalean complex. In: *Origin and Early Evolution of Angiosperms.* (Ed. C.B. Beck), pp. 241-299. Colombia University Press, New York.

Walsh, R.P.D. (1980). Runoff processes and models in the humid tropics. *Zeit. f. Geomorph. Suppl. Band* 36, 176-202.

Walsh, J.W.T. (1961). *The Science of Daylight.* MacDonald, London.

Walter, H. (1971). *Ecology of Tropical and Subtropical Vegetation.* Oliver and Boyd, Edinburgh.

Walters, M.B. and Field, C.B. (1987). Photosynthetic light acclimation in two rainforest *Piper* species with different ecological amplitudes. *Oecologia* 72, 449-456

Watson, D.J. (1958). The dependence of net assimilation rate upon leaf area index. *Annals of Botany* 22, 37-54.

Webb, L.J. (1958). Cyclones as an ecological factor in tropical lowland rainforest, North Queensland. *Australian Journal of Botany* 6, 220-228.

Webb, L.J. (1959). A physiognomic classification of Australian rainforests. *Journal of Ecology* 47, 551-569.

Webb, L.J. (1968). Environmental relationships of the structural types of Australian rainforest vegetation. *Ecology* 49, 296-311.

Webb, L.J., Tracey, J.G., Williams, W.T. and Lance, G.N. (1970). Studies in the numerical analysis of complex rain forest communities V: a comparison of the properties of floristic and physiognomic structural data. *Journal of Ecology* 58, 203-232.

Webb, L.J., Tracey, J.G. and Williams, W.T. (1972). Regeneration and pattern in the subtropical rain forest. *Journal of Ecology* 60, 675-695.

Webb, L.J. and Tracey, J.G. (1981). Australian rainforests: patterns and change. In: *Ecological Biogeography of Australia.* (Ed. A. Keast), pp. 607-683. Dr W. Junk Publishers, The Hague.

Weber, J.A., Jurik, T.W., Tenhunen, J.D. and Gates, D.M. (1985). Analysis of gas exchange in seedlings of *Acer saccharan*: integration of field and laboratory studies. *Oecologia (Berlin)* 65, 338-347.

Wellman, P. (1987). Eastern highlands of Australia; their uplift and erosion. *BMR Journal of Australian Geology and Geophysics* 10, 277-286.

Whitmore, T.C. (1974). Change with time and the role of cyclones in tropical rain forest on Kolombangara, Solomon Islands. *Commonwealth Forestry Institute, Paper* 46.

Whitmore, T.C. (1975). *Tropical Rain Forests of the Far East.* Oxford Science Publications, Oxford.

Whitmore, T.C. (1978). Gaps in the forest canopy. In: *Tropical Trees as Living Systems.* (Eds. P.B. Tomlinson and M.H. Zimmerman), pp. 639-655. Cambridge University Press, Cambridge.

Whitmore, T.C. (1984). *Tropical Rain Forests of the Far East (2nd. Ed.).* Oxford Science Publications, Oxford.

Whitmore, T.C. (1988). The influence of tree population dynamics on forest species composition. In: *Population Biology of Plants.* (Eds. D.J. Davy, M.J. Hutchings and A.R. Watkinson). Blackwell Scientific, Oxford.

Whitmore, T.C. (1989) . Canopy gaps and the two major groups of forest trees. *Ecology* 70, 536 - 538

Whitmore, T.C. and Wong, Y.K. (1959). Patterns of sunfleck and shade in tropical rain forest. *Malaysian Forester* 22, 50-62

Whittaker, R.H. (1975). *Communities and Ecosystems (2nd Ed.).* Macmillan, New York.

Williams, B.A. and Austin, R.B. (1977). Short note: an instrument for measuring the transmission of shortwave radiation by crop canopies. *Journal of Applied Ecology* 14, 987-991.

Wilmott, W.F., Trezise, D.L., O'Flynn, M.L., Holmes, P.R. and Hofmann, G.W. (1988). *Cairns Region.* Sheets 8064 & 8063, Queensland. Queensland Department of Mines.

Willmott, W.F. and Stephenson, P.J. (1989). *Rocks and Landscapes of the Cairns District.* Queensland Department of Mines. Qld. Government printer, Brisbane.

Wilson, M.F. and Crome, F.H.J. (1989). Patterns of seed rain at the edge of a tropical Queensland rainforest. *Journal of Tropical Ecology* 5, 301-308.

Woods, D.R. and Turner, N.C. (1971). Stomatal responses to changing light by four tree species of varying shade tolerance. *New Phytologist* 70, 77-84.

Woodward, F.I. (1983). Instruments for measurement of photosynthetically active radiation and red, far-red and blue light. *Journal of Applied Ecology* 20, 103 -115.

Woodward, F.I. and Yaqub, M. (1979). Integrators and sensors for measuring photosynthetically active radiation and temperature in the field. *Journal of Applied Ecology* 16, 545-552.

World Meteorological Organisation (1981). Meteorological Aspects of the Utilisation of Solar Radiation as an Energy Source. *Technical Note No.* 172, W.M.O. 557, Geneva.

Yoda, K. (1974). Three-dimensional distribution of light intensity in a tropical rain forest of West Malaysia. *Japanese Journal of Ecology* 24, 247-254.

APPENDIX A

BASIC PROGRAM FOR THE CALCULATION OF SOLAR DECLINATION, ALTITUDE AND AZIMUTH

```
0010    REM SOLAR DECLINATION, ALTITUDE AND AZIMUTH PROGRAM
0020    REM BY SM TURTON (1987)
0030    INPUT "LATITUDE (- FOR S HEM) IN DECIMAL DEG ";LA
0040    PRINT:INPUT"DAY #, MONTH # ";D,M
0050    INPUT "LEAP YEAR (Y OR N) ";L$:CLS
0060    IF L$="Y" THEN L=1 ELSE L=2
0080    TD=(INT(275*M/9)-L*INT((M+9)/12)+D-30)
0085    PI=4*ATN(1):CF=PI/180:LA=LA*CF
0090    DA=2*PI*(TD-.3)/365.25:REM  DAY  ANGLE
0100    REM SOLAR DECLINATION EQUATION
0110    SD=.006918-.399912*COS(DA)+.070257*SIN(DA)
0120    SD=SD-.006758*COS(2*DA)+.000907*SIN(2*DA)
0130    SD=SD-.002697*COS(3*DA)+.00148*SIN(3*DA)
0140    PRINT "DAY OF THE YEAR = ";TD
0150    PRINT "SOLAR DECLINATION = ";SD/CF:PRINT
0160    FOR H=0 TO 90 STEP 15:REM HOUR ANGLE OF THE SUN
0170    SA=SIN(LA)*SIN(SD)+COS(LA)*COS(SD)*COS(H*CF)
0180    SA=ATN(SA/SQR(1-SA^2))
0190    AZ=ATN(SIN(H*CF)/(COS(H*CF)*SIN(LA)-TAN(SD)*COS(LA)))
0200    IF AZ<0 THEN AZ=AZ+PI
0205    IF AZ=0 THEN 220
0210    IF LA<0 THEN AZ=PI-AZ
0220    PRINT"HOUR ANGLE ";H;
0230    PRINT "     ALTITUDE ";SA/CF;"     AZIMUTH ";AZ/CF
0240    NEXT H
0250    PRINT :PRINT "CLICK TO CONTINUE":WHILE MOUSE (0)<>1:WEND
0260    CLS:GOTO 10
0270    END
```

PROGRAM DETAILS

Lines 10-50:	The latitude of the site (treated as negative in the southern hemisphere), and the day and month are entered.
Lines 60-85:	This short algorithm calculates the day number (January 1st =1).
Lines 90-240:	The main algorithm that calculates solar declination, solar altitude, and solar azimuth for every hour from solar noon to sunrise/sunset. Remark (REM) statements are provided for various equations referred to in the text (Chapter 2).
Lines 250-270:	The values are displayed on the screen.

APPENDIX B

BASIC PROGRAM FOR THE SKY-CANOPY-GAP-IRRADIANCE (SCANGIR) MODEL

```
0001  REM WRITTEN BY SM TURTON (1987-88)
0002  DIM   R1(1000),R2(1000),R3(1000)
0005  GOSUB 2000
0006  F$="#####.#":G$="######.#":H$="#############.#"
0007  INPUT"OUTPUT FILE NAME";NA$
0008  OPEN "O",#1,NA$
0010  CLS
0023  DEF   FNB(X)=-ATN(X/SQR(-X*X+1))+1.5708
0024  DEF   FNA(X)=ATN(X/SQR(-X*X+1))
0110  CF=.0174533:PI=3.141592654#
0120  SC=1367:B=.91:A=.51:T=.7
0200  PRINT "INPUT PARAMETERS"
0210  PRINT :PRINT "LATITUDE OF SITE IN"
0220  PRINT "DECIMAL DEGREES (-VE FOR S HEM) ":INPUT LA
0225  IF ABS(LA)>66.5 THEN 210
0226  INPUT "DAY #, MONTH # ";D,M
0227  INPUT "LEAP YEAR (Y OR N) ";L$
0228  IF L$="Y" THEN L=1 ELSE L=2
0230  TD=(INT(275*M/9)-L*INT((M+9)/12)+D-30)
0232  IF TD>365 THEN 230
0234  PRINT "INCLINATION OF SURFACE FROM "
0235  PRINT "THE HORIZONTAL (DEG) ":INPUT BT
0236  IF BT>90 THEN 234
0237  PRINT "SURFACE AZIMUTH ANGLE"
0238  PRINT "EAST IS +VE, WEST IS -VE,"
0239  PRINT "NORTH IS 180, SOUTH IS 0 ":INPUT U
0240  PRINT "ENTER REQUIRED TIME INTERVALS "
0250  PRINT "BETWEEN IRRADIANCE ESTIMATES (IN SECS) ":INPUT K
0260  PRINT "ENTER GAP DIAMETER IN METRES ":INPUT GD
0270  PRINT "ENTER MEAN HEIGHT OF FOREST"
0280  PRINT "AROUND THE GAP IN METRES ":INPUT GH
0300  REM ECCENTRICITY CORRECTION EQUATION
0310  EO=1+.003*COS((2*PI*TD/365.25)*CF)
0320  REM DAY ANGLE EQUATION
0330  DA=(2*PI*(TD-1)/365.25)/CF
0340  REM SOLAR DECLINATION EQUATION
0350  SD=.006918-.399912*COS(DA*CF)+.070257*SIN(DA*CF)
0351  SD=SD-.006758*COS(2*DA*CF)+.000907*SIN(2*DA*CF)
0352  SD=SD-.002697*COS(3*DA*CF)+.00148*SIN(3*DA*CF)
0353  SD=SD*(180/PI)
0355  Z=K
0360  K=K/240
0400  REM SOLAR GEOMETRY FOR GAP
0405  IF GH=0 THEN VF=1:GOTO 500
0410  G=ATN(GH/(GD/2))/CF:REM GAP GEOMETRY
0430  REM SKY-VIEW FACTOR (%)
0440  VF=ATN(GD/(GH*2))/CF:VF=SIN(VF*CF):VF=VF*VF
0450  IF GH=0 THEN VF=1
0500  REM LOOP SIMULATION
0505  GOSUB 700
0510  FOR H=110 TO 0 STEP -K:REM MORNING
0511  GOSUB 520
0512  NEXT H
0515  FOR H=0-K TO -110 STEP -K:REM AFTERNOON
0516  GOSUB 520
0517  NEXT H
0518  GOTO 654
0520  REM SOLAR ALTITUDE EQUATION
```

```
0530   SA=SIN(LA*CF)*SIN(SD*CF)
0535   SA=SA+COS(LA*CF)*COS(SD*CF)*COS(H*CF)
0540   SA=FNA(SA):SA=SA/CF
0550   REM INCLINED SURFACE COMPUTATIONS
0555   TH=(SIN(LA*CF)*COS(BT*CF)-COS(LA*CF)*SIN(BT*CF)*COS(U*CF))
       *SIN(SD*CF)+(COS(LA*CF)*COS(BT*CF)+SIN(LA*CF)*SIN(BT*CF)
       *COS(U*CF))* COS(SD*CF)*COS(H*CF)+COS(SD*CF)
       *SIN(BT*CF)*SIN(U*CF)*SIN(H*CF)
0560   TH=FNB(TH):TH=TH/CF
0580   REM SOLAR RADIATION COMPONENTS
0590   M=1/SIN(SA*CF)
0595   GOSUB 2052
0596   BB=SC*EO*T^M*SIN(SA*CF):REM DIRECT-BEAM
0597   DD=A*(B*SC*EO*SIN(SA*CF)-BB):REM DIFFUSE CLOUDLESS SKY
0598   DD=.5*DD*(1+COS(BT*CF)):REM DIFFUSE INCLINED SURFACE CLOUDLESS
0599   D1=A*(B*SC*EO*SIN(SA*CF)-T1)/(1-A):REM DIFFUSE CLOUDY SKY
0600   D1=.5*D1*(1+COS(BT*CF)):REM DIFFUSE INCLINED SURFACE CLOUDY
0603   ZA=90-SA
0605   BB=BB*(COS(TH*CF)/COS(ZA*CF)):REM DIRECT INCLINED CLOUDLESS
0606   IF D1 >=T1 THEN D1=T1
0607   IF N=1 THEN 620
0608   B1=T1-D1
0609   B1=B1*(COS(TH*CF)/COS(ZA*CF)):REM DIRECT INCLINED CLOUDY
0610   T1=B1+D1:TT=T1:BB=B1:DD=D1
0620   IF 90-TH<G THEN BB=0
0621   F SA=<0 THEN DD=0:IF SA =<0 THEN BB=0
0627   IF BB<0 THEN BB=0
0628   IF SA<0 THEN SA=0
0633   DD=DD*VF:TT=BB+DD
0635   PRINT#1,USING "##.#";SA;:PRINT#1,USING F$;BB;
       :PRINT#1,USING F$;DD;:PRINT#1,USING F$;TT
0644   PRINT :PRINT "SOLAR ALTITUDE ";:PRINT USING F$;SA
0645   PRINT "BEAM";:PRINT USING F$;BB;:PRINT "  DIFFUSE";
       :PRINT USING F$;DD;:PRINT"  TOTAL";:PRINT USING F$;TT
0646   BB=BB*Z/1000:REM AVERAGES IN KJ/M
0647   DD=DD*Z/1000
0648   TT=TT*Z/1000
0649   R1=R1+(BB):R2=R2+(DD):R3=R3+(TT)
0652   RETURN
0654   CLOSE#1:CLS
0655   PRINT "DAILY INTEGRALS BASED ON ";Z/60;" MIN VALUES"
0660   PRINT "IN KILOJOULES PER SQ METRE"
0665   PRINT :PRINT "DIRECT-BEAM";:PRINT USING G$;R1
0666   PRINT "DIFFUSE-SKY";:PRINT USING G$;R2
0667   PRINT "TOTAL";:PRINT USING G$;R3
0680   PRINT :PRINT "MEAN DAILY FLUXES BASED ON ";Z/60; " MIN VALUES"
0681   PRINT "IN WATTS PER SQ METRE"
0682   WS=-TAN(LA*CF)*TAN(SD*CF):REM SUNRISE HOUR ANGLE
0683   WS=FNB(WS):WS=WS/CF
0684   DN=.13333333#*WS:REM DAYLENGTH IN HRS
0685   PRINT "DAYLENGTH (HRS)";:PRINT USING F$;DN :DN=DN*3600
0686   PRINT :PRINT "DIRECT-BEAM";:PRINT USING F$;R1*1000/DN
0687   PRINT "DIFFUSE-SKY";:PRINT USING F$;R2*1000/DN
0688   PRINT "TOTAL";:PRINT USING F$;R3*1000/DN
0696   GOTO 900
0700   REM DISPLAY ROUTINE
0705   CLS
0710   PRINT "DAY OF THE YEAR ";TD
```

```
0720    PRINT "LATITUDE ";LA;" DEGREES"
0721    PRINT "SOLAR DECLINATION ";:PRINT USING F$;SD
0725    PRINT "CLOUD-TYPE - ";C$
0730    PRINT "GAP DIAMETER ";GD;" METRES"
0740    PRINT "MEAN CANOPY HEIGHT ";GH;" METRES"
0745    PRINT "SLOPE ANGLE ";BT;" DEG"
0748    PRINT "ASPECT ";U;" DEG"
0780    PRINT "SKY VIEW FACTOR ";VF
0785    PRINT :PRINT "CLICK TO CONTINUE":WHILE MOUSE (0)<>1:WEND
0789    CLS
0790    PRINT :PRINT "RADIATION COMPONENTS WATTS PER SQ METRE"
0800    PRINT "AT THE CENTRE OF THE GAP":PRINT
0805    PRINT "VALUES ARE GIVEN EVERY ";Z/60;" MINS"
0810    RETURN
0900    PRINT :PRINT "CLICK TO CONTINUE":WHILE MOUSE (0)<>1:WEND
0910    GOTO2
0930    END
2000    REM SUBROUTINE FOR CLOUD TYPES
2005    CLS:PRINT "CLOUD TYPES"
2010    PRINT :PRINT "(1) CLOUDLESS"
2015    PRINT "(2) CIRRUS"
2020    PRINT "(3) CIRROSTRATUS"
2025    PRINT "(4) ALTOCUMULUS"
2030    PRINT "(5) ALTOSTRATUS"
2035    PRINT "(6) STRATOCUMULUS"
2040    PRINT "(7) STRATUS"
2041    PRINT "(8) NIMBOSTRATUS"
2042    PRINT :INPUT"SELECT OPTION (NUMBER) ";N
2043    IF N=1 THEN C$="CLOUDLESS"
2044    IF N=2 THEN C$="CIRRUS"
2045    IF N=3 THEN C$="CIRROSTRATUS"
2046    IF N=4 THEN C$="ALTOCUMULUS"
2047    IF N=5 THEN C$="ALTOSTRATUS"
2048    IF N=6 THEN C$="STRATOCUMULUS"
2049    IF N=7 THEN C$="STRATUS"
2050    IF N=8 THEN C$="NIMBOSTRATUS"
2051    RETURN
2052    REM CLOUD-IRRADIANCE REGRESSIONS
2053    IF N=1 THEN 2090
2055    IF N=2 THEN T1=-120.84+20.75*SA-.093*SA^2:REM CIRRUS
2060    IF N=3 THEN T1=-139.36+20.37*SA-.087*SA^2:REM CIRROSTRATUS
2065    IF N=4 THEN T1=-81.11+12.51*SA-.053*SA^2:REM ALTOCUMULUS
2070    IF N=5 THEN T1=-61.51+10.22*SA-.048*SA^2:REM ALTOSTRATUS
2075    IF N=6 THEN T1=-48.11+8.07*SA-.033*SA^2:REM STRATOCUMULUS
2080    IF N=7 THEN T1=-32.2+5.78*SA-.025*SA^2:REM STRATUS
2085    IF N=8 THEN T1=-10.42+3.82*SA-.024*SA^2:REM NIMBOSTRATUS
2088    IF T1<0 THEN T1=0
2090    RETURN
```

PROGRAM DETAILS

Lines 1-200:	Parameters are set, and variables and functions defined.
Lines 200-280:	Input parameters are entered, including sky conditions, latitude, day and month, slope angle and aspect, time interval required for irradiance estimates, diameter of the circular gap, and height of the surrounding forest.

Lines 300-633:	The main algorithm that calculates direct, diffuse and total irradiance at the prescibed interval for the particular set of input parameters. Remark (REM) statements are provided for various equations referred to in the text (Chapters 2 & 3).
Lines 635-654:	Routine that writes simulated data into a named ASCII file.
Lines 655-930:	The main screen output display routine.
Lines 2000-2090:	Routine which calculates total irradiance beneath the seven cloud types using the regression equations defined in Table 3.4.

APPENDIX C

DESCRIPTIVE STATISTICS APPLIED TO THE SCANGIR MODEL SIMULATIONS IN CHAPTER 4

	TOTAL IRRADIANCE (W m^{-2})				
SOLAR DECLINATION (Approximate date)	0° S mean±1 SD median (range) cv	10° S mean±1 SD median (range) cv	20° S mean±1 SD median (range) cv	30° S mean±1 SD median (range) cv	40° S mean±1 SD median (range) cv
-23.5° (Dec 22)	602.6±326.3 664.1 (5.1-1001.8) 54.2% *n* = 359	641.3±350.5 709.7 (3.8-1071.8) 54.7% *n* = 377	654.8±361.3 722.9 (0.7-1104.3) 55.5% *n* = 397	648.3±361.3 713.0 (4.2-1098.2) 55.7% *n* = 412	618.7±364.1 676.7 (9.6-1053.7) 55.9% *n* = 441
-20.0° (Jan 22/ Nov 22)	620.6±335.7 684.5 (5.2-1030.9) 54.1% *n* = 359	650.1±356.5 716.4 (1.6-1087.8) 54.8% *n* = 375	657.5±363.9 723.0 (0.6-1106.6) 55.4% *n* = 391	641.0±358.6 706.2 (0.4-1086.8) 55.9% *n* = 409	604.0±339.1 662.2 (5.0-1028.9) 56.1% *n* = 429
-11.0° (Feb 22/ Oct 22)	654.2±353.3 722.1 (5.5-1085.3) 54.0% *n* = 359	664.8±361.2 733.3 (4.0-1106.6) 54.3% *n* = 367	652.3±356.0 718.6 (3.7-1089.1) 54.6% *n* = 375	614.7±339.5 679.3 (1.3-1033.6) 55.2% *n* = 385	558.3±309.1 611.9 (3.7-941.9) 55.4% *n* = 395
0.0° (Mar 21/ Sep 23)	667.4±360.1 736.8 (5.6-1106.6) 53.9% *n* = 359	654.4±353.7 722.3 (4.9-1086.1) 54.1% *n* = 359	617.8±335.1 681.5 (4.1-1027.5) 54.2% *n* = 359	559.3±304.8 616.1 (3.1-933.1) 54.5% *n* = 359	481.1±263.8 528.9 (2.1-806.2) 54.8% *n* = 359
+11.0° (Apr 22/ Aug 22)	654.2±353.3 722.1 (5.5-1085.3) 54.0% *n* = 359	611.4±330.7 675.0 (4.0-1014.8) 54.1% *n* = 351	549.6±299.1 606.7 (1.0-914.9) 54.4% *n* = 343	472.5±254.4 520.8 (4.8-783.3) 53.8% *n* = 331	375.9±203.2 413.4 (2.6-625.2) 54.1% *n* = 319
+20.0° (May 22/ Jul 22)	620.6±335.7 684.5 (5.2-1030.9) 54.1% *n* = 359	562.2±304.7 623.8 (2.9-934.2) 54.2% *n* = 345	486.7±262.9 540.0 (2.9-807.6) 54.0% *n* = 329	393.7±212.5 433.7 (2.0-653.5) 54.0% *n* = 311	290.0±154.2 318.4 (3.9-479.0) 53.2% *n* = 287
+23.5 (Jun 22)	602.6±326.3 664.1 (5.1-1001.8) 54.2% *n* = 359	538.3±293.0 594.0 (1.1-896.4) 54.4% *n* = 343	458.9±246.9 506.1 (3.9-760.3) 53.8% *n* = 323	362.2±193.6 401.1 (4.2-598.7) 53.5% *n* = 301	253.2±135.5 277.8 (1.1-419.5) 53.5% *n* = 275

Table C.1. Statistical summary showing simulated total irradiance on a horizontal surface (W m^{-2}) above the forest (forest height to diameter ratio = 0:0) under cloudless skies. The mean, standard deviation, median, range and coefficient of variation (cv) are given for 0°, 10°, 20°, 30°, and 40° South at solar declinations (δ) approximately equal to the 22nd day of each month.

SOLAR DECLINATION (Approximate date)	0° S mean±1 SD median (range) cv	10° S mean±1 SD median (range) cv	20° S mean±1 SD median (range) cv	30° S mean±1 SD median (range) cv	40° S mean±1 SD median (range) cv
	TOTAL IRRADIANCE (W m^{-2})				
-23.5° (Dec 22)	545.7±354.3 634.2 (4.1-972.0) 64.9% n = 359	586.3±377.6 679.4 (3.1-1042.3) 64.4% n = 377	600.4±389.9 692.6 (0.6-1074.9) 65.0% n = 397	593.5±388.0 682.8 (3.3-1068.8) 65.5% n = 417	562.5±373.2 646.4 (7.7-1024.1) 66.4% n = 441
-20.0° (Jan 22/ Nov 22)	565.1±362.9 654.2 (4.2-1001.2) 64.2% n = 359	595.9±383.1 686.1 (1.3-1058.3) 64.3% n = 375	604.2±389.6 692.8 (0.5-1077.2) 64.5% n = 391	586.8±384.4 675.9 (0.3-1057.3) 65.5% n = 409	546.8±366.3 632.0 (4.0-999.2) 67.0% n = 429
-11.0° (Feb 22/ Oct 22)	599.1±381.2 691.8 (4.4-1055.8) 63.6% n = 359	611.3±387.7 703.0 (3.2-1077.2) 63.4% n = 367	597.4±383.4 688.3 (3.0-1059.7) 64.2% n = 375	588.9±366.3 649.1 (1.0-1003.9) 65.6% n = 385	500.3±335.9 581.9 (2.9-911.9) 67.1% n = 395
0.0° (Mar 21/ Sep 23)	612.9±387.9 706.5 (4.4-1077.2) 63.3% n = 359	599.3±381.5 692.0 (3.9-1056.6) 63.7% n = 359	561.3±363.1 651.3 (3.2-997.8) 64.7% n = 359	500.8±332.3 586.1 (2.5-903.1) 66.4% n = 359	416.9±291.5 499.2 (1.6-776.0) 69.9% n = 359
+11.0° (Apr 22/ Aug 22)	599.1±381.2 691.8 (4.4-1055.8) 63.6% n = 359	554.7±358.7 644.8 (3.2-985.1) 64.7% n = 351	490.7±326.6 576.6 (0.8-884.9) 66.6% n = 343	408.6±282.1 491.2 (3.8-753.1) 69.0% n = 331	299.9±227.8 114.7 (2.1-595.1) 75.9% n = 319
+20.0° (May 22/ Jul 22)	565.1±362.9 654.2 (4.2-1001.2) 64.2% n = 359	503.8±332.4 593.7 (2.3-904.2) 66.0% n = 345	423.8±290.7 510.3 (2.3-777.4) 68.6% n = 329	320.6±238.2 404.8 (1.6-623.4) 74.3% n = 311	187.2±160.4 108.4 (3.1-449.7) 85.7% n = 287
+23.5 (Jun 22)	545.7±354.3 634.2 (4.1-972.0) 64.9% n = 359	478.9±320.3 563.9 (0.9-866.3) 66.9% n = 343	392.5±275.2 476.5 (3.1-730.0) 70.1% n = 323	284.2±217.3 114.0 (3.4-568.6) 76.5% n = 301	90.4±30.6 104.6 (0.9-115.0) 33.8% n = 275

Table C.2. Statistical summary showing simulated total irradiance on a horizontal surface (W m^{-2}) at ground level at the centre of a circular gap (forest height to diameter ratio = 1:4) under cloudless skies. The mean, standard deviation, median, range and coefficient of variation (cv) are given for 0°, 10°, 20°, 30°, and 40° South at solar declinations (δ) approximately equal to the 22nd day of each month.

	TOTAL IRRADIANCE (W m^{-2})				
SOLAR DECLINATION (Approximate date)	0° S mean±1 SD median (range) cv	10° S mean±1 SD median (range) cv	20° S mean±1 SD median (range) cv	30° S mean±1 SD median (range) cv	40° S mean±1 SD median (range) cv
-23.5° (Dec 22)	403.8±389.9 75.5 (2.5-927.3) 96.6% n = 359	454.3±417.7 75.7 (1.9-998.0) 91.9% n = 377	473.3±429.9 75.7 (0.7-1104.3) 90.8% n = 397	464.2±427.5 75.7 (2.1-1024.7) 92.1% n = 417	428.6±409.2 75.6 (4.8-979.7) 95.5% n = 441
-20.0° (Jan 22/ Nov 22)	425.8±401.9 75.6 (2.6-956.7) 94.4% n = 359	465.8±423.9 75.7 (0.8-1014.1) 91.0% n = 375	476.2±430.9 75.7 (0.3-1033.2) 90.4% n = 391	456.1±423.4 75.6 (0.2-1013.1) 92.8% n = 409	409.5±399.7 75.5 (2.5-954.7) 97.6% n = 429
-11.0° (Feb 22/ Oct 22)	469.4±422.8 75.7 (2.7-1011.7) 90.1% n = 359	481.5±431.2 75.7 (2.0-1033.1) 89.6% n = 367	466.8±424.6 75.7 (1.9-1015.5) 90.9% n = 375	421.9±402.6 75.6 (0.7-959.4) 95.4% n = 385	345.7±362.2 75.2 (1.8-867.0) 101.7% n = 395
0.0° (Mar 21/ Sep 23)	482.3±431.6 75.7 (2.8-1033.2) 89.5% n = 359	469.6±423.2 75.7 (2.4-1012.4) 90.1% n = 359	424.2±400.5 75.6 (2.0-953.3) 94.4% n = 359	343.7±359.1 75.2 (1.6-858.1) 104.5% n = 359	218.1±277.9 74.2 (1.0-730.6) 127.5% n = 359
+11.0° (Apr 22/ Aug 22)	469.4±422.8 75.7 (2.7-1011.7) 90.1% n = 359	415.4±395.5 75.6 (2.0-940.5) 95.2% n = 351	330.8±350.7 75.2 (0.5-839.8) 106.0% n = 343	193.5±256.7 74.1 (2.4-707.7) 132.6% n = 331	62.4±18.7 71.7 (1.3-75.3) 29.9% n = 319
+20.0° (May 22/ Jul 22)	425.8±401.9 75.6 (2.6-956.7) 94.4% n = 359	347.0±360.1 75.3 (1.4-859.2) 103.8% n = 345	224.8±281.8 74.4 (1.5-732.0) 125.4% n = 329	63.0±18.6 72.3 (1.0-75.5) 29.5% n = 311	58.9±18.7 67.8 (1.9-73.3) 31.8% n = 287
+23.5 (Jun 22)	403.8±389.9 75.5 (2.5-927.3) 96.6% n = 359	313.9±341.0 75.0 (0.6-821.2) 108.6% n = 343	152.3±217.6 73.9 (2.0-684.6) 142.9% n = 323	62.4±18.4 71.3 (2.1-75.1) 29.7% n = 301	56.5±19.1 65.4 (0.5-71.8) 33.8% n = 275

Table C.3. Statistical summary showing simulated total irradiance on a horizontal surface (W m^{-2}) at ground level at the centre of a circular gap (forest height to diameter ratio = 1:2) under cloudless skies. The mean, standard deviation, median, range and coefficient of variation (cv) are given for 0°, 10°, 20°, 30°, and 40° South at solar declinations (δ) approximately equal to the 22nd day of each month.

SOLAR DECLINATION (Approximate date)	TOTAL IRRADIANCE (W m^{-2}) 0° S mean±1 SD median (range) cv	10° S mean±1 SD median (range) cv	20° S mean±1 SD median (range) cv	30° S mean±1 SD median (range) cv	40° S mean±1 SD median (range) cv
-23.5° (Dec 22)	146.5±296.1 30.0 (1.0-882.7) 202.2% n = 359	255.6±391.5 30.1 (0.8-953.7) 153.2% n = 377	286.4±414.8 30.1 (0.1-986.8) 144.8% n = 397	277.2±408.8 30.1 (0.8-980.6) 147.5% n = 417	223.6±368.6 30.0 (1.9-935.3) 164.8% n = 441
-20.0° (Jan 22/ Nov 22)	202.0±349.1 30.0 (1.0-912.2) 172.8% n = 359	274.0±404.7 30.1 (0.3-970.0) 147.7% n = 375	290.7±417.3 30.1 (0.1-989.1) 143.5% n = 391	266.4±400.8 30.1 (0.1-968.9) 150.4% n = 409	189.1±339.2 30.0 (1.0-910.1) 179.4% n = 429
-11.0° (Feb 22/ Oct 22)	274.7±404.4 30.1 (1.1-967.5) 147.2% n = 359	293.4±418.6 30.1 (0.8-989.1) 142.6% n = 367	274.5±405.4 30.1 (0.7-971.3) 147.7% n = 375	199.5±348.1 30.0 (0.3-914.9) 174.5% n = 385	26.4±6.9 30.0 (0.7-30.3) 26.3% n = 395
0.0° (Mar 21/ Sep 23)	299.0±420.6 30.1 (1.1-989.1) 140.7% n = 359	274.9±404.7 30.1 (1.0-968.2) 147.2% n = 359	192.2±341.3 30.0 (0.8-908.8) 177.6% n = 359	26.5±6.9 30.0 (0.6-30.3) 25.9% n = 359	26.0±7.2 29.7 (0.4-30.3) 27.8% n = 359
+11.0° (Apr 22/ Aug 22)	274.7±404.4 30.1 (1.1-967.5) 147.2% n = 359	174.7±324.6 30.0 (0.8-895.9) 185.8% n = 351	26.4±7.0 30.0 (0.2-30.3) 26.4% n = 343	26.0±7.1 29.6 (1.0-30.3) 27.1% n = 331	24.0±7.5 28.7 (0.5-30.1) 29.9% n = 319
+20.0° (May 22/ Jul 22)	202.0±349.1 30.0 (1.0-912.2) 172.8% n = 359	26.5±6.8 30.0 (0.6-30.3) 25.8% n = 345	26.1±7.1 29.8 (0.6-30.3) 50.3% n = 329	25.2±7.4 28.9 (0.4-30.2) 29.5% n = 311	23.6±7.5 27.1 (0.8-29.3) 31.8% n = 287
+23.5 (Jun 22)	146.5±296.1 30.0 (1.0-882.7) 202.2% n = 359	26.4±7.0 30.0 (0.2-30.3) 26.7% n = 343	25.9±7.1 29.5 (0.8-30.3) 27.5% n = 323	24.9±7.4 28.5 (0.8-30.0) 29.7% n = 301	22.6±7.7 26.1 (0.2-26.1) 53.5% n = 275

Table C.4. Statistical summary showing simulated total irradiance on a horizontal surface (W m^{-2}) at ground level at the centre of a circular gap (forest height to diameter ratio = 1:1) under cloudless skies. The mean, standard deviation, median, range and coefficient of variation (cv) are given for 0°, 10°, 20°, 30°, and 40° South at solar declinations (δ) approximately equal to the 22nd day of each month.

SOLAR DECLINATION (Approximate date)	TOTAL IRRADIANCE (W m^{-2}) 0° S mean±1 SD median (range) cv	10° S mean±1 SD median (range) cv	20° S mean±1 SD median (range) cv	30° S mean±1 SD median (range) cv	40° S mean±1 SD median (range) cv
-23.5° (Dec 22)	7.9±1.9 8.8 (0.3-8.9) 24.7% n = 359	49.5±192.0 8.7 (0.2-932.9) 387.9% n = 377	149.0±337.7 8.8 (0.3-966.1) 266.6% n = 397	131.9±319.2 8.8 (0.2-959.8) 241.9% n = 417	7.8±1.9 8.7 (0.6-8.9) 24.5% n = 441
-20.0° (Jan 22/ Nov 22)	7.9±1.9 8.7 (0.3-8.9) 24.4% n = 359	109.9±292.2 8.8 (0.1-949.2) 265.7% n = 375	151.5±340.5 8.8 (0.3-968.4) 224.7% n = 391	106.4±287.5 8.8 (0.3-948.1) 270.1% n = 409	7.8±2.0 8.7 (0.3-8.9) 25.6% n = 429
-11.0° (Feb 22/ Oct 22)	104.0±284.2 8.8 (0.3-946.7) 273.3% n = 359	154.9±343.8 8.8 (0.2-968.4) 221.9% n = 367	115.1±298.6 8.8 (0.2-950.6) 259.5% n = 375	7.8±2.0 8.7 (0.1-8.9) 25.6% n = 385	7.8±2.0 8.8 (0.2-8.9) 26.3% n = 395
0.0° (Mar 21/ Sep 23)	158.2±346.7 8.8 (0.3-968.4) 219.2% n = 359	109.2±290.9 8.8 (0.3-947.4) 266.4% n = 359	7.9±1.9 8.7 (0.2-8.9) 24.6% n = 359	7.8±2.0 8.8 (0.2-8.9) 25.9% n = 359	7.6±2.1 8.7 (0.1-8.9) 27.8% n = 359
+11.0° (Apr 22/ Aug 22)	104.0±284.2 8.8 (0.3-946.7) 273.3% n = 359	7.9±1.9 8.8 (0.2-8.9) 24.7% n = 351	7.8±2.0 8.8 (0.1-8.9) 26.4% n = 343	7.7±2.1 8.7 (0.3-8.9) 27.1% n = 331	7.3±2.2 8.4 (0.2-8.9) 29.9% n = 319
+20.0° (May 22/ Jul 22)	7.9±1.9 8.7 (0.3-8.9) 24.4% n = 359	7.8±2.0 8.8 (0.2-8.9) 25.7% n = 345	7.7±2.1 8.8 (0.2-8.9) 27.2% n = 329	7.4±2.2 8.5 (0.1-8.9) 29.5% n = 311	6.9±2.2 8.0 (0.2-8.6) 31.8% n = 287
+23.5 (Jun 22)	7.9±1.9 8.9 (0.3-8.9) 24.7% n = 359	7.8±2.1 8.8 (0.1-8.9) 26.7% n = 343	7.6±2.1 8.7 (0.2-8.9) 27.5% n = 323	7.3±2.1 8.4 (0.2-8.4) 29.7% n = 301	6.4±2.2 7.7 (0.1-8.5) 33.8% n = 275

Table C.5. Statistical summary showing simulated total irradiance on a horizontal surface (W m^{-2}) at ground level at the centre of a circular gap (forest height to diameter ratio = 2:1) under cloudless skies. The mean, standard deviation, median, range and coefficient of variation (cv) are given for 0°, 10°, 20°, 30°, and 40° South at solar declinations (δ) approximately equal to the 22nd day of each month.

SOLAR DECLINATION (Approximate date)	TOTAL IRRADIANCE (W m^{-2}) 0° S mean±1 SD median (range) cv	10° S mean±1 SD median (range) cv	20° S mean±1 SD median (range) cv	30° S mean±1 SD median (range) cv	40° S mean±1 SD median (range) cv
-23.5° (Dec 22)	3.6±0.9 4.0 (0.1-4.1) 24.8% n = 359	3.6±0.9 4.0 (0.1-4.1) 24.6% n = 377	92.8±278.0 4.0 (0.1-961.4) 299.5% n = 397	74.1±249.1 4.0 (0.1-955.2) 336.3% n = 417	3.6±0.9 4.0 (0.3-4.1) 24.4% n = 441
-20.0° (Jan 22/ Nov 22)	3.6±0.9 4.0 (0.1-4.1) 24.4% n = 359	3.6±0.9 4.0 (0.2-4.1) 23.7% n = 375	104.1±293.3 4.0 (0.1-963.7) 281.7% n = 391	3.6±0.9 4.0 (0.1-4.1) 24.7% n = 409	3.6±0.9 4.0 (0.1-4.1) 25.6% n = 429
-11.0° (Feb 22/ Oct 22)	3.6±0.9 4.0 (0.1-4.1) 23.9% n = 359	104.9±294.4 4.0 (0.1-963.7) 280.5% n = 367	3.6±0.9 4.0 (0.1-4.1) 24.4% n = 375	3.6±0.9 4.0 (0.2-4.1) 24.5% n = 385	3.6±0.9 4.0 (0.1-4.1) 26.4% n = 395
0.0° (Mar 21/ Sep 23)	101.9±290.6 4.0 (0.1-963.7) 285.0% n = 359	3.6±0.9 4.0 (0.1-4.1) 23.9% n = 359	3.6±0.9 4.0 (0.1-4.1) 24.6% n = 359	3.6±0.9 4.0 (0.1-4.1) 26.1% n = 359	3.5±0.9 4.0 (0.1-4.1) 27.8% n = 359
+11.0° (Apr 22/ Aug 22)	3.6±0.9 4.0 (0.1-4.1) 23.9% n = 359	3.6±0.9 4.0 (0.1-4.1) 24.7% n = 351	3.6±0.9 4.0 (0.2-4.1) 25.3% n = 343	3.5±0.9 4.0 (0.1-4.1) 27.1% n = 331	3.4±1.0 3.9 (0.1-4.1) 29.9% n = 319
+20.0° (May 22/ Jul 22)	3.6±0.9 4.0 (0.1-4.1) 24.4% n = 359	3.6±0.9 4.0 (0.1-4.1) 25.8% n = 345	3.5±0.9 4.0 (0.1-4.1) 27.3% n = 329	3.4±1.0 3.9 (0.1-4.1) 29.6% n = 311	3.2±1.0 3.7 (0.1-4.0) 31.8% n = 287
+23.5 (Jun 22)	3.6±0.9 4.0 (0.1-4.1) 24.8% n = 359	3.6±0.9 4.1 (0.2-4.1) 25.6% n = 343	3.5±1.0 4.0 (0.1-4.1) 27.5% n = 323	3.4±1.0 3.9 (0.1-4.1) 29.7% n = 301	3.1±1.0 3.5 (0.1-3.9) 32.8% n = 275

Table C.6. Statistical summary showing simulated total irradiance on a horizontal surface (W m^{-2}) at ground level at the centre of a circular gap (forest height to diameter ratio = 3:1) under cloudless skies. The mean, standard deviation, median, range and coefficient of variation (cv) are given for 0°, 10°, 20°, 30°, and 40° South at solar declinations (δ) approximately equal to the 22nd day of each month.

SOLAR DECLINATION (Approximate date)	TOTAL IRRADIANCE (W m^{-2}) 0° S mean±1 SD median (range) cv	10° S mean±1 SD median (range) cv	20° S mean±1 SD median (range) cv	30° S mean±1 SD median (range) cv	40° S mean±1 SD median (range) cv
-23.5°	2.0±0.5	2.1±0.5	67.3±241.3	31.7±165.5	2.0±0.5
(Dec 22)	2.3	2.3	2.3	2.3	2.3
	(0.1-2.3)	(0.1-2.3)	(0.1-959.7)	(0.1-953.5)	(0.1-2.3)
	24.6%	24.5%	358.4%	522.2%	24.5%
	n = 359	*n* = 377	*n* = 397	*n* = 417	*n* = 441
-20.0°	2.1±0.5	2.1±0.5	78.3±259.4	2.1±0.5	2.0±0.5
(Jan 22/	2.3	2.3	2.3	2.3	2.3
Nov 22)	(0.1-2.3)	(0.1-2.3)	(0.1-962.0)	(0.1-2.3)	(0.1-2.3)
	24.4%	23.6%	331.4%	24.6%	25.5%
	n = 359	*n* = 375	*n* = 391	*n* = 409	*n* = 429
-11.0°	2.1±0.5	77.7±258.4	2.1±0.5	2.1±0.5	2.0±0.5
(Feb 22/	2.3	2.3	4.0	2.3	2.3
Oct 22)	(0.1-2.3)	(0.1-962.0)	(0.1-2.3)	(0.1-2.3)	(0.1-2.3)
	23.8%	332.9%	24.2%	24.4%	26.2%
	n = 359	*n* = 367	*n* = 375	*n* = 385	*n* = 395
0.0°	79.3±261.0	2.1±0.5	2.1±0.5	2.0±0.5	2.0±0.5
(Mar 21/	2.3	2.3	2.3	2.3	2.3
Sep 23)	(0.1-962.0)	(0.1-2.3)	(0.1-2.3)	(0.1-2.3)	(0.1-2.3)
	329.1%	23.9%	24.7%	24.7%	26.5%
	n = 359	*n* = 359	*n* = 359	*n* = 359	*n* = 359
+11.0°	2.1±0.5	2.1±0.5	2.0±0.5	2.0±0.5	1.9±0.6
(Apr 22/	2.3	2.3	2.3	2.3	2.2
Aug 22)	(0.1-2.3)	(0.1-2.3)	(0.2-2.3)	(0.1-2.3)	(0.1-2.2)
	23.8%	24.6%	25.0%	27.0%	28.8%
	n = 359	*n* = 351	*n* = 343	*n* = 331	*n* = 319
+20.0°	2.1±0.5	2.0±0.5	2.0±0.5	1.9±0.6	1.8±0.6
(May 22/	2.3	2.3	2.3	2.2	2.1
Jul 22)	(0.1-2.3)	(0.1-2.3)	(0.1-2.3)	(0.1-2.2)	(0.1-2.3)
	24.4%	24.5%	25.9%	28.4%	31.9%
	n = 359	*n* = 345	*n* = 329	*n* = 311	*n* = 287
+23.5	2.0±0.5	2.0±0.5	2.0±0.5	1.9±0.6	1.8±0.6
(Jun 22)	2.3	2.3	2.3	2.2	2.0
	(0.1-2.3)	(0.2-2.3)	(0.1-2.3)	(0.1-2.3)	(0.1-2.2)
	24.6%	25.3%	27.4%	29.7%	32.6%
	n = 359	*n* = 343	*n* = 323	*n* = 301	*n* = 275

Table C.7. Statistical summary showing simulated total irradiance on a horizontal surface (W m^{-2}) at ground level at the centre of a circular gap (forest height to diameter ratio = 4:1) under cloudless skies. The mean, standard deviation, median, range and coefficient of variation (cv) are given for 0°, 10°, 20°, 30°, and 40° South at solar declinations (δ) approximately equal to the 22nd day of each month.

TOTAL IRRADIANCE (W m^{-2})	SOLAR DECLINATION (Approximate date) -23.5° (Dec 22)	0.0° (Mar 21/Sep 23)	+23.5° (Jun 22)
North 10°			
mean±1 SD	628.5±358.3	639.2±352.4	516.1±277.0
median	688.9	708.7	572.9
(range)	(0.7-1078.7)	(0.3-1071.5)	(3.9-850.1)
cv	57.0%	55.1%	53.7%
	n = 397	n = 361	n = 323
North 30°			
mean±1 SD	526.3±316.6	630.9±350.7	587.9±312.7
median	566.5	699.3	659.5
(range)	(0.6-937.6)	(0.3-960.5)	(3.6-957.0)
cv	60.2%	54.1%	53.2%
	n = 397	n = 361	n = 323
South 10°			
mean±1 SD	663.2±358.3	578.4±313.1	389.7±209.9
median	737.3	641.7	426.1
(range)	(0.6-994.9)	(0.3-960.5)	(3.9-649.7)
cv	54.0%	54.1%	53.9%
	n = 397	n = 361	n = 323
South 30°			
mean±1 SD	626.0±317.4	455.8±237.7	226.6±116.9
median	705.9	506.5	236.8
(range)	(0.6-994.9)	(0.3-742.6)	(3.6-380.1)
cv	50.7%	52.1%	51.6%
	n = 397	n = 361	n = 323
East/West 10°			
mean±1 SD	645.9±364.9	608.9±339.9	453.0±248.4
median	712.3	672.3	498.9
(range)	(0.7-1099.3)	(0.3-1027.2)	(3.9-758.2)
cv	56.5%	55.8%	54.8%
	n = 397	n = 361	n = 323
East/West 30°			
mean±1 SD	583.2±365.9	552.0±345.0	412.5±250.9
median	629.3	597.3	440.3
(range)	(0.6-1058.3)	(0.3-998.0)	(3.6-739.2)
cv	62.7%	62.5%	60.8%
	n = 397	n = 361	n = 323

Table C.8. Statistical summary showing simulated total irradiance (W m^{-2}) above the forest (forest height to diameter ratio = 0:0) at 20° South under cloudless skies. The mean, standard deviation, median, range and coefficient of variation (cv) are given for six slope inclinations at the solstices (June 22, δ = +23.5°; December 22, δ = -23.5°) and equinoxes (March 21/September 23, δ = 0.0°). Refer to Table C.1 for comparison with a horizontal surface at 20° S.

TOTAL IRRADIANCE (W m^{-2})	SOLAR DECLINATION (Approximate date) -23.5° (Dec 22)	0.0° (Mar 21/Sep 23)	+23.5° (Jun 22)
North 10°			
mean±1 SD	569.6±387.1	587.4±376.5	466.7±296.9
median	658.8	678.7	543.6
(range)	(0.7-1078.7)	(0.3-1042.0)	(3.1-820.0)
cv	68.0%	64.1%	63.6%
	n = 397	n = 361	n = 323
North 30°			
mean±1 SD	455.8±348.2	579.3±376.6	556.8±317.0
median	538.2	671.1	631.9
(range)	(0.5-910.1)	(0.2-1034.5)	(2.9-928.8)
cv	76.4%	65.0%	56.9%
	n = 397	n = 361	n = 323
South 10°			
mean±1 SD	613.3±381.8	516.4±344.3	297.5±237.8
median	707.2	611.7	117.3
(range)	(0.5-1069.5)	(0.3-931.1)	(3.1-619.7)
cv	62.3%	66.7%	79.9%
	n = 397	n = 361	n = 323
South 30°			
mean±1 SD	584.3±335.4	364.7±278.2	96.7±26.6
median	677.7	478.3	110.3
(range)	(0.5-967.5)	(0.2-714.9)	(2.9-113.0)
cv	57.4%	76.3%	27.5%
	n = 397	n = 361	n = 323
East/West 10°			
mean±1 SD	593.1±388.7	555.2±363.4	389.9±272.8
median	682.4	642.5	470.3
(range)	(0.5-1070.1)	(0.3-997.7)	(3.1-728.1)
cv	65.5%	65.4%	70.0%
	n = 397	n = 361	n = 323
East/West 30°			
mean±1 SD	529.8±385.0	498.3±363.2	352.7±265.3
median	601.4	571.0	312.0
(range)	(0.5-1030.6)	(0.2-970.0)	(2.9-711.0)
cv	72.7%	72.9%	75.3%
	n = 397	n = 361	n = 323

Table C.9. Statistical summary showing simulated total irradiance (W m^{-2}) at ground level at the centre of a circular gap (forest height to diameter ratio = 1:4) at 20° South under cloudless skies. The mean, standard deviation, median, range and coefficient of variation (cv) are given for six slope inclinations at the solstices (June 22, δ = +23.5°; December 22, δ = -23.5°) and equinoxes (March 21/September 23, δ = 0.0°). Refer to Table C.2 for comparison with a horizontal surface at 20° S.

TOTAL IRRADIANCE ($W\ m^{-2}$)	SOLAR DECLINATION (Approximate date) -23.5° (Dec 22)	0.0° (Mar 21/Sep 23)	+23.5° (Jun 22)
North 10°			
mean±1 SD	438.9±420.8	459.6±416.9	309.9±323.9
median	75.1	75.0	73.3
(range)	(0.3-1005.8)	(0.2-997.9)	(1.9-775.0)
cv	95.9%	90.7%	104.5%
	n = 397	n = 361	n = 323
North 30°			
mean±1 SD	293.9±352.3	455.4±416.2	448.2±364.5
median	70.3	70.5	590.6
(range)	(0.3-869.0)	(0.2-993.0)	(1.8-886.4)
cv	119.9%	91.4%	81.3%
	n = 397	n = 361	n = 323
South 10°			
mean±1 SD	482.9±428.1	356.8±372.4	64.3±17.7
median	662.2	75.0	73.3
(range)	(0.3-1025.7)	(0.2-886.9)	(1.9-75.1)
cv	88.6%	104.4%	27.5%
	n = 397	n = 361	n = 323
South 30°			
mean±1 SD	424.0±394.9	62.1±15.8	60.4±16.6
median	70.6	69.4	68.9
(range)	(0.3-926.3)	(0.2-70.6)	(1.8-70.6)
cv	93.1%	25.5%	27.5%
	n = 397	n = 361	n = 323
East/West 10°			
mean±1 SD	467.7±427.3	420.2±399.6	162.1±226.7
median	75.1	75.1	73.3
(range)	(0.3-1026.3)	(0.2-953.4)	(1.9-683.1)
cv	91.4%	95.1%	139.8%
	n = 397	n = 361	n = 323
East/West 30°			
mean±1 SD	428.4±404.1	394.8±378.1	194.1±242.6
median	70.6	70.6	70.2
(range)	(0.3-988.9)	(0.2-928.1)	(1.8-668.6)
cv	94.3%	95.8%	125.0%
	n = 397	n = 361	n = 323

Table C.10. Statistical summary showing simulated total irradiance ($W\ m^{-2}$) at ground level at the centre of a circular gap (forest height to diameter ratio = 1:2) at 20° South under cloudless skies. The mean, standard deviation, median, range and coefficient of variation (cv) are given for six slope inclinations at the solstices (June 22, δ = +23.5°; December 22, δ = -23.5°) and equinoxes (March 21/September 23, δ = 0.0°). Refer to Table C.3 for comparison with a horizontal surface at 20° S.

TOTAL IRRADIANCE (W m^{-2})	SOLAR DECLINATION (Approximate date)		
	-23.5° (Dec 22)	0.0° (Mar 21/Sep 23)	+23.5° (Jun 22)
North 10°			
mean±1 SD	246.0±388.7	269.1±397.8	25.7±7.1
median	29.8	29.9	29.3
(range)	(0.1-962.1)	(0.1-953.7)	(0.8-30.0)
cv	157.9%	147.8%	27.5%
	n = 397	n = 361	n = 323
North 30°			
mean±1 SD	24.8±6.2	267.4±397.5	258.2±360.9
median	27.5	28.1	27.6
(range)	(0.1-28.2)	(0.1-951.4)	(0.7-844.1)
cv	25.2%	148.6%	27.6%
	n = 397	n = 361	n = 323
South 10°			
mean±1 SD	289.8±415.4	26.4±6.7	25.7±7.1
median	29.9	29.5	29.3
(range)	(0.1-982.0)	(0.1-30.0)	(0.8-30.0)
cv	143.3%	25.5%	27.5%
	n = 397	n = 361	n = 323
South 30°			
mean±1 SD	24.8±6.2	24.8±6.3	24.2±6.7
median	27.5	27.7	27.6
(range)	(0.1-28.2)	(0.1-28.2)	(0.7-28.2)
cv	25.2%	25.5%	27.5%
	n = 397	n = 361	n = 323
East/West 10°			
mean±1 SD	284.5±412.2	199.8±346.7	25.7±7.1
median	29.8	29.7	29.3
(range)	(0.1-982.5)	(0.1-909.2)	(0.8-30.0)
cv	144.9%	173.5%	27.5%
	n = 397	n = 361	n = 323
East/West 30°			
mean±1 SD	264.1±388.4	210.7±343.6	24.2±6.7
median	27.7	27.7	27.6
(range)	(0.1-947.3)	(0.1-886.1)	(0.7-28.2)
cv	147.0%	163.0%	27.5%
	n = 397	n = 361	n = 323

Table C.11. Statistical summary showing simulated total irradiance (W m^{-2}) at ground level at the centre of a circular gap (forest height to diameter ratio = 1:1) at 20° South under cloudless skies. The mean, standard deviation, median, range and coefficient of variation (cv) are given for six slope inclinations at the solstices (June 22, δ = +23.5°; December 22, δ = -23.5°) and equinoxes (March 21/September 23, δ = 0.0°). Refer to Table C.4 for comparison with a horizontal surface at 20° S.

TOTAL IRRADIANCE (W m^{-2})	SOLAR DECLINATION (Approximate date) -23.5° (Dec 22)	0.0° (Mar 21/Sep 23)	+23.5° (Jun 22)
North 10°			
mean±1 SD	47.7±189.1	106.9±285.7	7.6±2.1
median	8.6	8.7	8.6
(range)	(0.0-941.5)	(0.0-932.9)	(0.2-8.8)
cv	396.7%	267.2%	27.5%
	n = 397	n = 361	n = 323
North 30°			
mean±1 SD	7.3±1.8	106.4±285.5	50.0±182.5
median	8.1	8.2	8.1
(range)	(0.0-8.3)	(0.0-931.9)	(0.2-824.1)
cv	25.2%	268.3%	365.1%
	n = 397	n = 361	n = 323
South 10°			
mean±1 SD	138.4±326.4	7.8±2.0	7.6±2.1
median	8.7	8.7	8.6
(range)	(0.0-961.4)	(0.0-8.8)	(0.2-8.8)
cv	235.9%	25.6%	27.5%
	n = 397	n = 361	n = 323
South 30°			
mean±1 SD	7.3±1.8	7.3±1.9	7.1±2.0
median	8.1	8.2	8.1
(range)	(0.0-8.3)	(0.0-8.3)	(0.2-8.3)
cv	25.2%	25.5%	27.6%
	n = 397	n = 361	n = 323
East/West 10°			
mean±1 SD	145.1±332.7	7.8±2.0	7.6±2.1
median	8.7	25.6	8.6
(range)	(0.0-961.9)	(0.0-8.8)	(0.2-8.8)
cv	229.4%	25.6%	27.5%
	n = 397	n = 361	n = 323
East/West 30°			
mean±1 SD	128.7±306.9	7.3±1.9	7.1±2.0
median	8.1	8.2	8.1
(range)	(0.0-927.8)	(0.0-8.3)	(0.2-8.3)
cv	238.4%	25.5%	27.6%
	n = 397	n = 361	n = 323

Table C.12. Statistical summary showing simulated total irradiance (W m^{-2}) at ground level at the centre of a circular gap (forest height to diameter ratio = 2:1) at 20° South under cloudless skies. The mean, standard deviation, median, range and coefficient of variation (cv) are given for six slope inclinations at the solstices (June 22, δ = +23.5°; December 22, δ = -23.5°) and equinoxes (March 21/September 23, δ = 0.0°). Refer to Table C.5 for comparison with a horizontal surface at 20° S.

TOTAL IRRADIANCE (W m^{-2})	SOLAR DECLINATION (Approximate date) -23.5° (Dec 22)	0.0° (Mar 21/Sep 23)	+23.5° (Jun 22)
North 10°			
mean±1 SD	3.5±1.0	3.6±1.0	3.5±1.0
median	4.0	4.0	4.0
(range)	(0.0-4.1)	(0.0-4.1)	(0.1-4.1)
cv	25.3%	25.5%	27.6%
	n = 397	n = 361	n = 323
North 30°			
mean±1 SD	3.4±0.8	3.4±0.9	3.3±0.9
median	3.7	3.7	3.7
(range)	(0.0-3.8)	(0.0-3.8)	(0.1-3.8)
cv	25.2%	25.5%	27.4%
	n = 397	n = 361	n = 323
South 10°			
mean±1 SD	77.7±255.2	3.6±1.0	3.5±1.0
median	4.0	4.0	4.0
(range)	(0.0-956.8)	(0.0-4.1)	(0.1-4.1)
cv	328.4%	25.5%	27.6%
	n = 397	n = 361	n = 323
South 30°			
mean±1 SD	3.4±0.8	3.4±0.9	3.3±0.9
median	3.7	3.7	3.7
(range)	(0.0-3.8)	(0.0-3.8)	(0.1-3.8)
cv	25.2%	25.5%	27.4%
	n = 397	n = 361	n = 323
East/West 10°			
mean±1 SD	91.8±275.8	3.6±0.9	3.5±1.0
median	4.0	4.0	4.0
(range)	(0.0-957.3)	(0.0-4.1)	(0.1-4.1)
cv	300.3%	25.5%	27.6%
	n = 397	n = 361	n = 323
East/West 30°			
mean±1 SD	73.7±242.3	3.4±0.9	3.3±0.9
median	3.7	3.7	3.7
(range)	(0.0-923.1)	(0.0-3.8)	(0.1-3.8)
cv	328.6%	25.5%	27.4%
	n = 397	n = 361	n = 323

Table C.13. Statistical summary showing simulated total irradiance (W m^{-2}) at ground level at the centre of a circular gap (forest height to diameter ratio = 3:1) at 20° South under cloudless skies. The mean, standard deviation, median, range and coefficient of variation (cv) are given for six slope inclinations at the solstices (June 22, δ = +23.5°; December 22, δ = -23.5°) and equinoxes (March 21/September 23, δ = 0.0°). Refer to Table C.6 for comparison with a horizontal surface at 20° S.

TOTAL IRRADIANCE (W m^{-2})	SOLAR DECLINATION (Approximate date) -23.5° (Dec 22)	0.0° (Mar 21/Sep 23)	+23.5° (Jun 22)
North 10°			
mean±1 SD	2.0±0.5	2.0±0.5	2.0±0.5
median	2.3	2.3	2.3
(range)	(0.0-2.3)	(0.0-2.3)	(0.1-2.3)
cv	25.2%	25.6%	27.5%
	n = 397	n = 361	n = 323
North 30°			
mean±1 SD	1.9±0.5	1.9±0.5	1.9±0.5
median	2.1	2.1	2.1
(range)	(0.0-2.2)	(0.0-2.2)	(0.1-2.2)
cv	25.3%	25.5%	27.6%
	n = 397	n = 361	n = 323
South 10°			
mean±1 SD	33.2±169.7	2.0±0.5	2.0±0.5
median	2.3	2.3	2.3
(range)	(0.0-955.1)	(0.0-2.3)	(0.1-2.3)
cv	510.9%	25.6%	27.5%
	n = 397	n = 361	n = 323
South 30°			
mean±1 SD	1.9±0.5	1.9±0.5	1.9±0.5
median	2.1	2.1	2.1
(range)	(0.0-2.2)	(0.0-2.2)	(0.1-2.2)
cv	25.3%	25.5%	27.6%
	n = 397	n = 361	n = 323
East/West 10°			
mean±1 SD	64.2±235.2	2.0±0.5	2.0±0.5
median	2.3	2.3	2.3
(range)	(0.0-955.6)	(0.0-2.3)	(0.1-2.3)
cv	366.3%	25.6%	27.5%
	n = 397	n = 361	n = 323
East/West 30°			
mean±1 SD	36.1±172.7	1.9±0.5	1.9±0.5
median	2.1	2.1	2.1
(range)	(0.0-916.6)	(0.0-2.2)	(0.1-2.2)
cv	478.7%	25.5%	27.6%
	n = 397	n = 361	n = 323

Table C.14. Statistical summary showing simulated total irradiance (W m^{-2}) at ground level at the centre of a circular gap (forest height to diameter ratio = 4:1) at 20° South under cloudless skies. The mean, standard deviation, median, range and coefficient of variation (cv) are given for six slope inclinations at the solstices (June 22, δ = +23.5°; December 22, δ = -23.5°) and equinoxes (March 21/September 23, δ = 0.0°). Refer to Table C.7 for comparison with a horizontal surface at 20° S.

TOTAL IRRADIANCE ($W\ m^{-2}$)	SOLAR DECLINATION (Approximate date) -23.5° (Dec 22)	0.0° (Mar 21/Sep 23)	+23.5° (Jun 22)
North 10°			
mean±1 SD	621.0±361.9	528.4±296.8	305.1±167.9
median	672.2	583.2	337.0
(range)	(9.6-1085.6)	(0.6-896.5)	(1.1-510.1)
cv	58.3%	56.2%	55.0%
	n = 441	n = 361	n = 275
North 30°			
mean±1 SD	576.1±361.5	575.2±331.5	384.9±218.2
median	609.6	633.7	429.2
(range)	(0.0-1057.2)	(0.6-989.4)	(1.0-649.0)
cv	62.7%	57.6%	56.7%
	n = 441	n = 361	n = 275
South 10°			
mean±1 SD	599.6±320.5	425.7±228.2	195.4±99.5
median	662.8	471.3	212.1
(range)	(9.6-992.0)	(0.6-704.6)	(1.1-318.4)
cv	53.5%	53.6%	50.9%
	n = 441	n = 361	n = 275
South 30°			
mean±1 SD	513.8±243.9	279.5±134.2	105.5±35.7
median	582.7	311.6	122.0
(range)	(0.9-787.6)	(0.6-436.8)	(1.0-134.1)
cv	47.5%	48.0%	33.8%
	n = 441	n = 361	n = 275
East/West 10°			
mean±1 SD	610.4±348.5	477.2±269.2	250.3±136.4
median	663.5	526.1	274.5
(range)	(9.6-1051.5)	(0.6-812.2)	(1.1-420.0)
cv	57.1%	56.4%	54.5%
	n = 441	n = 361	n = 275
East/West 30°			
mean±1 SD	553.1±355.8	425.7±228.2	231.8±138.1
median	580.1	471.3	236.8
(range)	(9.0-1028.9)	(0.6-704.6)	(1.0-419.7)
cv	64.3%	53.6%	59.6%
	n = 441	n = 361	n = 275

Table C.15. Statistical summary showing simulated total irradiance ($W\ m^{-2}$) above the forest (forest height to diameter ratio = 0:0) at 40° South under cloudless skies. The mean, standard deviation, median, range and coefficient of variation (cv) are given for six slope inclinations at the solstices (June 22, δ = +23.5°; December 22, δ = -23.5°) and equinoxes (March 21/September 23, δ = 0.0°). Refer to Table C.1 for comparison with a horizontal surface at 40° S.

TOTAL IRRADIANCE (W m^{-2})	SOLAR DECLINATION (Approximate date) -23.5° (Dec 22)	0.0° (Mar 21/Sep 23)	+23.5° (Jun 22)
North 10°			
mean±1 SD	563.3±389.2	474.3±319.5	250.2±182.0
median	642.2	553.7	311.1
(range)	(7.6-1056.3)	(0.5-866.5)	(0.9-481.6)
cv	69.1%	67.4%	72.6%
	n = 441	n = 361	n = 275
North 30°			
mean±1 SD	515.7±388.4	531.3±348.4	361.4±214.9
median	581.4	606.0	404.8
(range)	(7.2-1029.6)	(0.5-961.2)	(0.8-622.2)
cv	75.3%	65.6%	59.5%
	n = 441	n = 361	n = 275
South 10°			
mean±1 SD	545.0±347.4	344.2±259.4	83.7±30.4
median	632.9	441.8	103.8
(range)	(7.6-962.6)	(0.5-674.6)	(0.9-114.1)
cv	63.7%	75.4%	33.8%
	n = 441	n = 361	n = 275
South 30°			
mean±1 SD	456.9±275.4	96.8±27.2	84.4±28.5
median	554.5	111.0	97.6
(range)	(7.2-760.0)	(0.5-113.0)	(0.8-107.3)
cv	60.3%	28.1%	33.8%
	n = 441	n = 361	n = 275
East/West 10°			
mean±1 SD	555.3±373.1	416.8±292.1	129.9±109.6
median	633.8	496.2	103.8
(range)	(7.6-1022.1)	(0.5-782.2)	(0.9-391.6)
cv	67.2%	70.1%	84.4%
	n = 441	n = 361	n = 275
East/West 30°			
mean±1 SD	499.3±373.6	344.2±259.4	163.2±126.4
median	554.0	441.8	106.3
(range)	(7.2-1001.0)	(0.5-674.6)	(0.8-393.4)
cv	74.8%	75.4%	77.4%
	n = 441	n = 361	n = 275

Table C.16. Statistical summary showing simulated total irradiance (W m^{-2}) at ground level at the centre of a circular gap (forest height to diameter ratio = 1:4) at 40° South under cloudless skies. The mean, standard deviation, median, range and coefficient of variation (cv) are given for six slope inclinations at the solstices (June 22, δ = +23.5°; December 22, δ = -23.5°) and equinoxes (March 21/September 23, δ = 0.0°). Refer to Table C.2 for comparison with a horizontal surface at 40° S.

TOTAL IRRADIANCE (W m^{-2})	SOLAR DECLINATION (Approximate date) -23.5° (Dec 22)	0.0° (Mar 21/Sep 23)	+23.5° (Jun 22)
North 10°			
mean±1 SD	438.0±420.9	329.7±342.9	56.1±19.0
median	75.0	73.8	64.9
(range)	(4.8-1012.2)	(0.3-821.5)	(0.5-71.3)
cv	96.1%	90.7%	33.8%
	n = 441	n = 361	n = 275
North 30°			
mean±1 SD	394.3±409.9	418.6±382.6	257.8±242.9
median	70.5	69.3	61.0
(range)	(4.5-988.2)	(0.3-918.9)	(0.5-582.0)
cv	103.9%	91.0%	94.2%
	n = 441	n = 361	n = 275
South 10°			
mean±1 SD	388.7±386.8	64.3±18.1	56.1±18.9
median	75.0	73.8	64.9
(range)	(4.8-918.6)	(0.3-75.1)	(0.5-71.3)
cv	99.5%	28.1%	33.8%
	n = 441	n = 361	n = 275
South 30°			
mean±1 SD	62.0±15.2	60.5±17.0	52.7±17.8
median	69.2	69.3	61.0
(range)	(4.5-70.6)	(0.3-70.6)	(0.5-67.0)
cv	24.5%	25.5%	33.8%
	n = 441	n = 361	n = 275
East/West 10°			
mean±1 SD	425.5±407.1	233.6±287.1	56.1±19.0
median	75.0	73.8	64.9
(range)	(4.8-978.0)	(0.3-737.1)	(0.5-71.3)
cv	95.7%	122.9%	33.8%
	n = 441	n = 361	n = 275
East/West 30°			
mean±1 SD	397.3±388.9	394.8±378.1	52.7±17.8
median	70.5	70.6	33.8
(range)	(4.5-959.1)	(0.2-928.1)	(0.5-67.0)
cv	97.9%	95.8%	33.8%
	n = 441	n = 361	n = 275

Table C.17. Statistical summary showing simulated total irradiance (W m^{-2}) at ground level at the centre of a circular gap (forest height to diameter ratio = 1:2) at 40° South under cloudless skies. The mean, standard deviation, median, range and coefficient of variation (cv) are given for six slope inclinations at the solstices (June 22, δ = +23.5°; December 22, δ = -23.5°) and equinoxes (March 21/September 23, δ = 0.0°). Refer to Table C.3 for comparison with a horizontal surface at 40° S.

TOTAL IRRADIANCE (W m^{-2})	SOLAR DECLINATION (Approximate date) -23.5° (Dec 22)	0.0° (Mar 21/Sep 23)	+23.5° (Jun 22)
North 10°			
mean±1 SD	260.4±396.7	25.7±7.2	22.4±7.6
median	29.8	29.5	25.9
(range)	(1.9-968.2)	(0.1-30.0)	(0.2-28.5)
cv	152.4%	28.1%	33.8%
	n = 441	n = 361	n = 275
North 30°			
mean±1 SD	219.8±369.5	246.4±364.9	21.1±7.1
median	28.0	27.7	24.4
(range)	(1.8-946.8)	(0.1-876.6)	(0.2-26.8)
cv	168.1%	148.1%	50.9%
	n = 441	n = 361	n = 275
South 10°			
mean±1 SD	26.4±6.5	25.7±7.2	22.4±7.6
median	29.4	29.5	25.9
(range)	(1.9-30.0)	(0.1-30.0)	(0.2-28.5)
cv	24.5%	28.1%	33.8%
	n = 441	n = 361	n = 275
South 30°			
mean±1 SD	24.8±6.1	24.2±6.8	21.1±7.1
median	27.7	27.7	24.4
(range)	(1.8-28.2)	(0.1-28.2)	(0.2-26.8)
cv	24.5%	28.1%	33.8%
	n = 441	n = 361	n = 275
East/West 10°			
mean±1 SD	226.3±369.2	25.7±7.2	22.4±7.6
median	29.7	29.5	25.9
(range)	(1.9-933.9)	(0.1-30.0)	(0.2-28.5)
cv	163.2%	28.1%	33.8%
	n = 441	n = 361	n = 275
East/West 30°			
mean±1 SD	233.5±363.7	25.7±7.2	21.1±7.1
median	27.7	29.5	24.4
(range)	(1.8-917.3)	(0.1-30.0)	(0.2-26.8)
cv	155.8%	28.1%	33.8%
	n = 441	n = 361	n = 275

Table C.18. Statistical summary showing simulated total irradiance (W m^{-2}) at ground level at the centre of a circular gap (forest height to diameter ratio = 1:1) at 40° South under cloudless skies. The mean, standard deviation, median, range and coefficient of variation (cv) are given for six slope inclinations at the solstices (June 22, δ = +23.5°; December 22, δ = -23.5°) and equinoxes (March 21/September 23, δ = 0.0°). Refer to Table C.4 for comparison with a horizontal surface at 40° S.

TOTAL IRRADIANCE (W m^{-2})	SOLAR DECLINATION (Approximate date) -23.5° (Dec 22)	0.0° (Mar 21/Sep 23)	+23.5° (Jun 22)
North 10°			
mean±1 SD	123.6±307.7	7.6±2.1	6.6±2.2
median	8.7	8.7	7.6
(range)	(0.6-947.4)	(0.3-8.8)	(0.1-8.4)
cv	396.7%	27.0%	33.9%
	n = 441	n = 361	n = 275
North 30°			
mean±1 SD	42.7±177.1	98.7±262.9	6.2±2.1
median	8.2	8.2	7.2
(range)	(0.5-927.3)	(0.3-856.7)	(0.1-7.9)
cv	414.9%	266.5%	33.8%
	n = 441	n = 361	n = 275
South 10°			
mean±1 SD	7.8±1.9	7.6±2.1	6.6±2.2
median	8.7	8.7	7.6
(range)	(0.6-8.8)	(0.3-8.8)	(0.1-8.4)
cv	24.5%	27.0%	33.9%
	n = 441	n = 361	n = 275
South 30°			
mean±1 SD	7.3±1.8	7.2±1.9	6.2±2.1
median	8.1	8.2	7.2
(range)	(0.0-8.3)	(0.3-8.3)	(0.1-7.9)
cv	24.6%	27.0%	33.8%
	n = 441	n = 361	n = 275
East/West 10°			
mean±1 SD	7.8±1.9	7.6±2.1	6.6±2.2
median	8.7	8.7	7.6
(range)	(0.6-8.8)	(0.3-8.8)	(0.1-8.4)
cv	24.5%	27.0%	33.9%
	n = 441	n = 361	n = 275
East/West 30°			
mean±1 SD	91.6±257.3	7.6±2.1	6.2±2.1
median	8.1	8.7	7.2
(range)	(0.5-897.6)	(0.3-8.8)	(0.1-7.9)
cv	280.8%	27.0%	33.8%
	n = 441	n = 361	n = 275

Table C.19. Statistical summary showing simulated total irradiance (W m^{-2}) at ground level at the centre of a circular gap (forest height to diameter ratio = 2:1) at 40° South under cloudless skies. The mean, standard deviation, median, range and coefficient of variation (cv) are given for six slope inclinations at the solstices (June 22, δ = +23.5°; December 22, δ = -23.5°) and equinoxes (March 21/September 23, δ = 0.0°). Refer to Table C.5 for comparison with a horizontal surface at 40° S.

TOTAL IRRADIANCE (W m^{-2})	SOLAR DECLINATION (Approximate date) -23.5° (Dec 22)	0.0° (Mar 21/Sep 23)	+23.5° (Jun 22)
North 10°			
mean±1 SD	69.3±239.6	3.5±1.0	3.1±1.0
median	4.0	4.0	3.5
(range)	(0.3-942.8)	(0.0-4.1)	(0.1-3.9)
cv	345.5%	27.2%	32.6%
	n = 441	n = 361	n = 275
North 30°			
mean±1 SD	3.3±0.8	3.3±0.9	2.9±0.9
median	3.7	3.7	3.3
(range)	(0.2-3.8)	(0.1-3.8)	(0.1-3.6)
cv	24.6%	27.0%	32.6%
	n = 441	n = 361	n = 275
South 10°			
mean±1 SD	3.6±0.9	3.5±1.0	3.1±1.0
median	4.0	4.0	3.5
(range)	(0.3-4.1)	(0.1-4.1)	(0.1-3.9)
cv	24.5%	27.2%	32.6%
	n = 441	n = 361	n = 275
South 30°			
mean±1 SD	3.3±0.8	3.3±0.9	2.9±0.9
median	3.7	3.7	3.3
(range)	(0.0-3.8)	(0.1-3.8)	(0.1-3.6)
cv	24.6%	27.0%	32.6%
	n = 441	n = 361	n = 275
East/West 10°			
mean±1 SD	3.6±0.9	3.5±0.9	3.0±1.0
median	4.0	4.0	3.5
(range)	(0.3-4.1)	(0.0-4.1)	(0.1-3.9)
cv	24.5%	27.2%	32.6%
	n = 441	n = 361	n = 275
East/West 30°			
mean±1 SD	3.3±0.8	3.5±0.9	2.9±0.9
median	3.7	4.0	3.3
(range)	(0.2-3.8)	(0.1-4.1)	(0.1-3.6)
cv	24.6%	27.2%	32.6%
	n = 441	n = 361	n = 275

Table C.20. Statistical summary showing simulated total irradiance (W m^{-2}) at ground level at the centre of a circular gap (forest height to diameter ratio = 3:1) at 40° South under cloudless skies. The mean, standard deviation, median, range and coefficient of variation (cv) are given for six slope inclinations at the solstices (June 22, δ = +23.5°; December 22, δ = -23.5°) and equinoxes (March 21/September 23, δ = 0.0°). Refer to Table C.6 for comparison with a horizontal surface at 40° S.

TOTAL IRRADIANCE (W m^{-2})	SOLAR DECLINATION (Approximate date) -23.5° (Dec 22)	0.0° (Mar 21/Sep 23)	+23.5° (Jun 22)
North 10°			
mean±1 SD	29.7±158.9	2.0±0.5	1.7±0.6
median	2.3	2.3	2.0
(range)	(0.1-941.1)	(0.0-2.3)	(0.1-2.2)
cv	535.2%	27.1%	32.7%
	n = 441	n = 361	n = 275
North 30°			
mean±1 SD	1.9±0.5	1.9±0.5	1.6±0.5
median	2.1	2.1	1.9
(range)	(0.0-2.2)	(0.0-2.2)	(0.1-2.1)
cv	24.6%	27.3%	32.7%
	n = 441	n = 361	n = 275
South 10°			
mean±1 SD	2.0±0.5	2.0±0.5	1.7±0.6
median	2.3	2.1	2.0
(range)	(0.1-2.3)	(0.1-2.2)	(0.0-2.2)
cv	24.6%	27.3%	33.3%
	n = 441	n = 361	n = 275
South 30°			
mean±1 SD	1.9±0.5	1.9±0.5	1.6±0.5
median	2.1	2.1	1.9
(range)	(0.1-2.2)	(0.0-2.2)	(0.1-2.1)
cv	24.6%	25.5%	32.7%
	n = 441	n = 361	n = 275
East/West 10°			
mean±1 SD	2.0±0.5	2.0±0.5	1.7±0.6
median	2.3	2.3	2.0
(range)	(0.1-2.3)	(0.1-2.3)	(0.1-2.2)
	24.6%	27.1%	32.7%
	n = 441	n = 361	n = 275
East/West 30°			
mean±1 SD	1.9±0.5	1.9±0.5	1.6±0.5
median	2.1	2.3	1.9
(range)	(0.1-2.2)	(0.1-2.3)	(0.1-2.1)
cv	24.6%	27.1%	32.7%
	n = 441	n = 361	n = 275

Table C.21. Statistical summary showing simulated total irradiance (W m^{-2}) at ground level at the centre of a circular gap (forest height to diameter ratio = 4:1) at 40° South under cloudless skies. The mean, standard deviation, median, range and coefficient of variation (cv) are given for six slope inclinations at the solstices (June 22, δ = +23.5°; December 22, δ = -23.5°) and equinoxes (March 21/September 23, δ = 0.0°). Refer to Table C.7 for comparison with a horizontal surface at 40° S.

TOTAL IRRADIANCE (W m^{-2})	SOLAR DECLINATION (Approximate date) -23.5° (Dec 22)	0.0° (Mar 21/Sep 23)	+23.5° (Jun 22)
Cirrostratus			
mean±1 SD	588.0±288.7	544.6±261.2	403.9±188.1
median	635.0	598.3	450.3
(range)	(6.2-972.1)	(0.4-861.0)	(0.3-620.3)
cv	49.1%	47.9%	46.6%
	n = 397	n = 361	n = 323
Altostratus			
mean±1 SD	287.9±137.9	270.2±125.6	203.3±93.7
median	314.5	299.9	227.2
(range)	(0.3-463.5)	(3.9-419.0)	(0.4-310.2)
cv	47.9%	46.5%	46.1%
	n = 397	n = 361	n = 323
Stratus			
mean±1 SD	170.6±83.4	159.3±75.2	119.2±55.2
median	185.3	174.9	135.5
(range)	(2.0-280.8)	(2.3-250.1)	(0.6-182.7)
cv	48.9%	47.2%	46.2%
	n = 397	n = 361	n = 323

Table C.22. Statistical summary showing simulated total irradiance (W m^{-2}) above the forest (forest height to diameter ratio = 0:0) at 20° South under cloudy skies. The mean, standard deviation, median, range and coefficient of variation (cv) are given for three cloud types at the solstices (June 22, δ = +23.5°; December 22, δ = -23.5°) and equinoxes (March 21/September 23, δ = 0.0°). Refer to Table C.1 for comparison with a cloudless sky at 20° S.

TOTAL IRRADIANCE (W m^{-2})	SOLAR DECLINATION (Approximate date) -23.5° (Dec 22)	0.0° (Mar 21/Sep 23)	+23.5° (Jun 22)
Cirrostratus			
mean±1 SD	529.2±282.9	485.7±253.6	347.9±182.1
median	575.0	539.9	399.4
(range)	(5.0-915.2)	(0.3-796.0)	(0.2-560.9)
cv	53.5%	52.2%	52.3%
	n = 397	n = 361	n = 323
Altostratus			
mean±1 SD	230.3±110.4	216.2±100.5	162.7±74.9
median	251.6	239.9	181.7
(range)	(2.4-370.8)	(3.1-335.2)	(0.3-248.2)
cv	47.9%	46.5%	46.1%
	n = 397	n = 361	n = 323
Stratus			
mean±1 SD	136.4±66.7	127.4±60.1	93.4±44.2
median	148.2	139.9	106.8
(range)	(1.6-224.7)	(1.9-200.1)	(0.5-146.1)
cv	48.9%	47.2%	46.3%
	n = 397	n = 361	n = 323

Table C.23. Statistical summary showing simulated total irradiance (W m^{-2}) at ground level at the centre of a circular gap (forest height to diameter ratio = 1:4) at 20° South under cloudy skies. The mean, standard deviation, median, range and coefficient of variation (cv) are given for three cloud types at the solstices (June 22, δ = +23.5°; December 22, δ = -23.5°) and equinoxes (March 21/September 23, δ = 0.0°). Refer to Table C.2 for comparison with a cloudless sky at 20° S.

TOTAL IRRADIANCE (W m^{-2})	SOLAR DECLINATION (Approximate date) -23.5° (Dec 22)	0.0° (Mar 21/Sep 23)	+23.5° (Jun 22)
Cirrostratus			
mean±1 SD	403.7±294.2	354.2±260.5	166.7±136.1
median	484.8	146.0	127.2
(range)	(3.1-829.8)	(0.2-698.5)	(0.2-471.7)
cv	72.9%	73.5%	81.6%
	n = 397	*n* = 361	*n* = 323
Altostratus			
mean±1 SD	143.9±68.9	135.1±62.8	101.7±46.9
median	157.3	149.9	113.6
(range)	(1.5-231.8)	(2.0-209.5)	(0.2-155.1)
cv	47.9%	46.5%	46.1%
	n = 397	*n* = 361	*n* = 323
Stratus			
mean±1 SD	85.3±41.7	79.6±37.6	59.6±27.6
median	92.6	87.5	66.7
(range)	(1.0-140.4)	(1.2-125.0)	(0.3-91.3)
cv	48.9%	47.2%	46.3%
	n = 397	*n* = 361	*n* = 323

Table C.24. Statistical summary showing simulated total irradiance (W m^{-2}) at ground level at the centre of a circular gap (forest height to diameter ratio = 1:2) at 20° South under cloudy skies. The mean, standard deviation, median, range and coefficient of variation (cv) are given for three cloud types at the solstices (June 22, δ = +23.5°; December 22, δ = -23.5°) and equinoxes (March 21/September 23, δ = 0.0°). Refer to Table C.3 for comparison with a cloudless sky at 20° S.

TOTAL IRRADIANCE (W m^{-2})	SOLAR DECLINATION (Approximate date) -23.5° (Dec 22)	0.0° (Mar 21/Sep 23)	+23.5° (Jun 22)
Cirrostratus			
mean±1 SD	236.5±283.5	162.8±219.3	46.1±14.8
median	60.1	58.4	50.9
(range)	(1.2-744.5)	(0.1-601.0)	(0.1-59.4)
cv	119.9%	134.7%	32.0%
	n = 397	*n* = 361	*n* = 323
Altostratus			
mean±1 SD	57.6±27.6	54.0±25.1	40.7±18.7
median	62.9	60.0	45.4
(range)	(0.6-92.7)	(0.8-83.8)	(0.1-62.0)
cv	47.9%	46.5%	46.1%
	n = 397	*n* = 361	*n* = 323
Stratus			
mean±1 SD	34.1±16.7	31.9±15.0	23.8±11.0
median	37.1	35.0	26.7
(range)	(0.4-56.2)	(0.5-50.0)	(0.1-36.5)
cv	48.9%	47.2%	46.3%
	n = 397	*n* = 361	*n* = 323

Table C.25. Statistical summary showing simulated total irradiance (W m^{-2}) at ground level at the centre of a circular gap (forest height to diameter ratio = 1:1) at 20° South under cloudy skies. The mean, standard deviation, median, range and coefficient of variation (cv) are given for three cloud types at the solstices (June 22, δ = +23.5°; December 22, δ = -23.5°) and equinoxes (March 21/September 23, δ = 0.0°). Refer to Table C.4 for comparison with a cloudless sky at 20° S.

TOTAL IRRADIANCE (W m^{-2})	SOLAR DECLINATION (Approximate date) -23.5° (Dec 22)	0.0° (Mar 21/Sep 23)	+23.5° (Jun 22)
Cirrostratus			
mean±1 SD	120.2±239.7	15.4±4.7	13.6±4.3
median	17.7	17.2	15.0
(range)	(0.4-704.3)	(0.0-19.2)	(0.0-17.5)
cv	199.4%	30.6%	32.0%
	n = 397	n = 361	n = 323
Altostratus			
mean±1 SD	16.9±8.1	15.9±7.4	12.0±5.5
median	18.5	17.6	13.4
(range)	(0.2-27.3)	(0.2-24.6)	(0.0-18.2)
cv	47.9%	46.5%	46.1%
	n = 397	n = 361	n = 323
Stratus			
mean±1 SD	10.0±4.9	9.4±4.4	7.0±3.2
median	10.9	10.3	7.9
(range)	(0.1-16.5)	(0.1-14.7)	(0.0-10.7)
cv	48.9%	47.2%	46.3%
	n = 397	n = 361	n = 323

Table C.26. Statistical summary showing simulated total irradiance (W m^{-2}) at ground level at the centre of a circular gap (forest height to diameter ratio = 2:1) at 20° South under cloudy skies. The mean, standard deviation, median, range and coefficient of variation (cv) are given for three cloud types at the solstices (June 22, δ = +23.5°; December 22, δ = -23.5°) and equinoxes (March 21/September 23, δ = 0.0°). Refer to Table C.5 for comparison with a cloudless sky at 20° S.

TOTAL IRRADIANCE (W m^{-2})	SOLAR DECLINATION (Approximate date) -23.5° (Dec 22)	0.0° (Mar 21/Sep 23)	+23.5° (Jun 22)
Cirrostratus			
mean±1 SD	74.9±202.1	7.1±2.2	6.2±2.0
median	8.1	7.9	6.9
(range)	(0.2-695.2)	(0.0-8.8)	(0.0-8.0)
cv	269.7%	30.6%	32.0%
	n = 397	n = 361	n = 323
Altostratus			
mean±1 SD	7.8±3.7	7.3±3.4	5.5±2.5
median	8.5	8.1	6.1
(range)	(0.1-12.5)	(0.1-11.3)	(0.0-8.4)
cv	47.9%	46.5%	46.1%
	n = 397	n = 361	n = 323
Stratus			
mean±1 SD	4.6±2.3	4.3±2.0	3.2±1.5
median	5.0	4.7	3.6
(range)	(0.1-7.6)	(0.1-6.8)	(0.0-4.9)
cv	48.9%	47.2%	46.3%
	n = 397	n = 361	n = 323

Table C.27. Statistical summary showing simulated total irradiance (W m^{-2}) at ground level at the centre of a circular gap (forest height to diameter ratio = 3:1) at 20° South under cloudy skies. The mean, standard deviation, median, range and coefficient of variation (cv) are given for three cloud types at the solstices (June 22, δ = +23.5°; December 22, δ = -23.5°) and equinoxes (March 21/September 23, δ = 0.0°). Refer to Table C.6 for comparison with a cloudless sky at 20° S.

TOTAL IRRADIANCE (W m^{-2})	SOLAR DECLINATION (Approximate date) -23.5° (Dec 22)	0.0° (Mar 21/Sep 23)	+23.5° (Jun 22)
Cirrostratus			
mean±1 SD	54.2±177.3	4.0±1.2	3.5±1.1
median	4.6	4.5	3.9
(range)	(0.1-691.9)	(0.0-5.0)	(0.0-4.6)
cv	327.315%	30.6%	32.1%
	n = 397	n = 361	n = 323
Altostratus			
mean±1 SD	4.4±2.1	4.2±1.9	3.1±1.4
median	4.8	4.6	3.5
(range)	(0.0-7.1)	(0.1-6.4)	(0.0-4.8)
cv	47.9%	46.5%	46.1%
	n = 397	n = 361	n = 323
Stratus			
mean±1 SD	2.6±1.3	2.4±1.2	1.8±0.9
median	2.9	2.7	2.1
(range)	(0.0-4.3)	(0.0-3.8)	(0.0-2.8)
cv	48.9%	47.2%	46.3%
	n = 397	n = 361	n = 323

Table C.28. Statistical summary showing simulated total irradiance (W m^{-2}) at ground level at the centre of a circular gap (forest height to diameter ratio = 4:1) at 20° South under cloudy skies. The mean, standard deviation, median, range and coefficient of variation (cv) are given for three cloud types at the solstices (June 22, δ = +23.5°; December 22, δ = -23.5°) and equinoxes (March 21/September 23, δ = 0.0°). Refer to Table C.7 for comparison with a cloudless sky at 20° S.

APPENDIX D

BASIC PROGRAMS FOR SORTING PPFD DATA INTO LINEAR AND LOGARITHMIC CLASS INTERVALS

```
0005  REM PROGRAM TO COMPUTE FREQUENCY DISTRIBUTION OF PPFD
0006  REM USING 35 LINEAR AND 35 LOGARITHMIC CLASS INTERVALS
0007  REM WRITTEN BY SM TURTON (1986)
0010  INPUT "NAME OF FILE";I$
0020  INPUT "NAME OF OUTPUT FILE (LINEAR CLASSES)";OA$
0035  OPEN "I", #1, I$
0040  OPEN "O", #2, OA$
0050  IF EOF(1) THEN 1000
0060  INPUT#1, T$
0070  INPUT#1, C6,Q1,M$
0080  INPUT#1, C7,Q2,M$
0090  INPUT#1, C8,Q3,M$
0100  INPUT#1, C9,Q4,M$
0110  INPUT#1, C10,Q5,M$
0120  INPUT#1, C11,Q6,M$
0130  INPUT#1, C12,Q7,M$
0140  INPUT#1, C13,Q8,M$
0150  INPUT#1, C14,Q9,M$
0155  INPUT#1, Z$
0160  REM CALIBRATION CONVERSIONS
0165  Q1=Q1*100
0170  Q2=Q2*52.935
0175  Q3=Q3*58.393
0180  Q4=Q4*64.131
0185  Q5=Q5*58.705
0190  Q6=Q6*45.045
0195  Q7=Q7*77.970
0196  Q8=Q8*67.712
0200  Q9=Q9*54.744
0210  A=1:B=0:X=2520
0220  PRINT#2, T$

0300  REM LINEAR CLASSES SORTING ROUTINE
0315  FOR K=0 TO 2448 STEP 72
0316  J=(K+72)/72
0317  PRINT J,J
0320  IF Q1>K THEN 325
0325  IF Q1<K+72 THEN 330 ELSE 340
0330  PRINT#2, J,A,B,B,B,B,B,B,B,B
0331  Q1=X
0340  IF Q2>K THEN 345
0345  IF Q2<K+72 THEN 350 ELSE 360
0350  PRINT#2, J,B,A,B,B,B,B,B,B,B
0351  Q2=X
0360  IF Q3>K THEN 365
0365  IF Q3<K+72 THEN 370 ELSE 380
0370  PRINT#2, J, B,B,A,B,B,B,B,B,B
0371  Q3=X
0380  IF Q4>K THEN 385
0385  IF Q4<K+72 THEN 390 ELSE 400
0390  PRINT#2, J,B,B,B,A,B,B,B,B,B
0391  Q4=X
0400  IF Q5>K THEN 405
0405  IF Q5<K+72 THEN 410 ELSE 440
0410  PRINT#2, J,B,B,B,B,A,B,B,B,B
0411  Q5=X
0440  IF Q6>K THEN 445
0445  IF Q6<K+72 THEN 450 ELSE 460
```

```
0450   PRINT#2,  J,B,B,B,B,B,A,B,B,B
0451   Q6=X
0460   IF Q7>K THEN 465
0465   IF Q7<K+72 THEN 470 ELSE 480
0470   PRINT#2,  J,B,B,B,B,B,B,A,B,B
0471   Q7=X
0480   IF Q8>K THEN 485
0485   IF Q8<K+72 THEN 490 ELSE 495
0490   PRINT#2,  J,B,B,B,B,B,B,B,A,B
0491   Q8=X
0495   IF Q9>K THEN 500
0500   IF Q9<K+72 THEN 505 ELSE 520
0505   PRINT#2,  J,B,B,B,B,B,B,B,B,A
0506   Q9=X
0520   NEXT K
0700   GOTO 50
1000   CLOSE

0300   REM LOGARITHMIC SORTING ROUTINE
0305   FOR M=0 TO 33 STEP 1
0306   J=M+2
0307   K=M/10
0310   Z=10
0316   I=K+O.1
0318   K=Z^K:I=Z^I
0319   PRINT  J,K,I
0320   IF Q1>K THEN 325
0325   IF Q1<I THEN 330 ELSE 340
0330   PRINT#2,  J,A,B,B,B,B,B,B,B,B
0331   Q1=X
0340   IF Q2>K THEN 345
0345   IF Q2<I THEN 350 ELSE 360
0350   PRINT#2,  J,B,A,B,B,B,B,B,B,B
0351   Q2=X
0360   IF Q3>K THEN 365
0365   IF Q3<I THEN 370 ELSE 380
0370   PRINT#2,  J,B,B,A,B,B,B,B,B,B
0371   Q3=X
0380   IF Q4>K THEN 385
0385   IF Q4<I THEN 390 ELSE 400
0390   PRINT#2,  J,B,B,B,A,B,B,B,B,B
0391   Q4=X
0400   IF Q5>K THEN 405
0405   IF Q5<I THEN 410 ELSE 440
0410   PRINT#2,  J,B,B,B,B,A,B,B,B,B
0411   Q5=X
0440   IF Q6>K THEN 445
0445   IF Q6<I THEN 450 ELSE 460
0450   PRINT#2,  J,B,B,B,B,B,A,B,B,B
0451   Q6=X
0460   IF Q7>K THEN 465
0465   IF Q7<I THEN 470 ELSE 480
0470   PRINT#2,  J,B,B,B,B,B,B,A,B,B
0471   Q7=X
0480   IF Q8>K THEN 485
0485   IF Q8<I THEN 490 ELSE 500
0490   PRINT#2,  J,B,B,B,B,B,B,B,A,B
0491   Q8=X
```

```
0500   IF Q9>K THEN 505
0505   IF Q9<I THEN 510 ELSE 520
0510   PRINT#2,  J,B,B,B,B,B,B,B,B,A
0511   Q9=X
0520   NEXT M
0700   GOTO 50
1000 CLOSE
```

PROGRAM DETAILS

Lines 5-50:	Details of names of input and output files are entered
Lines 60-200:	Input ASCII data from the data logger is converted into PPFD fluxes (μ mol m^{-2} s^{-1}).
Lines 210-220:	Parameters are set to a maximum of 2520 μ mol m^{-2} s^{-1} for linear classes and 2512 μ mol m^{-2} s^{-1} for logarithmic classes (refer to Table 6.17)
Lines 300-1000:	Routine for sorting PPFD data into either 35 linear or 35 logarithmic class intervals as per Table 6.17. The data is written to a named ASCII file.